[redacted]

WADC TECHNICAL REPORT 55-305, PART I

(Title Unclassified)

STRUCTURAL DESIGN FOR AERODYNAMIC HEATING

PART I

DESIGN INFORMATION (U)

W. H. Dukes and A. Schnitt
Bell Aircraft Corporation
Buffalo, New York

[redacted]

October 1955

Aircraft Laboratory
Contract No. AF33(616)-2581
Task No. 13719

Wright Air Development Center
Air Research and Development Command
United States Air Force
Wright-Patterson Air Force Base, Ohio

[redacted]

FOREWORD

On 23 August 1954, Bell Aircraft Corporation initiated a program for WADC in accordance with USAF Contract No. AF 33(616)-2581, Project No. 1368, "Construction Techniques and Application of New Materials," to study structural design for aerodynamic heating with range of investigation to extend to Mach 20. The contract was administered under the direction of the Structures Branch, Aircraft Laboratory, Directorate of Development, Wright Air Development Center, with Lt. Roger Brislawn acting as Technical Project Officer.

Messrs. W. H. Dukes and A. Schnitt were responsible for the study organization and for the technical direction of the work accomplished. The editing of the manuscript for this volume was performed by Mr. H. Stafford.

ABSTRACT

The aerodynamic aspects of aerodynamic heating are explained for the structures engineer. Charts and nomographs facilitate the calculation of heat transfer coefficients, equilibrium temperatures, and associated functions to a velocity of 24,000 feet per second.

Mechanical and physical property curves are presented for structural materials, as well as insulating and cooling materials for use at temperatures up to 2400°F. Other curves show thermal gradients and stresses developed in a T section structural element. These cover a wide range of aerodynamic and geometric parameters. Tables are included to show the strength of unstable structural elements for a range of materials and temperatures, both at short- and long-time loading. Temperature gradient effects in a column are also included.

Design of pressure vessels is facilitated by tables that show weight and thickness, and by curves of buckling coefficients for vessels integral with the airframe. Design curves are given for various forms of structural insulation for both transient and steady-state conditions.

PUBLICATION REVIEW

This report has been reviewed and is approved.

FOR THE COMMANDER

D. D. McKee
Colonel, USAF
Chief of Aircraft Laboratory
Directorate of Development

[redacted]

[redacted]

TABLE OF CONTENTS

INTRODUCTION

This volume is Part I of a three-part final report which summarizes the results of a comprehensive study of the structural design of airframes subjected to aerodynamic heating as a result of flight up to Mach 20,

The objectives, methods of approach, and principal results of the study are given in detail in Parts II and III. Some of these results are presented in the form of design charts and methods having application beyond the study, since they contain data of general interest to the stress analyst concerned with the design of structures for use at elevated temperatures. This information has been abstracted and grouped for ready reference in this part of the report.

Since much of the information contained herein is of the type found in Structures Manuals devoted to room-temperature applications, it is presented in the format of a Design Manual. The information is not intended to be a complete treatment of the subject, but is only that which was required for the general study. It may, however, form the basis for a more complete design manual, and the format is such that additional material can be conveniently included. Alternatively, sections can be removed from this part of the report, and can be incorporated in individual Structures Manuals with minimum reorganization. The data of each section are preceded by a brief discussion of the subject matter, and typical examples are given for its use. More complete discussions, together with derivations of methods, can be found in Part II.

Section 1.0 of this volume presents a simplified method and charts for the rapid estimation of structural skin temperatures and heat fluxes due to aerodynamic heating.

In Section 2.0 is a compilation of mechanical and physical properties of materials which may be useful in elevated temperature structures. Included are both metallic and nonmetallic load-carrying materials, as well as insulation and cooling fluids.

Section 3.0 presents curves from which temperature gradients and corresponding thermal stresses can be calculated for structures convectively heated by external contact with the boundary layer.

The design curves of Section 4.0 are concerned with the buckling of plates and stable section columns operating at elevated temperatures, and sustaining load under these conditions for an extended period of time. Curves are also given from which the effect of a temperature gradient on the stability of a column can be determined.

Section 5.0 applies to the design of pressure vessels and contains tables which facilitate the rapid estimation of weights for vessels of a variety of shapes and materials. For the design of integral pressure vessels, buckling coefficients are given for both pressure-stabilized and ring-stabilized cylindrical shells.

For the design of structures that are insulated as protection from aerodynamic heating effects, Section 6.0 presents tables for obtaining structural temperatures and the required amounts of insulation for a number of insulation types.

For maximum usefulness of the graphical data of this part of the report, many curves are presented as "carpet" plots, and Appendix I is included to explain the use of these graphical presentations.

SECTION 1.0

AERODYNAMIC HEATING

By C.M. Schmidt, A. Hanawalt, and W. H. Dukes

[redacted]

[redacted]

TABLE OF CONTENTS

NOMENCLATURE

a = sonic velocity (ft/sec)

c = specific heat of skin element (BTU/lb °F)

G = irradiation, such as from sun and atmosphere (BTU/ft^2hr)

h_c = heat transfer coefficient ($BTU/ft^2hr°R$)

P_δ = local stream static pressure (lb/ft^2)

P_∞ = ambient pressure (lb/ft^2)

r = recovery factor (dimensionless)

T_r = recovery temperature (°R)

T_T = total temperature (°R)

T_W = body wall temperature (°R)

T' = boundary layer reference temperature (°R)

T_δ = local stream temperature, outside of boundary layer (°R)

T_∞ = ambient temperature (°R)

V_δ = local stream velocity outside of boundary layer (ft/sec)

V_∞ = stream velocity in front of shock (ft/sec)

w = specific weight of skin element (lb/ft^3)

X = effective distance (ft)

y = thickness of skin element (in.)

α = surface absorptivity (dimensionless)

δ = flow deflection angle for a plate (degrees)

ϵ = surface emissivity (dimensionless)

θ = time (sec)

θ_c = semivertex angle of cone (degrees)

σ = Stefan-Boltzmann constant = 0.173×10^{-8} $BTU/ft^2hr°R^4$

SECTION 1.0

AERODYNAMIC HEATING

1.1 GENERAL

Presented in this section is a simplified method for determining the aerodynamic heating that occurs on aircraft traveling at high speeds. The information of this volume is not intended to be a comprehensive discussion of the mechanism of heat transfer, but rather a design manual for preliminary structural investigations which can be used with a minimum amount of fluid flow and thermodynamic background. The major limitations and the range of applicability are explained, and typical examples clarify the procedures. The method given herein is largely a compilation of working curves based, with some slight modifications, upon Reference 1.

Wherever relative motion exists between a real fluid and a body, the particles of fluid in a thin layer near the body are retarded by viscous frictional forces. This thin layer of fluid is called the "flow boundary layer" and within it the kinetic energy of the fluid stream is converted into heat. Heat is then transferred to the body at a rate which is proportional to the temperature difference between the boundary layer and the body surface, and the coefficient of heat transfer. The heat transfer coefficient expresses the ability of the boundary layer to transport heat to the body surface, and its value therefore depends upon: (1) the type of flow within the boundary layer, (2) the local pressure, (3) the boundary layer fluid properties, (4) the boundary layer thickness, (5) the local velocity outside of the boundary layer, and (6) the wall temperature.

Unless the structure is cooled, these conditions may lead to an increase in surface temperature; the rate of increase depends upon the instantaneous rate of heat input and the heat capacity of the surface structure. As the surface temperature increases, it begins to dissipate a significant amount of heat by radiation. Ultimately, if the aerodynamic heating conditions persist for a sufficient time, a state of equilibrium is reached where the heat input from the boundary layer equals the radiant heat loss.

This section of the report is concerned with predicting, with a minimum of computation, the transient and steady state heating effects described previously. The method used is applicable particularly to flight speeds of less than Mach 10 and altitudes below 250,000 feet. For the purposes of this study, the method has been extended to Mach 20, but should be used with caution. The several assumptions involved are discussed in the following.

Very high temperatures are encountered within the boundary layer at high Mach numbers. At temperatures approaching 5400°R, the oxygen molecules begin to dissociate; at temperatures of about 10,000°R, inonization becomes significant. The thermal effects of transient dissociation of air are not well understood, but indications are that heating rates to a cool skin may not be altered significantly. Therefore, dissociation effects have not been included in the presentation.

At hypersonic speeds, interaction between the shock wave and the boundary layer near the leading edge has a pronounced effect on the heating rate, on the expansion side of the body, but only a small effect on the pressure side. Furthermore, the effect decreases with increasing pressure and, since the critical heating conditions inevitably occur on the pressure side, the interaction effect has been neglected.

At Mach numbers greater than 10, temperatures in the boundary layer are such that radiation from the boundary layer to the wall of the vehicle may become significant. In the present state of the art, this effect is not well understood and has been neglected in this section.

The methods given in this section for the calculations of aerodynamic effects are based upon boundary layer theory. Since some distance is required behind the entering edge for the boundary layer to become established, it is evident that these methods do not apply in the areas of wing leading edges and fuselage nose. Since the problem of aerodynamic heating of leading edges is too specialized to absorb the attentions of the structures engineer, its inclusion in this section is not appropriate. Methods of analysis can be found, however, in References 5, 6, and 7.

ALL AERODYNAMIC HEATING CALCULATIONS ARE BASED UPON LOCAL VALUES, JUST OUTSIDE THE BOUNDRY LAYER, RATHER THAN AMBIENT VALUES, OF PRESSURE, TEMPERATURE, AND VELOCITY IN THE FREE STREAM. Consequently, the curves presented in this section give both ambient pressures and temperatures at all altitudes up to 250,000 feet, and also the ratios of pressure, temperature, and velocity as the flow passes through the shock. Two nomographs permit the simple evaluation of the heat transfer coefficient for the two types of boundary layer, turbulent and laminar. Curves of stagnation temperature rise simplify the calculation of boundary layer temperatures.

The method is explained by which heat transfer coefficients and boundary layer temperatures are used to calculate transient skin temperatures, and, for steady state conditions, tables of equilibrium skin temperatures are included.

1.2 ATMOSPHERIC PROPERTIES

Since all aerodynamic heating calculations are dependent upon atmospheric pressure and temperature, Figures 1.2-1 and 1.2-2 show the variation of these characteristics with altitude for the NACA standard atmosphere (Reference 2), the ANA standard hot atmosphere (Reference 3), and the ICAO standard atmosphere (Reference 8).

The properties of the atmosphere at any altitude have variations of the same order of magnitude as at sea level. However, if the ambient temperature is above normal at low altitude, it tends to be below normal in the stratosphere (35,000 to 105,000 feet), and vice versa. The ANA standard hot atmosphere represents the highest temperatures that can reasonably be expected at any altitude, and hence it is a combination of summer temperatures at low altitudes and winter temperatures in the stratosphere.

Having the atmospheric temperature from Figure 1.2-1, the corresponding sonic velocity can be readily calculated from the expression

$$a = 49.02\sqrt{T_\infty} \ .$$

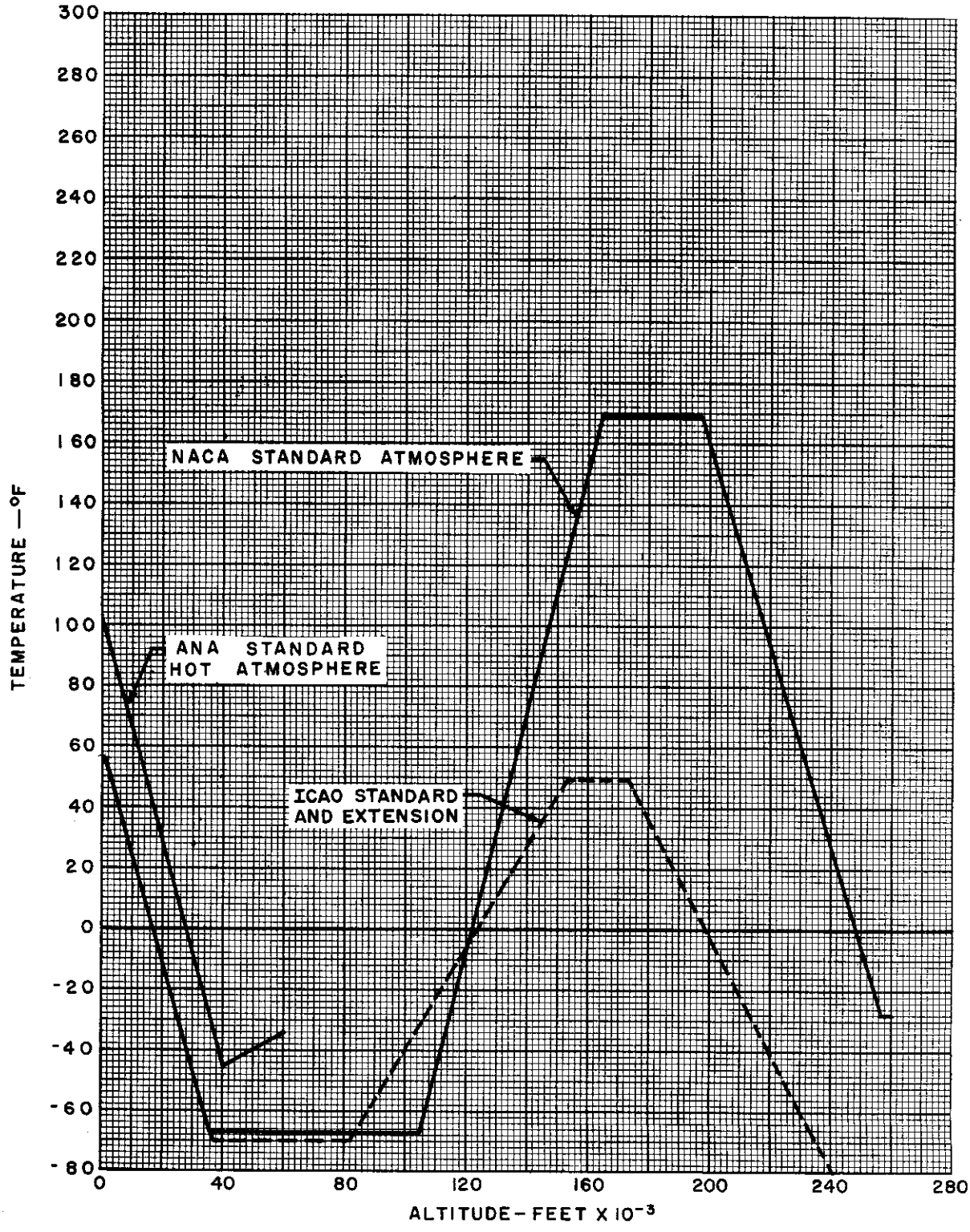

Figure 1.2-1. Properties of Standard Atmosphere — Temperature Variation

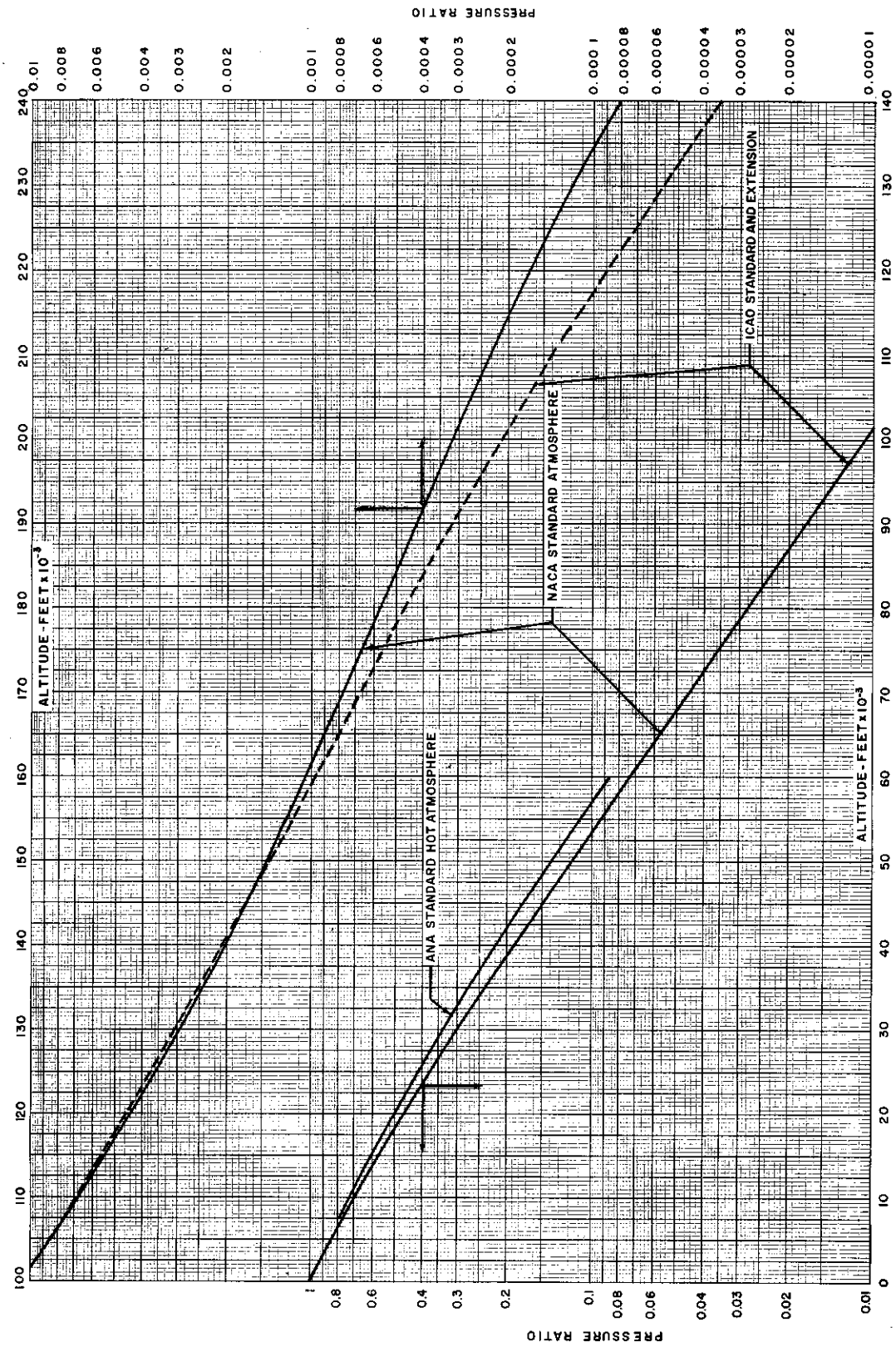

Figure 1.2-2. Properties of Standard Atmosphere — Pressure Ratio

1.3 LOCAL FREE STREAM CONDITIONS

The deflection of a uniform supersonic air stream, produced by any obstacle in the stream, results in the formation of a shock or expansion wave depending upon the means by which the stream is deflected. This difference can be shown by considering a thin flat plate in the stream, inclined at a small positive angle of attack. Referring to the following diagram, the flow deflection δ produces a shock wave below the plate and an expansion above.

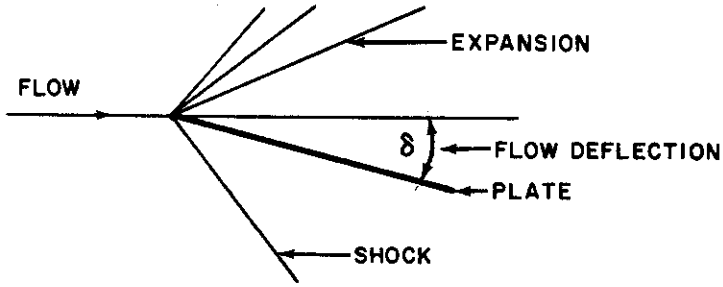

As the air flows through a shock wave, it is compressed (raised to a higher static pressure), its velocity is reduced, and its temperature rises as a result of the compression. Opposite effects occur as the flow passes through an expansion wave.

Since aerodynamic heating calculations are based upon the local free stream conditions at the point on the body under consideration, it is necessary to know the changes that take place in the airstream as it passes through shocks or expansions caused by deflection. Such information, presented in this section, has been calculated from data in Reference 4.

The changes in pressure, velocity, and temperature across the shock or expansion are presented in ratio form in Figures 1.3-1, 1.3-2, and 1.3-3. Static pressure and temperature behind the shock are obtained by multiplying the appropriate ratios by the ambient pressure and temperature obtained from Figures 1.2-1 and 1.2-2. Free-stream velocity behind the shock is the product of the vehicle velocity and the ratio from Figure 1.3-3. Similar curves, for flow through an expansion, are given in Figures 1.3-4 and 1.3-5.

It will be noted that changes in free stream conditions through a shock wave are dependent upon the body shape. Curves are presented for the two important cases of a flat plate inclined at a positive angle of attack and a cone at zero angle of attack.

The flat plate curves should be used for wing surfaces and similar flat areas over which the flow is essentially two-dimensional. For three-dimensional flow, such as occurs around the nose of a fuselage or body, the curves for a cone should be used. If the nose is at an angle of attack, or is an ogive or other nonconical shape, a value of semivertex angle θ_c should be selected so that the fictitious cone defined by this angle has the same inclination between its surface and the air stream as the tangent to the actual surface at the point under consideration.

Where more than one flow deflection occurs in the stream, the changes in flow characteristics at each deflection are found from the curves and applied progressively. Across the lower surface of a double-wedge wing, the first flow deflection, δ_1 (see the following diagram), produces a shock, while the second deflection, δ_2, occurs through an expansion.

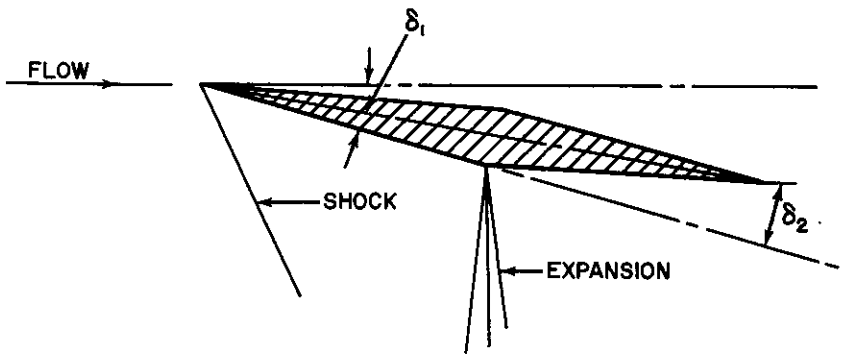

In the case of a cone followed by a cylinder, typical of many supersonic bodies, it is usual to determine flow conditions on the cylinder by applying the flat plate curves directly, and using a flow deflection angle equal to the local incidence between the point on the cylinder and the free stream. This neglects the cross flow around the circumference of the cylinder and replaces the conical shock expansion by a plane shock.

EXAMPLE

A double wedge airfoil having a total wedge angle of 10° is inclined at 4° positive angle of attack at a speed of Mach 5.0 at an altitude of 80,000 ft. Find static pressure, temperature, and velocity of the local free stream across the lower surface. Assume NACA standard atmosphere. From Figure 1.2-1, temperature at 80,000 ft = -67.5°F = 392.5°R; from Figure 1.2-2, pressure ratio at 80,000 ft = 0.027. Using a sea-level pressure of 2116 lb/ft^2, the ambient pressure at altitude becomes 59.2 lb/ft^2. Sonic speed at 80,000 ft = $49.02\sqrt{392.5}$ = 971 ft/sec, so that aircraft velocity = 971 x 5.0 = 4855 ft/sec.

Flow deflection at the airfoil nose equals $4 + 1/2 \cdot 10 = 9°$ and a shock wave is produced. From Figures 1.3-1, 1.3-2, and 1.3-3, the pressure, velocity, and temperature ratios are respectively 2.75, 0.961, and 1.38, so that over the first wedge of the airfoil, lower surface, static pressure = 163 lb/ft^2, velocity = 4665 ft/sec, and temperature = 541°R. Sonic velocity = $49.02\sqrt{541}$ = 1142 ft/sec. Local Mach number = 4665/1142 = 4.08.

At the junction of the two wedges, flow deflection equals 10°, and an expansion is produced. From Figures 1.3-4 and 1.3-5, the ratios are: pressure -0.32, velocity -1.04, and temperature 0.725. Over the aft part of the airfoil lower surface, therefore, the free stream conditions are: pressure = 163 x 0.32 = 52.2 lb/ft^2, velocity = 4665 x 1.04 = 4850 ft/sec, and temperature = 541 x 0.725 = 393°R.

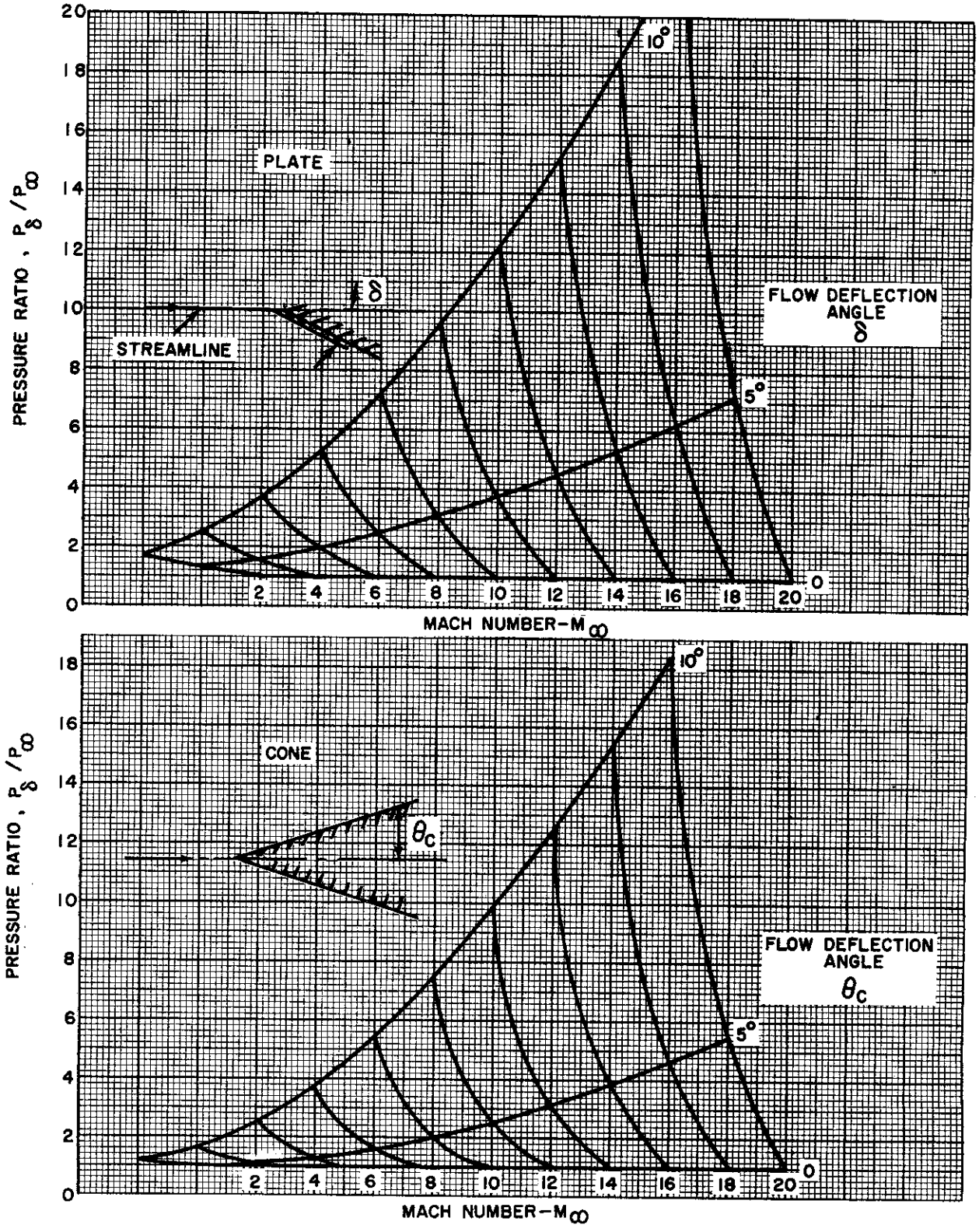

Figure 1.3-1. Static Pressure Ratio Across Shock for Plates and Cones

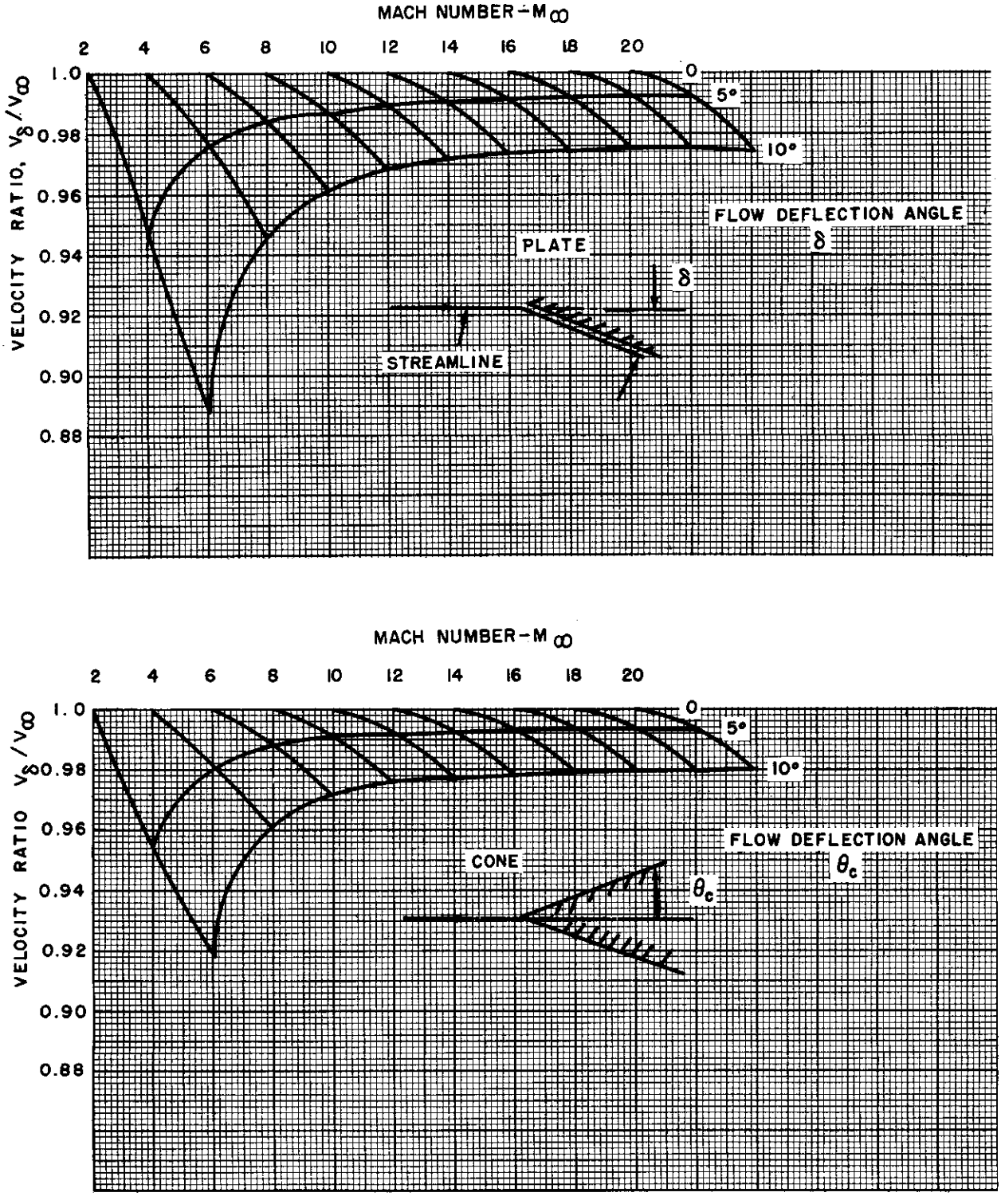

Figure 1.3-2. Velocity Ratio Across Shock for Plates and Cones

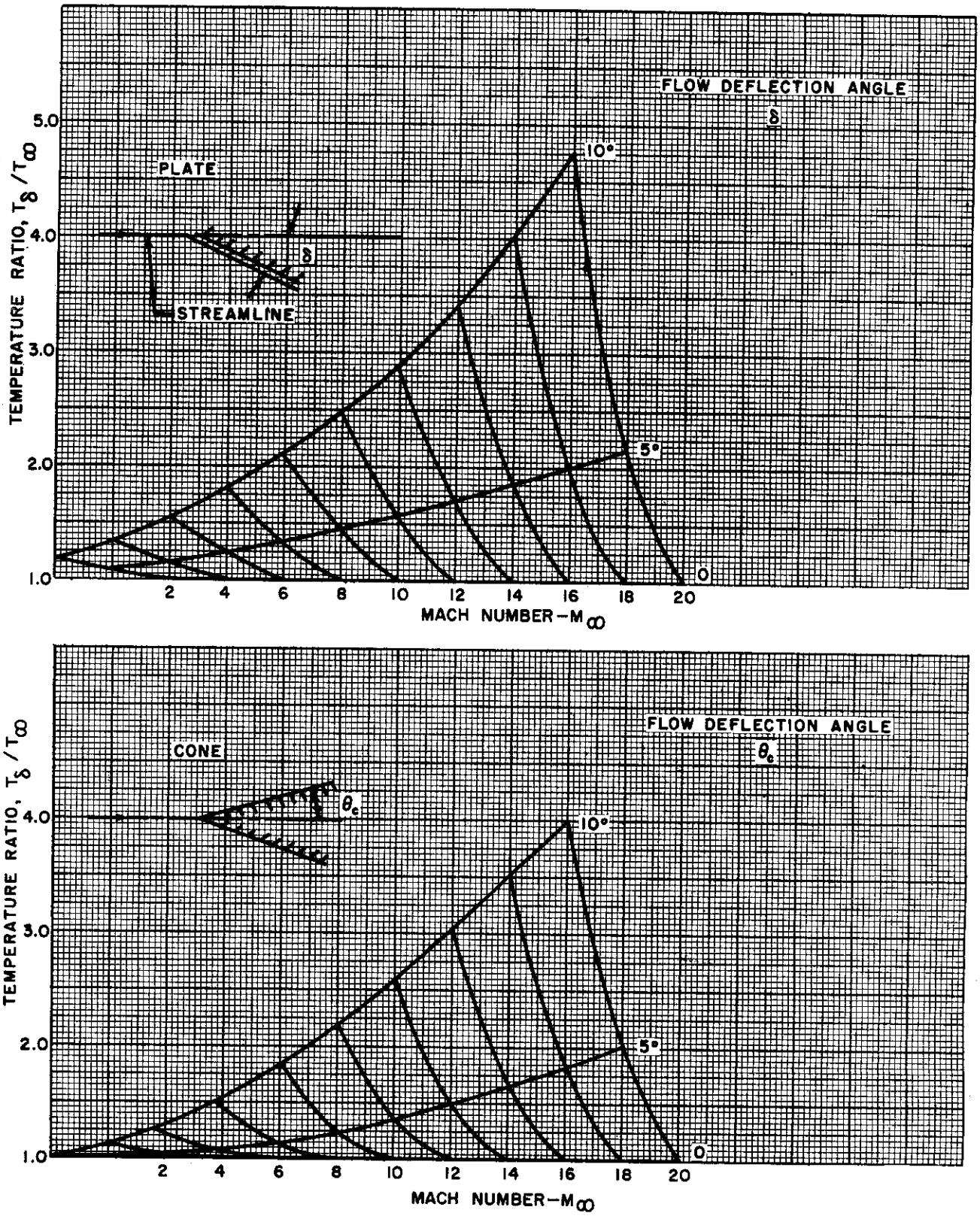

Figure 1.3-3. Temperature Ratio Across Shock for Plates and Cones

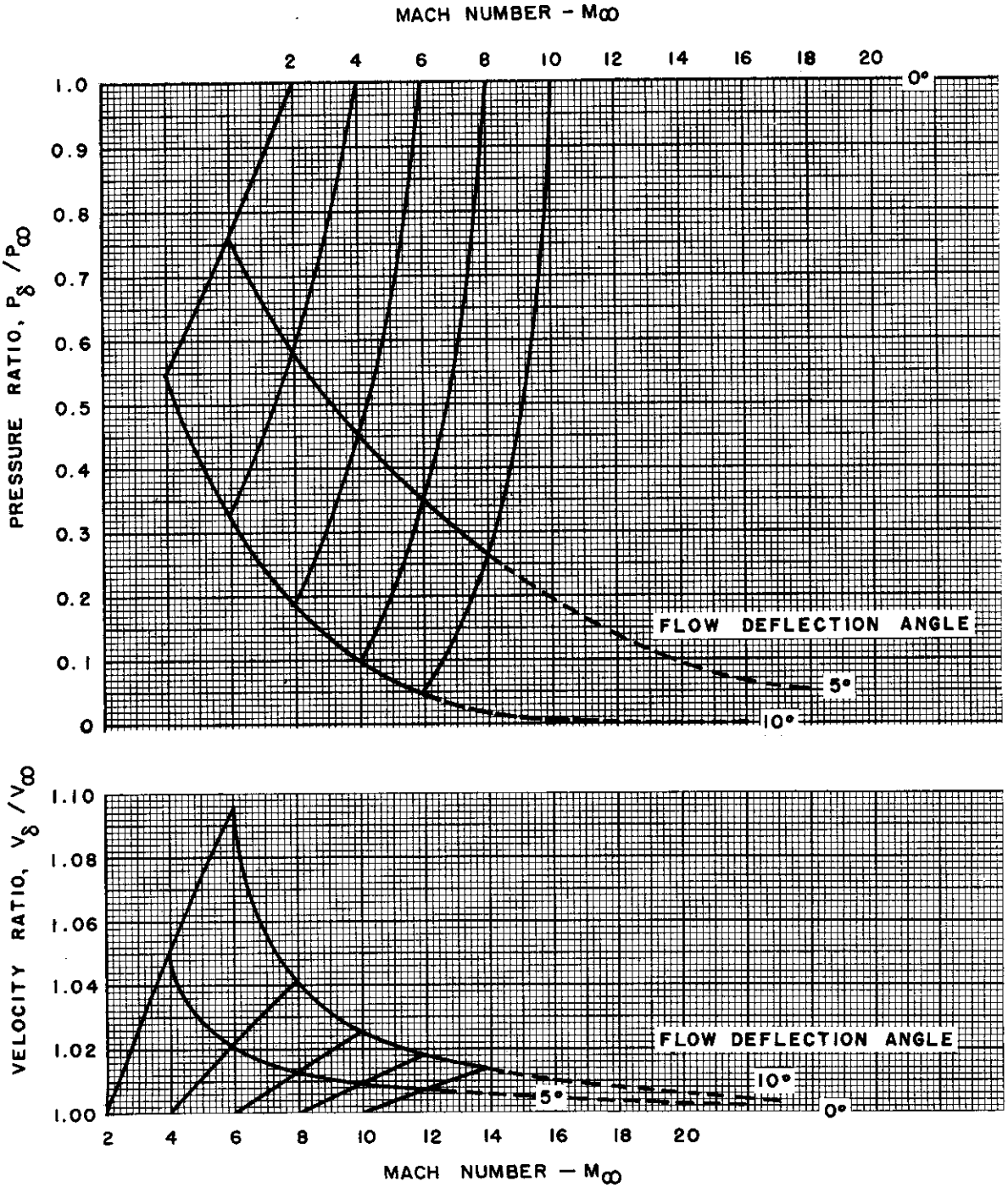

Figure 1.3-4. Pressure and Velocity Ratios Across an Expansion

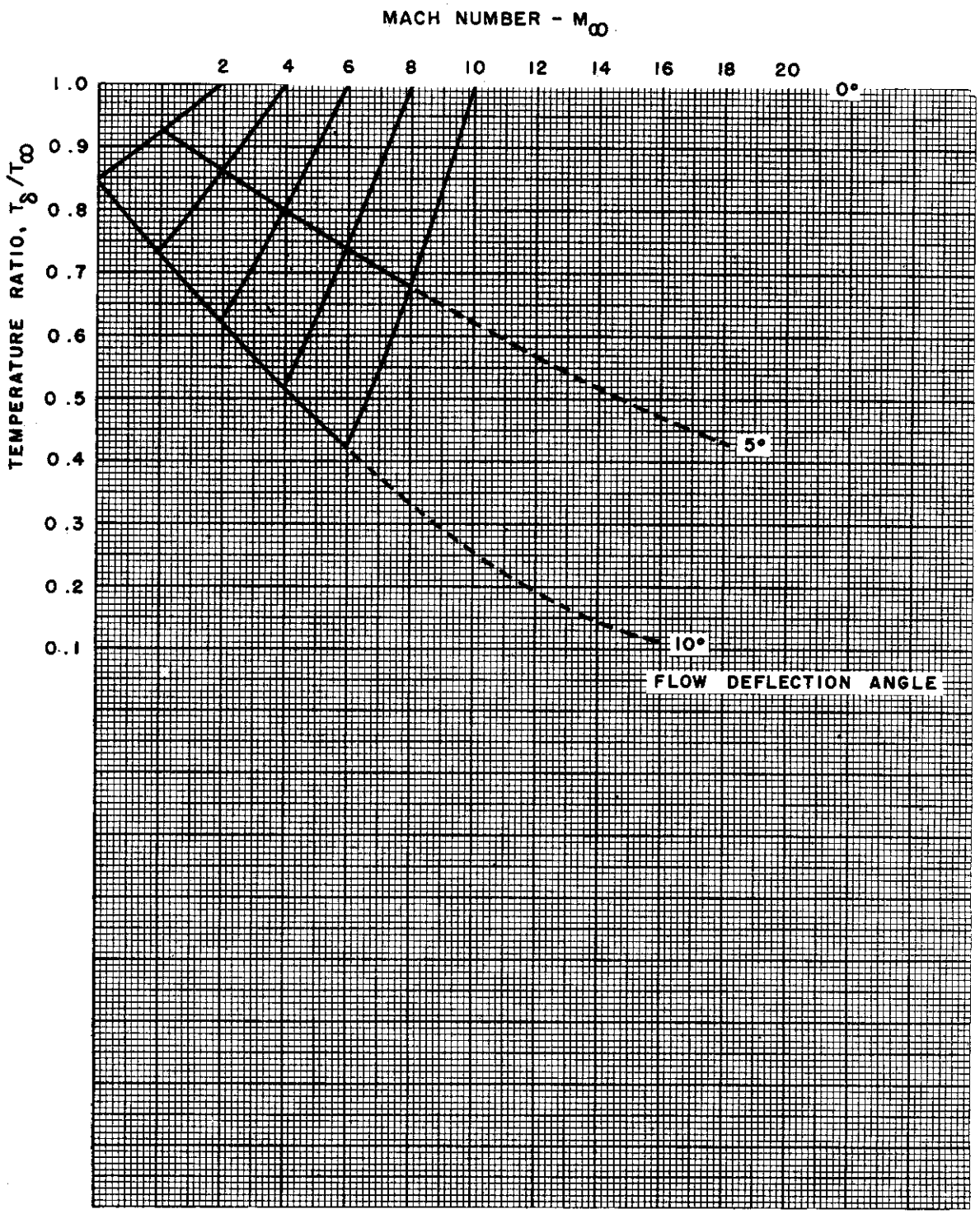

Figure 1.3-5. Temperature Ratios Across an Expansion

1.4 HEAT TRANSFER COEFFICIENTS

The significance of the heat transfer coefficient in the determination of structural temperatures has been explained in Section 1.1. This subsection presents two nomographs for the computation of heat transfer coefficients. However, before this can be done, it is necessary to determine the type of flow in the boundary layer and a reference temperature.

The numerical value of the heat transfer coefficient depends significantly upon the type of flow in the boundary layer, whether it be laminar or turbulent, to the extent that turbulent heat transfer coefficients may be several times larger than those produced by laminar flow, all other conditions being equal. Generally, the flow will be laminar near the leading edge and will become less stable as the distance from the leading edge increases, until at some point a slight disturbance will cause the flow to become turbulent. No reliable theory has yet been set forth to determine the location of the transition region. Thus, for conservative design, the flow may be assumed turbulent aft of the leading edge. However, many investigators have used a Reynolds number of 2.8×10^6 to locate the transition point, and this is suggested for use for high-altitude conditions where extensive areas of laminar flow may exist.

The heat transfer coefficient is influenced by the physical characteristics of the air in the boundary layer, and these, in turn, depend upon temperature. Since the temperature in the boundary layer varies through its thickness, a reference temperature, T' is used to evaluate the air properties. This reference temperature is conveniently obtained by the use of Figure 1.4-1 for which a wall temperature, T_w, must first be assumed.

EXAMPLE

Wall temperature, $T_w = 450°R$; local free stream temperature, $T_\delta = 400°R$; and local free stream velocity = 4000 ft/sec. Find the reference temperature for turbulent flow.

Lay a straight-edge from 400°R on the T_δ scale to 450°R on the T_w scale and read 425°R on the $\left(\frac{T_w + T_\delta}{2}\right)$ scale, see line 1 of Figure 1.4-1. Lay a straight-edge from 425°R on the $\left(\frac{T_w + T_\delta}{2}\right)$ scale to 4000 ft/sec on the turbulent velocity scale, see line 2 of Figure 1.4-1. Read $T' = 675°R$.

Heat transfer coefficients for turbulent and laminar flow are given by the nomographs in Figures 1.4-2 and 1.4-3, respectively. These charts are based upon the following equations:

$$h_c \text{ (turbulent)} = \frac{0.0334}{(T')^{0.576}} \frac{(V_\delta P_\delta)^{0.8}}{(X)^{0.2}}$$

$$h_c \text{ (laminar)} = \frac{0.00963}{(T')^{0.04}} \left(\frac{V_\delta P_\delta}{X}\right)^{0.5}$$

These equations are taken, with slight modifications, from Reference 1. Both include the following assumptions:

(1) Two-dimensional flat plate flow without pressure or temperature gradients.

(2) No effect of dissociation or shock-boundary layer interaction.

Note that in using Figures 1.4-2 and 1.4-3, the local free stream values of pressure and velocity must be used as calculated in Section 1.3. The altitude scale, included in these illustrations for convenience, may be used if the pressure ratio across the shock is small enough to be assumed equal to one. The pressure-altitude relationship shown is for the NACA standard atmosphere. The figures contain a scale for heat transfer coefficient on a cone and include a correction to the flat plate theory for three-dimensional effects.

If necessary, the use of these nomographs can be extended to lower pressures (higher altitudes) in the following manner. Multiply the actual pressure by the factor 10^n, where n is any convenient value, and obtain the heat transfer coefficient in the usual manner. Divide the value obtained from the nomograph by the factors $10^{0.8n}$ and $10^{0.5n}$ for turbulent and laminar flow, respectively.

EXAMPLE

Local free stream velocity = 1000 ft/sec, pressure = 23 lb/ft^2, and the reference temperature, T′, = 400°R. Find the heat transfer coefficient on a cone at a point 10 feet behind the nose if the flow is turbulent.

In Figure 1.4-2 (turbulent flow), lay a straight-edge from 23 lb/ft^2 on the pressure scale to 1000 ft/sec on the velocity scale and note the intersection point on the line marked Ref. 1. See line 1 on Figure 1.4-2. Lay a straight-edge from the intersection on reference line 1 to 10 feet on the length scale and note the intersection point on reference line 2. Lay a straight-edge from the intersection point on reference line 2 to 400°R on the reference temperature scale. Read a heat transfer coefficient of 2.4 BTU/ft^2°F hr, for flow over a cone.

A similar example is shown for laminar flow on Figure 1.4-3 for a local velocity of 1000 ft/sec, a local pressure of 59 lb/ft^2, and a reference temperature of 400°R. At a distance of 5 feet from the leading edge of a wedge, a heat transfer coefficient of 0.82 BTU/ft^2°F hr is indicated.

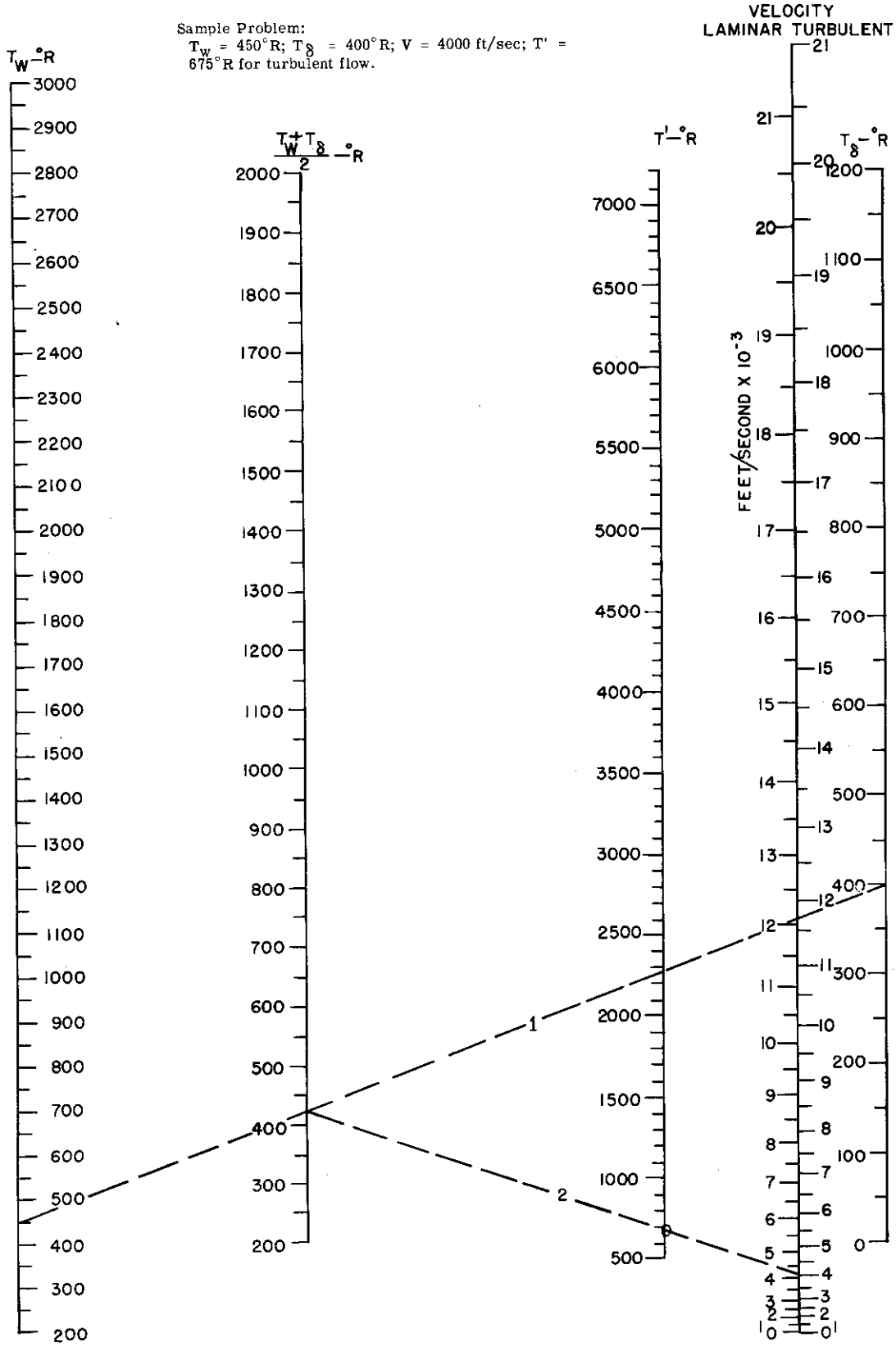

Figure 1.4-1. Reference Temperature — Laminar and Turbulent Flow

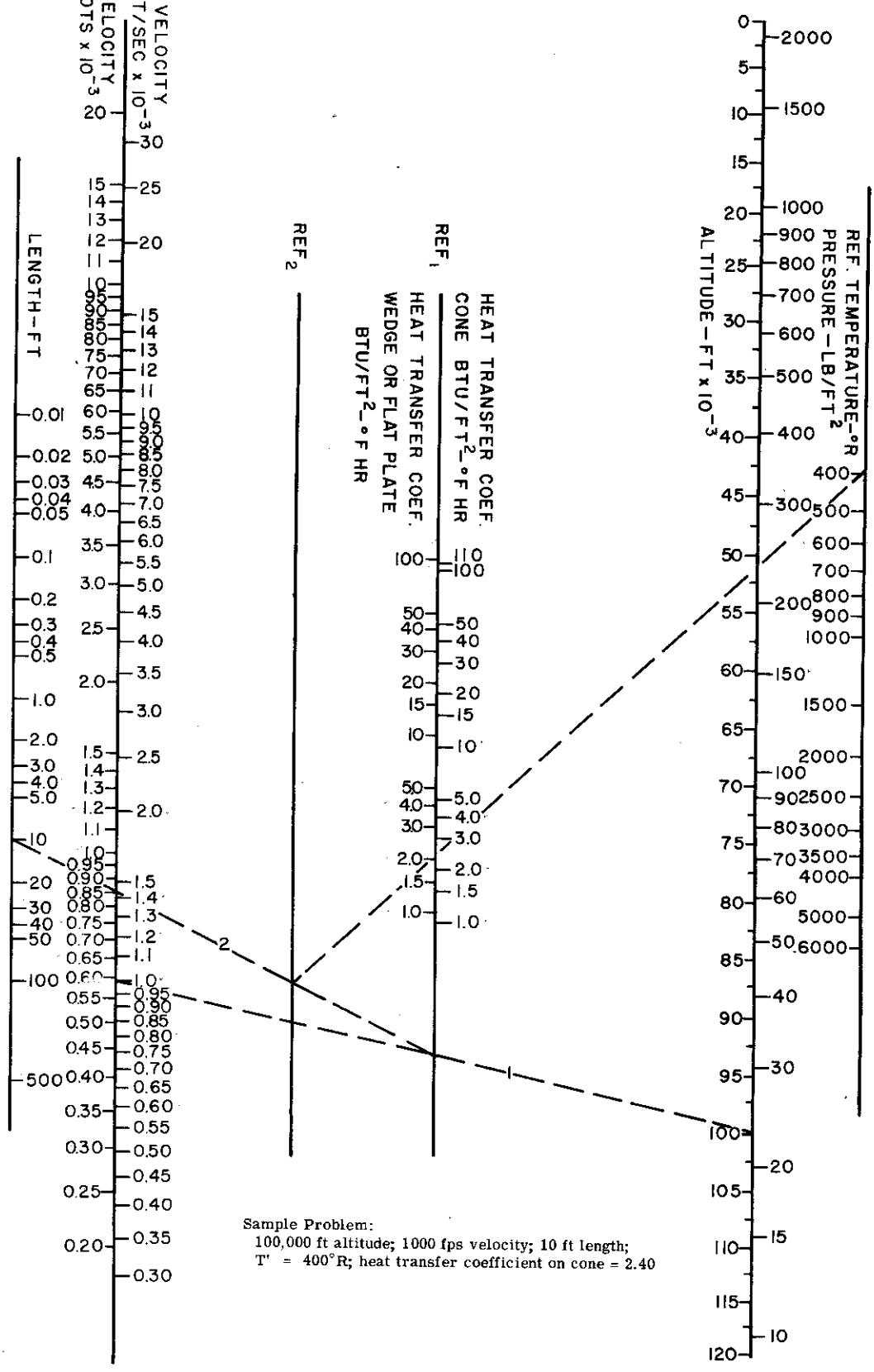

Figure 1.4-2. Heat Transfer Coefficient for Wedge and Cone, Turbulent Flow

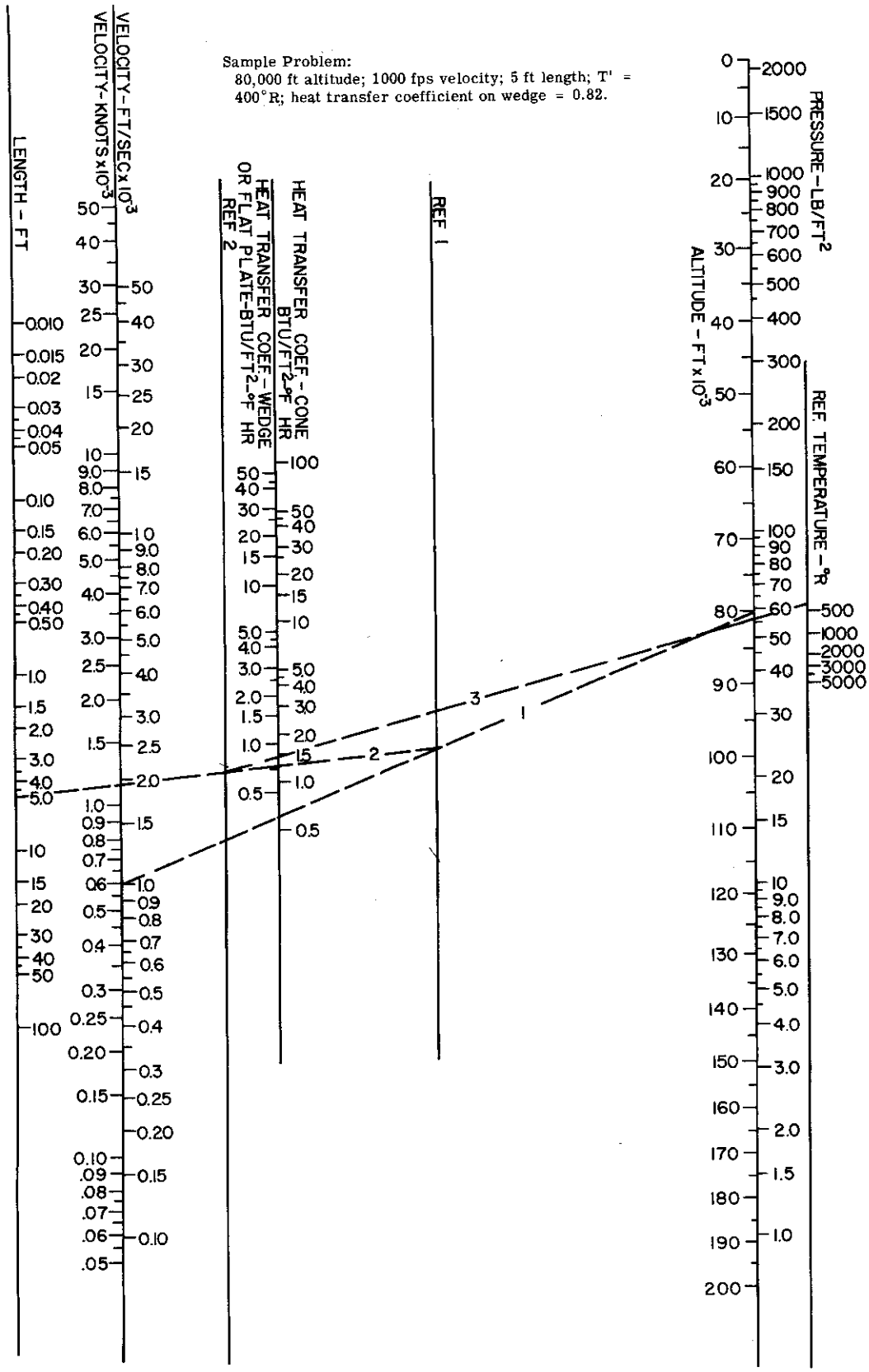

Figure 1.4-3. Heat Transfer Coefficient for Wedge and Cone, Laminar Flow

1.5 STAGNATION AND RECOVERY TEMPERATURES

In Section 1.1, it was explained that particles of fluid in a boundary layer are retarded by viscous frictional forces, so that some or all of their kinetic energy is converted into heat. The difference between the temperature reached by the boundary layer and the temperature of the body surface is the potential which forces heat into the structure.

If a particle is reduced to zero velocity, the resulting temperature is called stagnation temperature and is denoted by T_T. Convenient methods of determining the stagnation temperature rise, or the difference between the local free stream temperature T_δ and the final stagnation temperature T_T, are presented in Figures 1.5-1, 1.5-2, and 1.5-3. These curves are calculated from the equation

$$V_\delta^2 = 12{,}003 \left\{ T_T - T_\delta + \frac{1572}{e^{\left(\frac{5500}{T_T}\right)} - 1} - \frac{1572}{e^{\left(\frac{5500}{T_\delta}\right)} - 1} \right\} .$$

This equation represents a refinement over the more usual conversion of kinetic energy to heat energy since it includes the effect of temperature on the specific heat of the air.

The use of Figures 1.5-1 through 1.5-3 for the case when the local free-stream temperature is 400°R is evident from the curves, but some explanation is necessary for the case when T_δ does not equal 400°R. In using these curves, the stagnation temperature rise, ΔT_T, is first evaluated, appropriate to the velocity, from the curve marked T_δ = 400°R. At the intersection of the line corresponding to the stagnation temperature rise for T_δ = 400°R, and the left-hand curve for the actual value of T_δ read on the lower horizontal scale the additional increment of stagnation temperature rise, $\Delta\left(\Delta T_T\right)$. Add the two increments of stagnation temperature rise.

EXAMPLE

Find the stagnation temperature for a local free-stream velocity of 4500 ft/sec and a local free-stream temperature of 1000°R.

From Figure 1.5-1, the stagnation temperature rise corresponding to T_δ = 400°R = 1560°R. The intersection of the horizontal 1560° line with the curve for T_δ = 1000°R gives an additional increment of stagnation temperature rise of $\Delta\left(\Delta T_T\right)$ = -85°R. Therefore, total rise = 1560° - 85° = 1475°R, so that stagnation temperature = 2475°R.

The velocity of the air particles within the boundary layer is zero at the surface and increases to the local free-stream velocity, V_δ, at the edge of the boundary layer. Similarly, a temperature gradient exists within the boundary layer and causes heat flow to the structural surface and to the local free stream. If radiation is excluded and the aircraft surface is not internally leased or cooled, but is assumed to reach a state of equilibrium with the boundary layer, the temperature attained by the surface is called the recovery temperature, T_r. Because of the loss of heat to the local free stream, the recovery temperature for air is always less than the stagnation temperature. The ratio between the recovery temperature rise and the stagnation temperature rise is known as the recovery factor, $r = \frac{T_r - T_\delta}{T_T - T_\delta}$, and, for the practical purposes of this manual, it can be taken as 0.85 if the boundary layer is laminar and 0.90 if it is turbulent.

EXAMPLE

Find the recovery temperature for the previous example. Assume turbulent flow. Stagnation temperature rise = 1475°R. For turbulent flow, recovery factor = 0.90, so that recovery temperature rise = 1328°R. Recovery temperature = 1328° + 1000° = 2328°R.

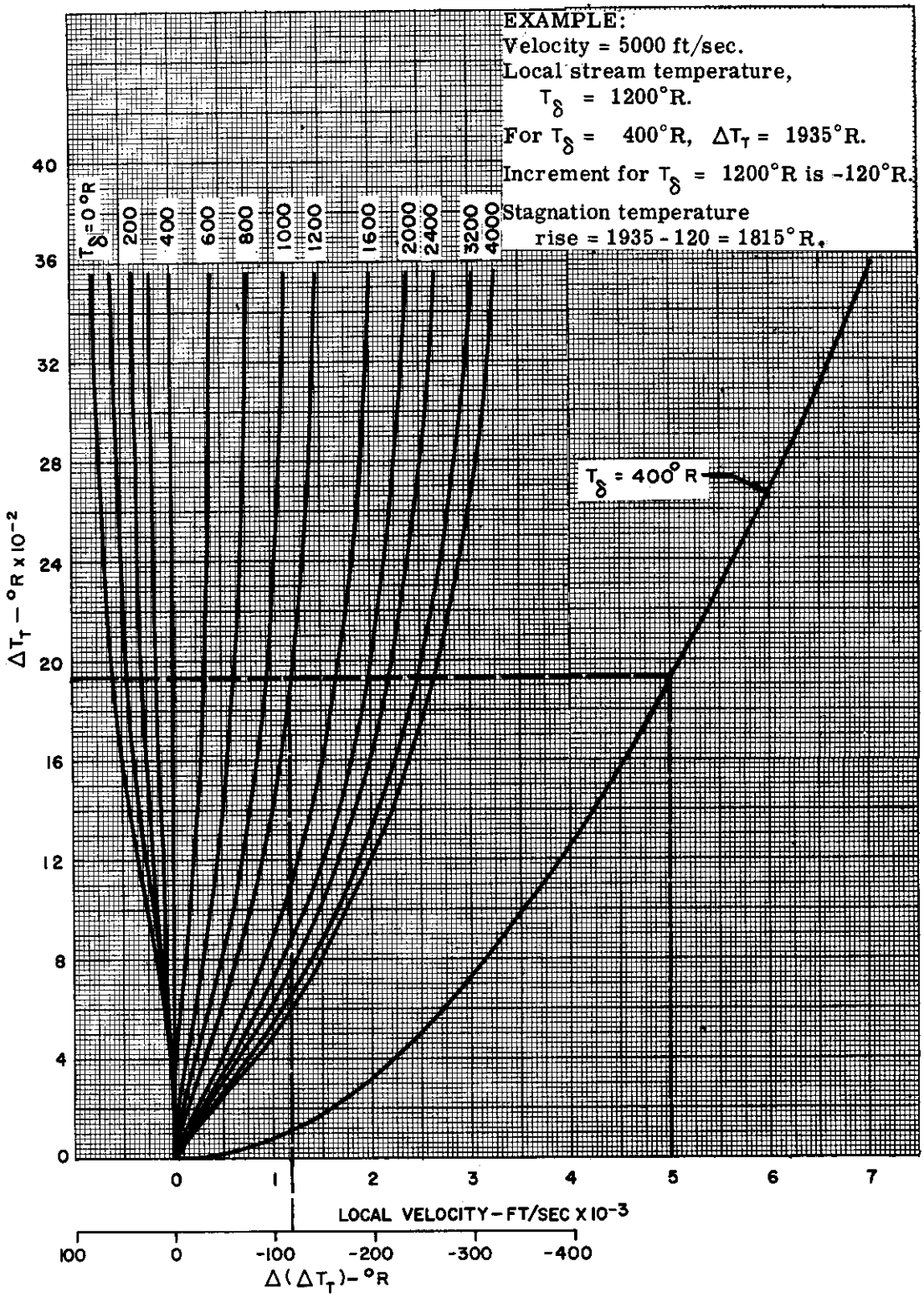

Figure 1.5-1. Stagnation Temperature Rise, 0 to 7000 ft/sec

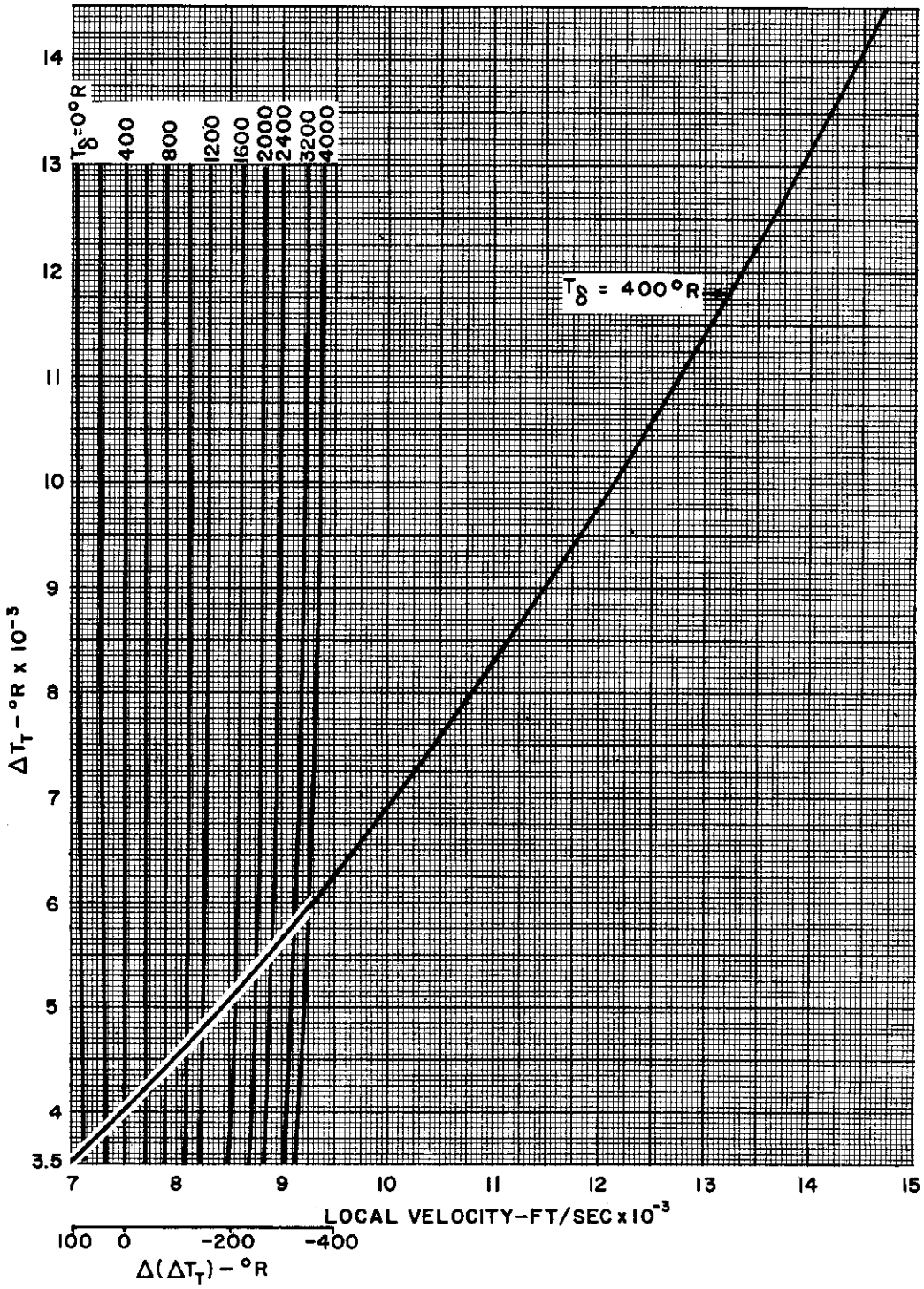

Figure 1.5-2. Stagnation Temperature Rise, 7000 to 15,000 ft/sec

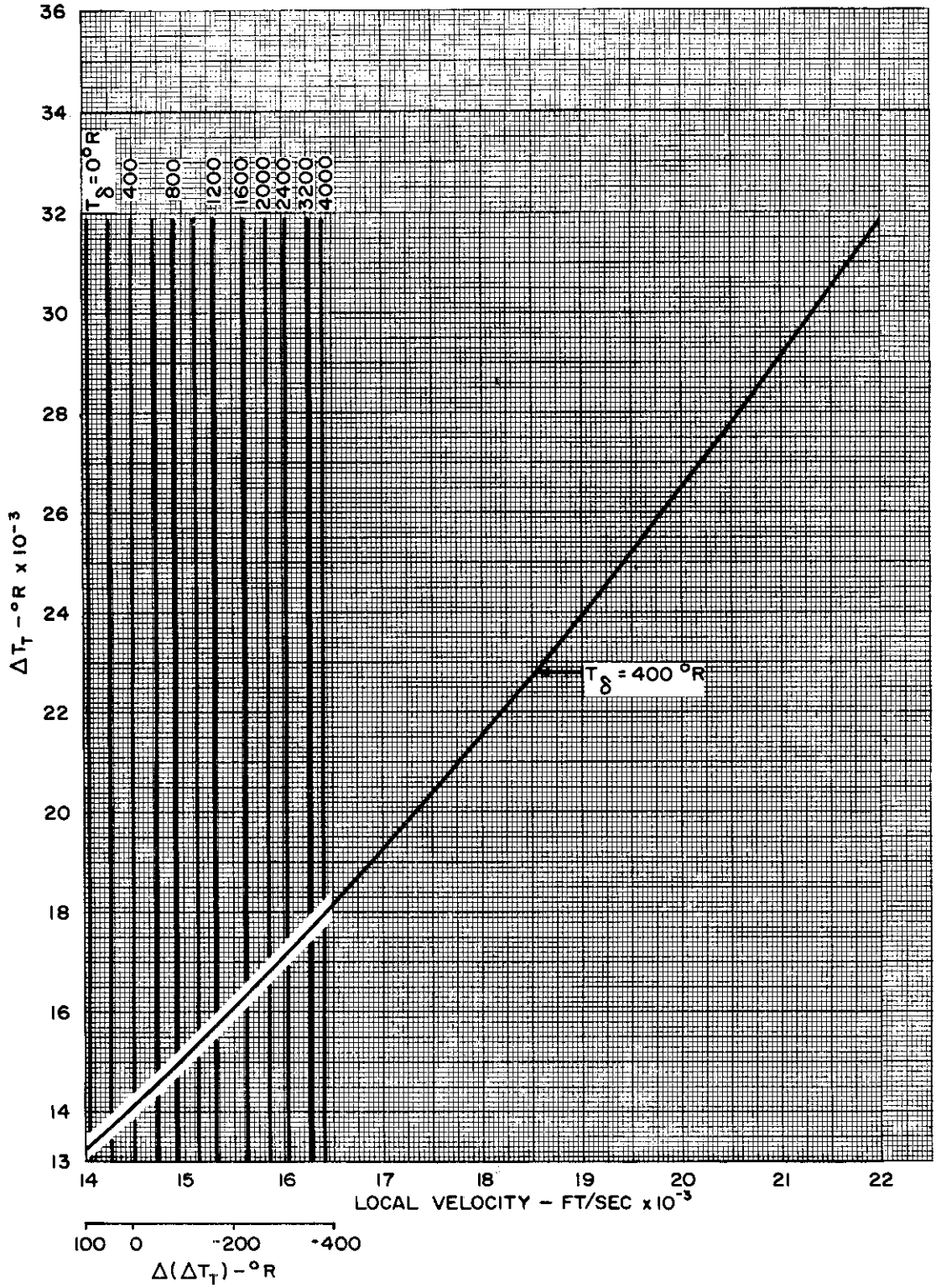

Figure 1.5-3. Stagnation Temperature Rise, 14,000 to 22,000 ft/sec

1.6 TRANSIENT TEMPERATURES

Methods have been presented in the previous subsections for calculating heat transfer coefficients and boundary layer recovery temperatures, and these may now be used to calculate transient skin temperatures. The heat transfer equation for an aircraft skin is

$$\frac{dT_w}{d\theta} = \frac{1}{300\, w\, c\, y}\left[h_c(T_r - T_w) + \alpha G - \sigma \epsilon T_w^4\right].$$

In this equation, the first term within the brackets is the convective heat input. The second term is the heat input by radiation from the sun and atmosphere, and the third term is the heat loss by radiation from the surface. The solar and nocturnal irradiation terms are usually negligible, and the heat radiated from the surface is generally small for skin temperatures below 400°R. The term $w\, c\, y$ expresses the heat capacity of unit area of skin.

Values of surface emissivity, ϵ, and skin specific heat, c, will be found for various skin temperatures in Section 2.0. Note that a large value of emissivity at surface temperature is desirable to minimize structural temperatures. Where this value is low, as with aluminum alloy skin, higher values can be obtained with suitable paint.

This differential equation is conveniently solved by numerical integration using one of the many methods that are available. One such method expresses the skin temperature in a Taylor series, retaining only the first two terms

$$T_{w(\theta_3)} = T_{w(\theta_2)} + \left[\Delta\theta_{(2-3)} \frac{dT_{w(\theta_2)}}{d\theta}\right] + \left[\frac{\left(\Delta\theta_{(2-3)}\right)^2}{2} \frac{d^2T_{w(\theta_2)}}{d\theta^2}\right].$$

The second derivative is approximated by

$$\frac{d^2T_{w(\theta_2)}}{d\theta^2} = \frac{\left[\frac{dT_{w(\theta_2)}}{d\theta}\right] - \left[\frac{dT_{w(\theta_1)}}{d\theta}\right]}{\Delta\theta_{(1-2)}}$$

The equation for T_w is thus reduced to functions of the time increments $\Delta\theta$ and the first derivative $dT_w/d\theta$. The first derivative is calculated from the equation given at the beginning of this section.

For simplicity, these equations are written for the particular times θ_1, θ_2, and θ_3, but they apply generally. The notation $\Delta\theta_{(2-3)}$ refers to the time increment between θ_2 and θ_3.

A check on the proper choice of time intervals is provided by the term

$$\left[\frac{\left(\Delta\theta_{(2-3)}\right)^2}{2} \frac{d^2T_{w(\theta_2)}}{d\theta^2}\right]$$

The time interval should be chosen such that this is small compared with the terms to which it is being added.

EXAMPLE

The following table shows the first three steps of a transient temperature calculation. The example is for a skin thickness of 0.05 inch and a distance 1 foot aft of the leading edge. Assumed are turbulent flow, a flat plate at zero angle of attack, a surface emissivity of 0.90, and ANA standard hot atmosphere. Solar radiation times the surface absorptivity is taken at 70 BTU/ft^2 hr.

EXAMPLE OF TRANSIENT TEMPERATURE CALCULATIONS

x = 1 ft
y = 0.05 in.
300 w c y = 300 x 173 x 0.21 x 0.05 = 583

Turbulent flow
Flat plate at zero angle of attack
ANA standard hot atmosphere

1	2	3	4	5	6	7	8
Time (sec)	Altitude Flight Plan (ft)	V (ft/sec)	P_∞ Fig. 1.2-2 (lb/ft^2)	T_∞ Fig. 1.2-1 (°R)	V_δ / V_∞ Fig. 1.3-2	P_δ / P_∞ Fig. 1.3-1	T_δ / T_∞ Fig. 1.3-3
0	38,000	728	431.8	422	1.0	1.0	1.0
2	37,700	728	438.0	423	1.0	1.0	1.0
4	37,500	757	442.3	424	1.0	1.0	1.0

9	10	11	12	13	14	15	16
V_δ (3) x (6) (ft/sec)	P_δ (4) x (7) (lb/ft^2)	T_δ (5) x (8) (°R)	ΔT_T Fig. 1.5-1 (°R)	$r \Delta T$ 0.9 x (12) (°R)	T' Fig. 1.4-1 (°R)	h Fig. 1.4-2 ($BTU/ft^2 hr\,°R$)	T_r (11)+(13) (°R)
728	431.8	422	44	39.6	450.5	24.8	461.6
728	438.0	423	44	39.6	451.0	25.0	462.6
757	442.3	424	48	43.2	452.3	26.1	467.2

17	18	19	20	21	22	23
$T_r - T_w$ (16) - (23) (°R)	$h(T_r - T_w)$ (15) x (17) ($BTU/ft^2 hr$)	$G\alpha$ ($BTU/ft^2 hr$)	$\sigma \epsilon T_w^4$ ($BTU/ft^2 hr$)	$\frac{\Delta\theta\, dT_w/d\theta}{\Delta\theta[(18)+(19)-(20)]}{583}$ (°R)	$\frac{(\Delta\theta)^2}{2}\frac{\Delta^2 T_w}{\Delta\theta^2}$ (°R)	T_w (°R)
0	0	70	70	0		461.6
1.0	25.0	70	70	0.086	0.043	461.6
5.5	143.5	70	70	0.492	0.203	461.7
						462.4

Column 22 is calculated, using the approximation given in the text, as follows:

Column 21 for present time minus column 21 for the previous time, divided by $\Delta\theta$ for the previous time interval and multiplied by $\frac{(\Delta\theta)}{2}$ for the present time interval. Column 23 is calculated by adding to the previous value the sum of columns 21 and 22.

1.7 EQUILIBRIUM TEMPERATURES

As explained in Section 1.1, if steady conditions of aircraft speed, altitude, and angle of attack are maintained for a sufficient time, a steady state will ultimately be reached in which the convective heat input is exactly balanced by the radiant heat loss from the surface. Referring to the equation of Section 1.6, this condition is achieved when $dT_W/d\theta = 0$ or $h_c(T_r - T_W) = \sigma\epsilon T_W^4$, neglecting solar and nocturnal radiation. This equation has been solved for a flat plate, and the results are presented in Figures 1.7-1 through 1.7-3 for the conditions of laminar and turbulent flow.

The carpet plots in Figures 1.7-1 and 1.7-3 give the radiation equilibrium temperatures for a one-foot station, an angle of attack of 5° and a surface emissivity of 0.9. Other quadrants of these figures give corrections to the equilibrium temperature for various values of surface emissivity, distance from the leading edge, and angle of attack. Figure 1.7-2 is an enlargement, for greater ease and accuracy of reading, of the most useful portion of the turbulent flow curves.

It will be noted in Figures 1.71 and 1.7-3 that the curves giving the correction for various angles of attack include altitude differences for the case of turbulent flow, but not for laminar flow. Actually, the altitude effect is present in both cases. But, because of the smaller significance of pressure on the laminar heat transfer coefficient, the allowance for altitude in the angle-of-attack correction is neglected.

Figures 1.7-1 through 1.7-3 are based upon the ICAO standard atmosphere, but they may be used, to a good approximation, for any other atmosphere by selecting a modified altitude value to equate the ambient pressure of the ICAO atmosphere to that of the new atmosphere.

EXAMPLE

Find the equilibrium temperature 10 feet from the leading edge of a flat plate inclined at 10° angle of attack if the altitude is 200,000 ft, velocity is 15,000 ft/sec, and surface emissivity is 0.60.

From Figure 1.7-1, upper right-hand quadrant, at 200,000 ft altitude and 15,000 ft/sec velocity, a temperature of 1290°F is shown. Following the broken line across the figure gives, for a surface emissivity of 0.6, a temperature on the left-hand horizontal scale of 1460°F. The same broken line is continued down to a distance value of 10 feet, giving a temperature on the lower vertical scale of 1270°F. Finally, continuing across to 10° angle of attack at 200,000 ft altitude gives a temperature on the right-hand horizontal scale of 1595°F,

The same example, indicated on the laminar flow diagram, Figure 1.7-3, gives a final equilibrium temperature of 1240°F.

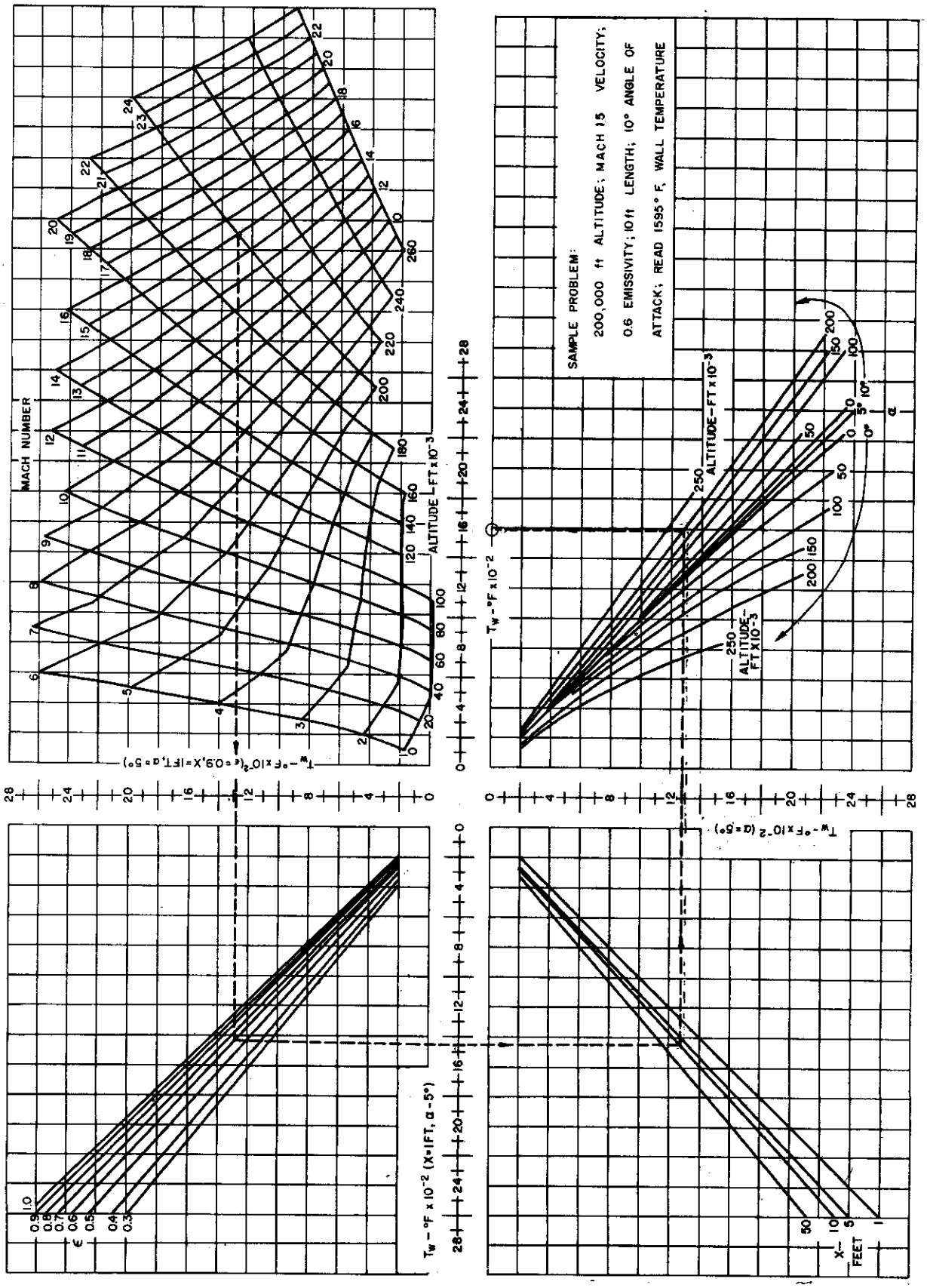

Figure 1.7-1. Equilibrium Wall Temperature, Turbulent Flow — ICAO Standard Atmosphere

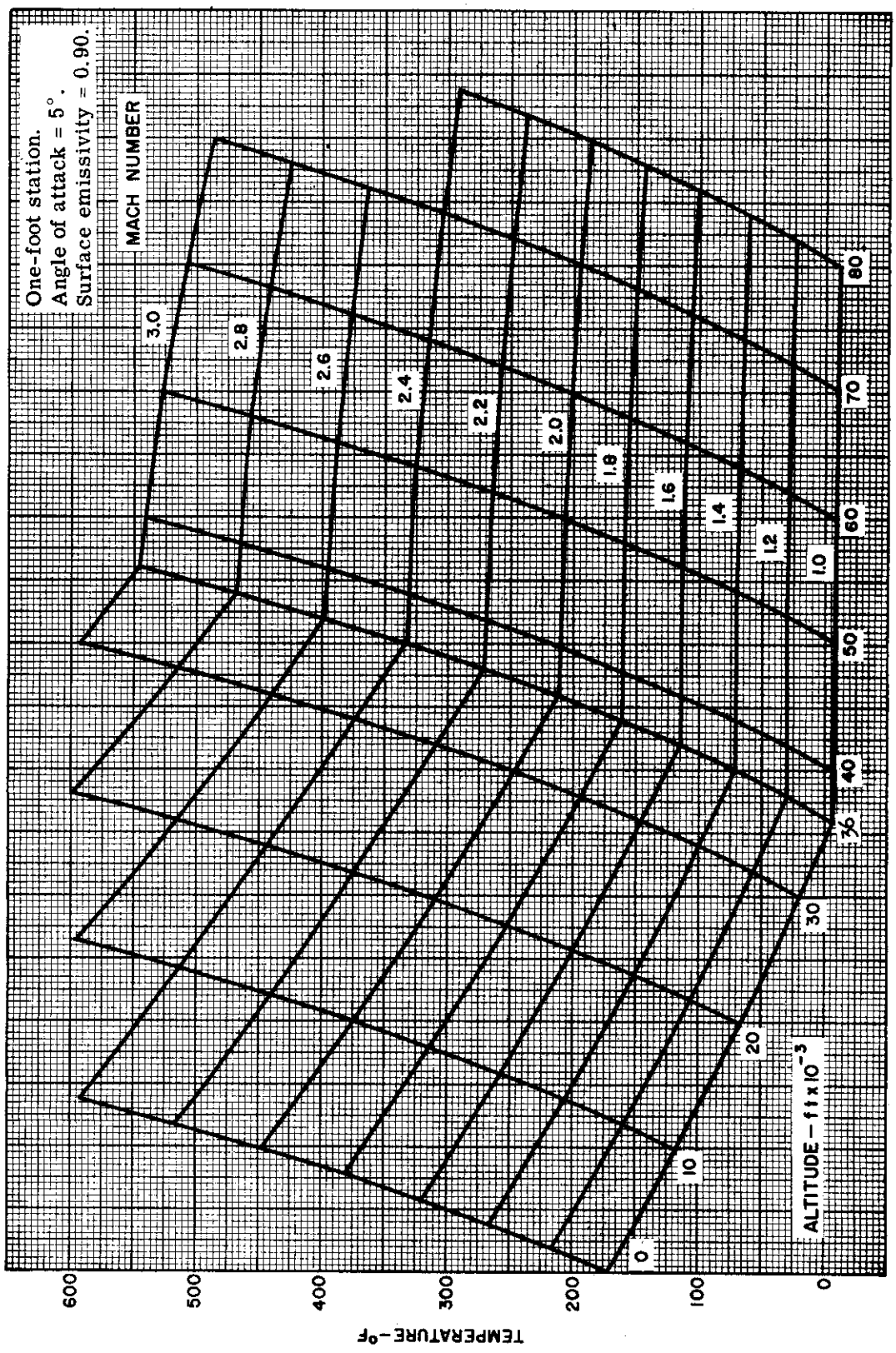

Figure 1.7-2. Equilibrium Wall Temperature, Turbulent Flow — ICAO Standard Atmosphere

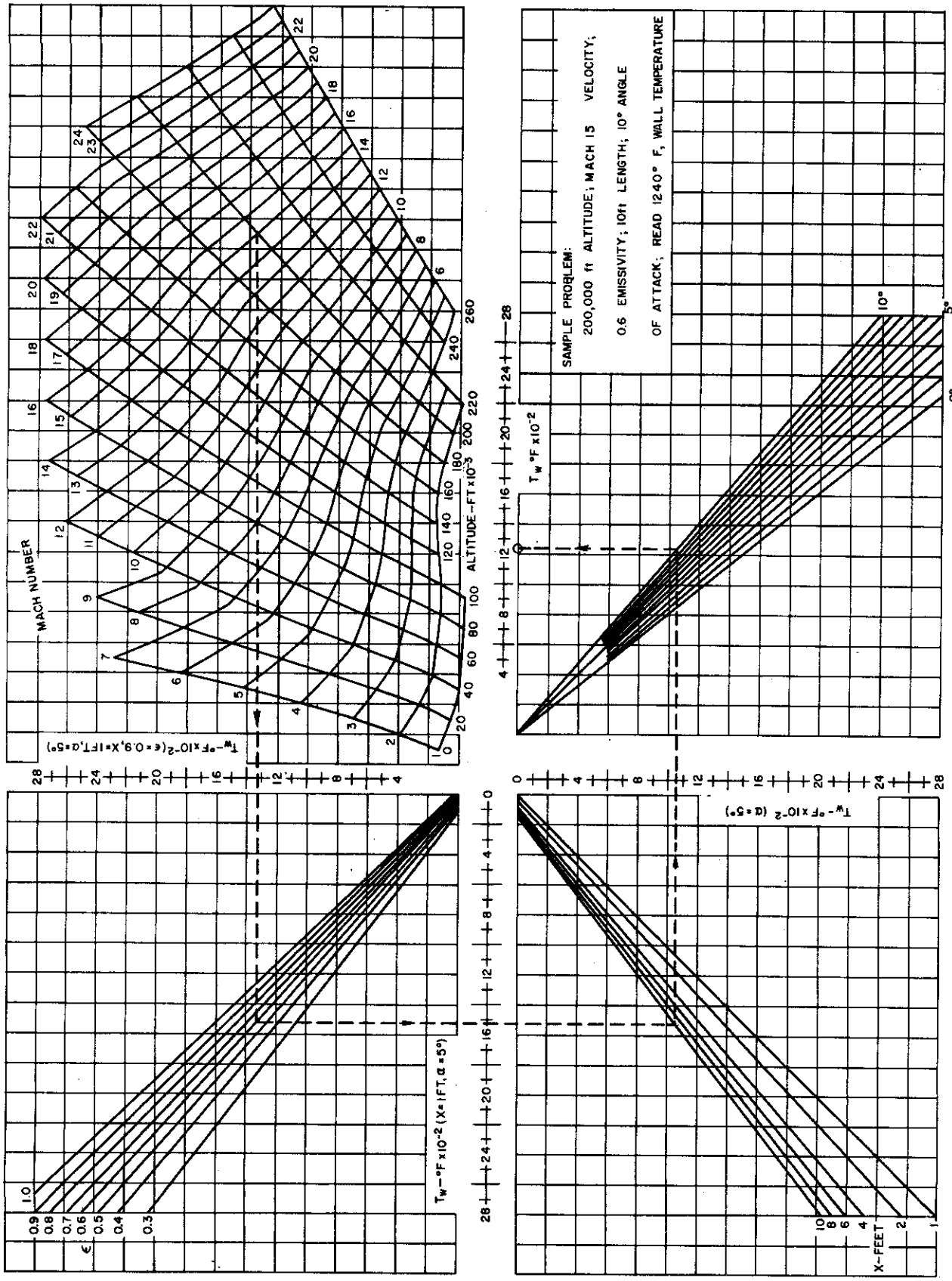

Figure 1.7-3. Equilibrium Wall Temperature, Laminar Flow — ICAO Standard Atmosphere

[redacted]

REFERENCES

(1) Eckert, E. R. G., "Survey on Heat Transfer at High Speeds", WADC Technical Report 54-70, April 1954.

(2) Warfield, C. N., "Tentative Tables for the Properties of the Upper Atmosphere", NACA TN 1200, January 1947.

(3) "Atmospheric Properties - Extreme Cold and Hot; Standard for Aeronautical Design", ANA Bulletin No. 421, 24 September 1953.

(4) "Equations, Tables and Charts for Compressible Flow", NACA Report 1135, 1953.

(5) Goldstein, Sydney, "Modern Developments in Fluid Dynamics", Vol. II, First Edition, Clarendon Press (Oxford), 1938, page 631.

(6) Korobkin, I., "Discussion of Laminar Heat Transfer Coefficients for Spheres and Cylinders in Incompressible Flow", Transaction of the ASME, Preprint.

(7) Gruenewald, K. H., and Lobb, R. K., "New Laminar and Turbulent Heat Transfer Data Applicable to Practical Body Shapes for High Mach Number Flight", Third Navy Symposium on Aeroballistics, Technical Session IV, US Navy Bureau of Ordnance, 20 October 1954.

(8) "Manual of the ICAO Standard Atmosphere", NACA TN 3182, May 1954.

[redacted]

SECTION 2.0

PROPERTIES OF MATERIALS

By J. Padlog

TABLE OF CONTENTS

SECTION 2.0

PROPERTIES OF MATERIALS

2.1 GENERAL

This section contains a collection of mechanical, thermal, and physical properties of materials having the potential for structural use in future high-speed aircraft. The data include properties of metallic and nonmetallic airframe materials, insulating materials, and cooling liquids. These have been selected to satisfy, so far as possible, the requirements of aircraft operating at speeds up to Mach 20. Materials are considered in this section only if available commercially, and if a useful amount of design information exists. Limited data on other materials having significant possibilities for high-speed airframes, but at present only in the experimental stage, will be found in Part II.

The information in this section is considered necessary for the stress and thermal analyses of structures exposed to aerodynamic heating and for the design of insulating and cooling systems for structures protected from these high-speed effects.

Material properties are taken from reports of various universities and government and military establishments, from brochures and reports of material manufacturers, from publications of various engineering institutions, from standard text books, and from tests conducted by Bell Aircraft Corporation in connection with other projects. A complete list of references is presented in Part II.

2.2 STRUCTURAL

In Figures 2.2-1 through 2.2-52, properties are presented for the following structural materials, arranged in the order shown:

2024-T3	Aluminum Alloy - clad
7075-T6	Aluminum Alloy
FSI-H24	Magnesium Alloy
RC C-110M	Titanium Alloy
Alloy Steel	200,000 psi Tensile Strength
18-8, 3/4-hard	Stainless Steel
17-7PH	Stainless Steel
Inconel X	Nickel Base Alloy
L-605	Cobalt Base Alloy
Molybdenum	Alloys
Alite 212	Aluminum Oxide

Among the properties of structural materials, emphasis has been placed on sheet and extruded stock, since these predominate in stressed skin construction. Higher strengths can generally be achieved in bar or forged materials, so that values for sheet may be conservatively used for all cases if more complete data are unavailable.

As higher temperatures are reached, particularly for the newer materials, available data become meager and show increased scatter. This scatter is due to the additional variables introduced

at elevated temperatures. Among these variables are (1) test temperature and rate of loading, (2) previous temperature-load history, (3) relationship between test temperature and heat treating temperature, (4) differences in techniques of elevated temperature testing, and (5) differences in manufacturing techniques and chemical composition for the new materials.

Some reduction in scatter has been obtained by comparing properties nondimensionally in terms of room-temperature properties, and drawing a conservative, average curve through the points so obtained. This curve has then been reduced, where possible, to 90% probability values by using "B" value room temperature properties from ANC-5. Where no differentiation between "A" and "B" values is given in ANC-5, the single value has been used.

For each structural material, mechanical property curves are presented against temperature for yield and ultimate strengths, elastic moduli and elongation, physical properties, coefficient of expansion, and specific heat and thermal conductivity. Stress-strain curves are given at various temperatures, and the graphs are presented in carpet form to simplify interpolation. Tangent and secant moduli curves plotted against stress at various temperatures have been prepared from the stress-strain curves. Where data are available, creep and stress-rupture information is given for each material on a master creep curve in which time and temperature effects are combined by using the Larson-Miller parameter. Generally, creep data are available only for comparatively large total strains. The use of the Larson-Miller parameter permits creep data to be derived, for small total strains, from the short-time stress-strain curves. For intermediate strain values, the master creep curves have been interpolated.

When materials are heat-treated to develop required mechanical strengths, the use of such materials at temperatures above that used for heat treatment produces annealing, and a reduction of properties at all temperatures. The extent of this annealing is dependent upon the temperature at which the material is used and the total exposure time at this temperature. Generally, it is not efficient to use a material in such a condition because, at such temperatures, the strength-density ratio can be exceeded by higher temperature materials. When temperatures exceed 1300°F, however, the range of available materials becomes very limited and it may be necessary to work beyond the heat-treating temperatures. For this reason, curves are included to show the effect of exposure to 1600°F for two hours on the mechanical properties of Inconel X.

Presented in Part II is general information on various structural materials, such as heat-treatment, temperature, resistance to oxidation, cost, availability, and ease of fabrication.

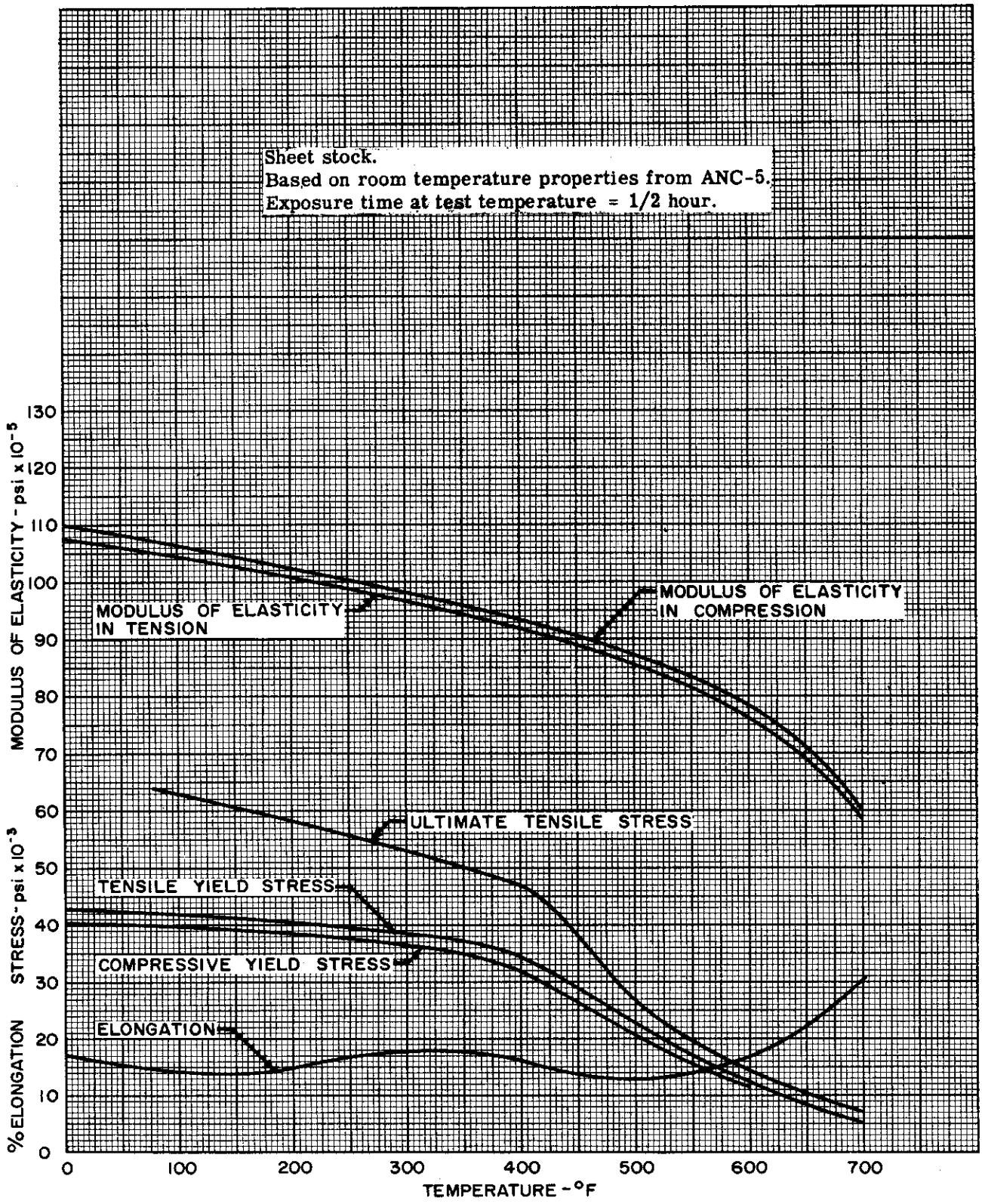

Figure 2.2-1. 2024-T3 Aluminum Alloy Clad Sheet — Mechanical Properties

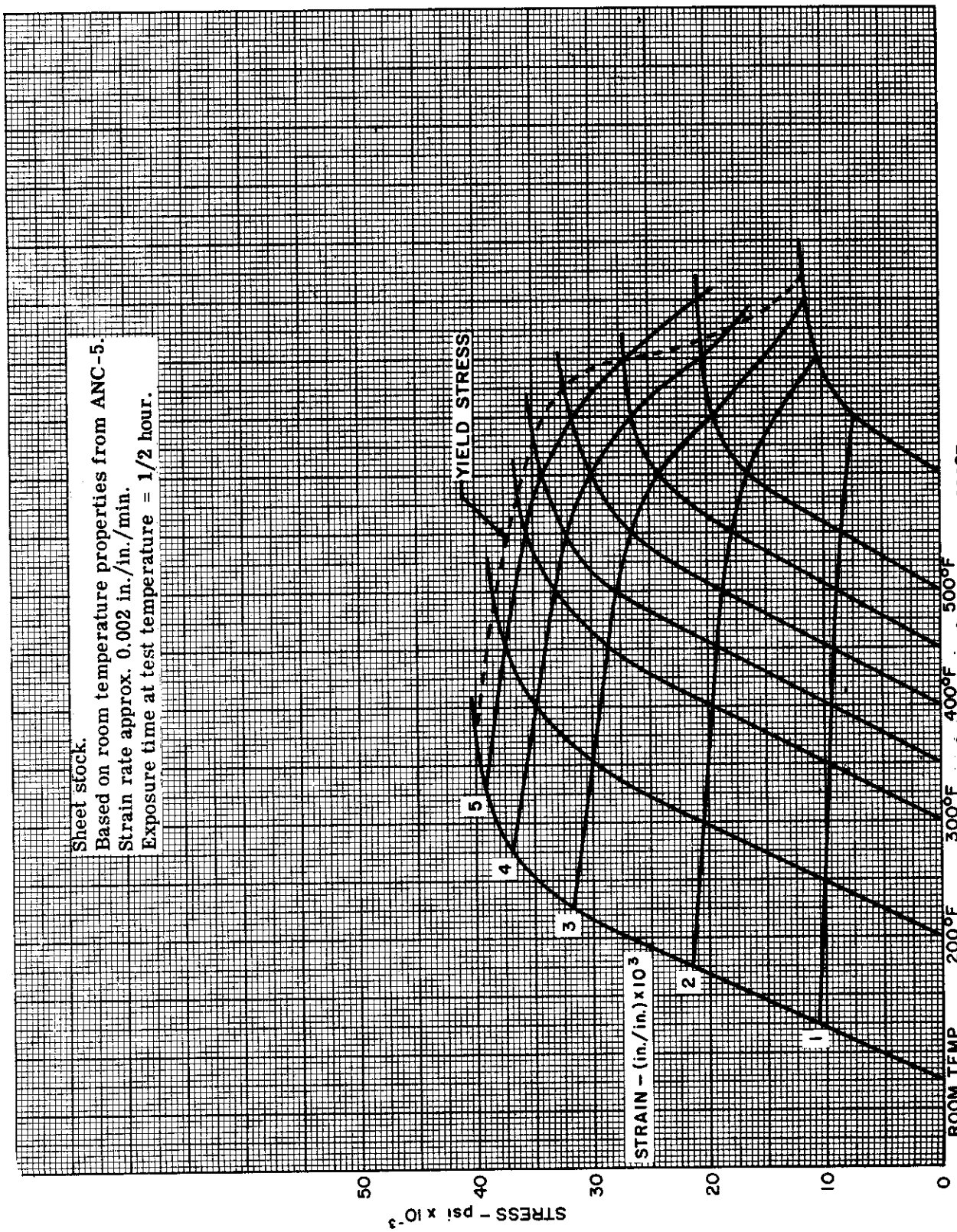

Figure 2.2-2. 2024-T3 Aluminum Alloy Clad Sheet — Short-Time Compressive Stress-Strain Curves at Elevated Temperatures

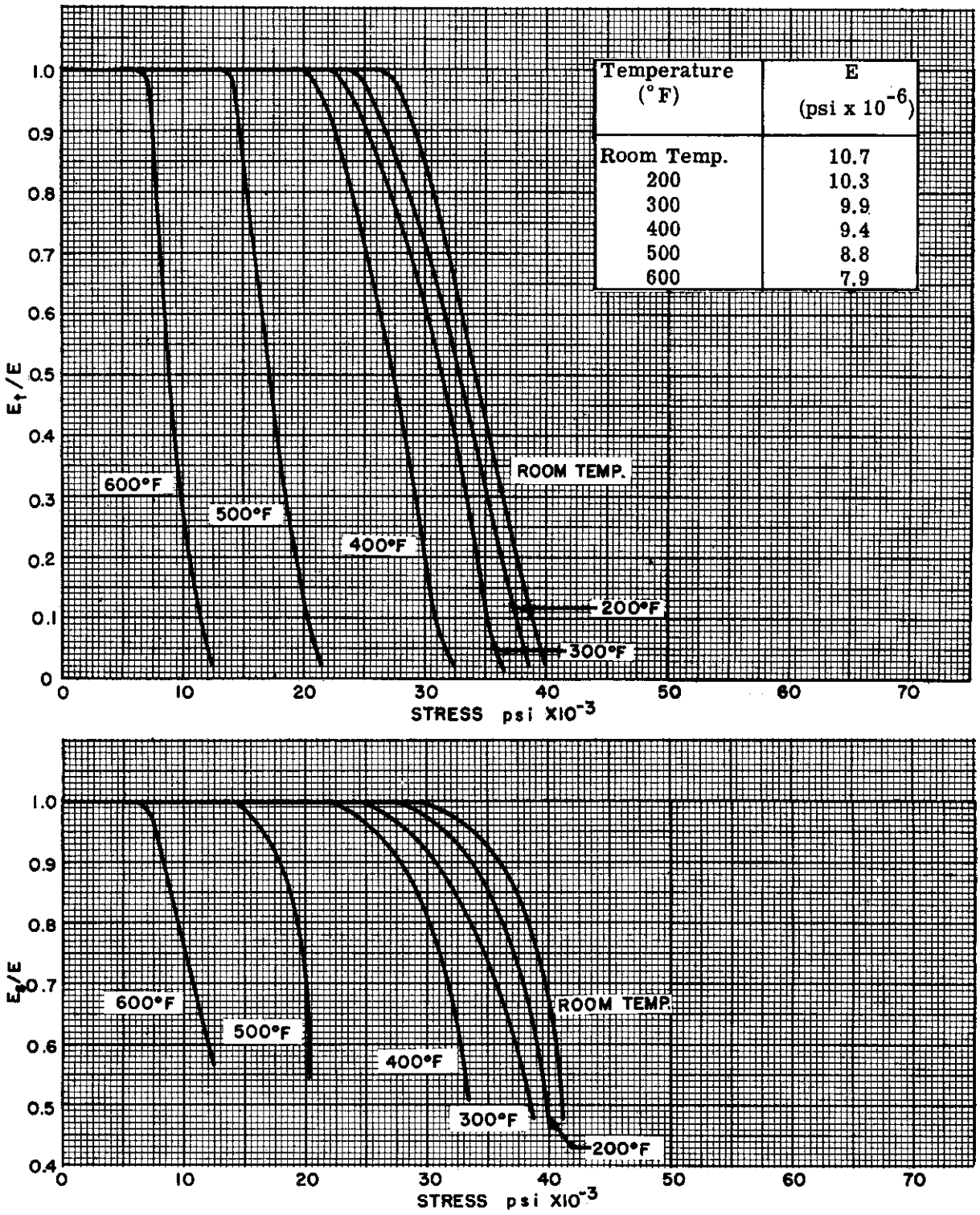

Figure 2.2-3. 2024-T3 Aluminum Alloy Clad Sheet — Tangent and Secant Moduli in Compression

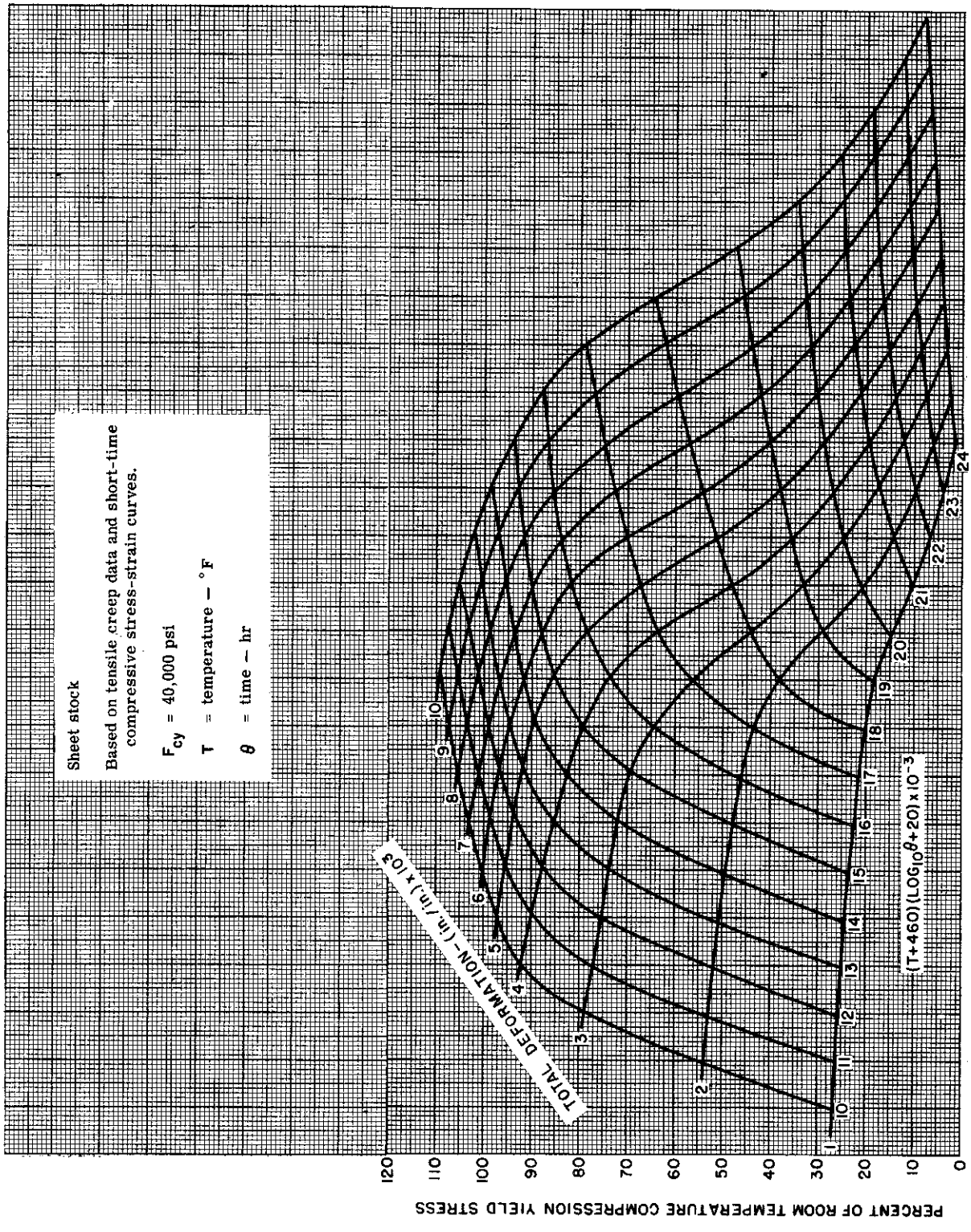

Figure 2.2-4. 2024-T3 Aluminum Alloy Clad Sheet — Master Creep Curves

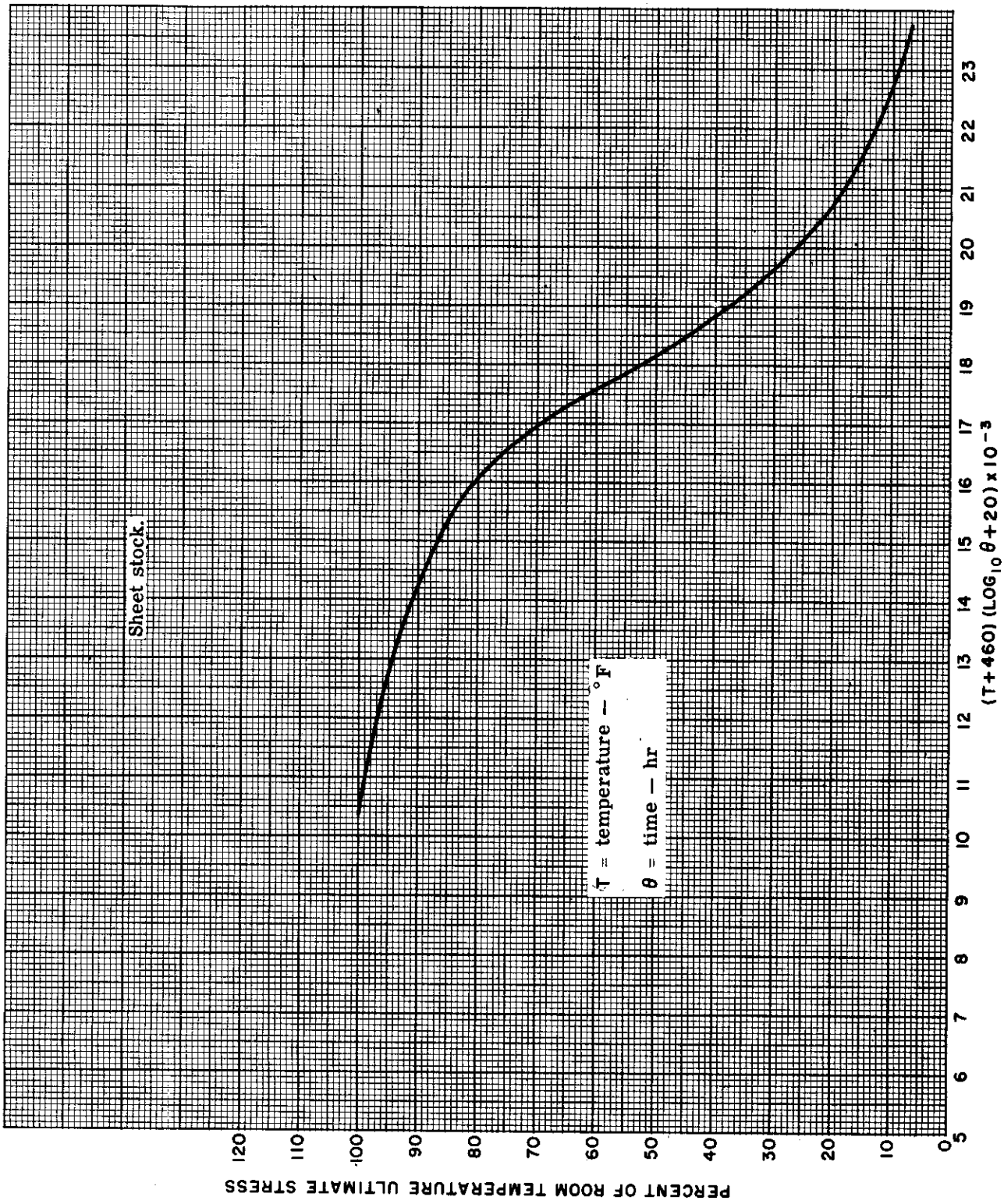

Figure 2.2-5. 2024-T3 Aluminum Alloy Clad Sheet — Master Rupture Curve

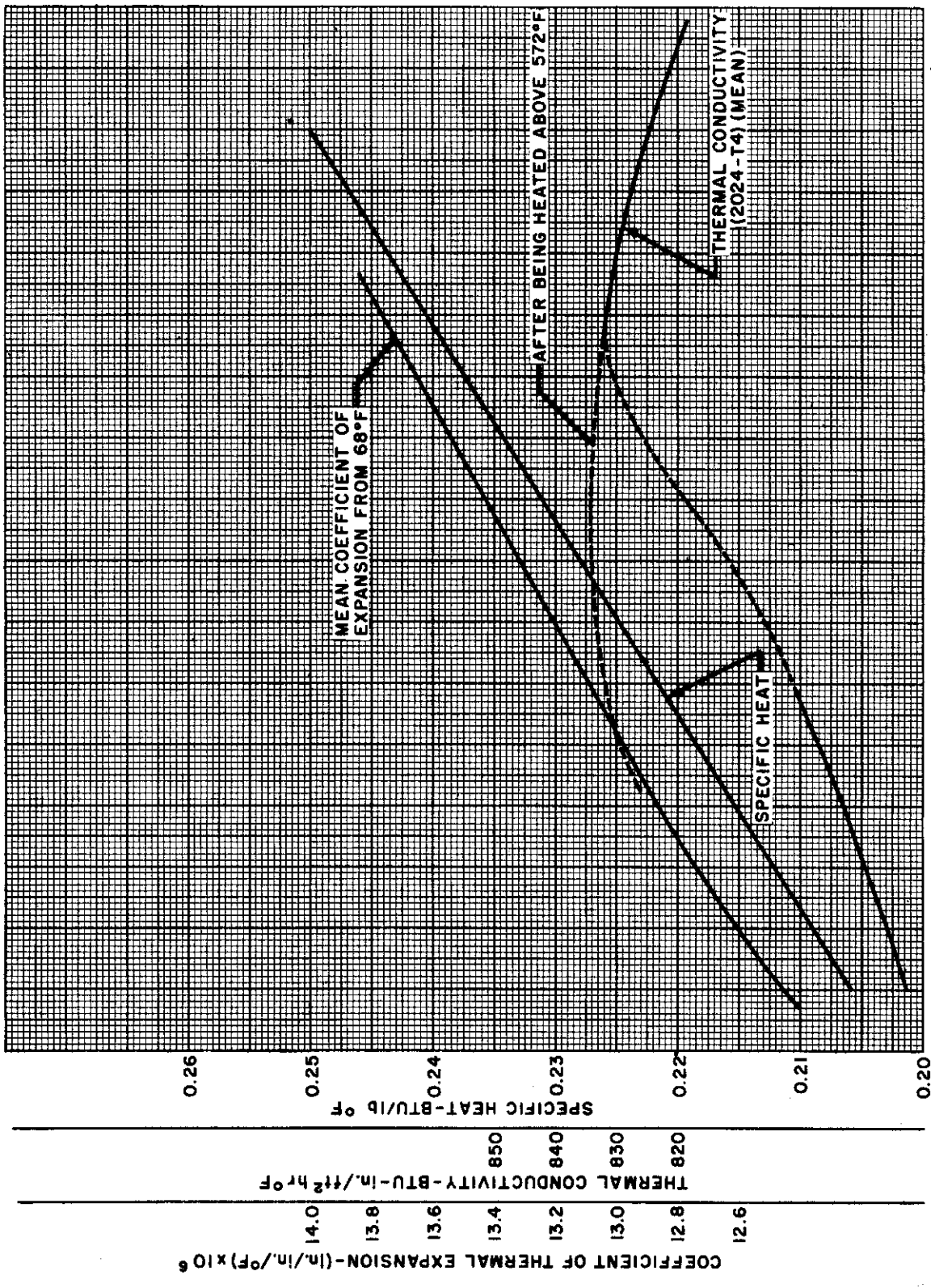

Figure 2.2-6. 2024-T3 Aluminum Alloy Clad Sheet — Thermal Properties

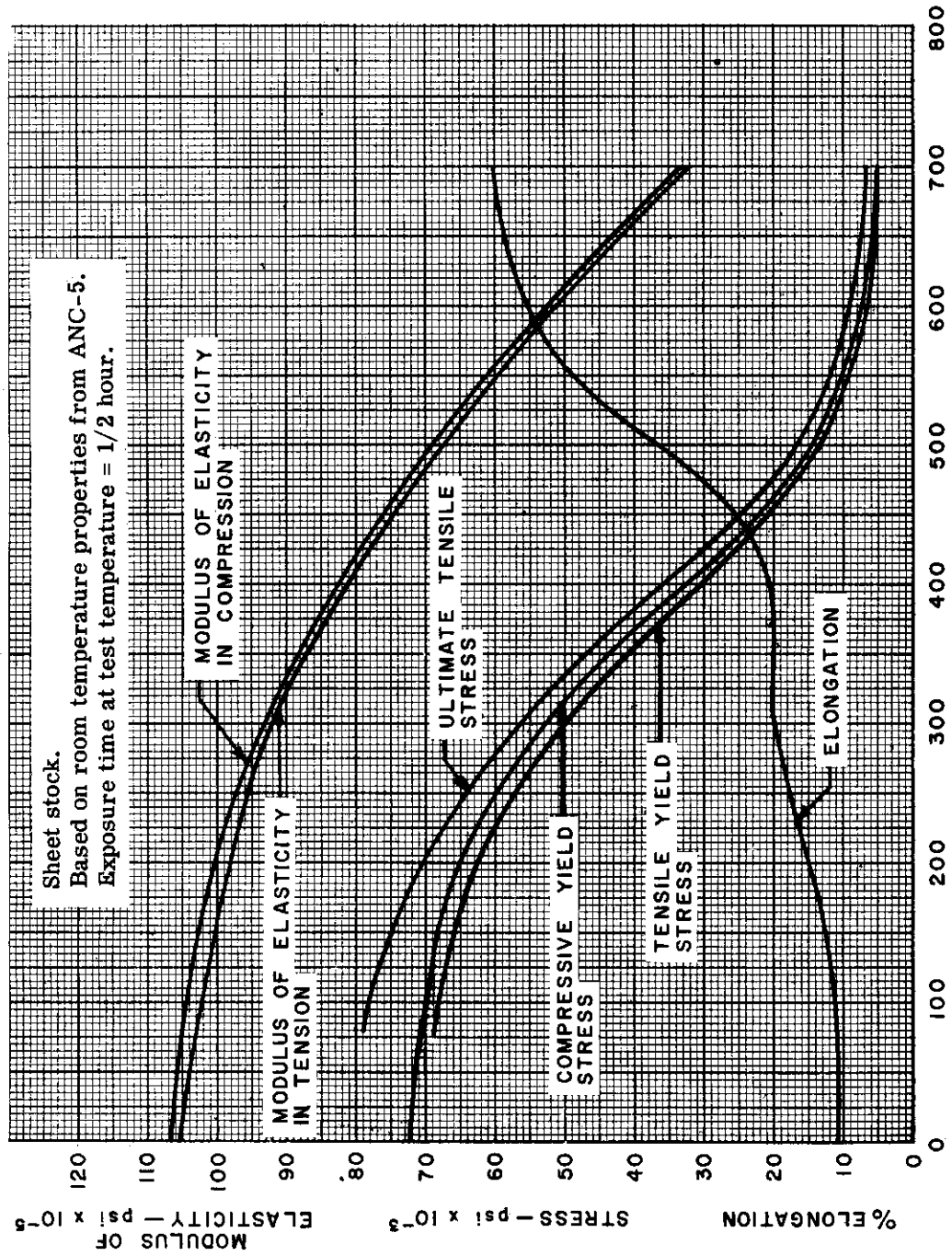

Figure 2.2-7. 7075-T6 Aluminum Alloy — Mechanical Properties

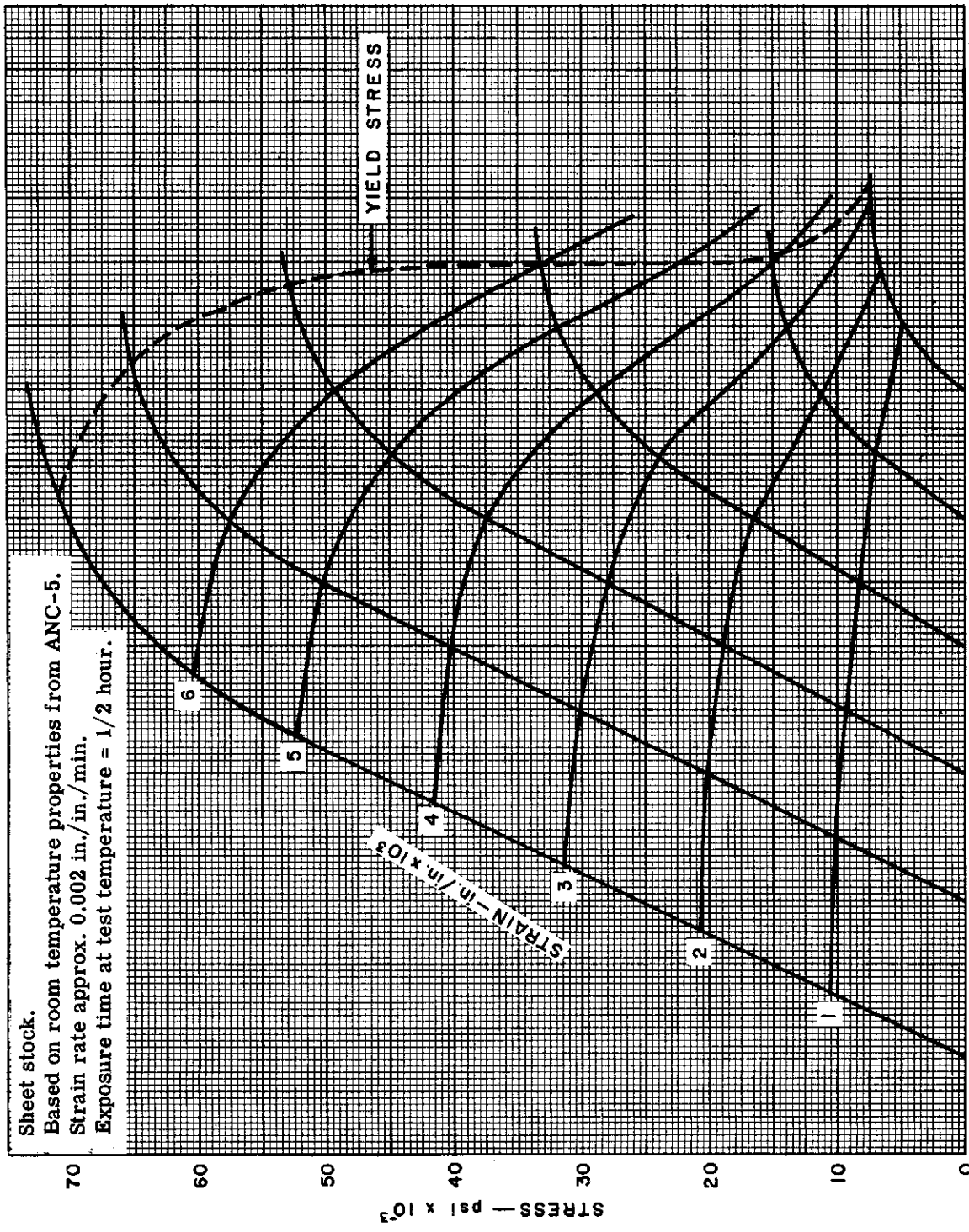

Figure 2.2-8. 7075-T6 Aluminum Alloy — Compressive Stress-Strain Curves

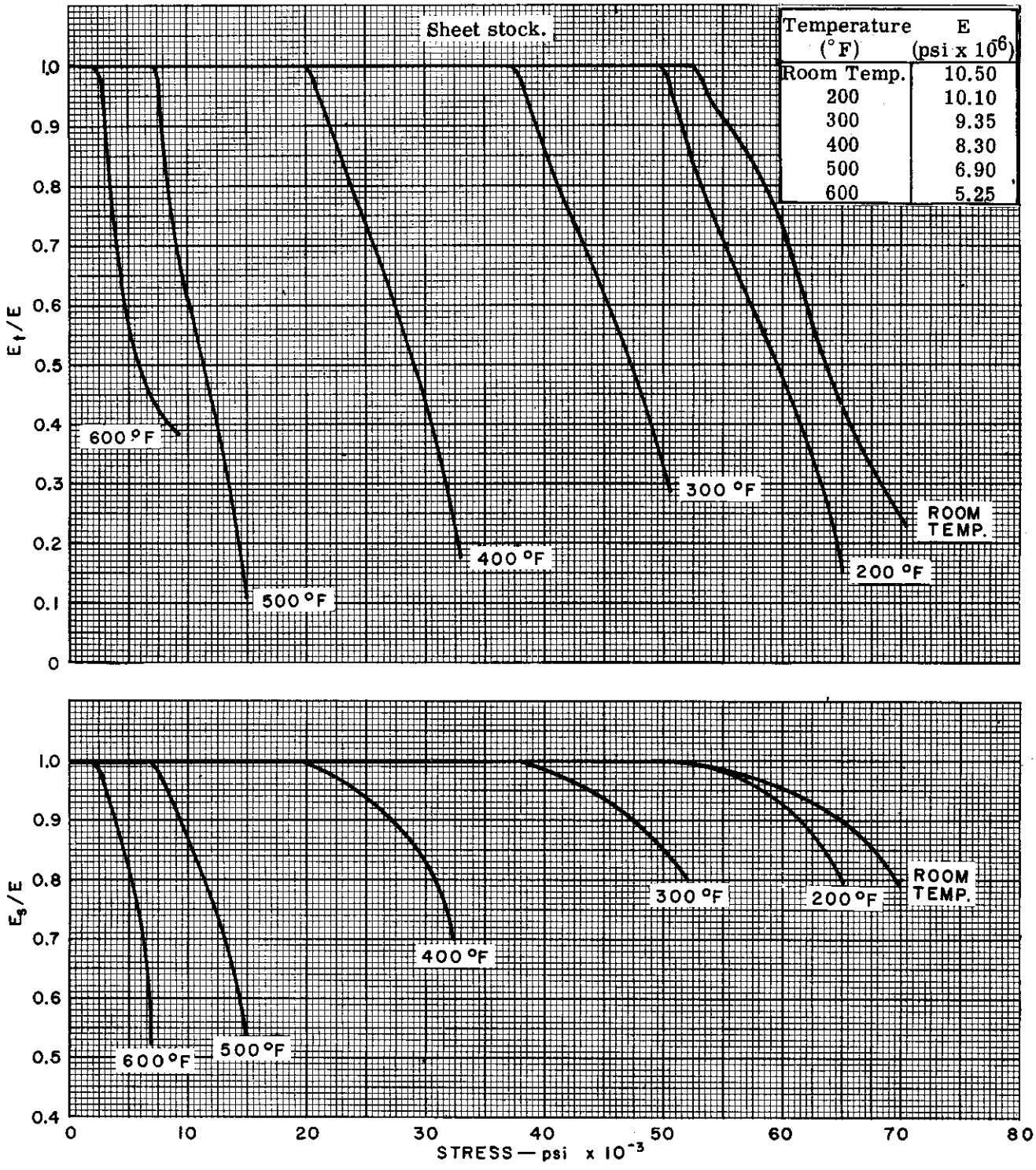

Figure 2.2-9. 7075-T6 Aluminum Alloy — Tangent and Secant Moduli in Compression

[redacted]

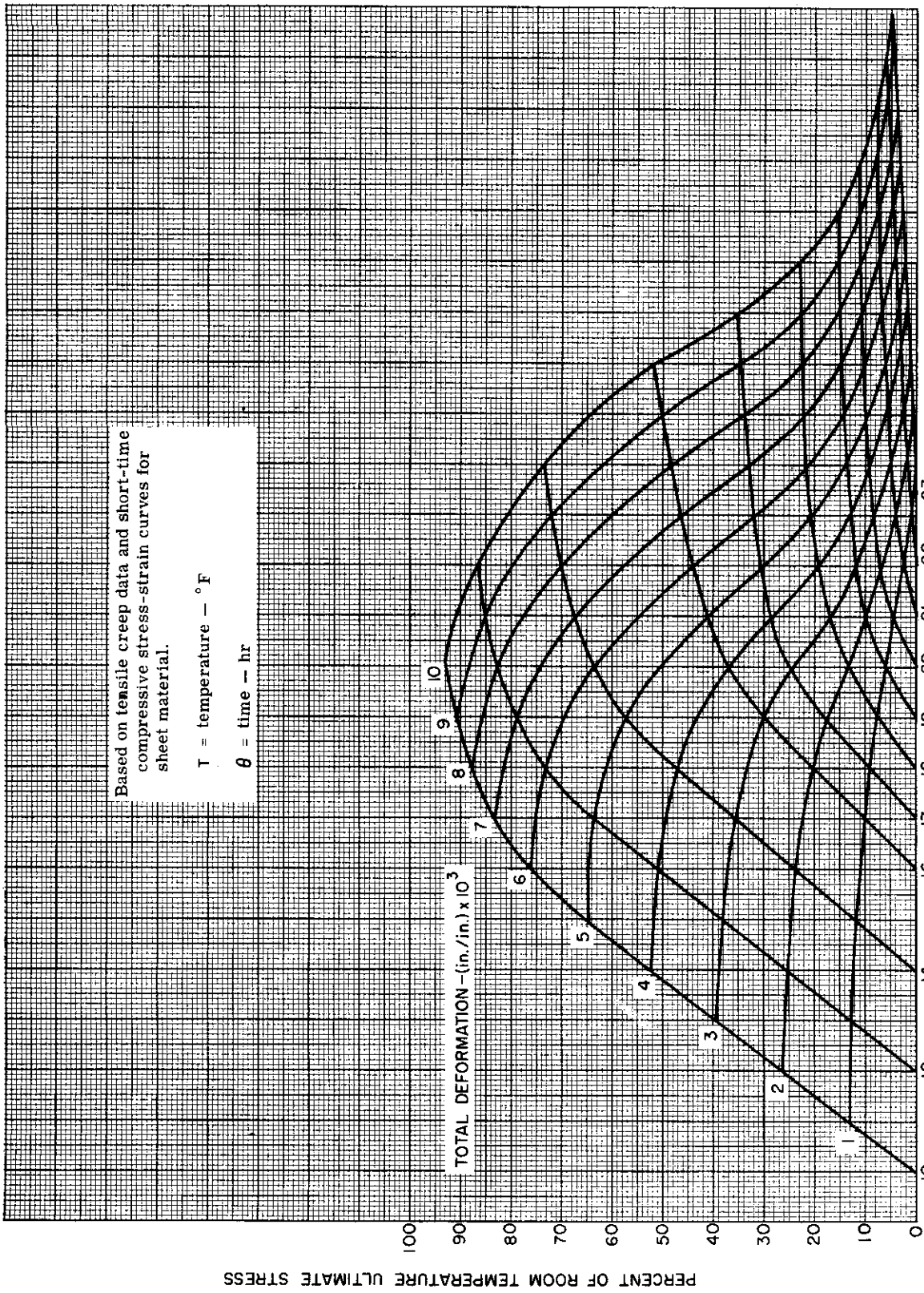

Figure 2.2-10. 7075-T6 Aluminum Alloy — Master Creep Curve

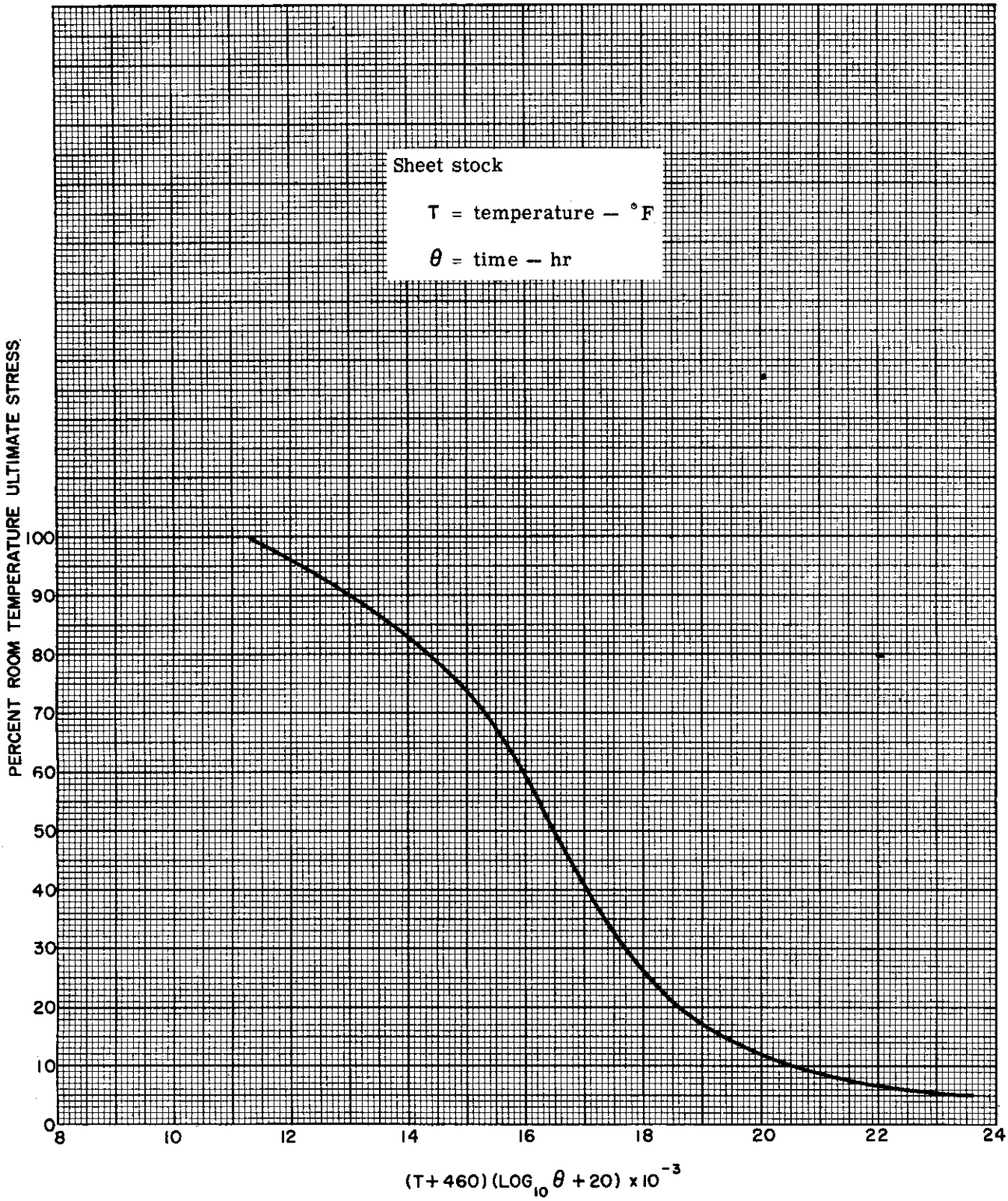

Figure 2.2-11. 7075-T6 Aluminum Alloy — Master Rupture Curve

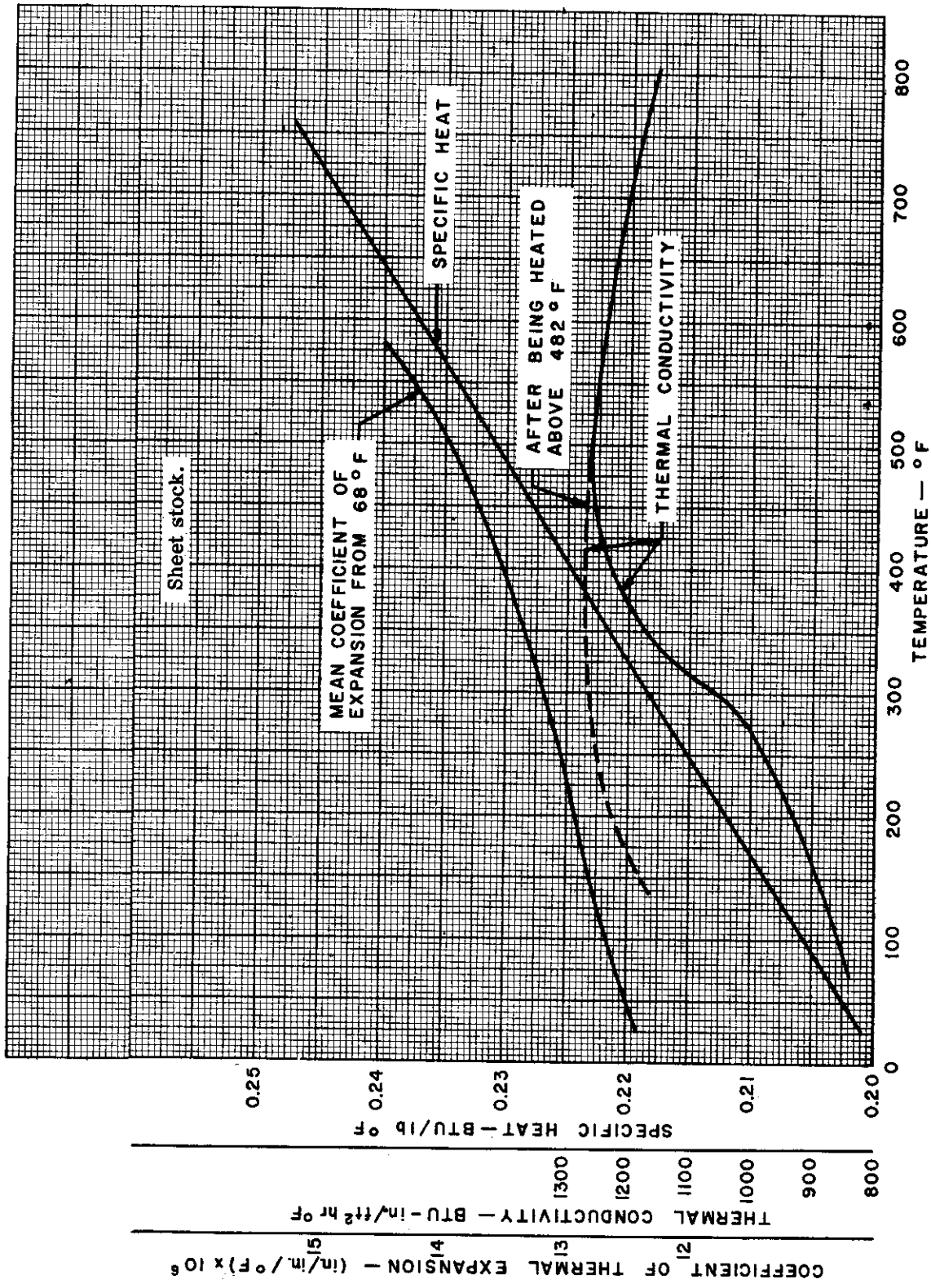

Figure 2.2-12. 7075-T6 Aluminum Alloy — Thermal Properties

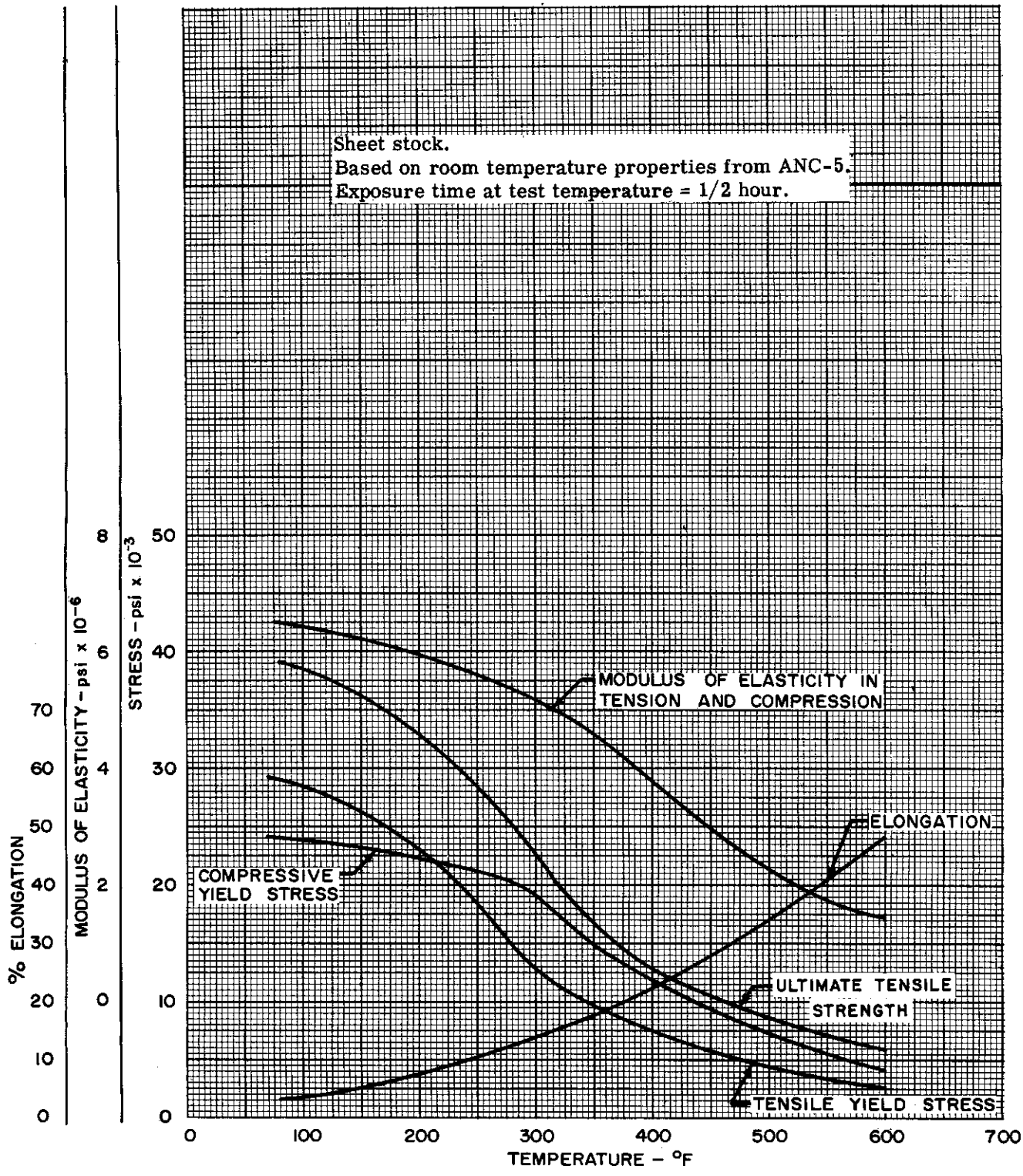

Figure 2.2-13. FSI-H24 Magnesium Alloy — Mechanical Properties

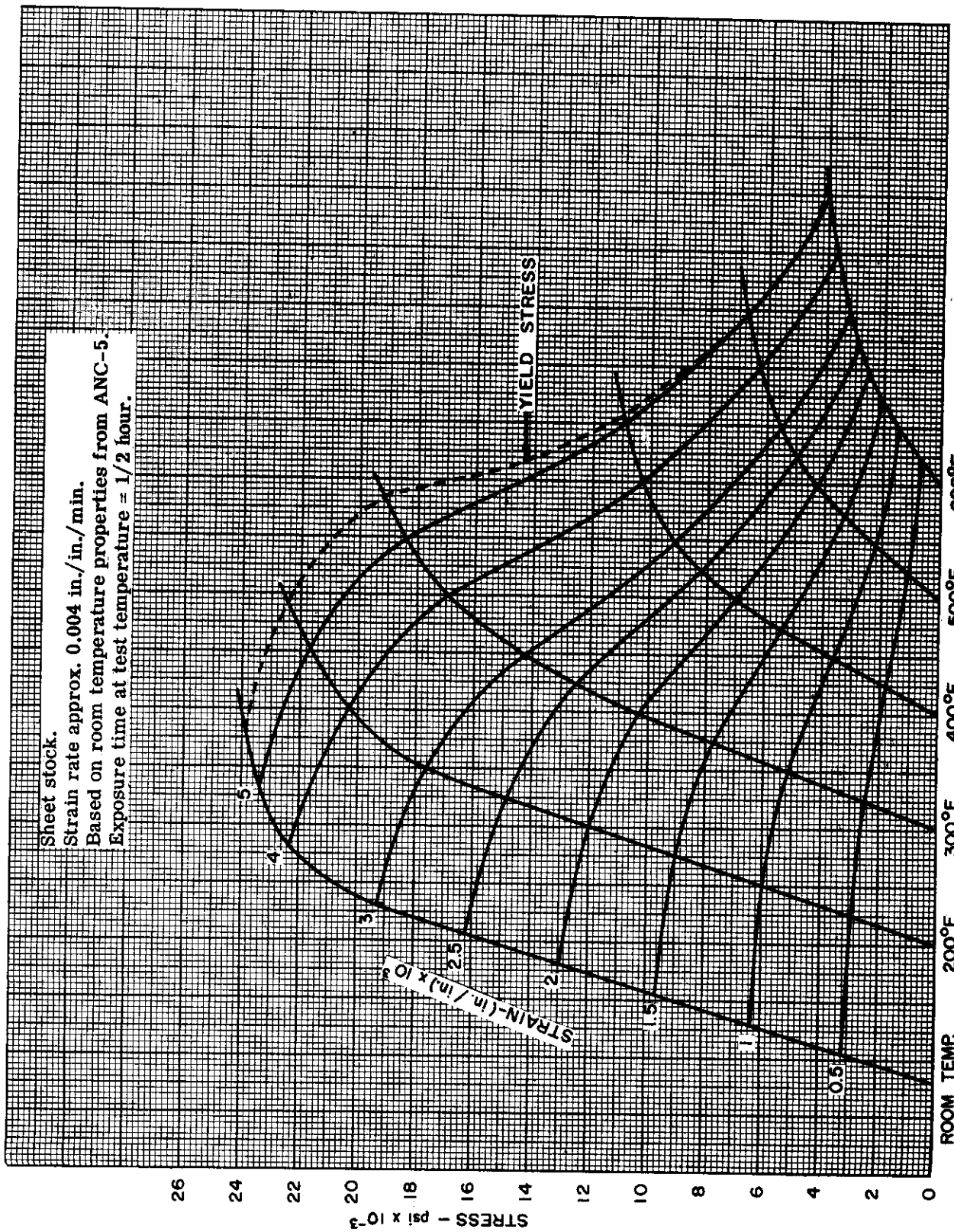

Figure 2.2-14. FSI-H24 Magnesium Alloy — Compressive Stress-Strain Curves

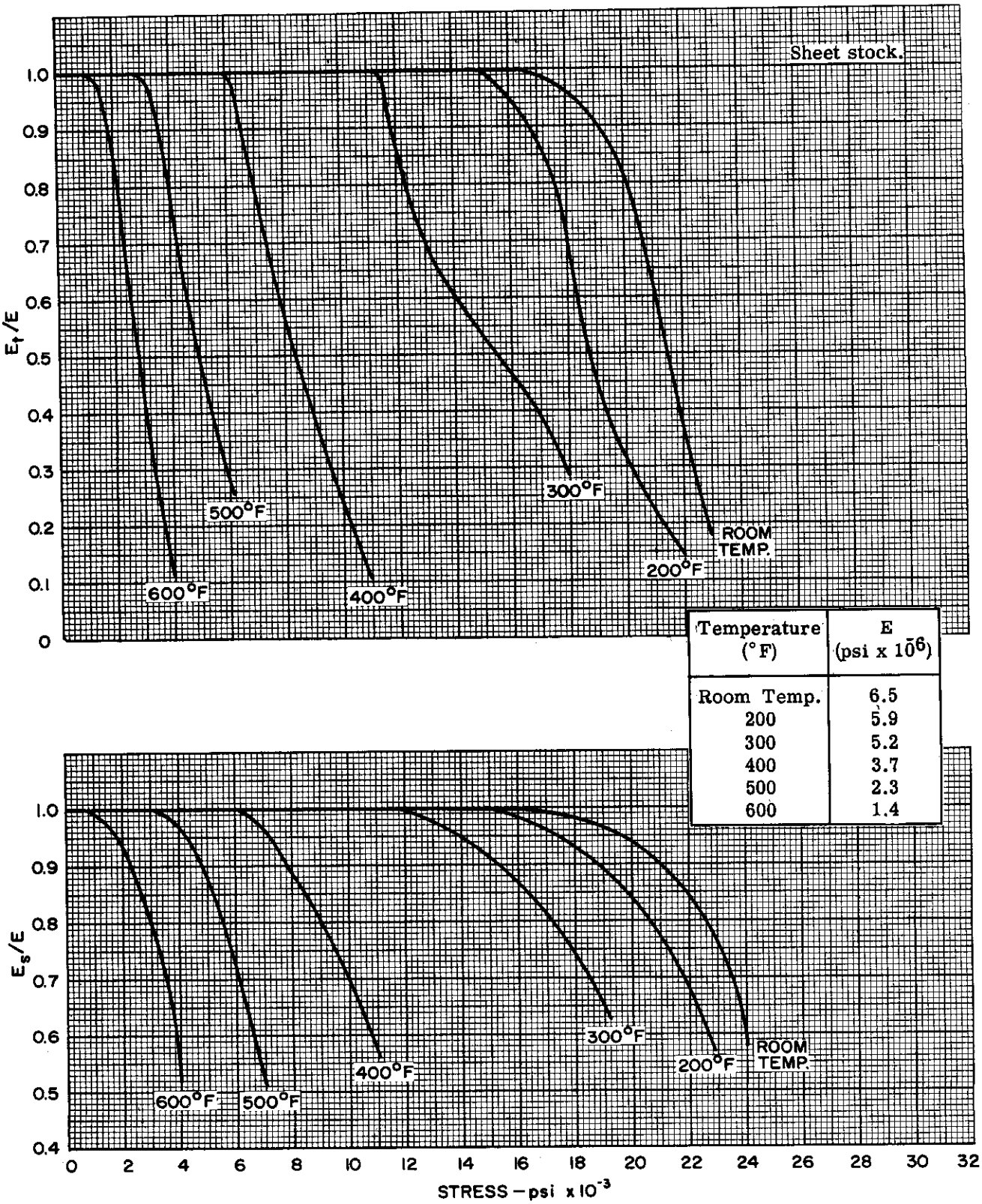

Temperature (°F)	E (psi x 10^6)
Room Temp.	6.5
200	5.9
300	5.2
400	3.7
500	2.3
600	1.4

Figure 2.2-15. FSI-H24 Magnesium Alloy — Tangent and Secant Moduli in Compression

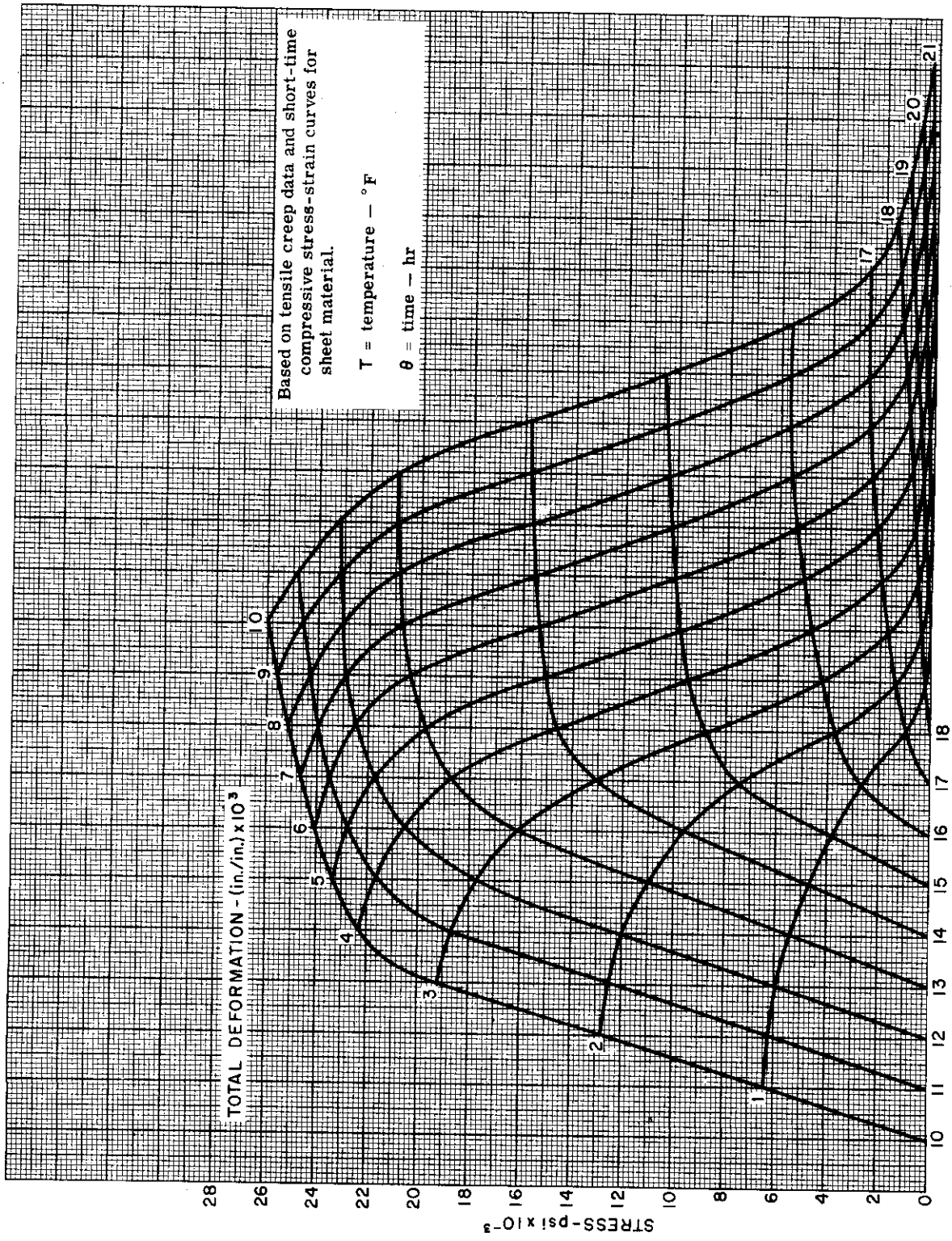

Figure 2.2-16. FSI-H24 Magnesium Alloy — Master Creep Curves

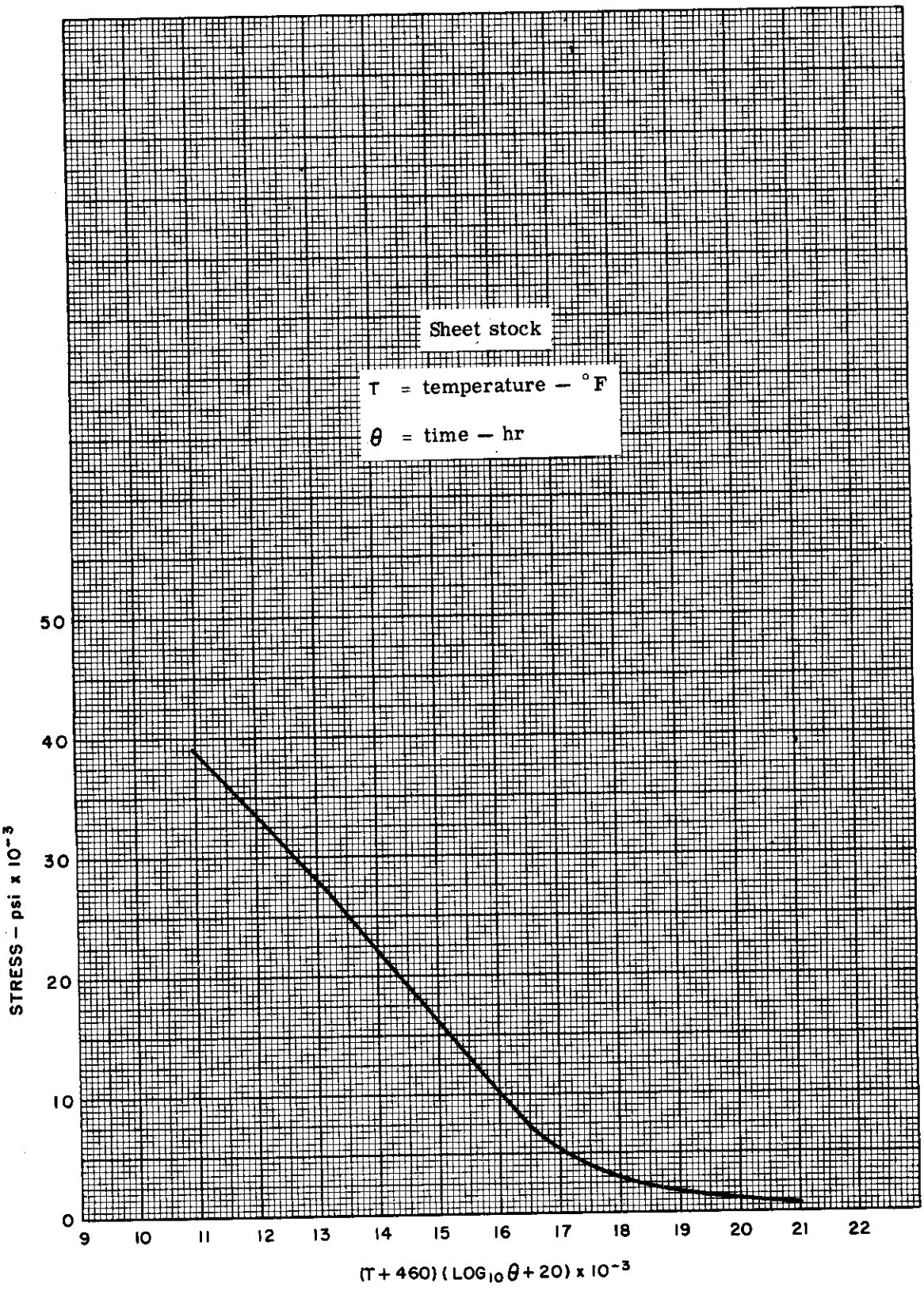

Figure 2.2-17. FSI-H24 Magnesium Alloy — Master Rupture Curve

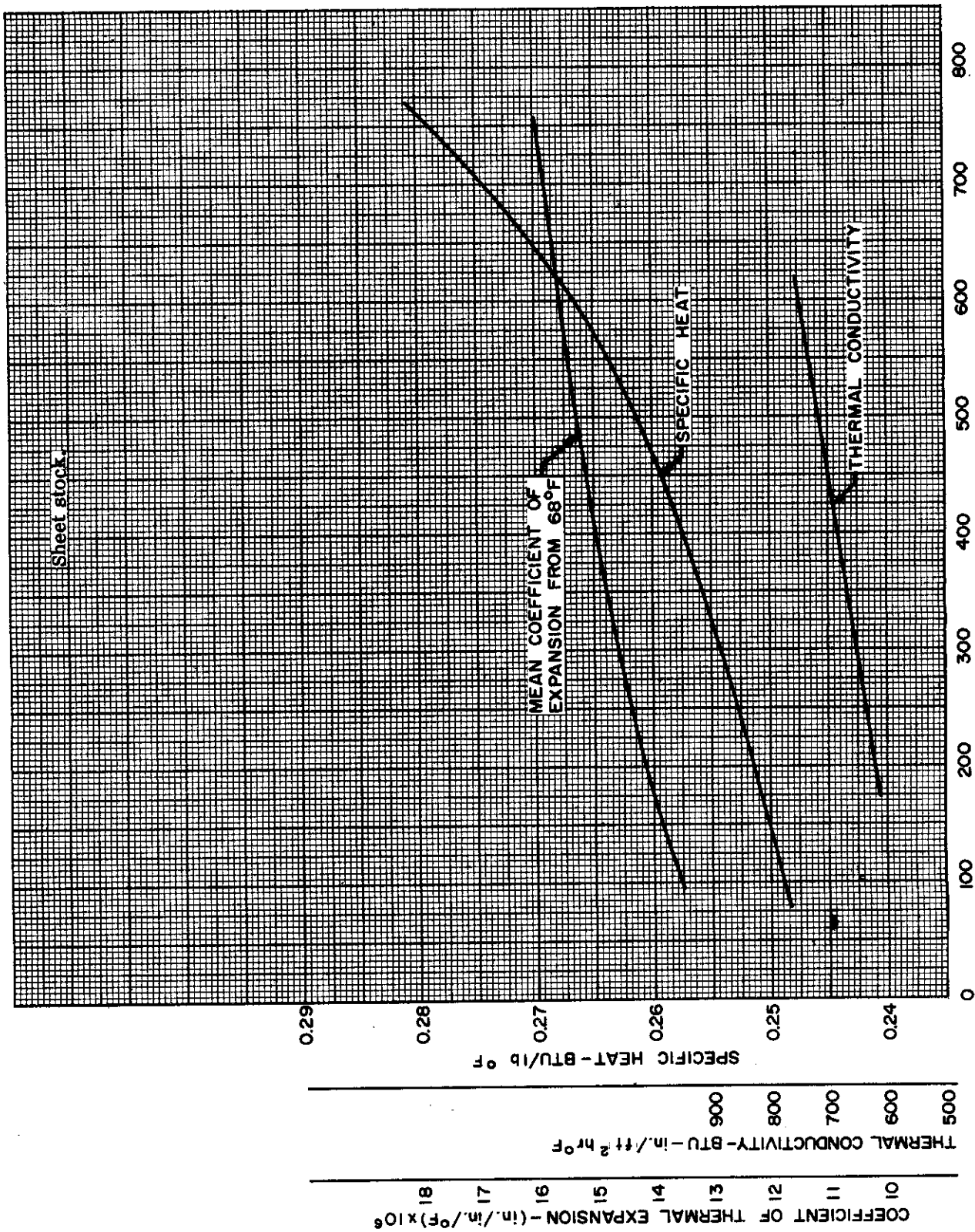

Figure 2.2-18. FSI-H24 Magnesium Alloy — Thermal Properties

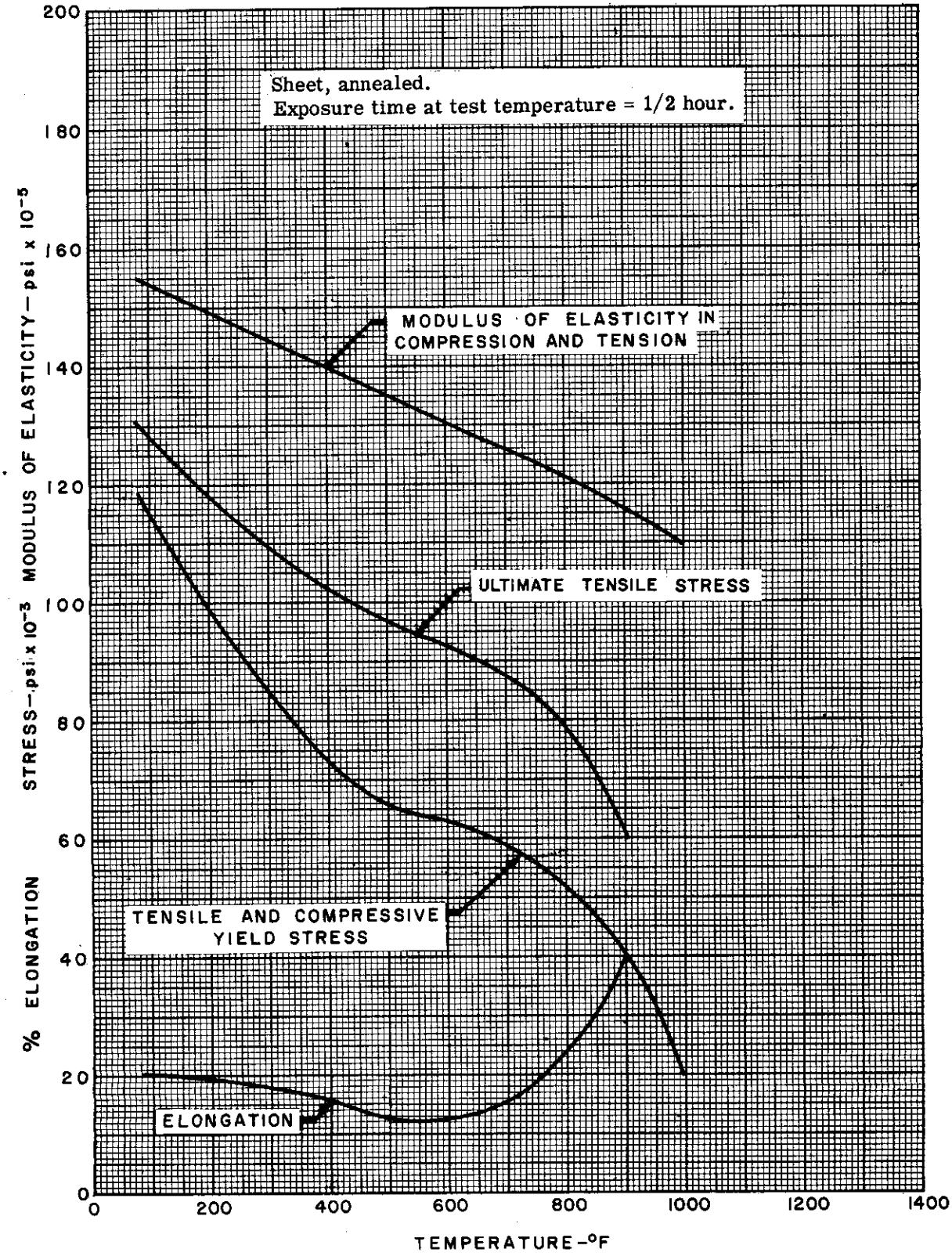

Figure 2.2-19. RC C-110M Titanium Alloy — Mechanical Properties

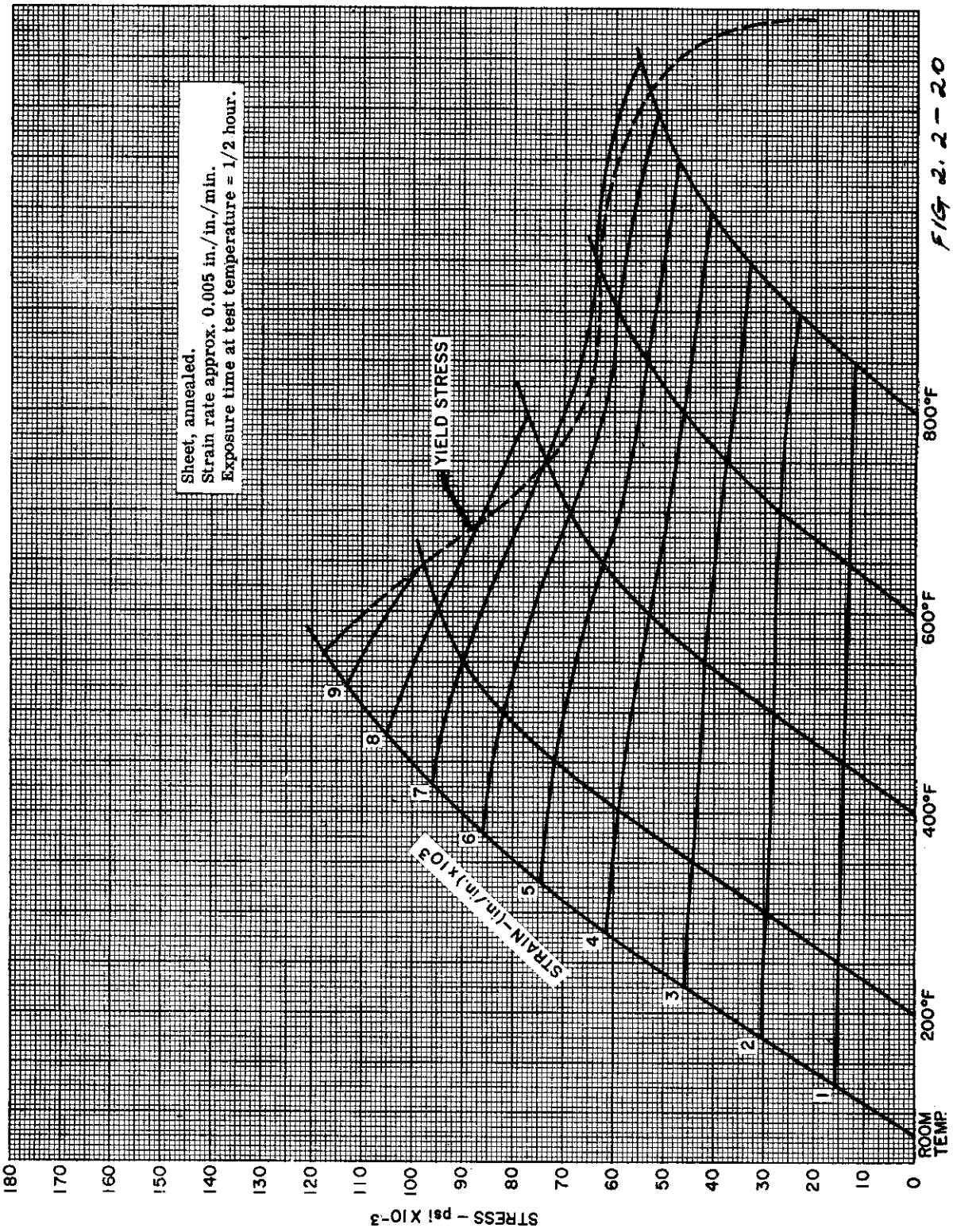

Figure 2.2-20. RC C-110M Titanium Alloy — Compressive Stress-Strain Curves

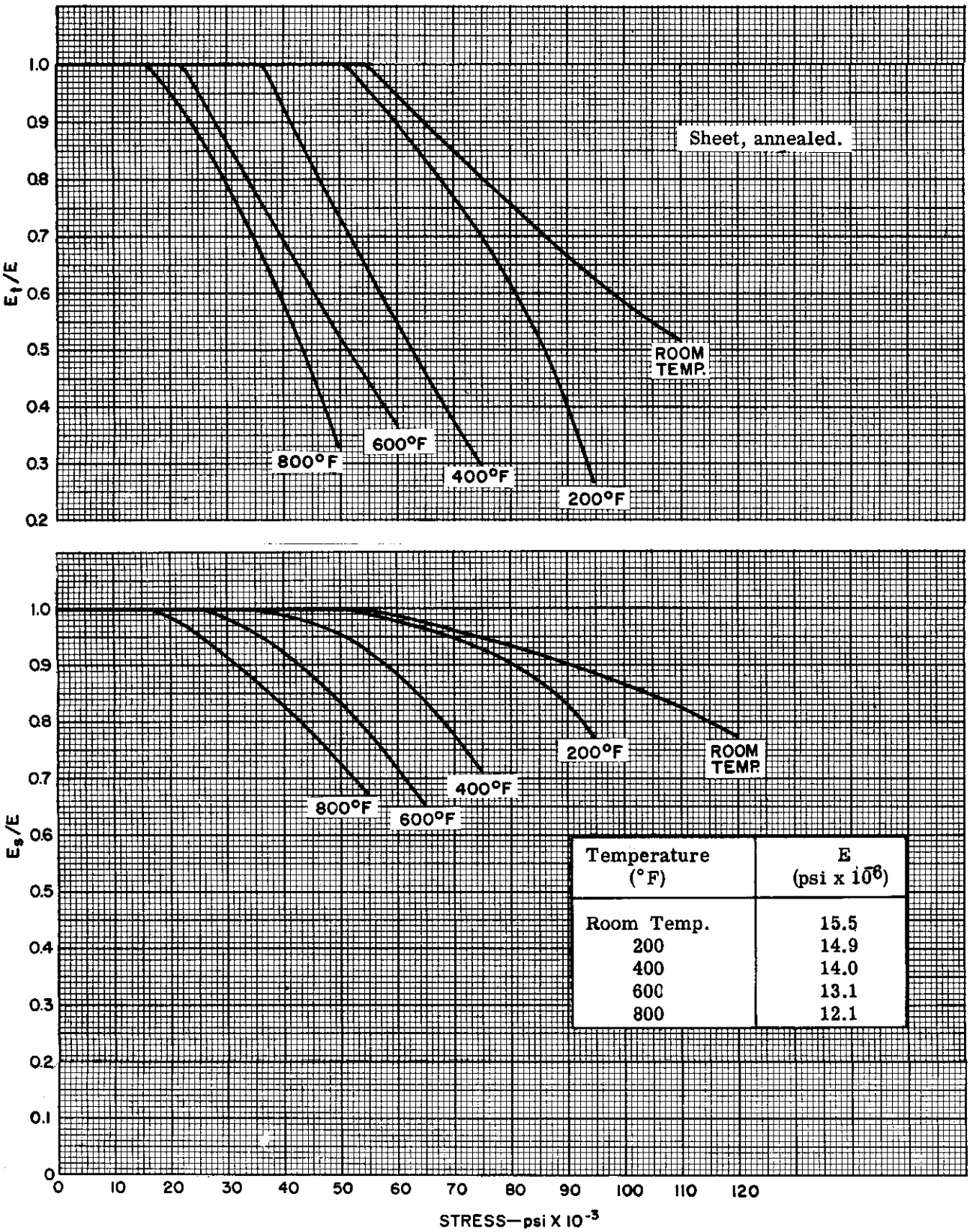

Temperature (°F)	E (psi x 10^6)
Room Temp.	15.5
200	14.9
400	14.0
600	13.1
800	12.1

Figure 2.2-21. RC C-110M Titanium — Target and Secant Moduli in Compression

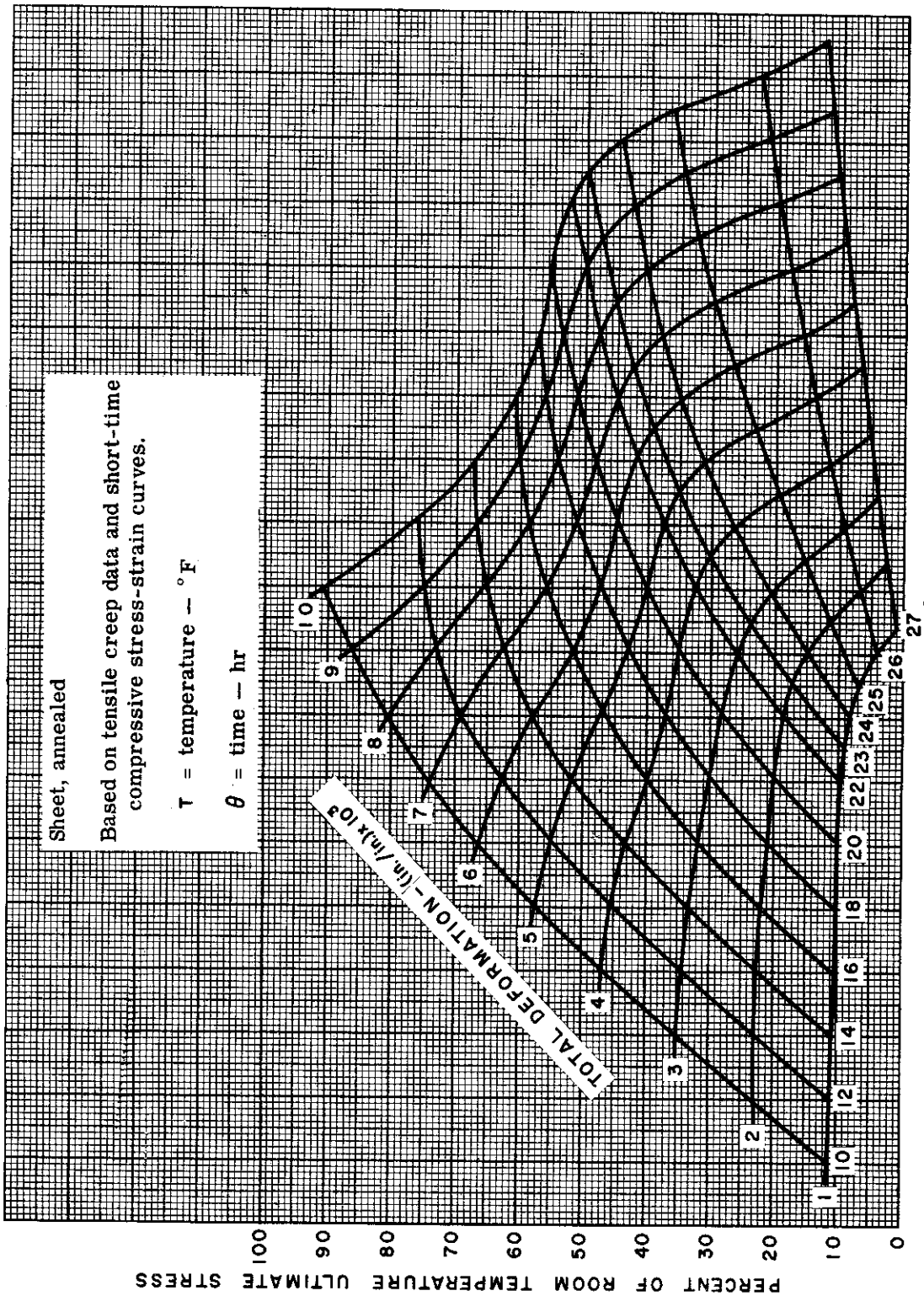

Figure 2-2-22. RC C-110M Titanium Alloy — Master Creep Curves

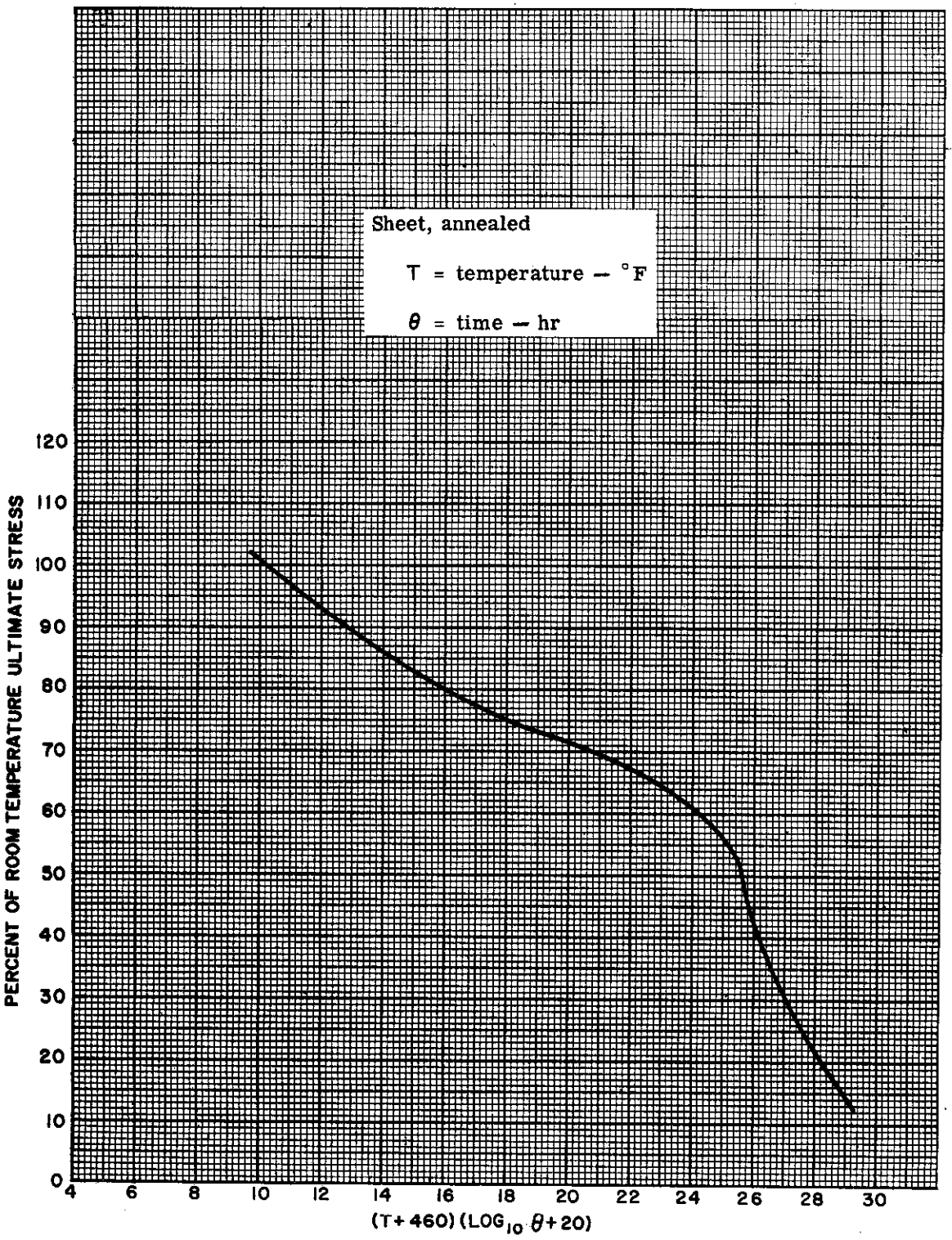

Figure 2.2-23. RC C-110M Titanium Alloy — Master Rupture Curve

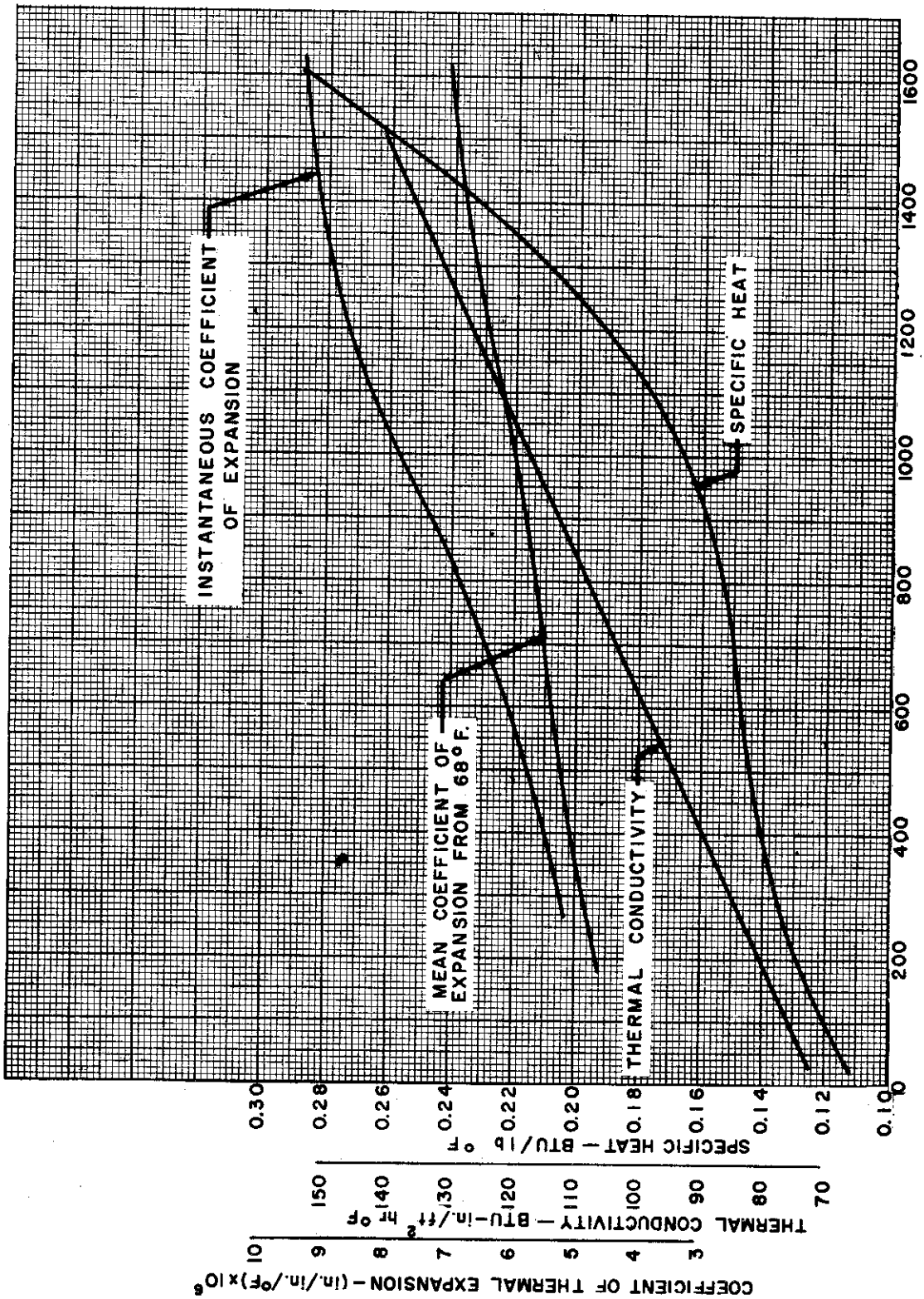

Figure 2.2-24. RC C-110M Titanium Alloy — Thermal Properties

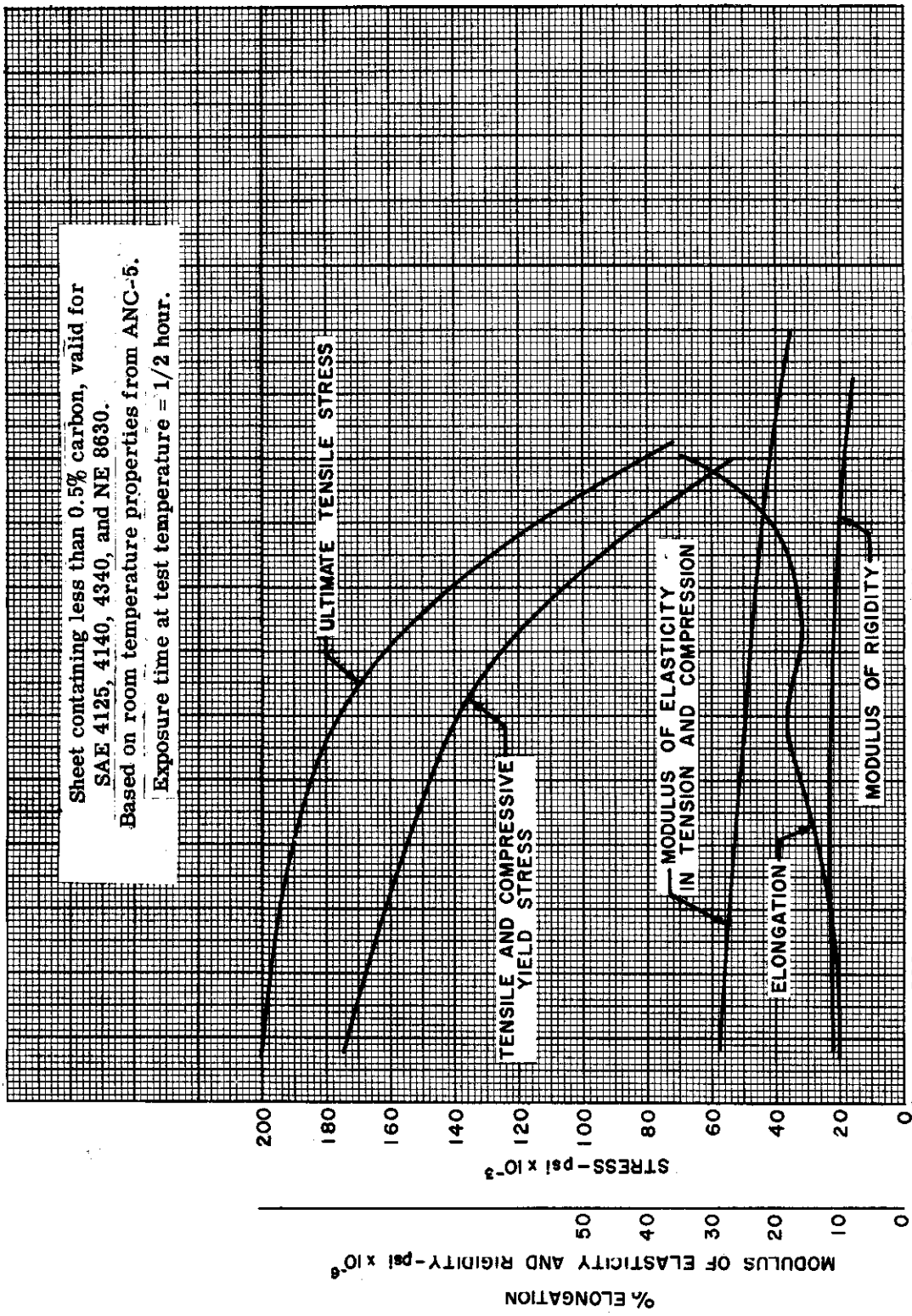

Figure 2.2-25. Alloy Steel – Heat-Treated to 200,000 psi – Mechanical Properties

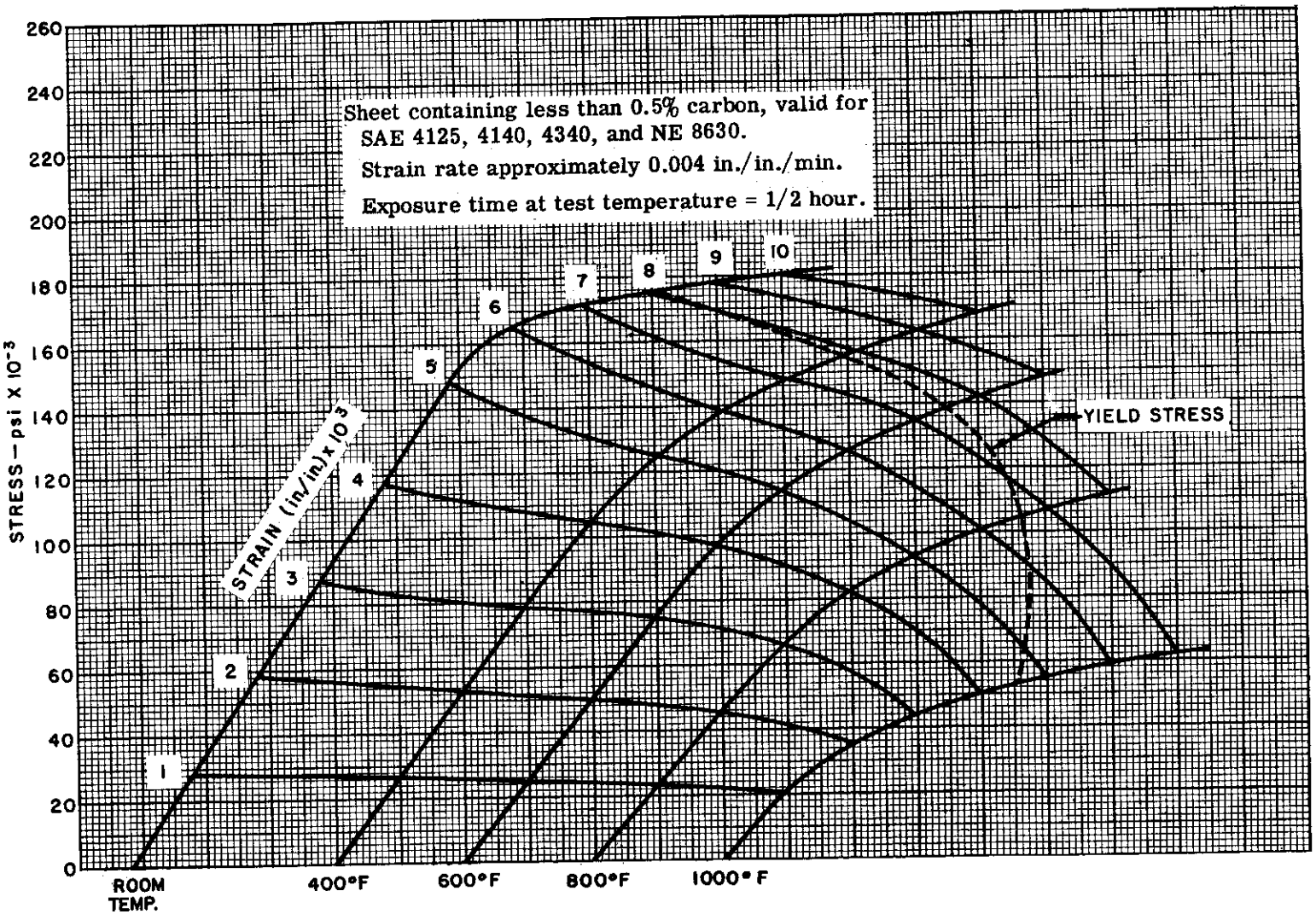

Figure 2.2-26. Alloy Steel -- Heat-Treated to 200,000 psi -- Compressive Stress-Strain Curves

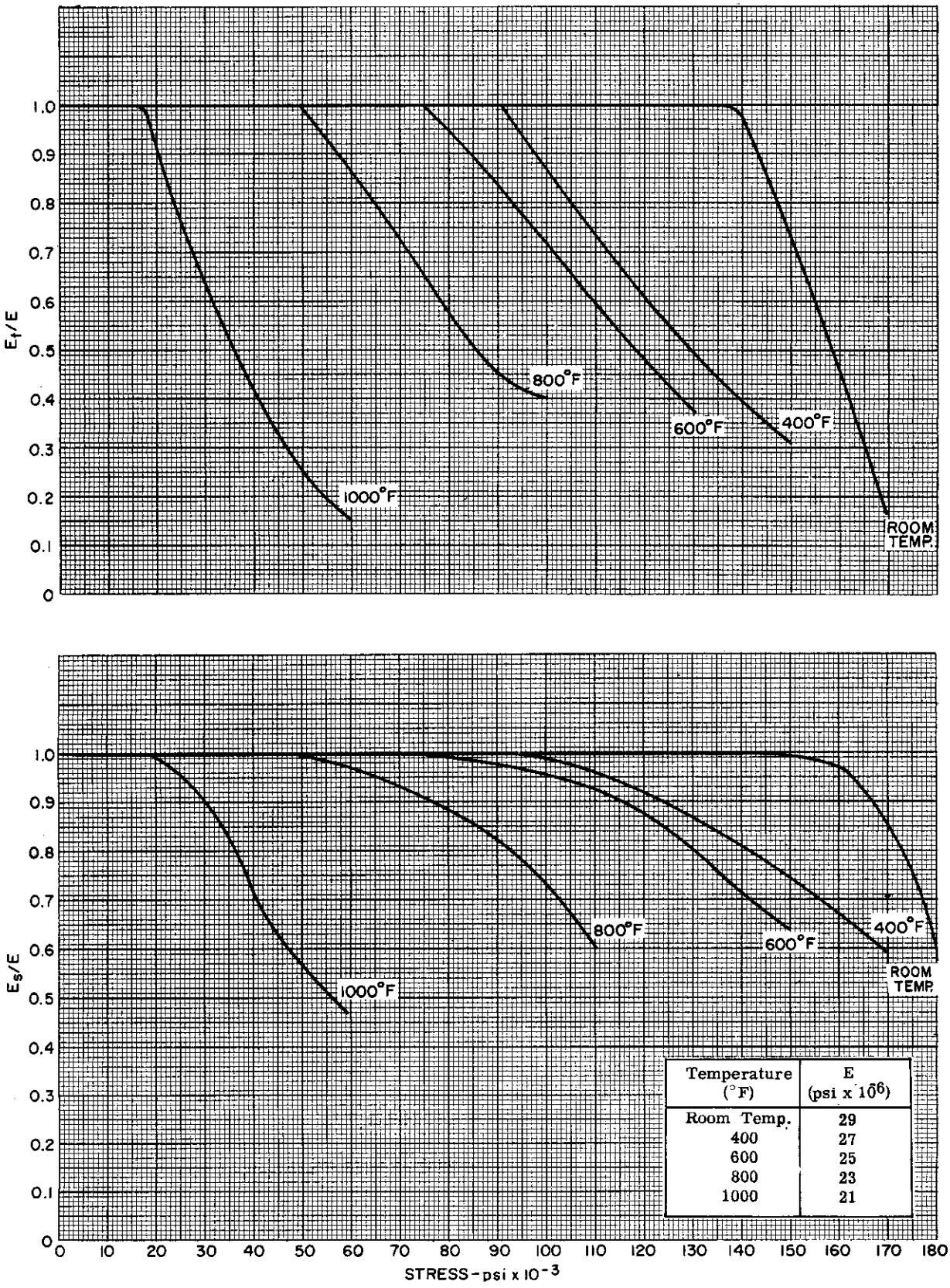

Temperature (°F)	E (psi x 10^6)
Room Temp.	29
400	27
600	25
800	23
1000	21

Figure 2.2-27. Alloy Steel — Heat-Treated to 200,000 psi — Tangent and Secant Moduli in Compression

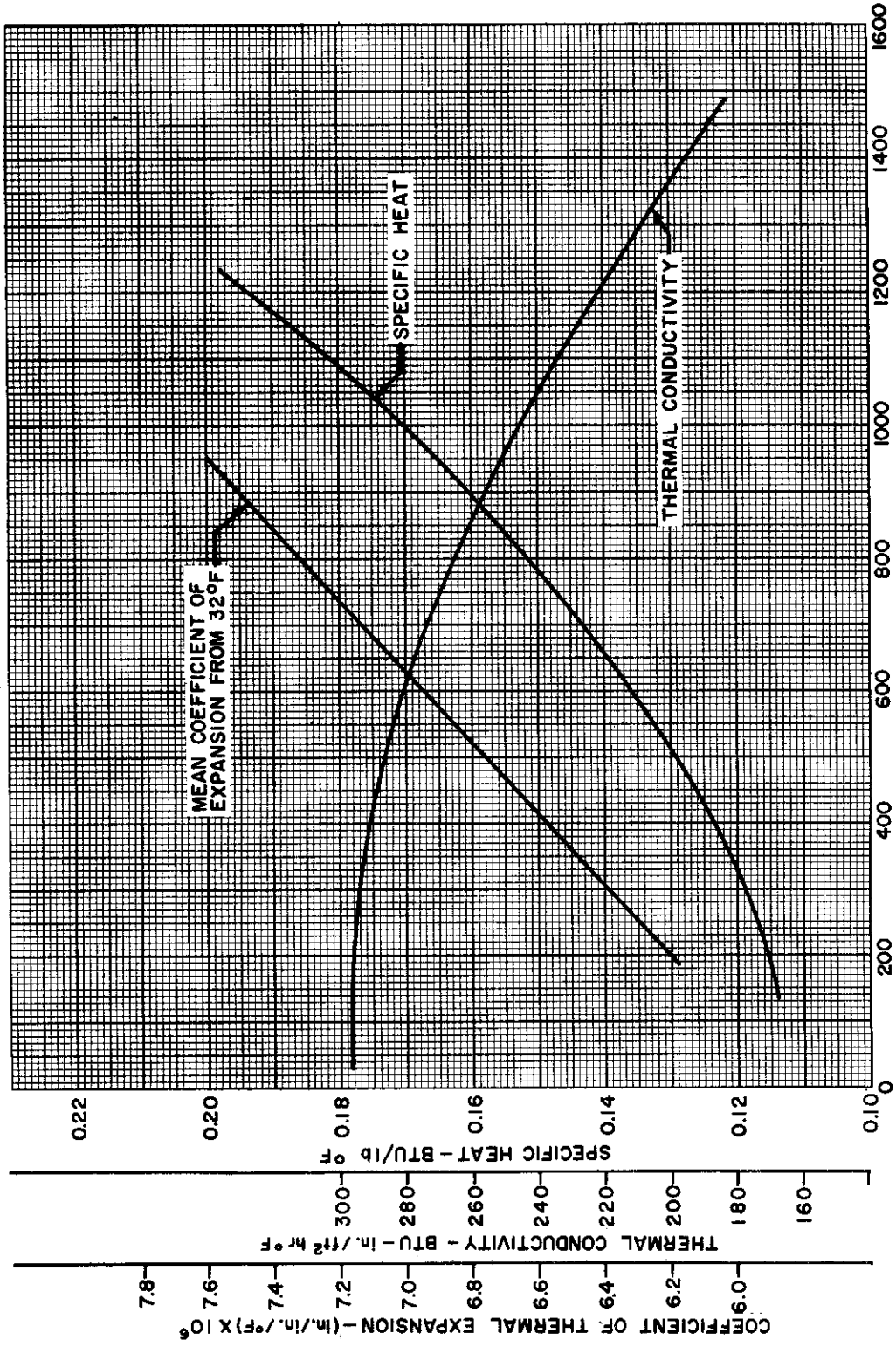

Figure 2.2-28. Alloy Steel — Heat-Treated to 200,000 psi — Thermal Properties

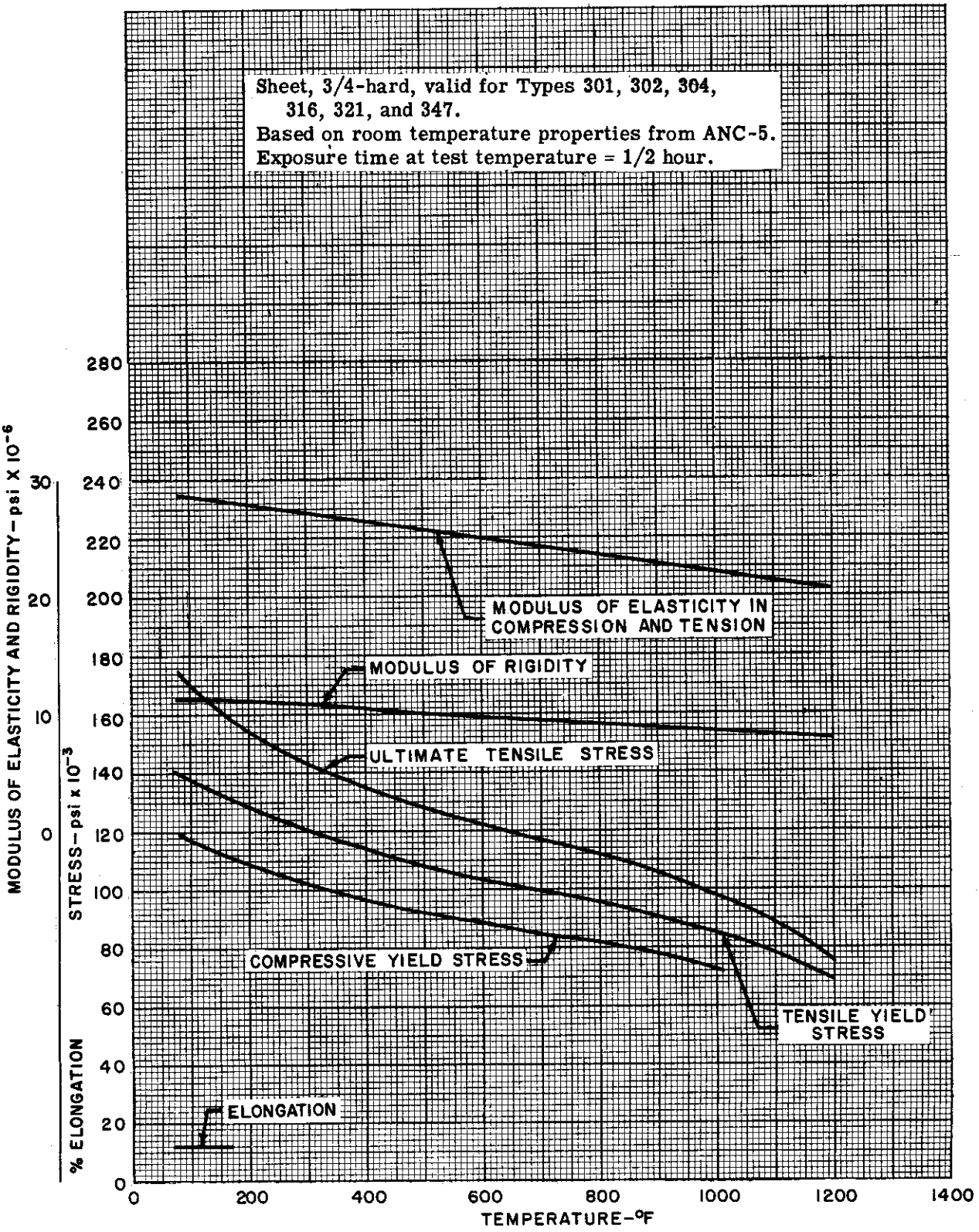

Figure 2.2-29. 18-8 Stainless Steel — Mechanical Properties

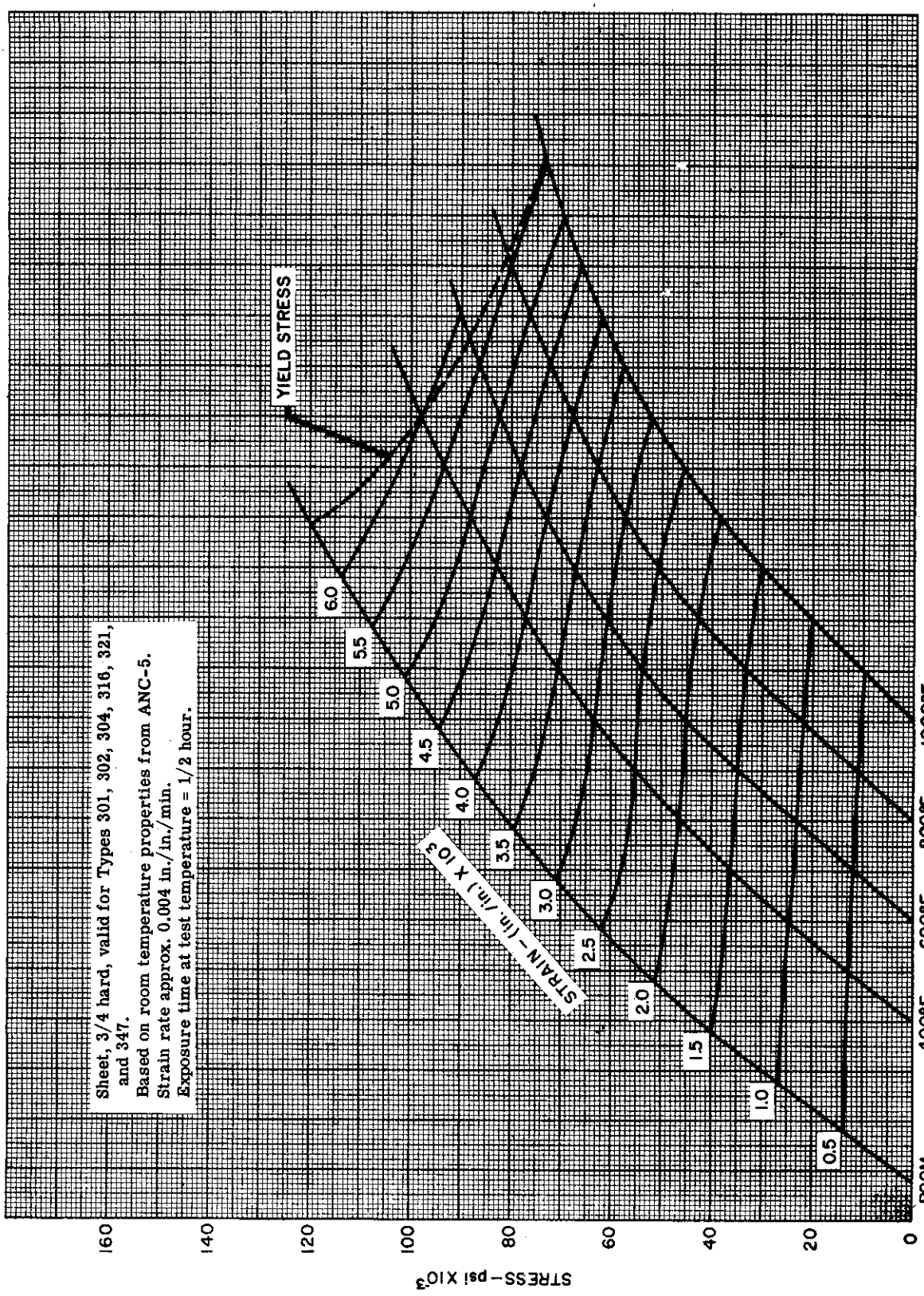

Figure 2.2-30. 18-8 Stainless Steel — Compressive Stress-Strain Curves

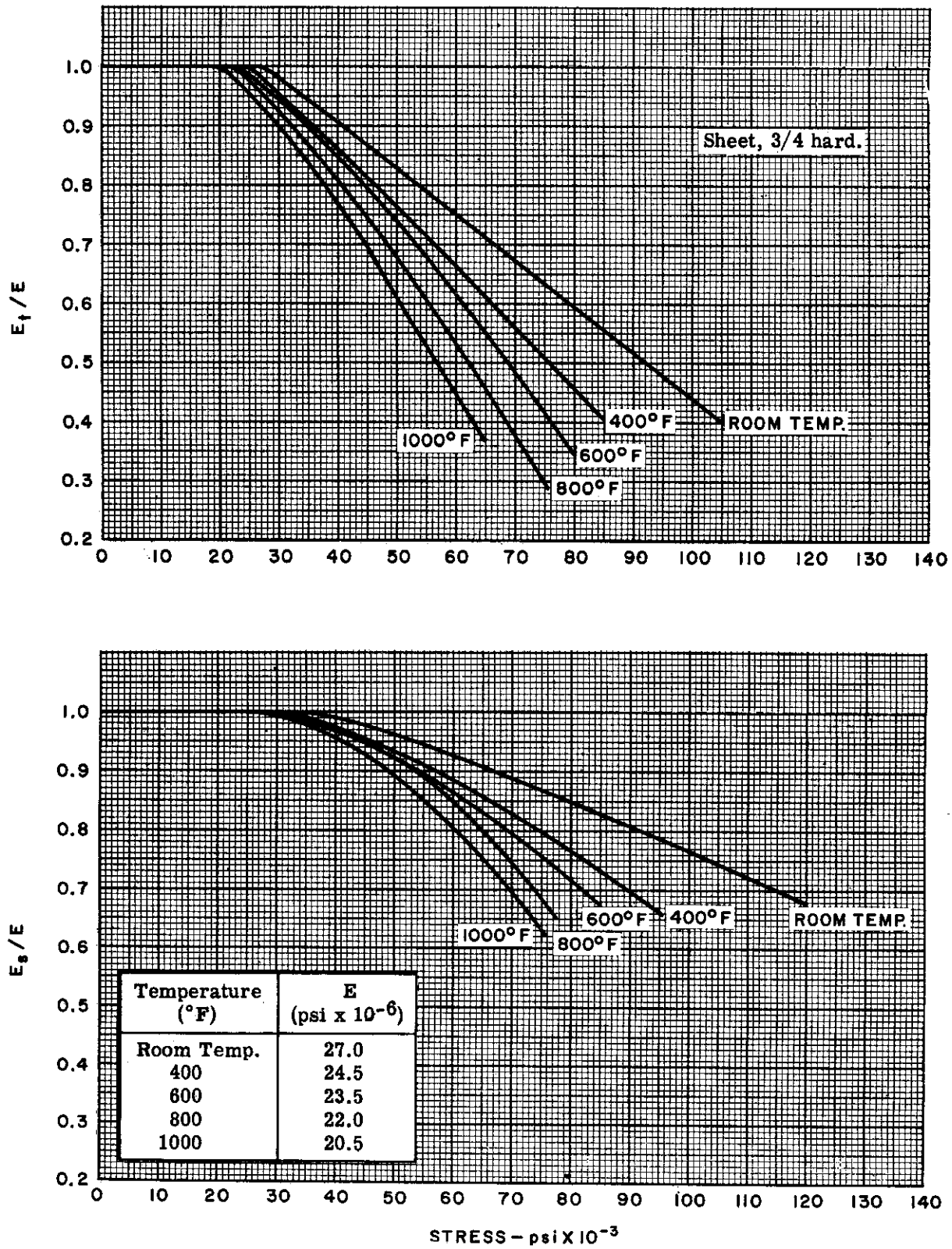

Temperature (°F)	E (psi x 10^{-6})
Room Temp.	27.0
400	24.5
600	23.5
800	22.0
1000	20.5

Figure 2.2-31. 18-8 Stainless Steel — Tangent and Secant Moduli in Compression

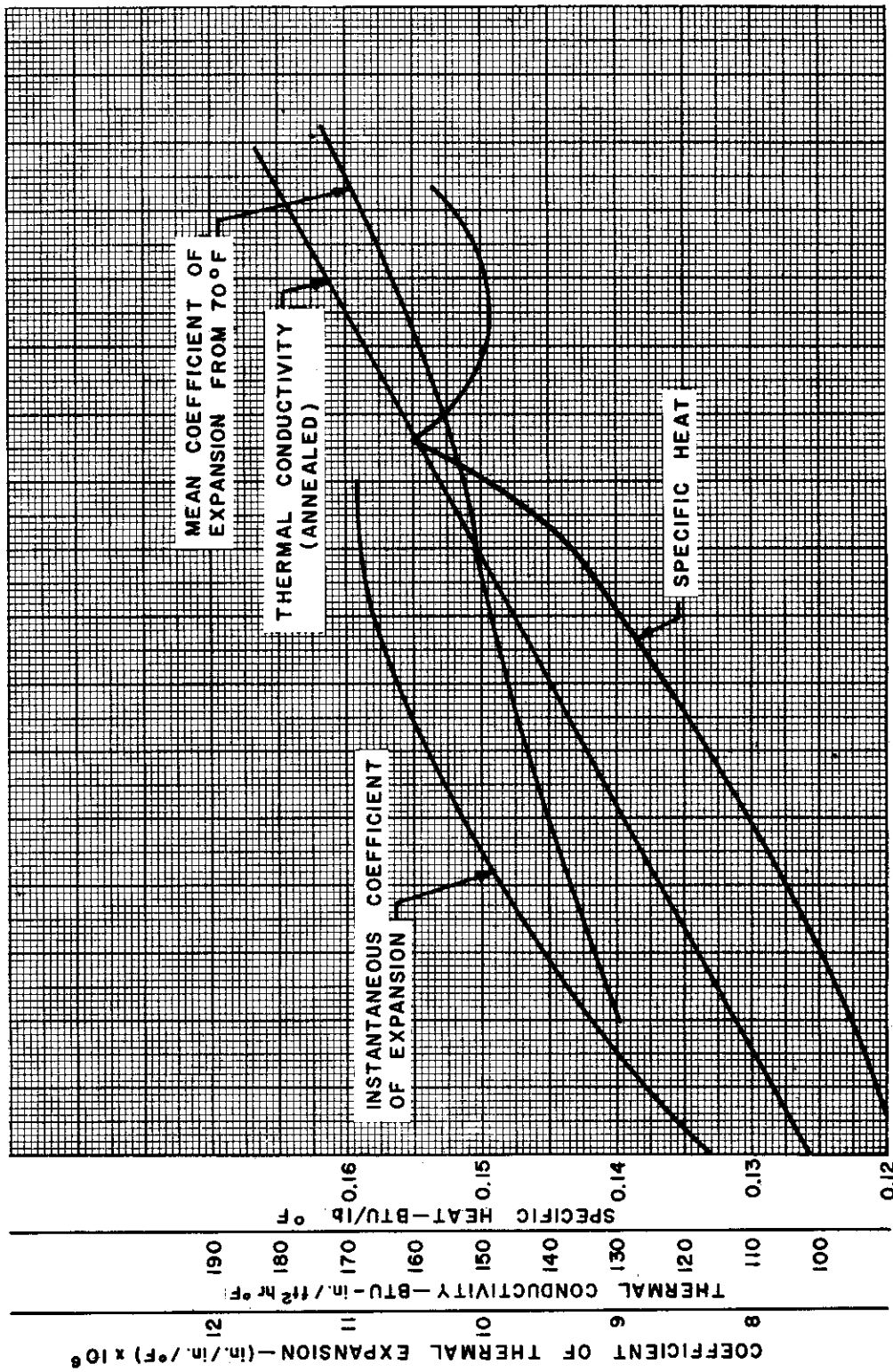

Figure 2.2-32. 18-8 Stainless Steel — Thermal Properties

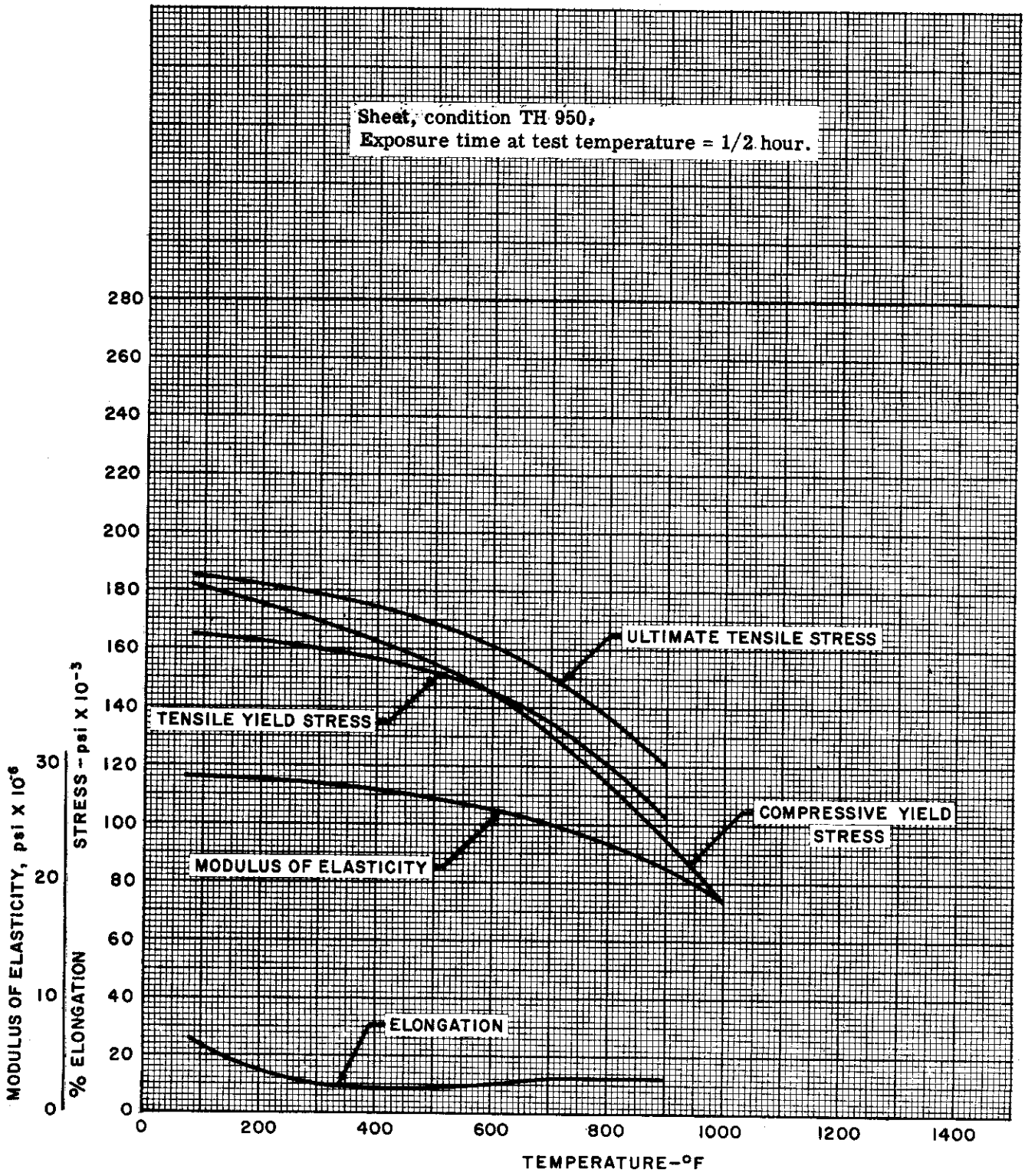

Figure 2.2-33. 17-7PH Stainless Steel — Mechanical Properties

[redacted]

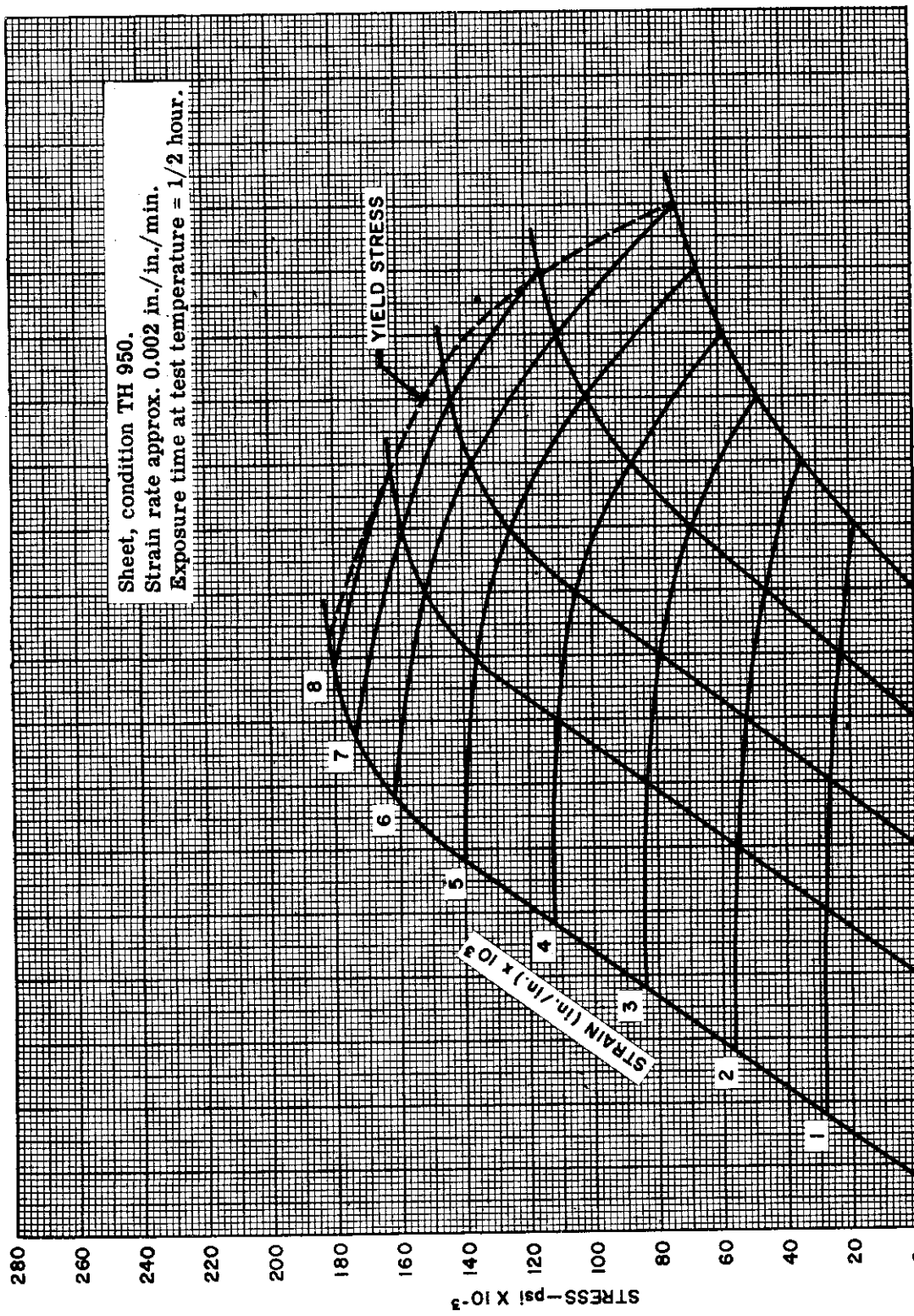

Figure 2.2-34. 17-7PH Stainless Steel — Compressive Stress-Strain Curves

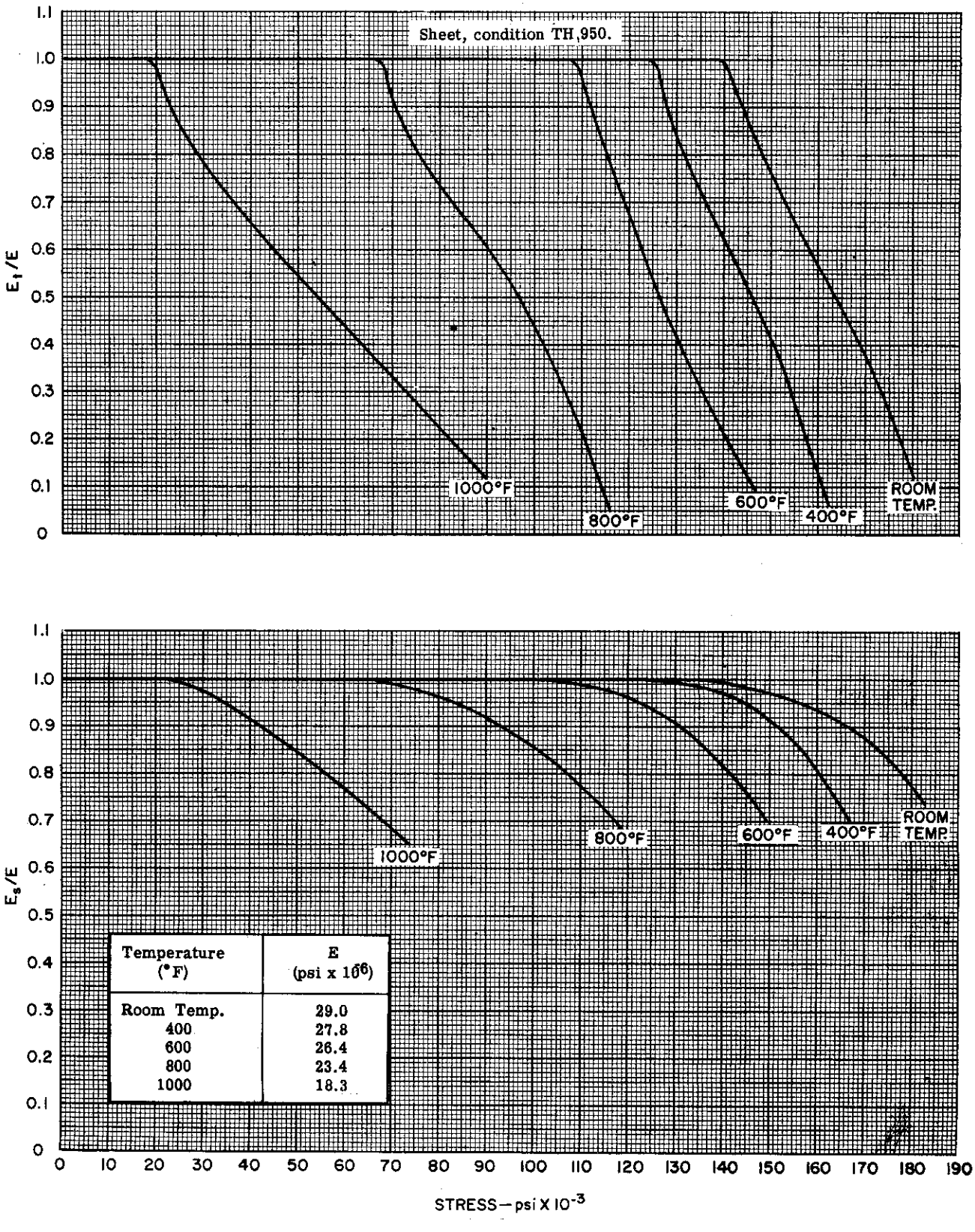

Figure 2.2-35. 17-7PH Stainless Steel — Tangent and Secant Moduli in Compression

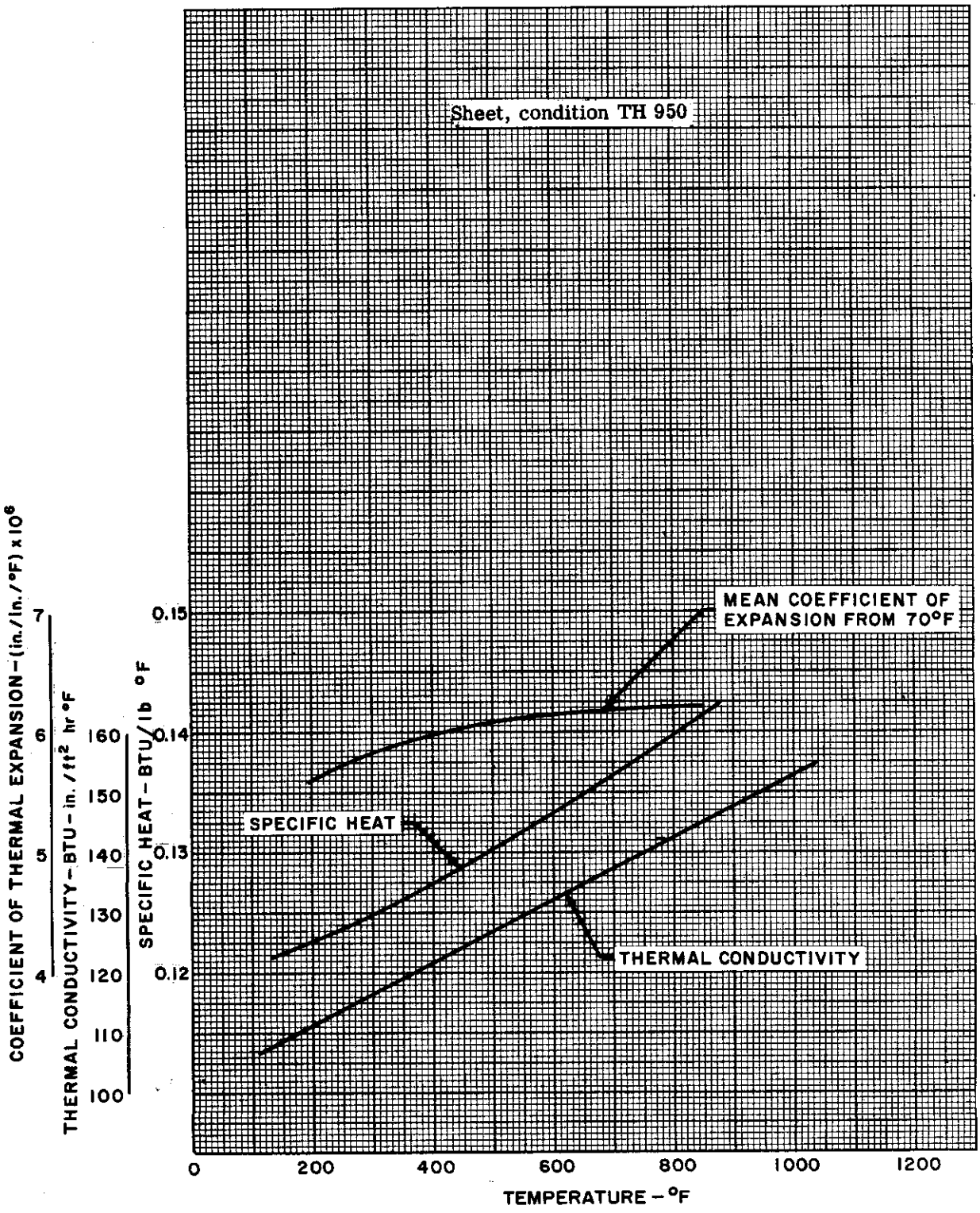

Figure 2.2-36. 17-7PH Stainless Steel — Thermal Properties

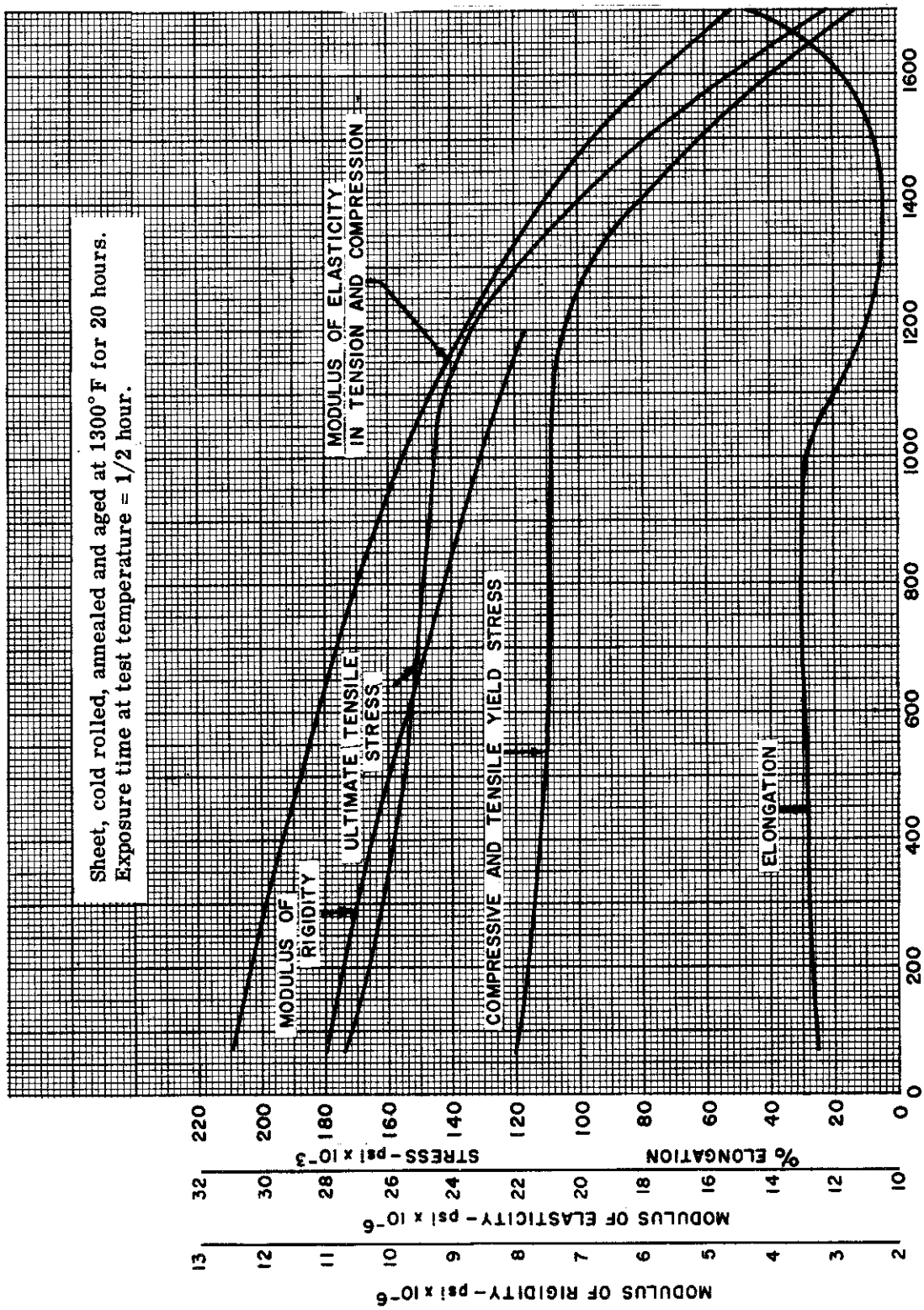

Figure 2.2-37. Inconel X Sheet — Short-Time Mechanical Properties

[redacted]

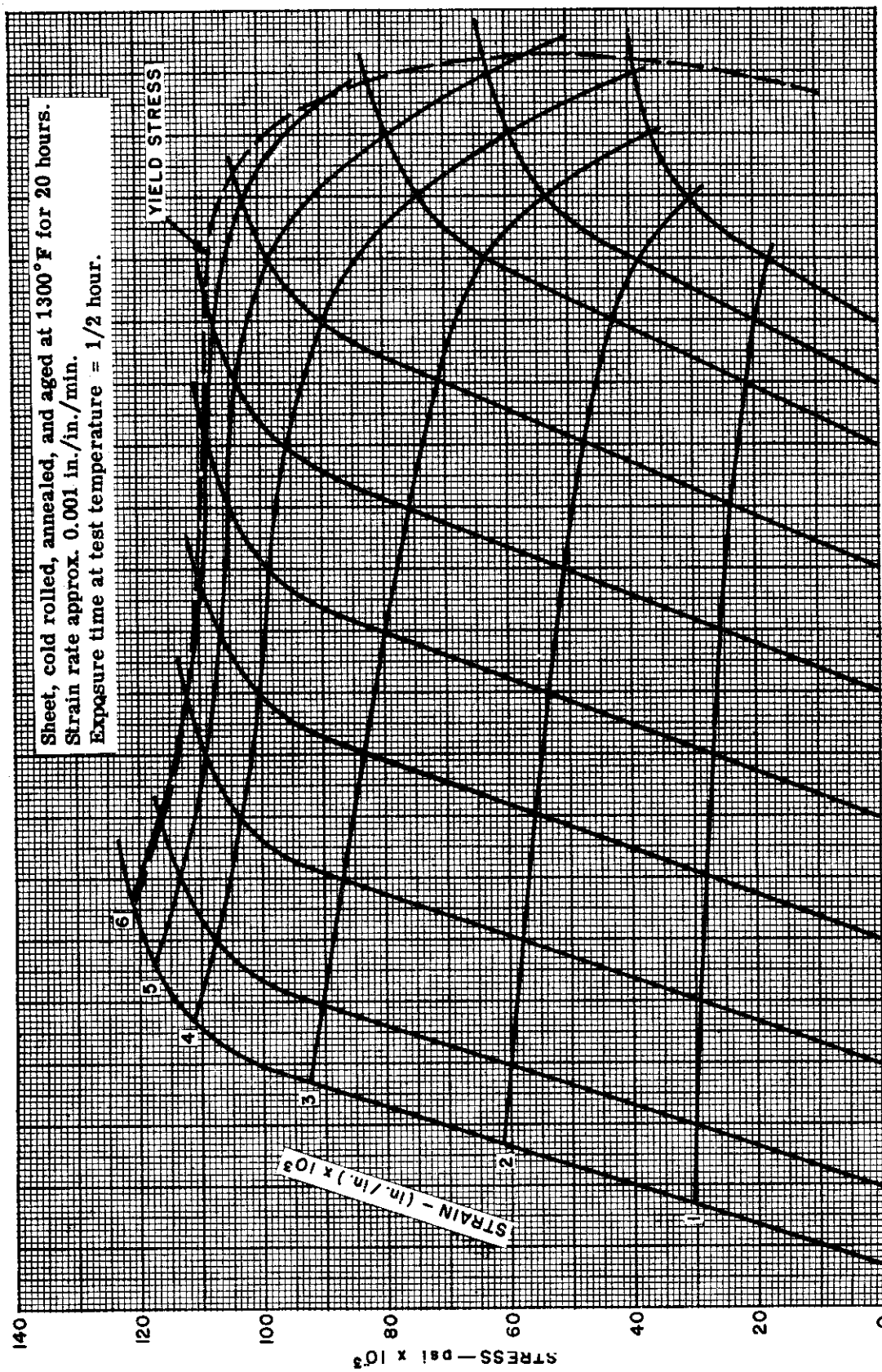

Figure 2.2-38. Inconel X Sheet — Short-Time Compressive Stress-Strain Curves

[redacted]

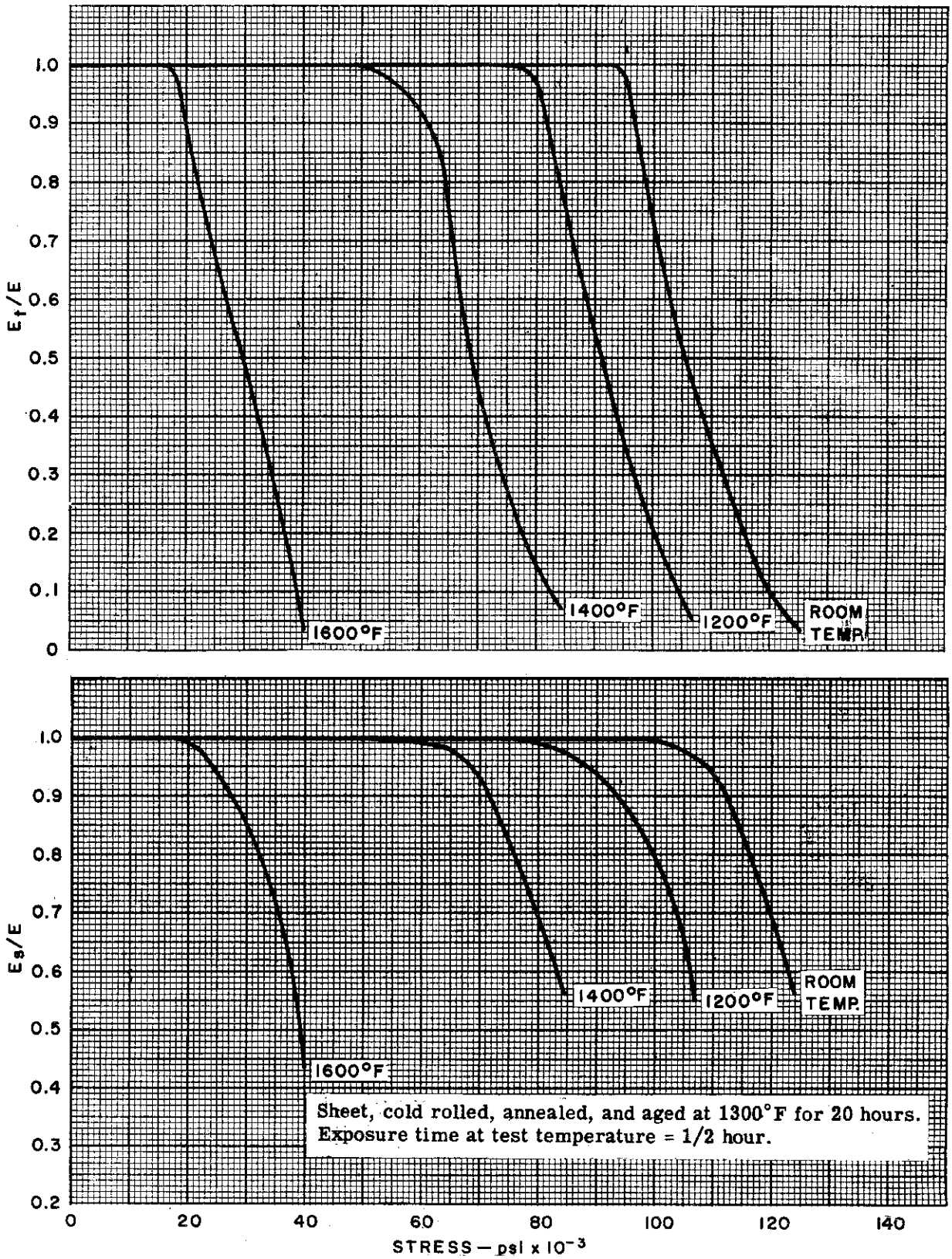

Figure 2.2-39. Inconel X Sheet — Tangent and Secant Moduli in Compression

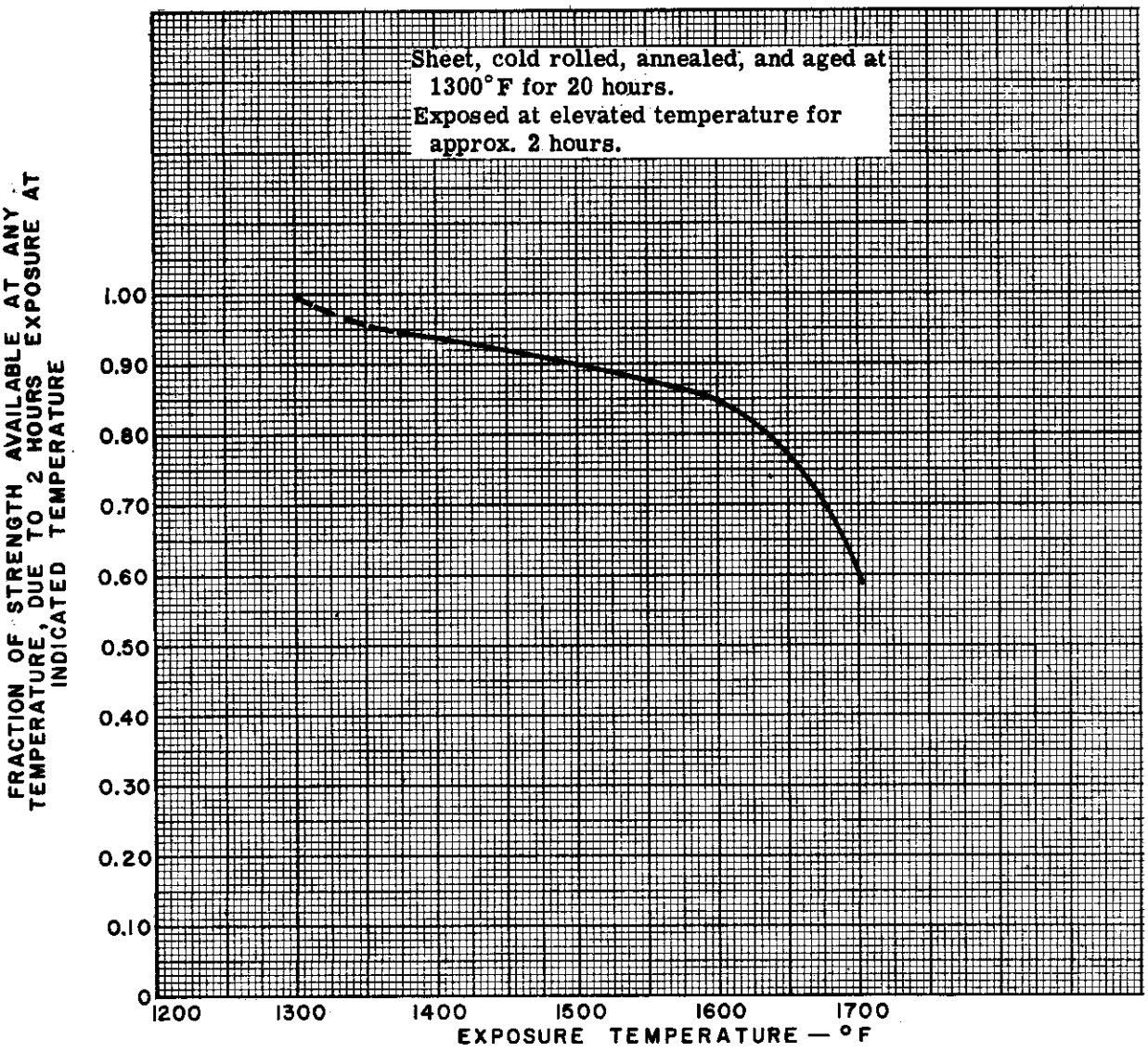

Figure 2.2-40. Inconel X Sheet — Reduction in Short-Time Tensile Strength — 2 Hours Exposure

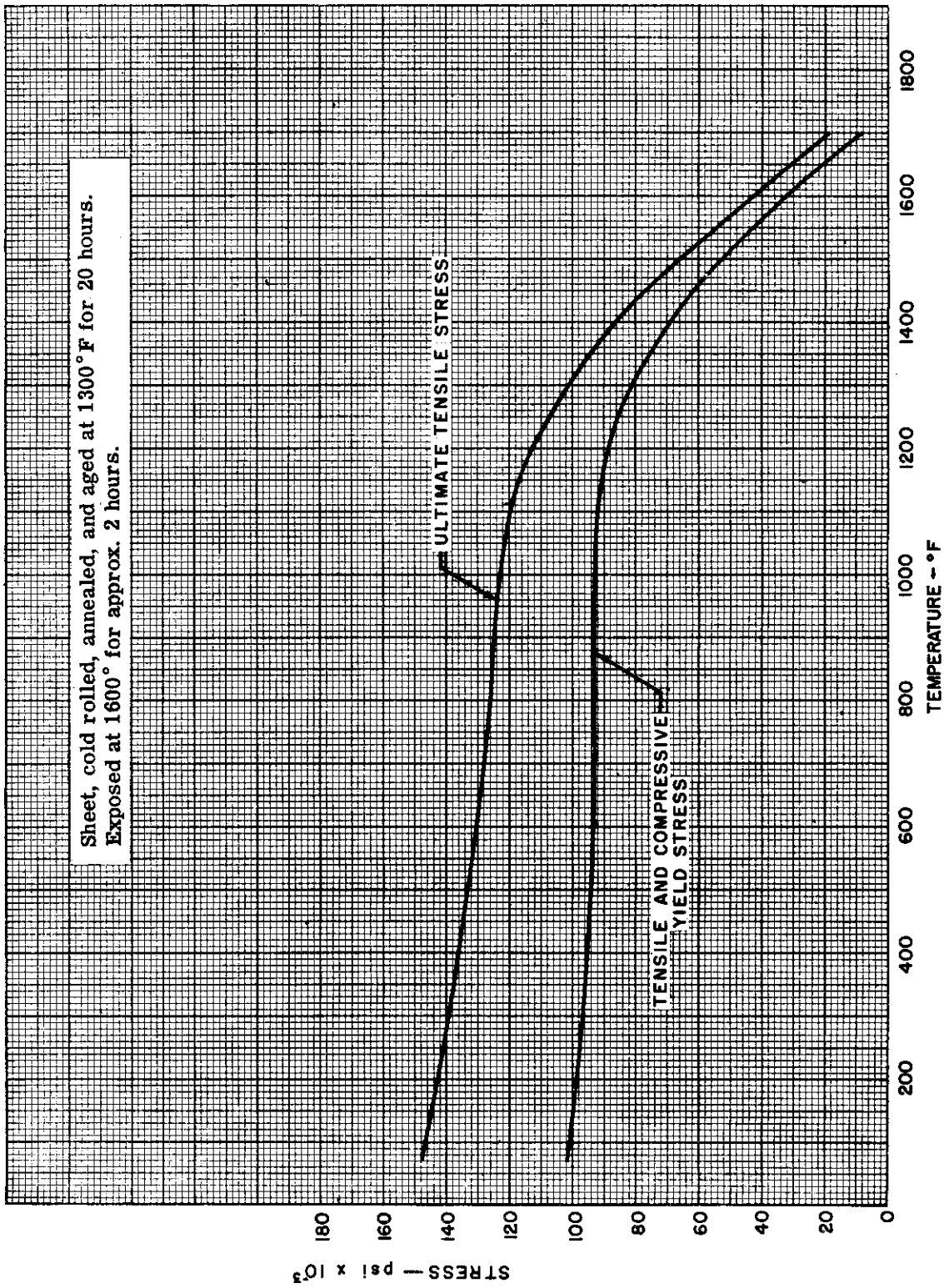

Figure 2.2-41. Inconel X Sheet — Short-Time Mechanical Properties After Exposure at 1600°F

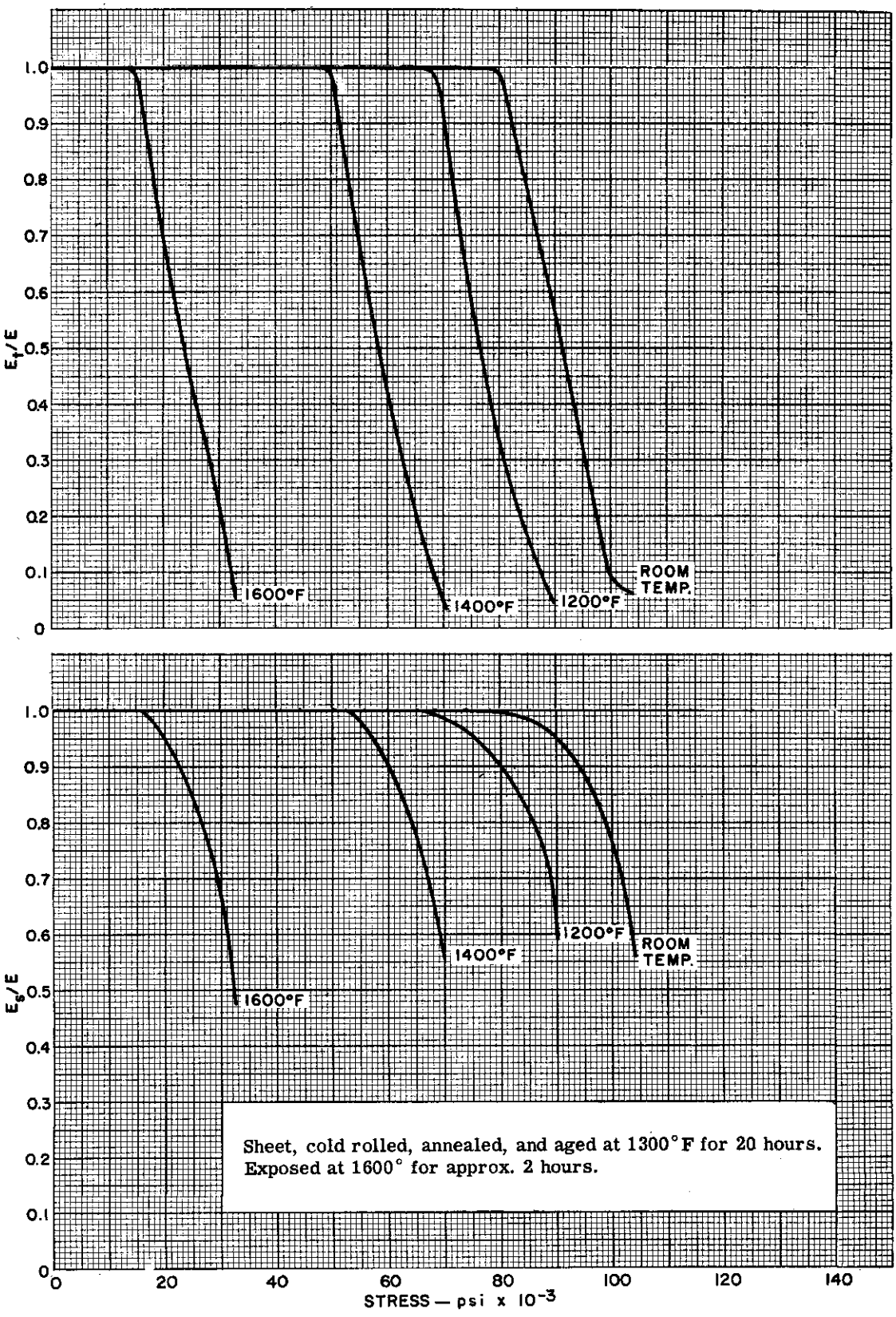

Figure 2.2-42. Inconel X Sheet — Tangent and Secant Moduli in Compression After Exposure at 1600°F

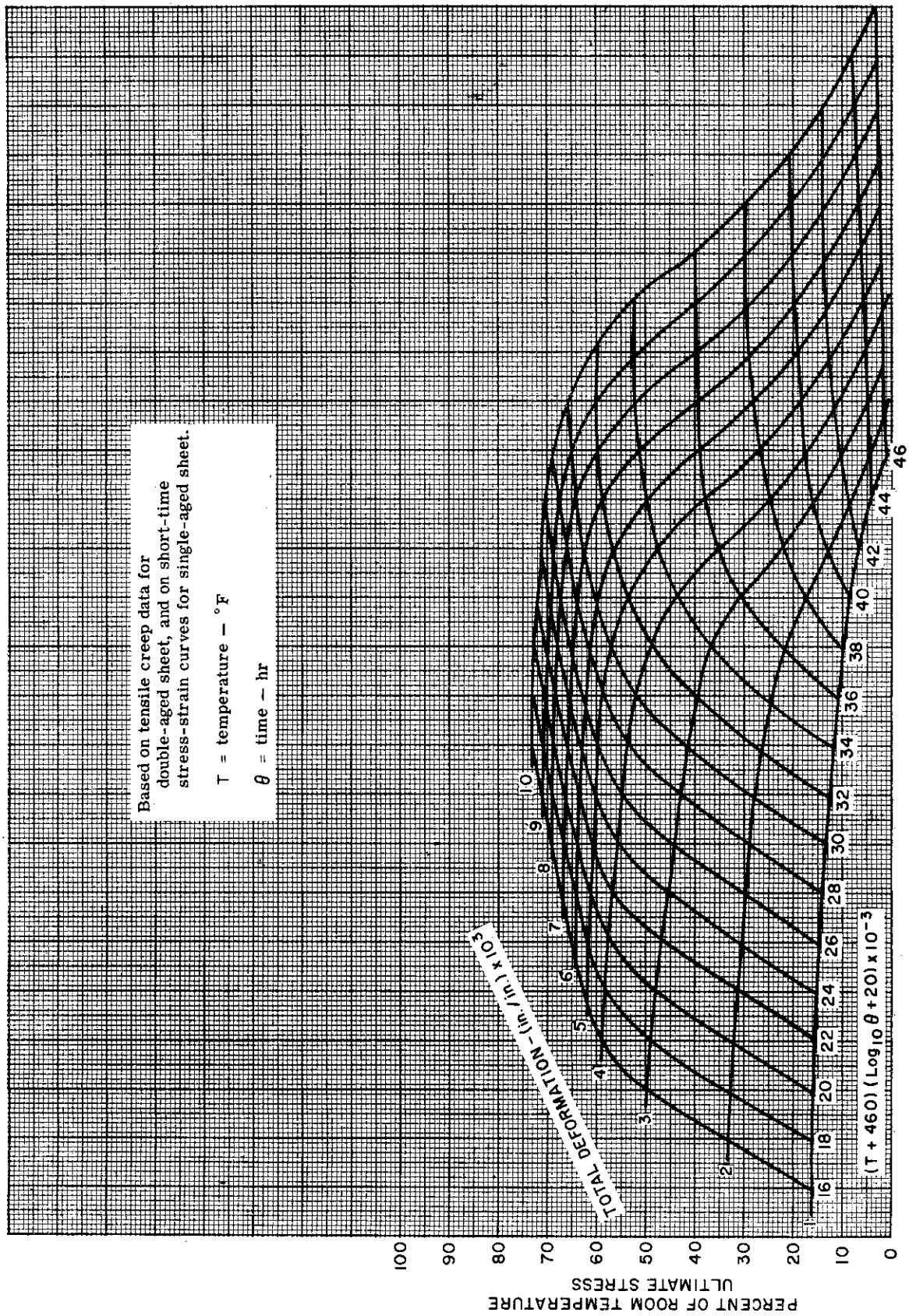

Figure 2.2-43. Inconel X Sheet at Elevated Temperatures — Master Creep Curves

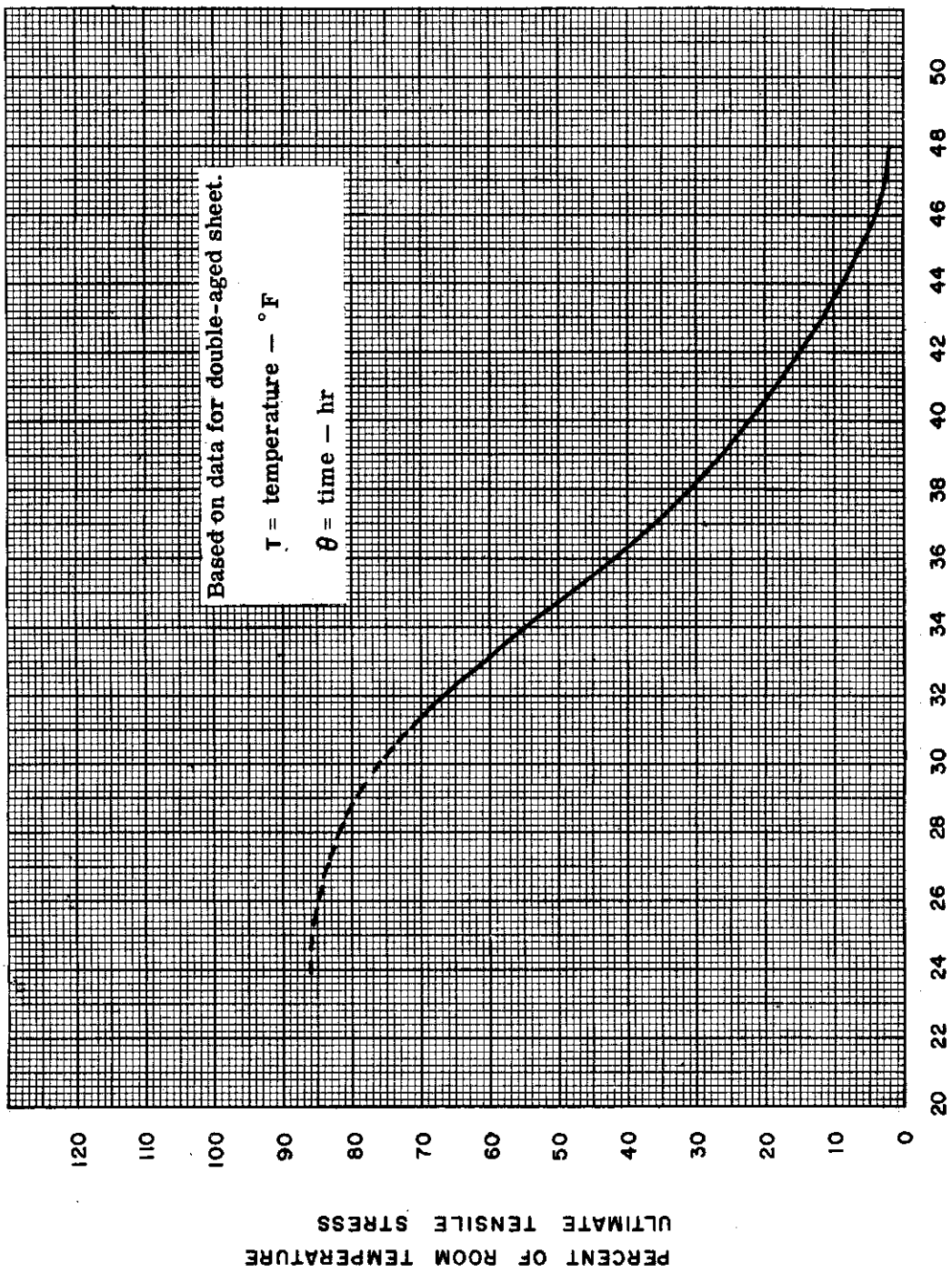

Figure 2.2-44. Inconel X Sheet at Elevated Temperatures — Master Rupture Curve

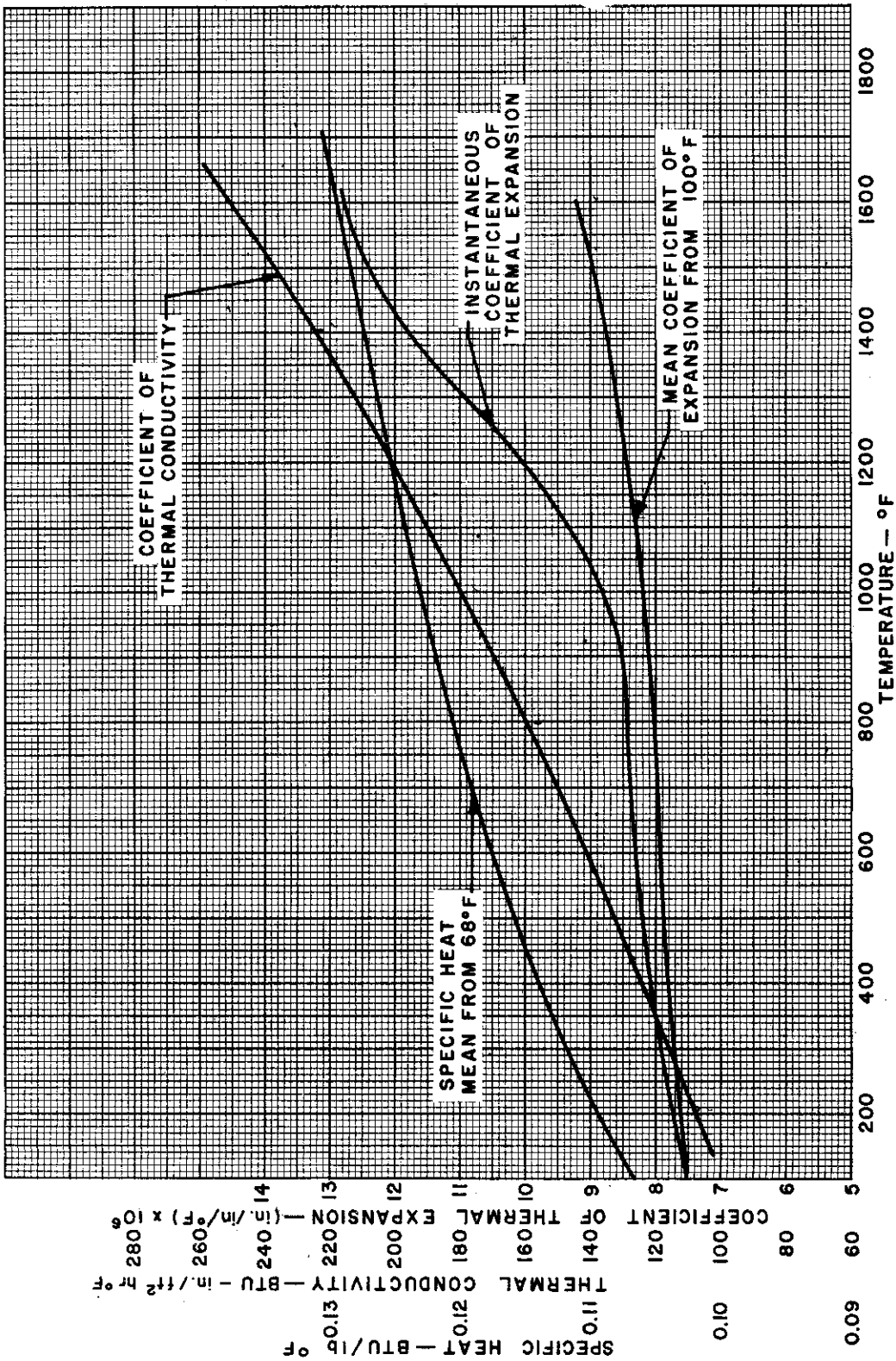

Figure 2.2-45. Inconel X Sheet at Elevated Temperatures — Thermal Properties

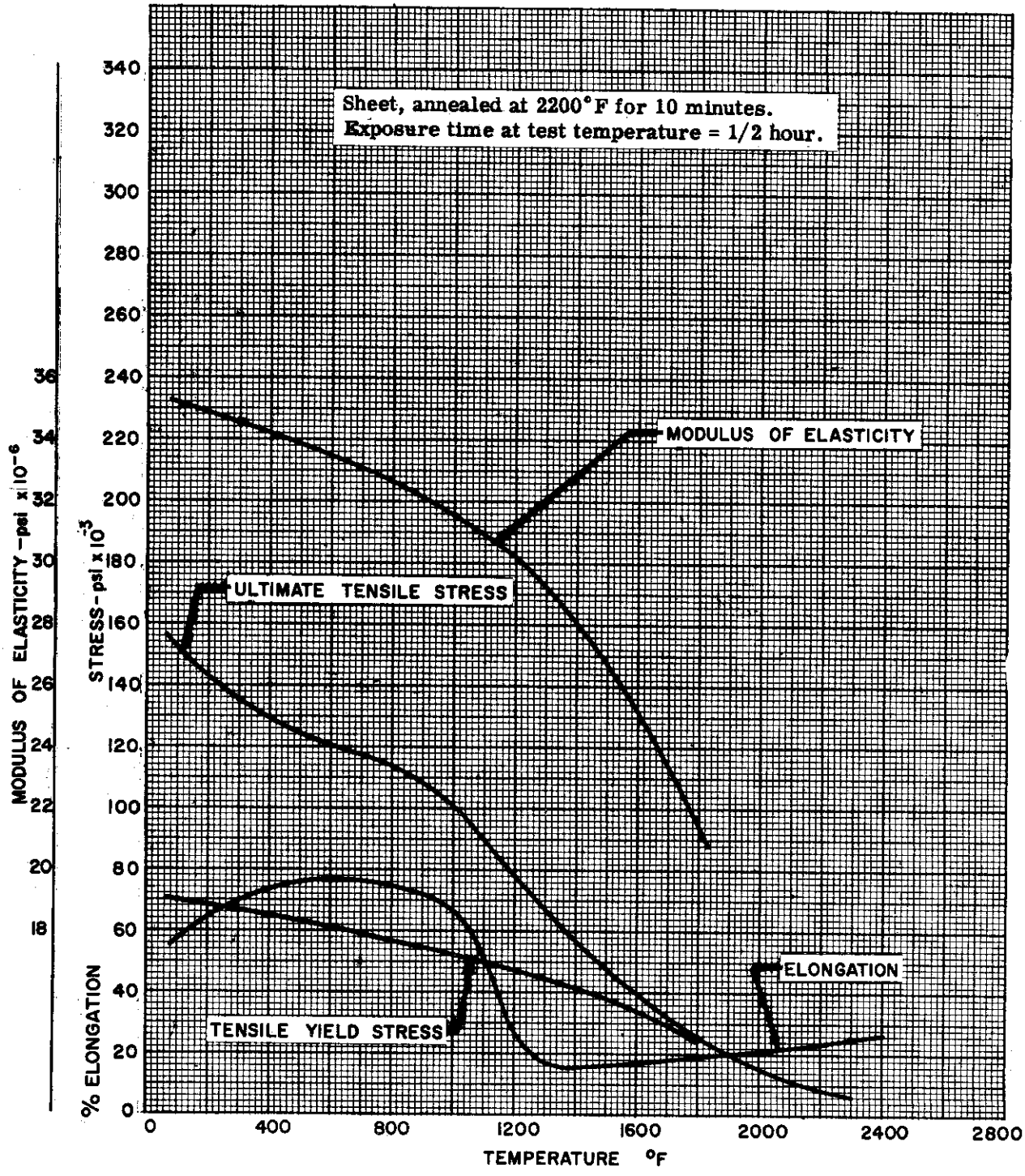

Figure 2.2-46. Haynes Alloy No. 25 (L-605) — Mechanical Properties

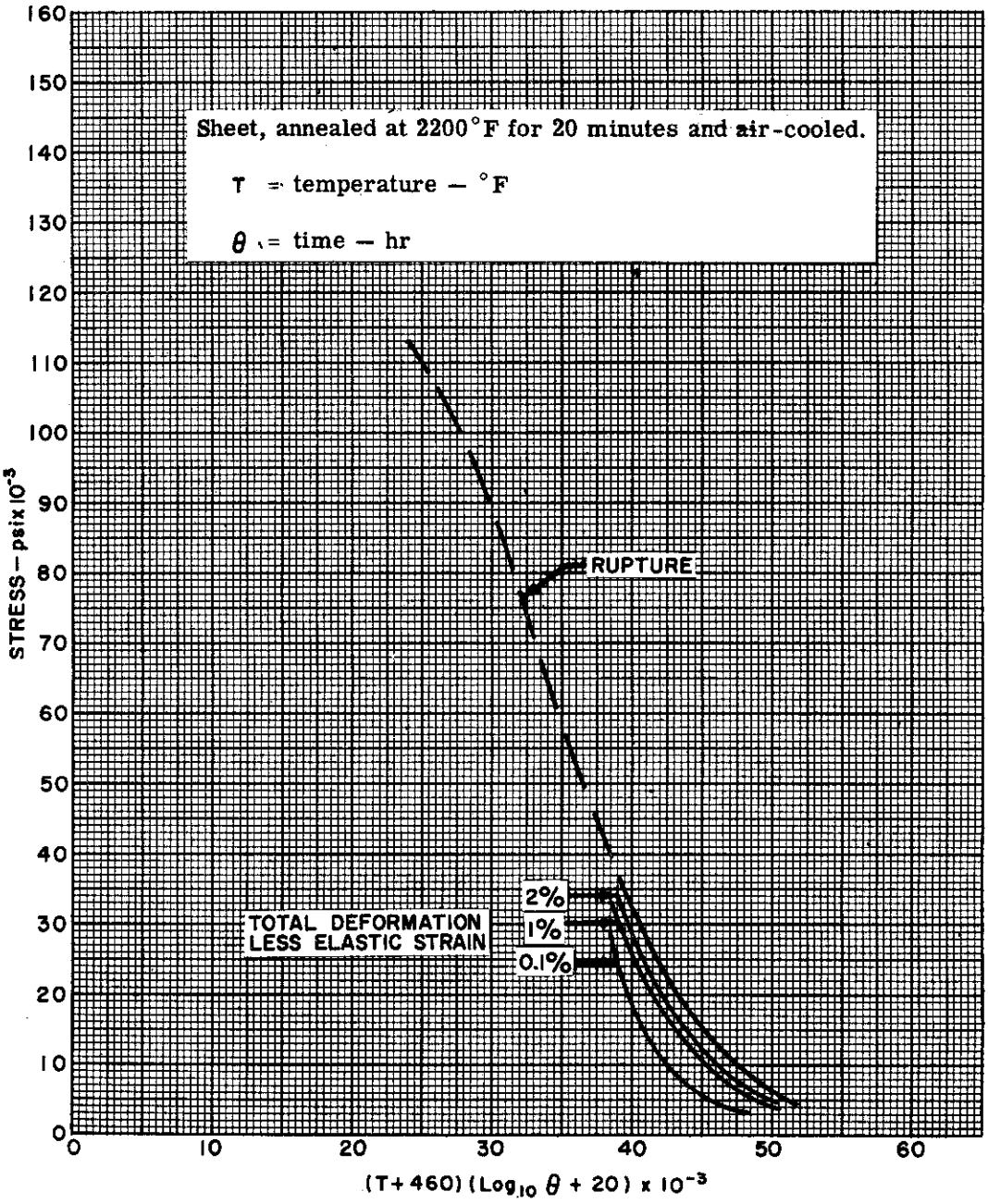

Figure 2.2-47. Haynes Alloy No. 25 (L-605) — Master Creep and Rupture Curves

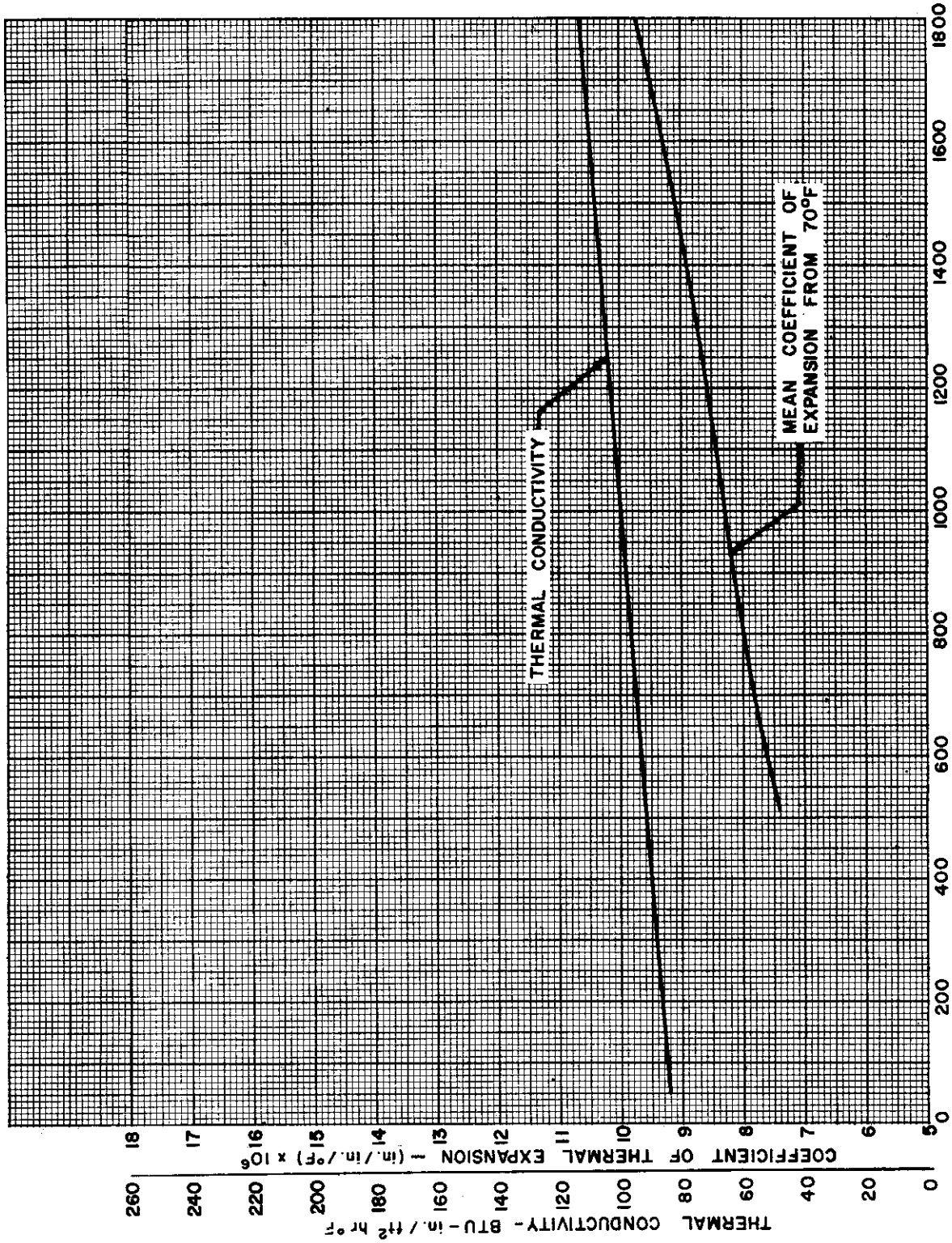

Figure 2.2-48. Haynes Alloy No. 25 (L-605) — Thermal Properties

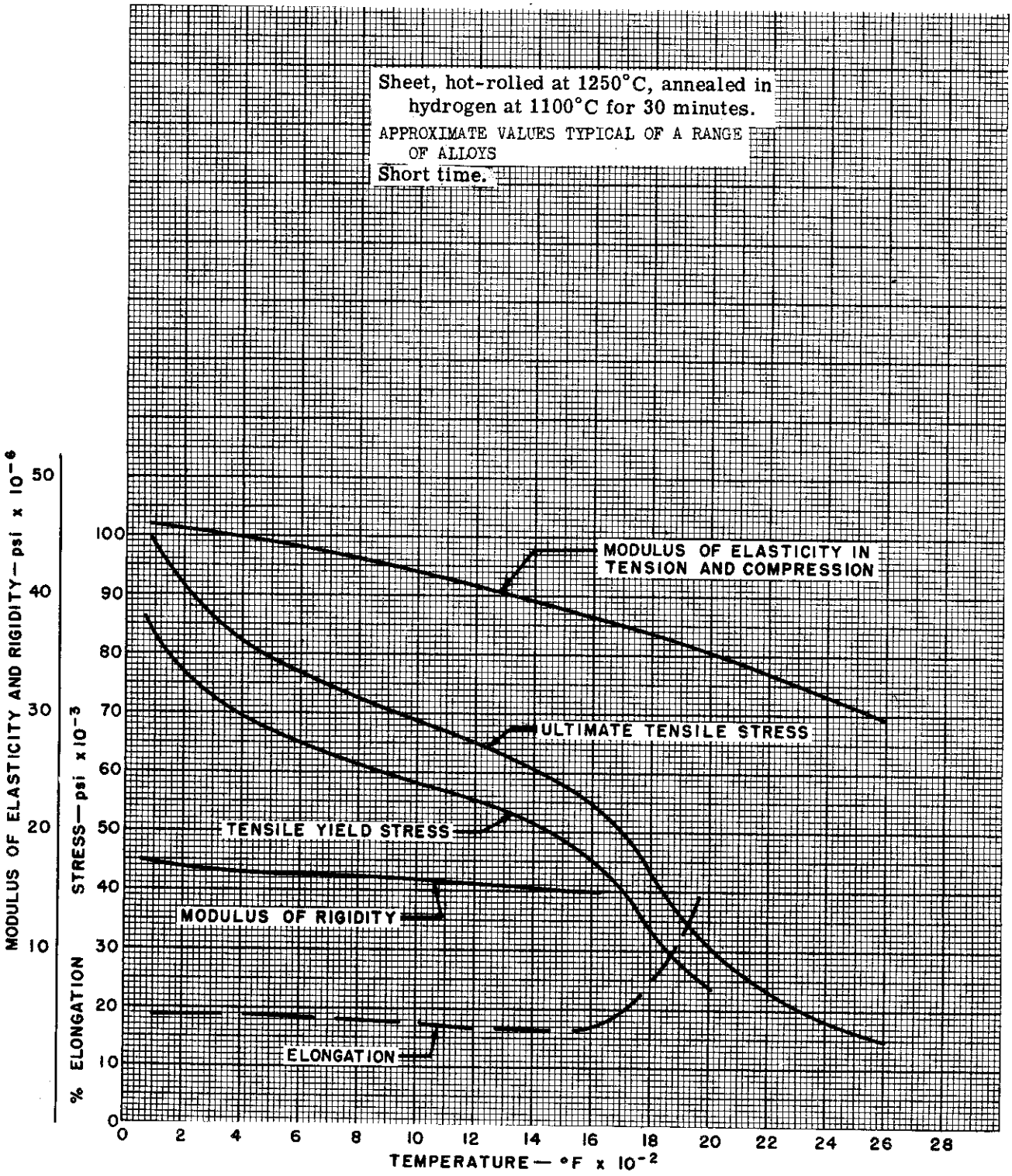

Figure 2.2-49. Molybdenum Base Alloys — Mechanical Properties

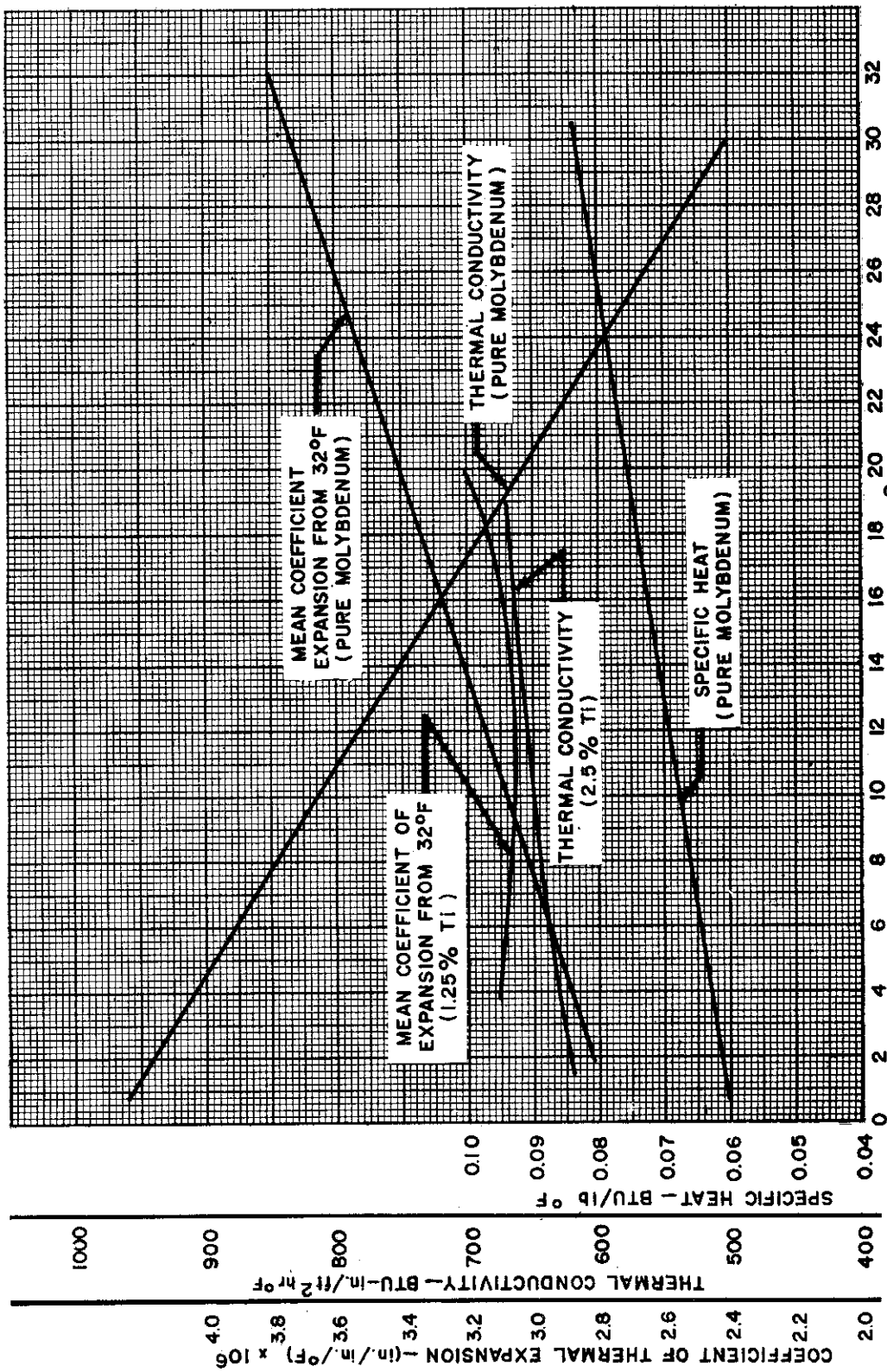

Figure 2.2-50. Molybdenum Base Alloys — Thermal Properties

[redacted]

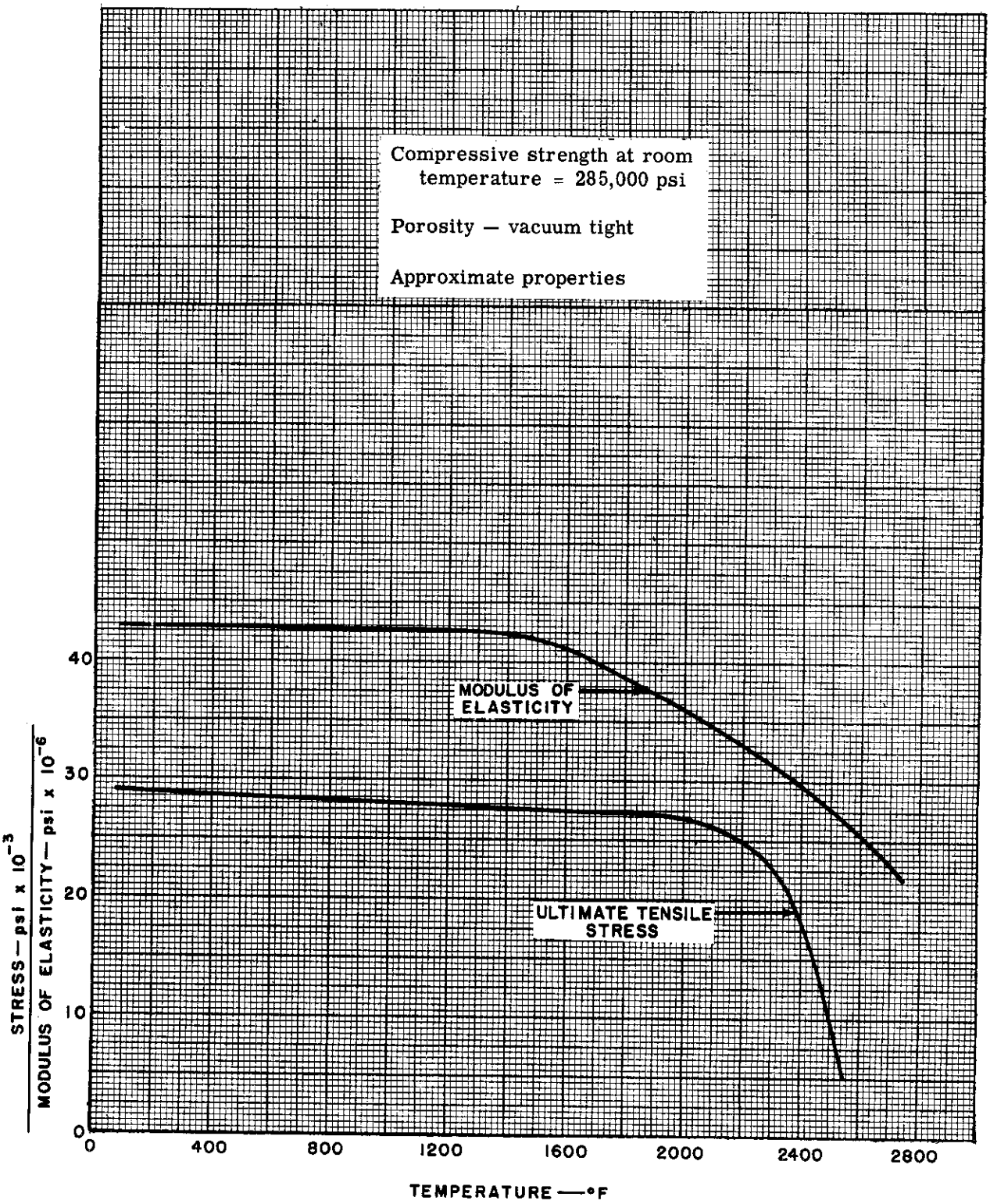

Figure 2.2-51. Alite AE-212 (Sintered Aluminum Oxide) — Mechanical Properties

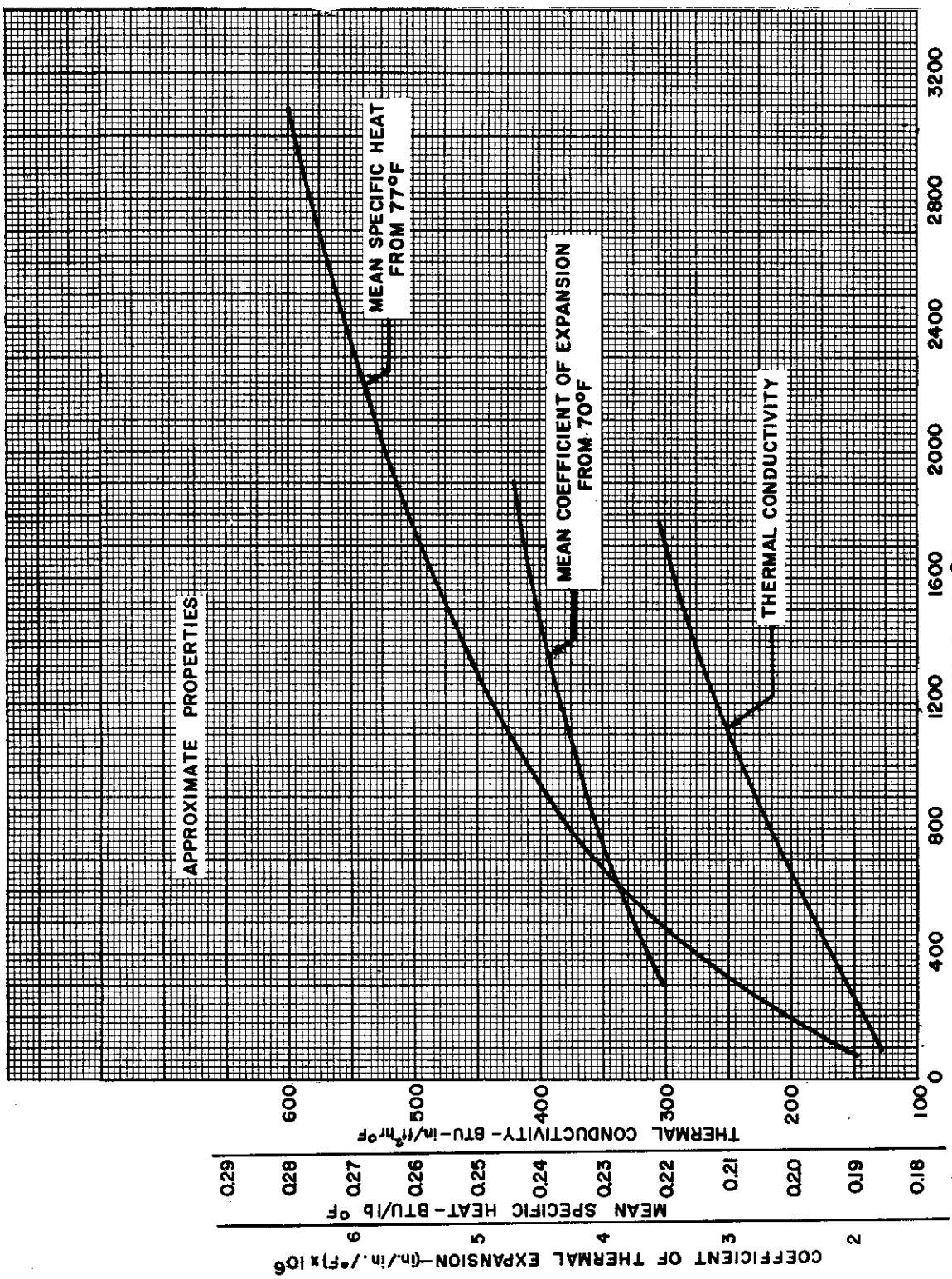

Figure 2.2-52. Alite AE-212 (Sintered Aluminum Oxide) — Thermal Properties

2.3 INSULATION

In Figures 2.3-1 through 2.3-4, curves of conductivity plotted against temperature are presented for various insulating materials, including air, which have been shown in Part II to be sufficiently efficient for airframe use. It should be noted that the conductivity of air is independent of pressure, until the pressure is reduced below 10.0 mm of mercury.

The use of air spaces as a means of insulating structure requires a knowledge of the normal emissivity of the surfaces bounding the space, so that heat transfer by radiation can be calculated. Emissivity is a function of both the surface material and its condition. Since the surface condition is dependent upon the initial condition, the temperature, and the type and degree of atmospheric contamination, it cannot be defined precisely; considerable scatter is generally found in test data. The most useful and available data on surface emissivity is presented in Figures 2.3-5 through 2.3-12 against the variable of surface temperature, for a variety of materials and surface conditions.

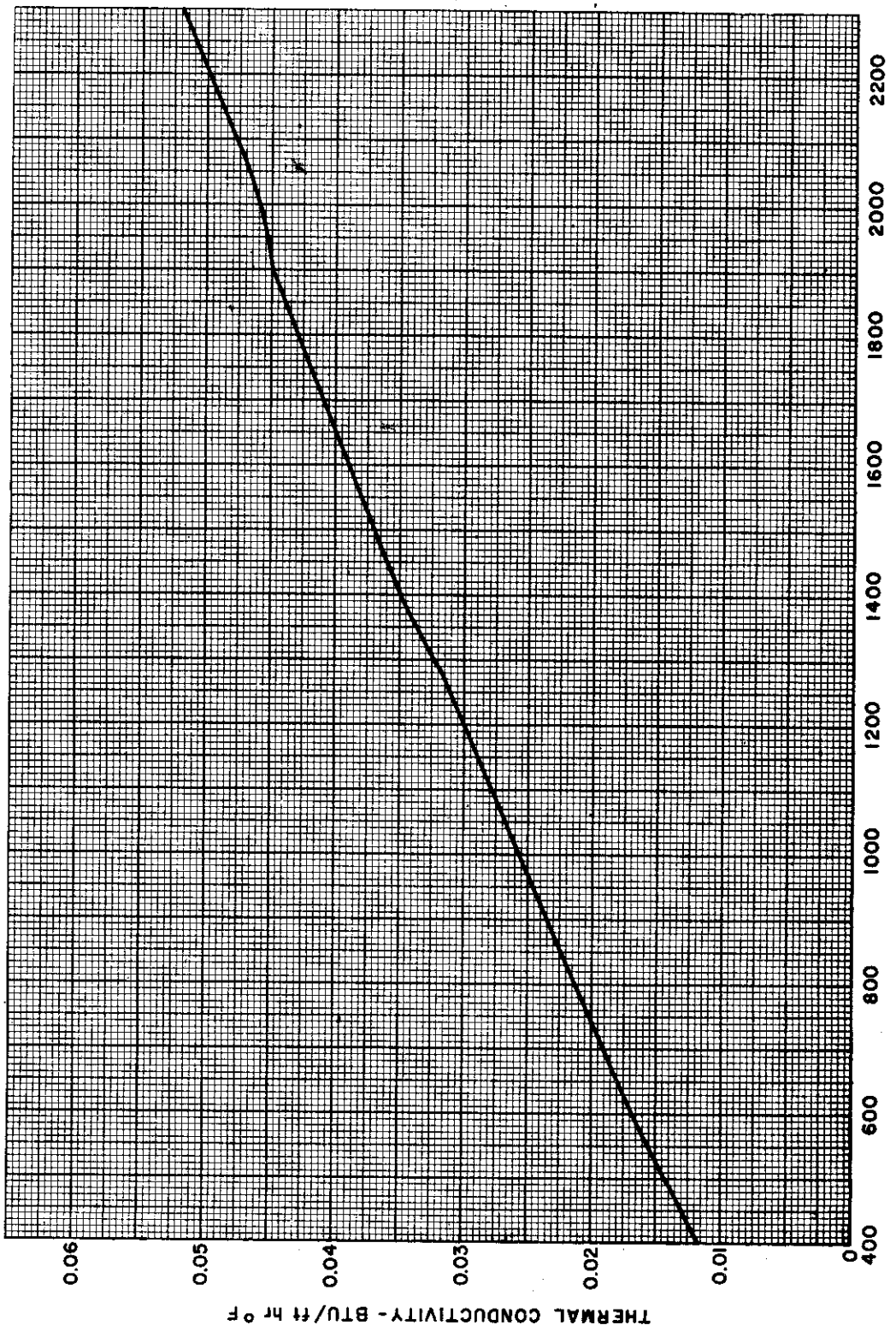

Figure 2.3-1. Thermal Conductivity of Air

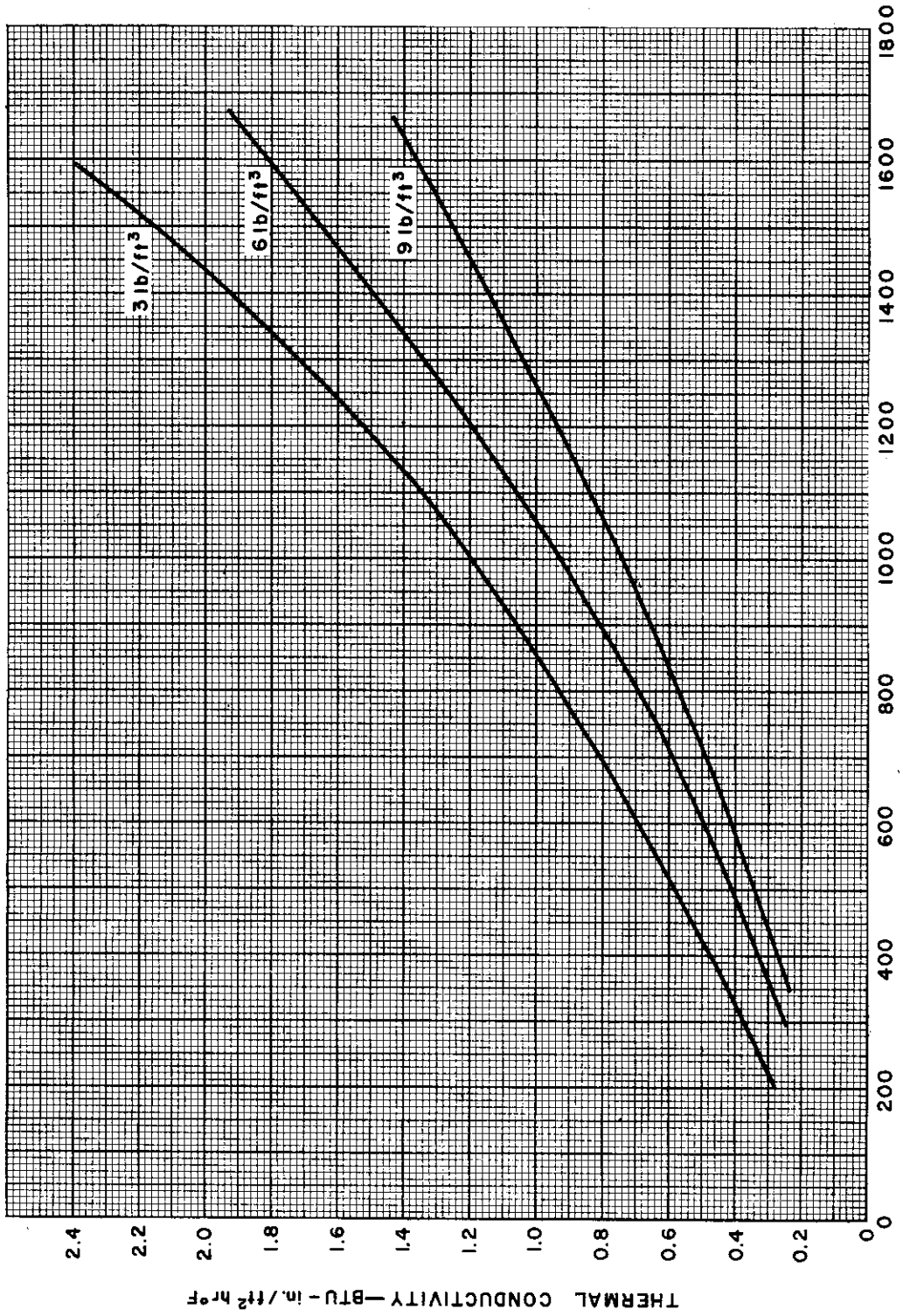

Figure 2.3-2. Thermal Conductivity of Refrasil

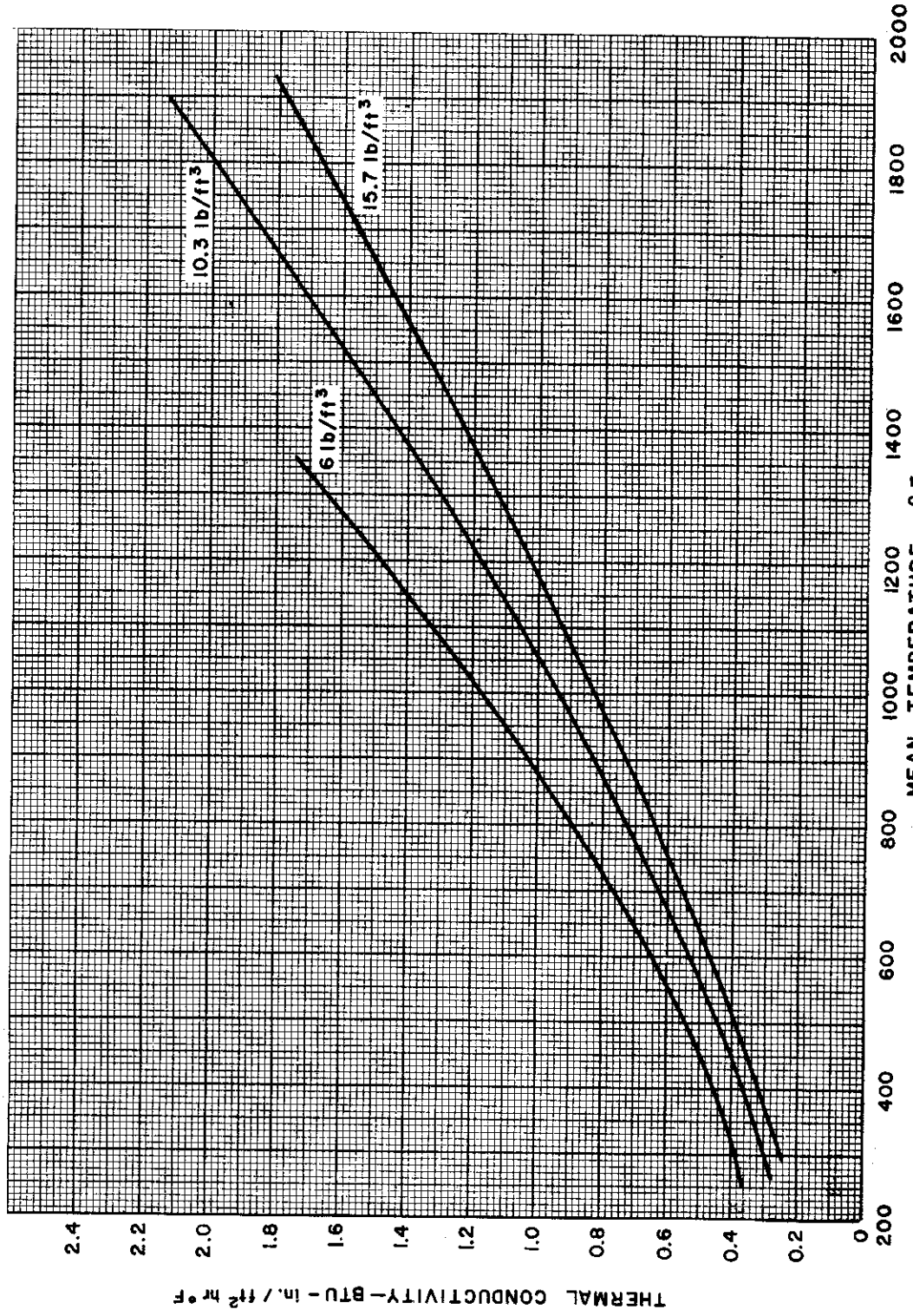

Figure 2.3-3. Thermal Conductivity of Fiberfrax

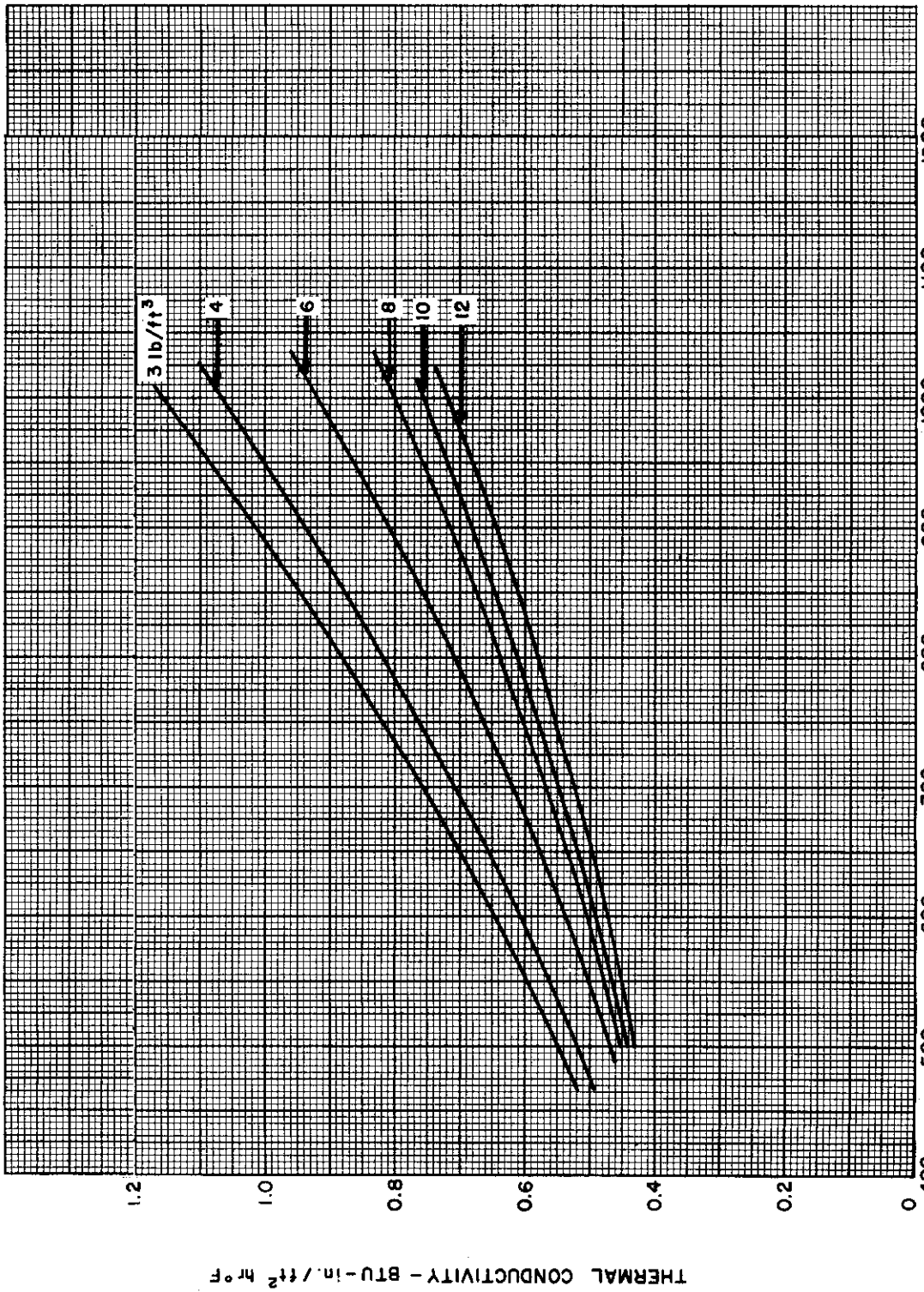

Figure 2.3-4. Thermal Conductivity of Thermoflex

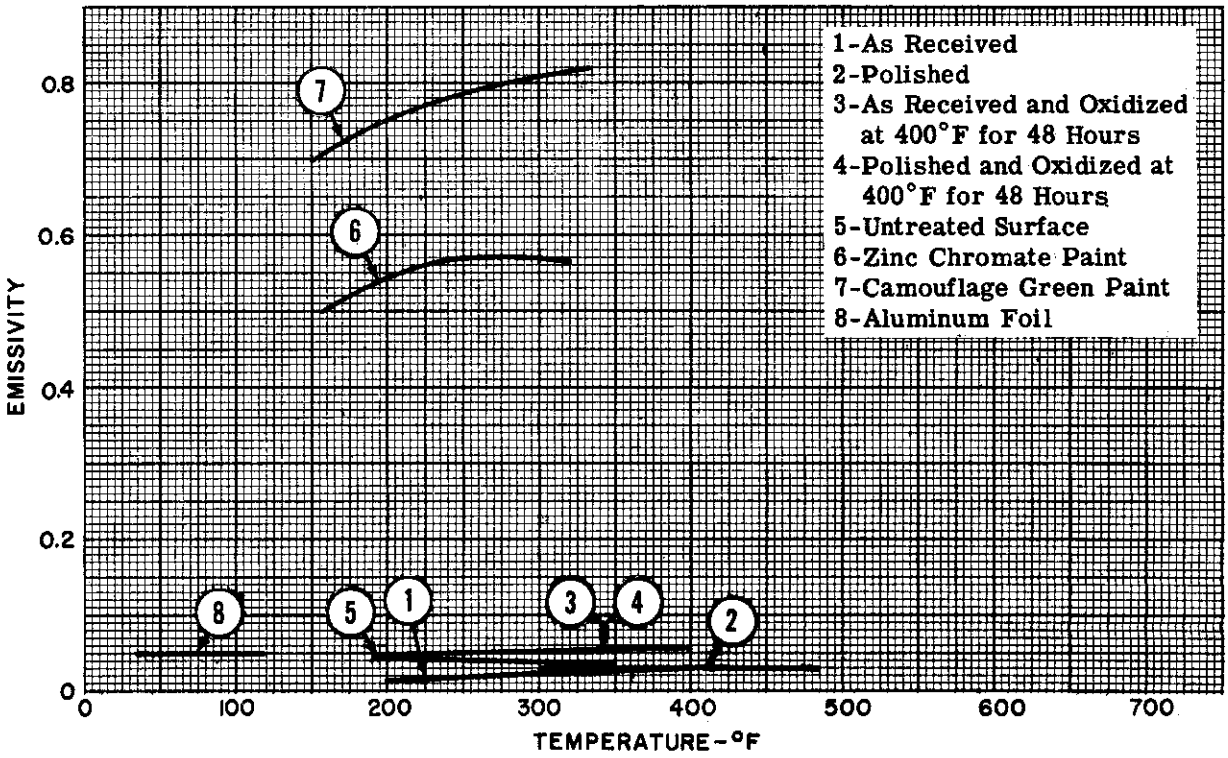

Figure 2.3-5. Emissivity of Alclad

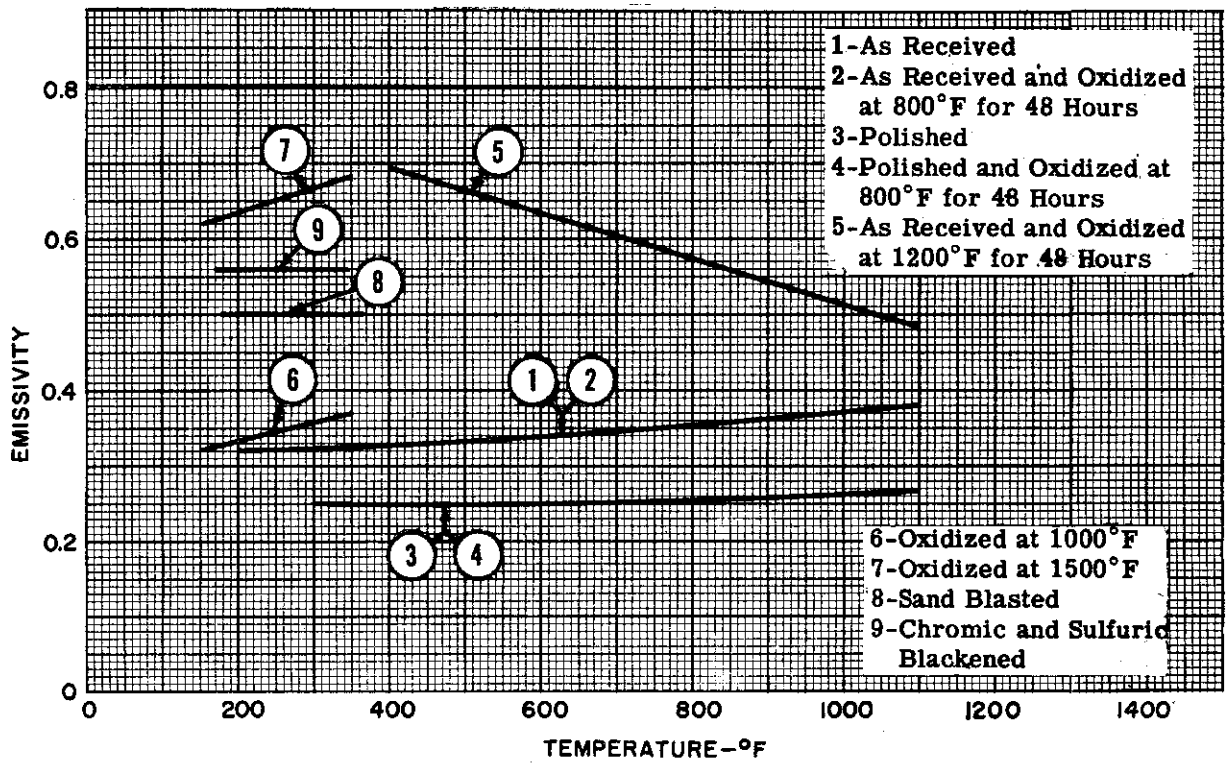

Figure 2.3-6. Emissivity of Stainless Steel

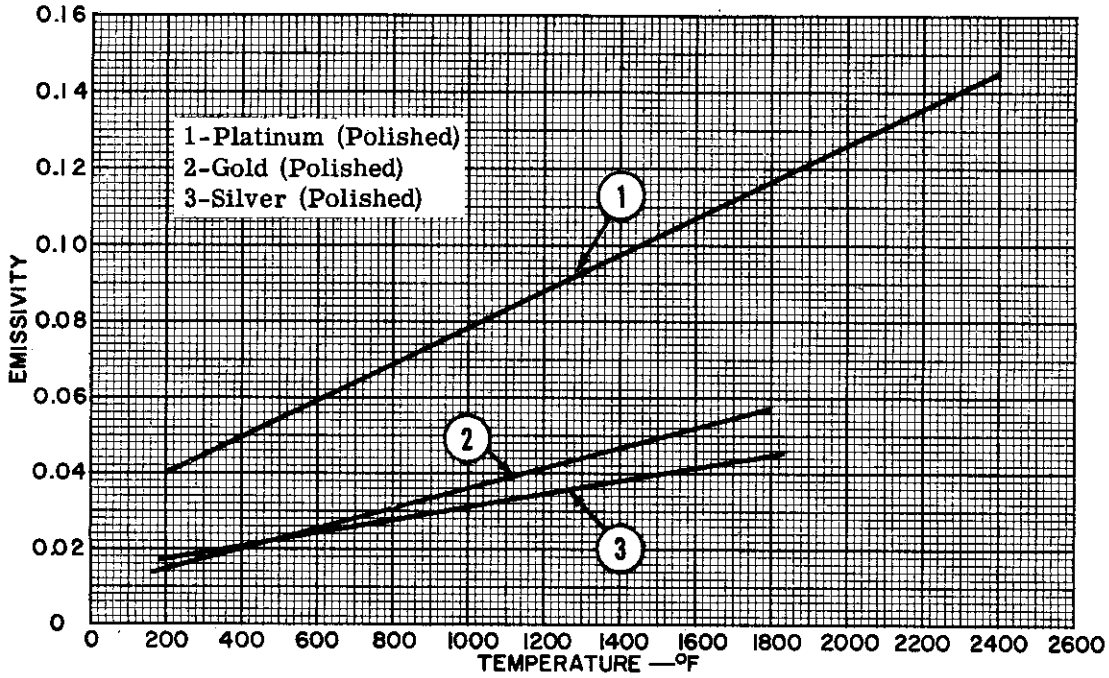

Figure 2.3-7. Emissivity of Precious Metals

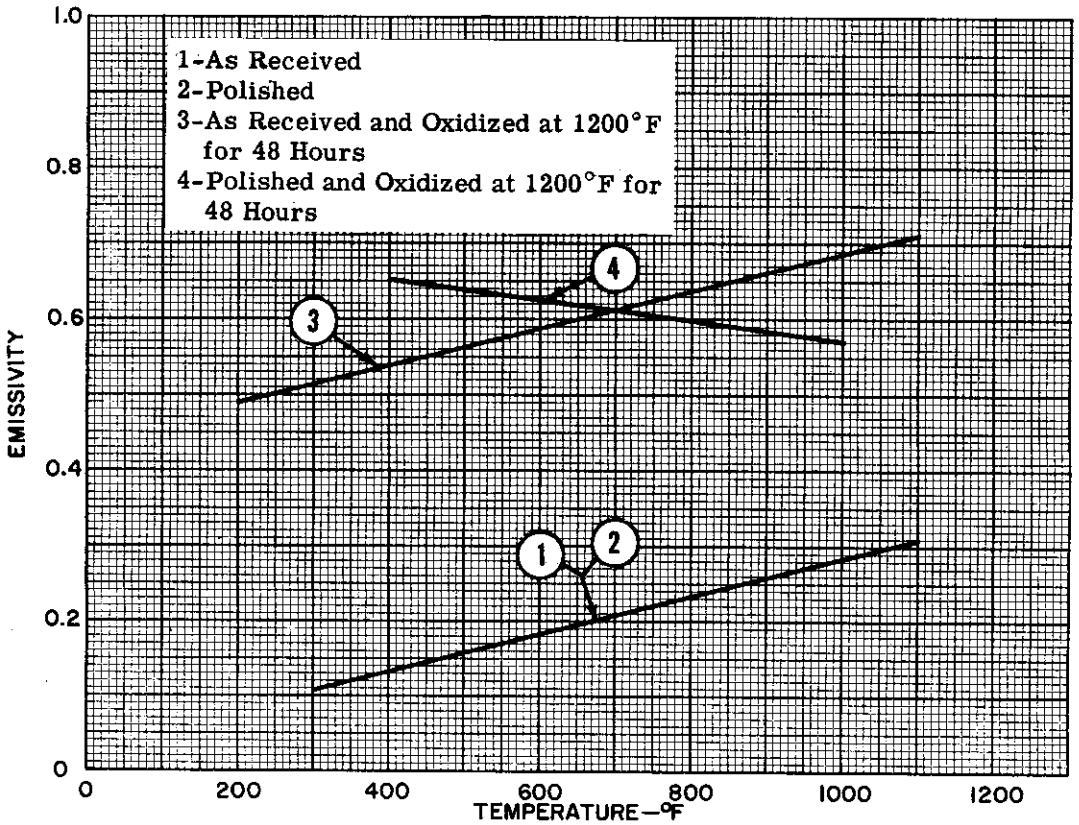

Figure 2.3-8. Emissivity of Monel

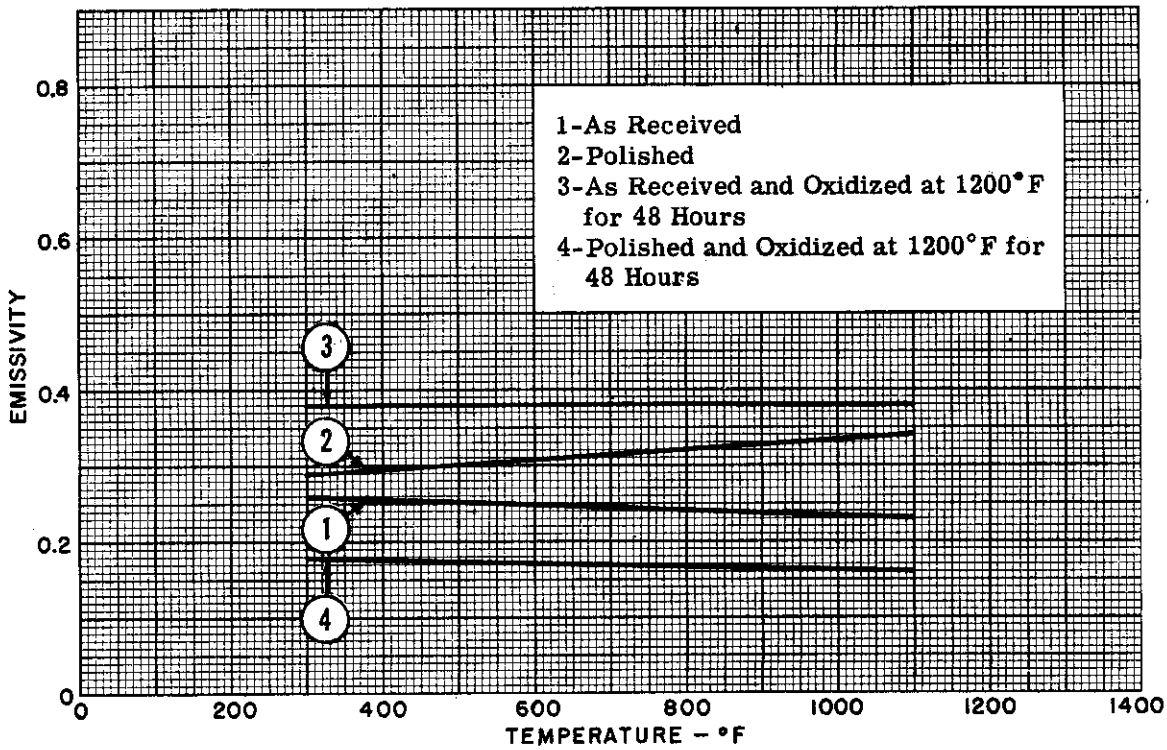

Figure 2.3-9. Emissivity of Inconel X

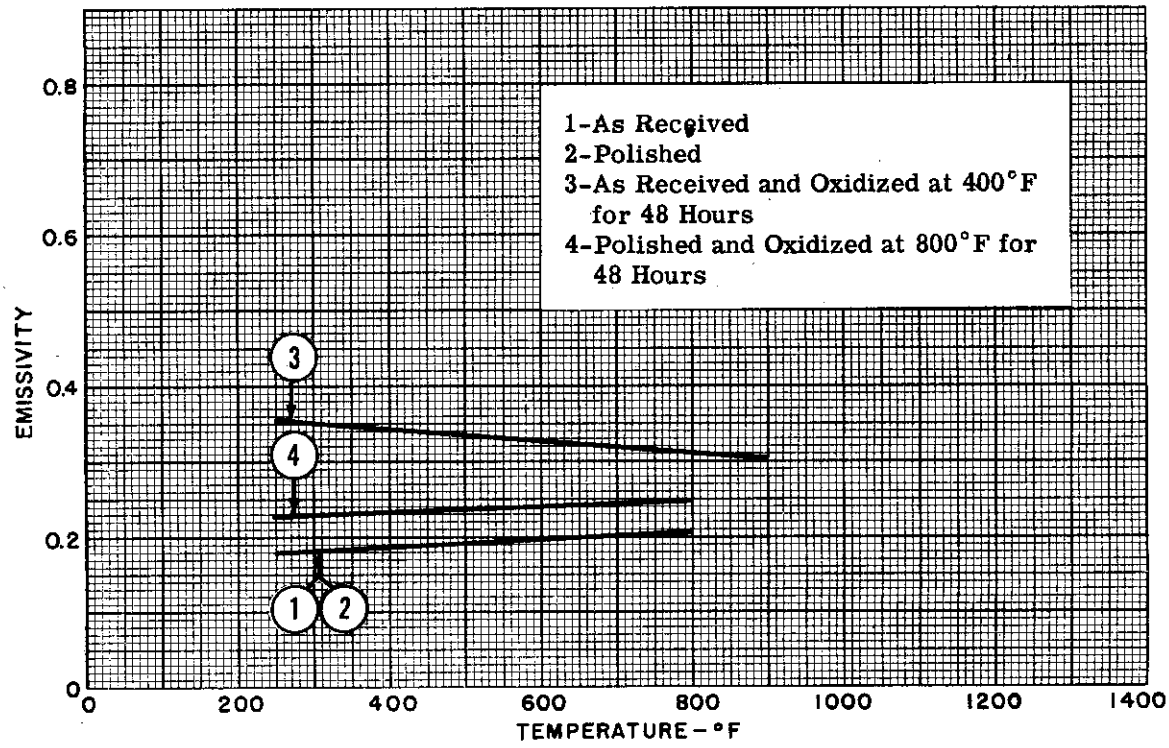

Figure 2.3-10. Emissivity of Titanium

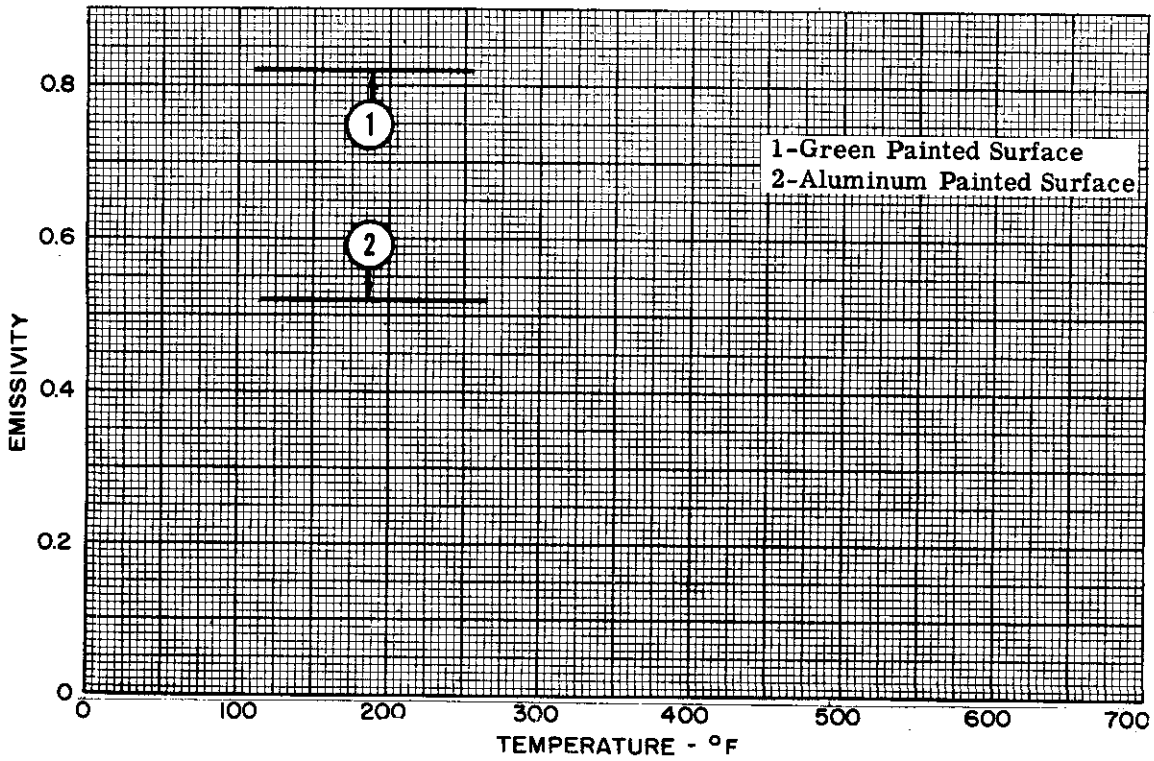

Figure 2.3-11. Emissivity of Painted Nonmetallic Surfaces

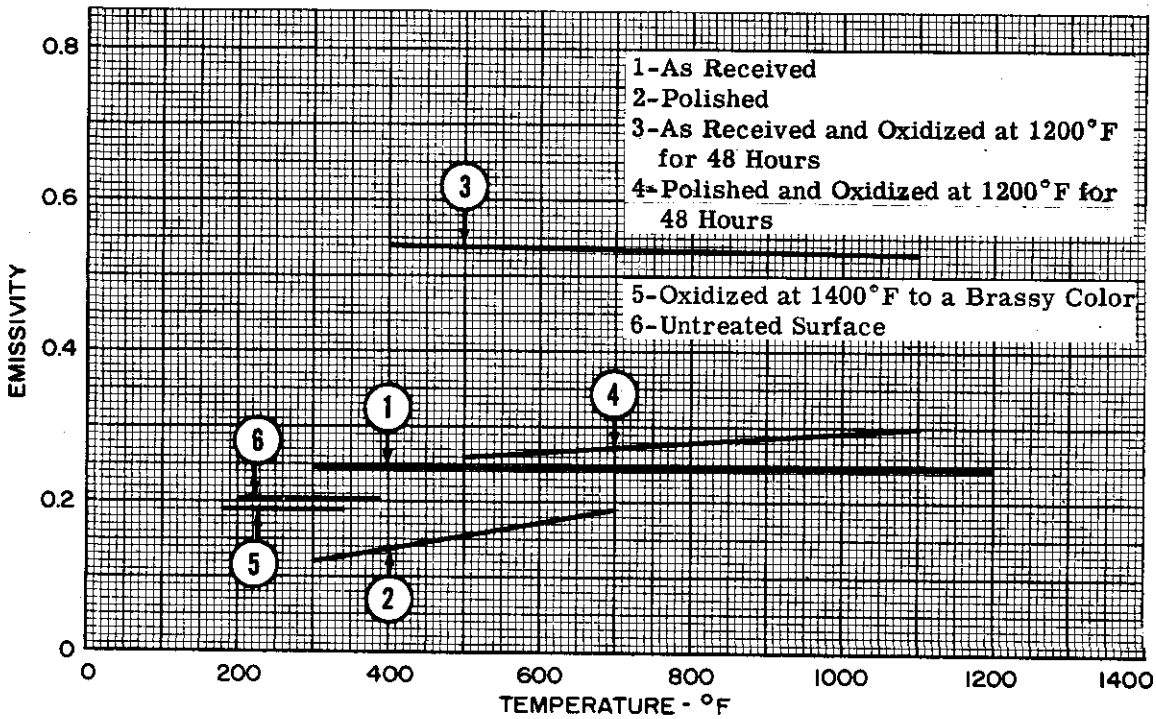

Figure 2.3-12. Emissivity of Inconel

2.4 COOLING

To assist in the design of structural cooling systems, Figures 2.4-1 and 2.4-2 show the total heat capacity of various coolants, plotted against temperature. Two levels of cooling effort are anticipated with these curves. For systems absorbing a relatively small heat flux, such as may occur when cooling is used in combination with insulation, Figure 2.4-1 applies. Utilizing these coolants permits low structural temperatures and, hence, the use of standard aluminum alloys as structural material. For regions of high-intensity heat flux, such as occur at leading edges during flight at high Mach numbers, the large heat capacity of the light metals, as shown in Figure 2.4-2, is desirable. For each material, this graph indicates the vapor pressure at two extreme temperatures; vapor pressures at intermediate temperatures are given in Figures 2.4-3 through 2.4-5.

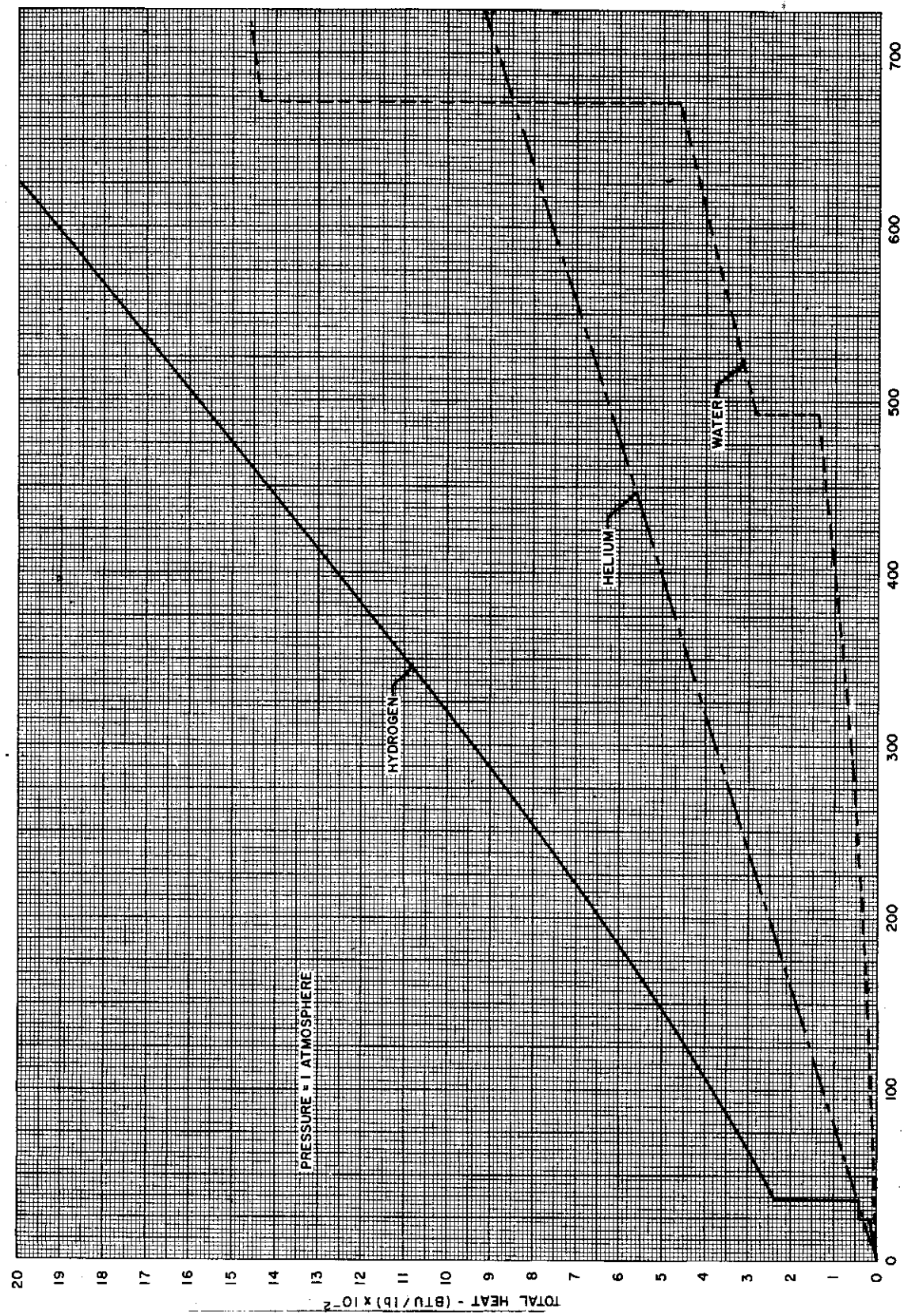

Figure 2.4-1. Heat Capacity of Various Coolants

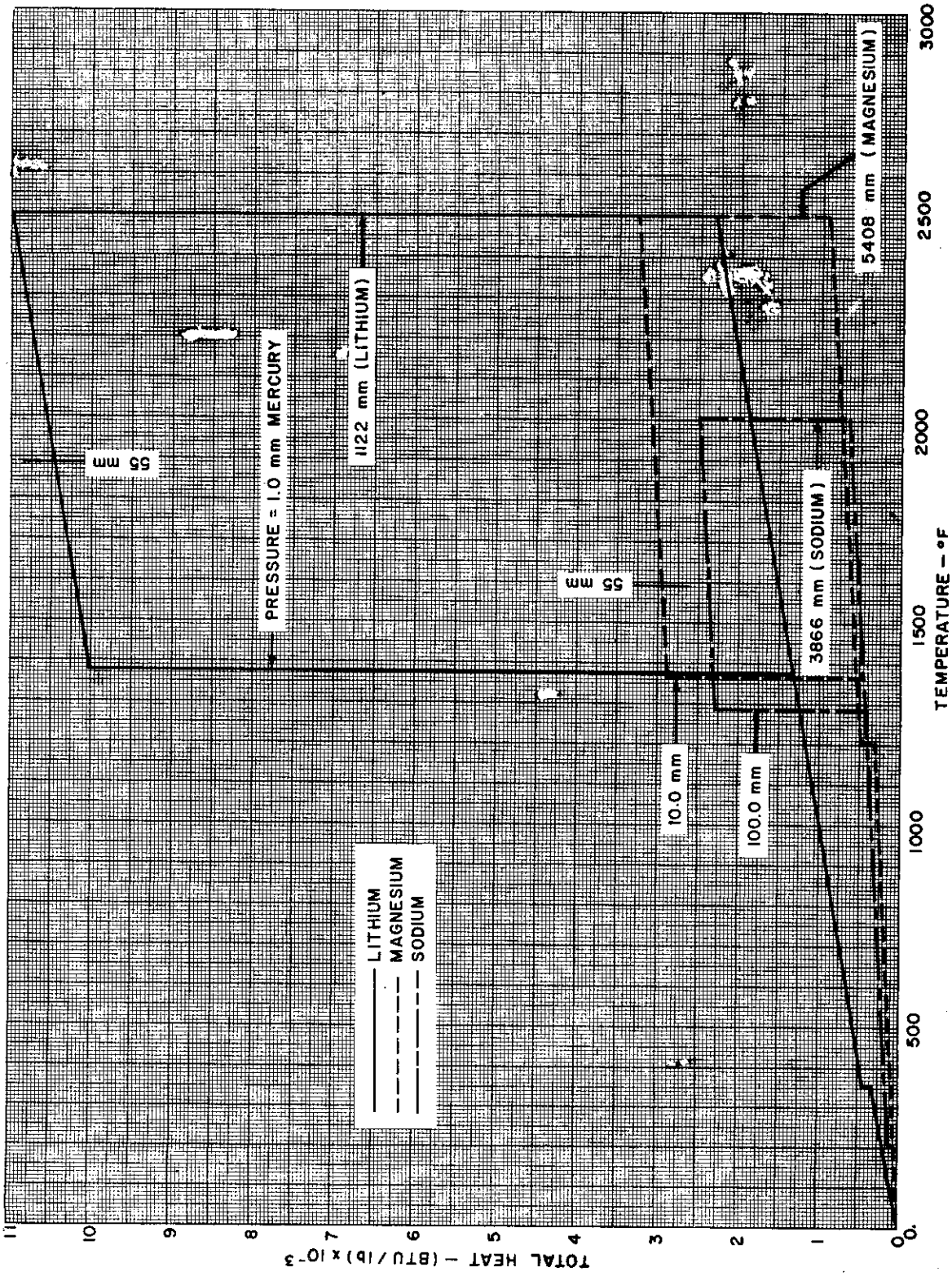

Figure 2.4-2. Heat Capacity of Various Coolants

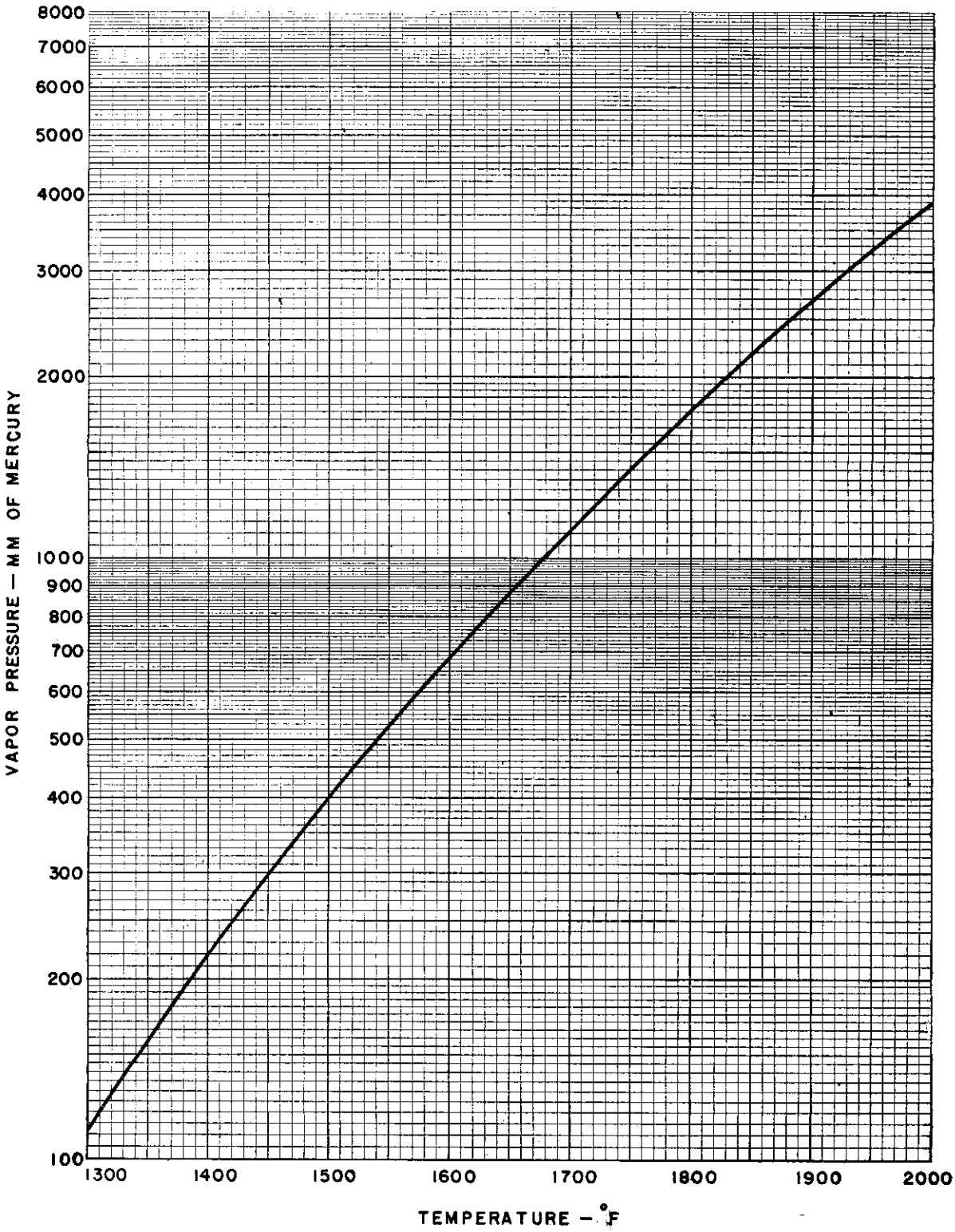

Figure 2.4-3. Vapor Pressure vs. Temperature — Sodium

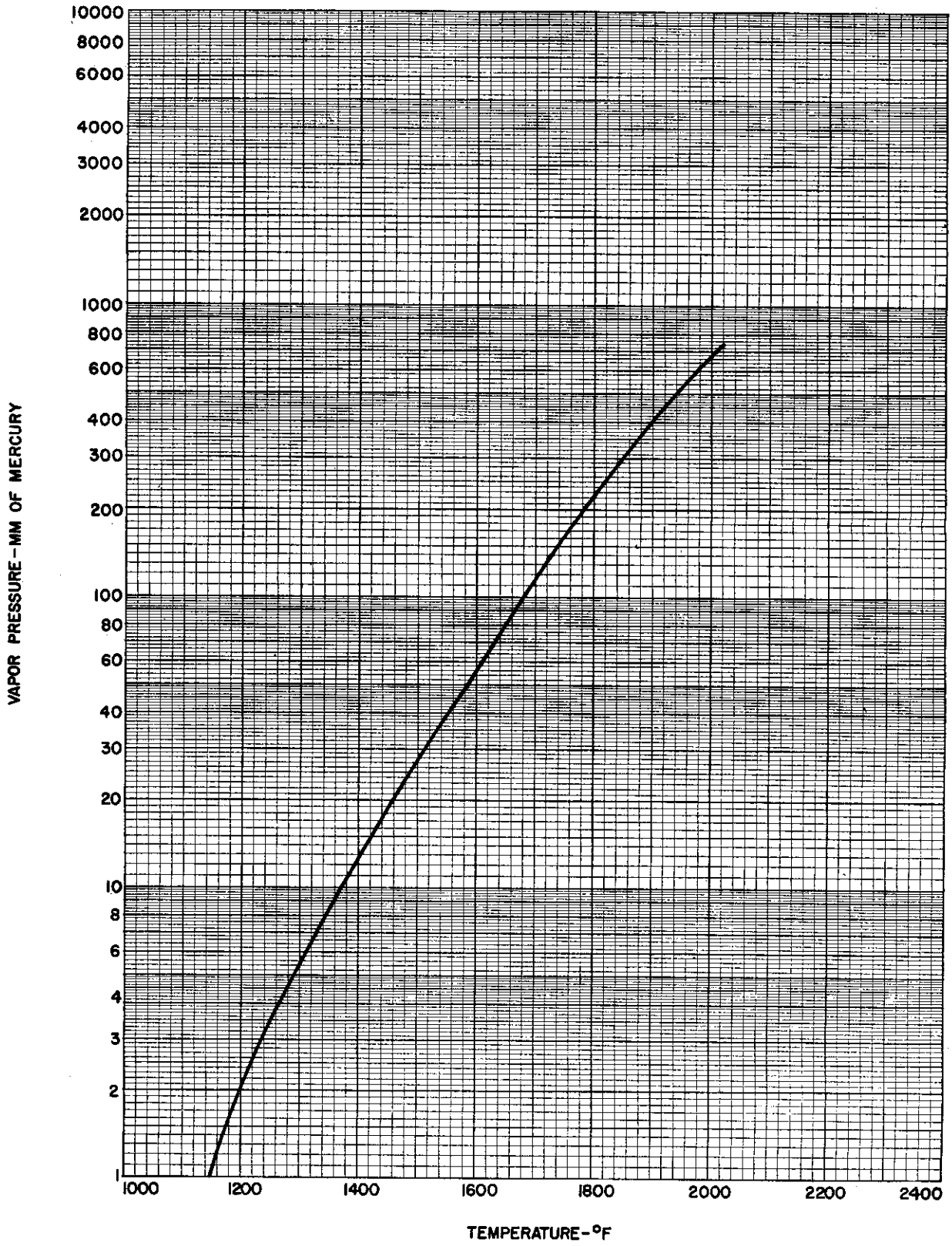

Figure 2.4-4. Vapor Pressure vs. Temperature — Magnesium

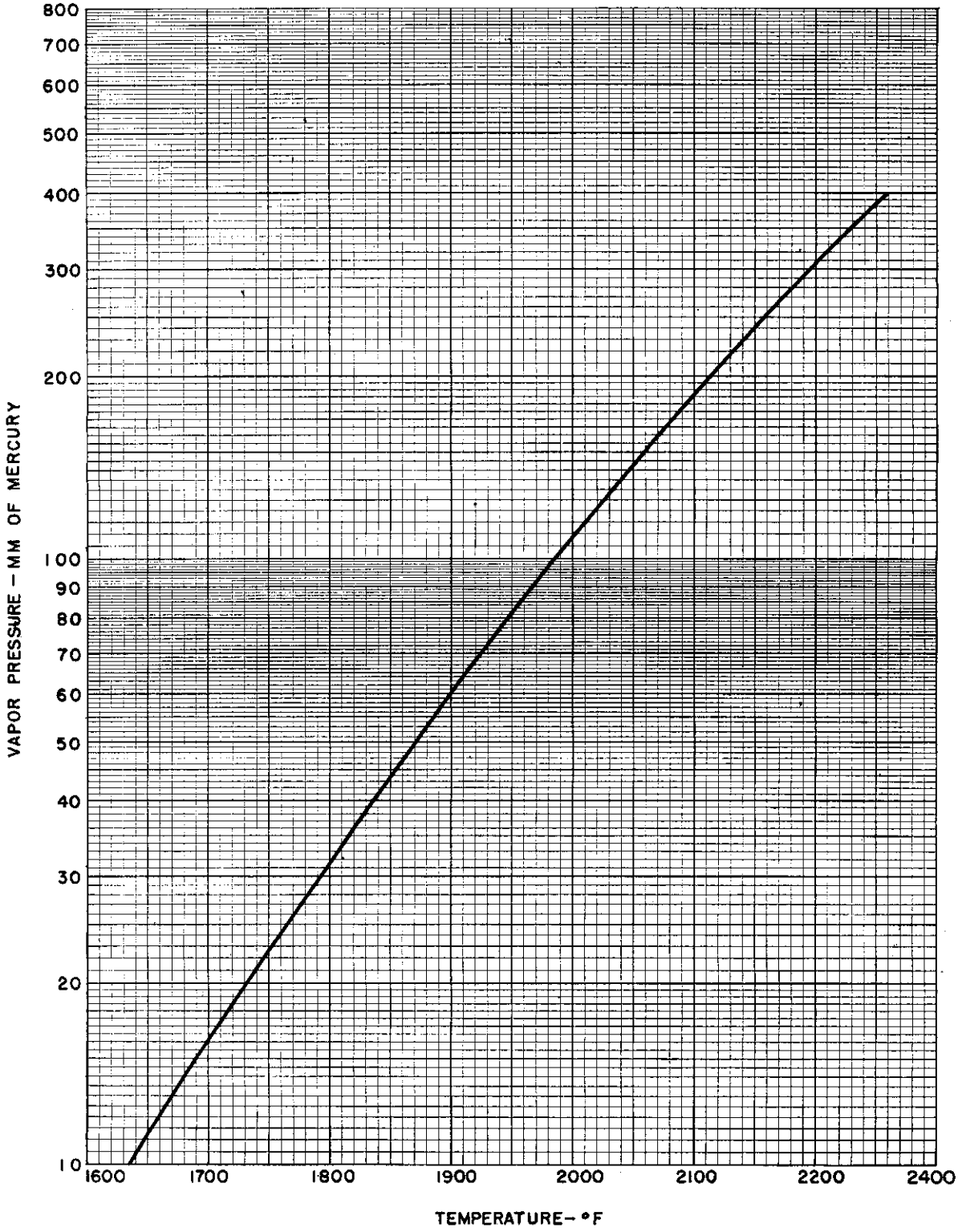

Figure 2.4-5. Vapor Pressure vs. Temperature — Lithium

[redacted]

SECTION 3.0

TEMPERATURE GRADIENTS AND THERMAL STRESSES

By M. A. Brull and M. A. Goldberg

[redacted]

[redacted]

[redacted]

TABLE OF CONTENTS

NOMENCLATURE

a = thermal diffusivity of section material = $\frac{k}{wc} \times 1.93 \times 10^{-6}$ (in.^{2}/sec)

A = total cross-sectional area of T section (in.^{2})

b_s = width of skin element of T section (in.)

b_w = web depth (in.)

c = specific heat of structural material (BTU/lb°F)

E = modulus of elasticity of structure material (lb/in.^{2})

h = heat transfer coefficient (BTU/ft^{2}hr°F)

h_e = effective heat transfer coefficient for structural joint (BTU/ft^{2}hr°F)

i = subscript indicating skin station (i = 1, 2,..6)

j = subscript indicating web station (j = I, II,..IV)

k = thermal conductivity of structure material (Btu in./ft^{2}hr°F)

M = joint resistance ratio = $\frac{2k}{b_s h_e}$

$P = 2\tau_s / b_s$

$R = 2b_w / b_s$

$S = \tau_w / 2\tau_s$

t_i = temperature in the ith skin element (°F)

T_a = initial structural temperature (°F)

T_j = temperature in the jth web element (°F)

T_{aw} = adiabatic wall temperature (°F)

u_{av} = weighted average temperature ratio

$u_i = t_i / T_{aw}$

$v_j = T_j \ T_{aw}$

w = specific weight of structural material (lb/in.^{3})

α = coefficient of expansion of structure material (in./in.°F)

$\delta = h(b_2/2)/k$ = dimensionless heat transfer

$\bar{\theta}$ = time (sec)

[redacted]

NOMENCLATURE (cont)

$\theta = a\bar{\theta}/(b_s/2)^2$ = dimensionless time

$\bar{\sigma}_i = \sigma_i / \alpha E T_{aw}$ = dimensionless thermal stress

σ_i = thermal stress at station i or j

σ_s = maximum thermal stress in skin

σ_w = maximum thermal stress in web

τ_s = skin thickness (in.)

τ_w = web thickness (in.)

[redacted]

[redacted]

SECTION 3.0

TEMPERATURE GRADIENTS AND THERMAL STRESSES

3.1 GENERAL

When a conventional airframe structure is heated externally by convective heating from the boundary layer, there is an appreciable time lag before the heat penetrates to the interior of the structure, so that temperature gradients are established. Because of the resulting differential expansion of the structure, thermal stresses are produced. Similar, but reversed, conditions exist during deceleration of an aircraft when the temperature of the outer skin is reduced rapidly by the cool boundary layer of lower speeds, while the internal structure remains hot.

These temperature gradients are clearly transient and will vanish if the aircraft flies at a speed, angle of attack, and altitude that are constant for a sufficient length of time. Additional temperature gradients are produced by differences in heating conditions over the surface of the aircraft, but these gradients vary with time only to the extent that external aerodynamic conditions change, and may therefore be calculated by the methods of Section 1.0. Methods are given in this section by which temperature gradients and thermal stresses, resulting from the resistance of the structure to heat conduction, may be readily calculated.

Evidently, the environmental conditions of Mach number, altitude, angle of attack, and type of flow not only vary continuously during a transient type of flight condition, but are dependent on the flight plan for the particular aircraft. Clearly, there is an infinite number of flight plans, considering all types of aircraft. The conduction problem is dealt with in a generalized manner, therefore, by first considering the case of constant environmental conditions; that is, the aircraft is assumed to start and continue its flight at steady values of Mach number, altitude, etc. Methods are then presented by which approximate temperature gradients and thermal stresses can be obtained for the practical case of variable environmental conditions, by using the solutions for constant conditions.

Since the internal conduction problem is time-dependent, it leads to a linear, partial differential equation of the second order. The boundary conditions imposed by the convective heat input and the geometric shape of the structure make it impractical to solve this equation analytically as each specific case arises, but electrical computing machines have been used successfully to solve it for a wide range of conditions. In this section, these numerical results are given for both temperature distributions and thermal stresses. It should be noted that these results apply only to a structure heated convectively. Errors arise if the surface temperature reaches a value where radiation from the surface is significant. However, this is not an important limitation since an aircraft capable of reaching such speeds will probably be forced, by the thermal stress problem, to use unconventional structure.

To present valid results for the widest possible range of structures, such as integral and non-integral multiweb beams, skin stringer and stiffened panel construction, and ring-stiffened shells, the problem is idealized by considering a structure composed of a series of T sections as shown in the following diagram. In the idealization, isolating cuts are made at points where no heat flow occurs chordwise along the skin and also in the case of a multiweb wing, at the plane of symmetry. This latter case neglects the differences in aerodynamic conditions between upper and lower surfaces, and it is further assumed that the aerodynamic flow is two-dimensional so that no spanwise heat flow occurs.

[redacted]

[redacted]

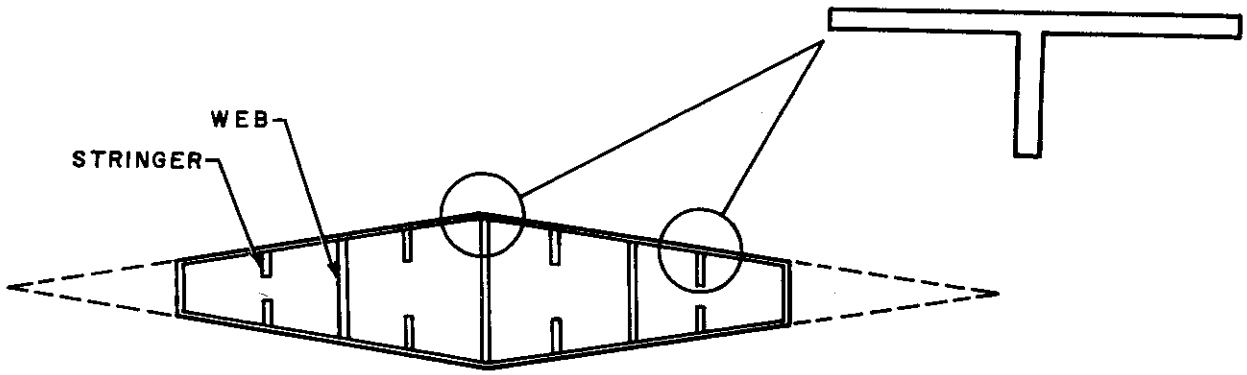

It has been found experimentally in a built-up structure that the conventional type of riveted or bolted joint produces an important additional resistance to heat flow across the interface between adjacent surfaces. To treat both integral and attached stiffeners simultaneously, the formulation of the heat flow problem provides for a thermal joint resistance between the skin and the web of the T section.

The geometric proportions of the T section are conveniently expressed by three nondimensional parameters R, S, and P, while the aerodynamic heat input conditions are represented by the nondimensional parameter δ. Various joint resistances are accounted for by the parameter M. For perfect conduction between the skin and web, M is equal to zero; for a perfectly insulated joint, M becomes infinite. It is shown in Part II that δ and P need not be considered separately and that temperatures and stresses depend only upon δ / P.

The temperature calculations, carried out generally and for a wide range of values of the parameters R, δ/P, and M, are presented in Section 3.2. Only one value of S is included since this parameter has been shown, in Part II, to have a small effect on temperature gradients.

In the case of thermal stresses, it is not possible to present completely generalized results because the thermal stresses depend not only upon the local geometry of the member being studied, but also upon the restraint conditions existing within the structure. In Section 3.3, maximum thermal stresses are presented for the most frequently encountered configurations, while methods are available in Part II to carry out thermal stress calculations for any other case. Such calculations may be based upon the temperature data of Section 3.2.

As discussed previously, these procedures are developed for the case of constant aerodynamic conditions, that is, constant boundary layer temperature and constant heat transfer coefficient, whereas in the practical case these functions vary with time. The problem of temperature gradients with a varying heat transfer coefficient is presently solved for one particular case (see Part II). A simple numerical procedure is given in Section 3.4 for the case of constant heat transfer coefficient and varying boundary layer temperature. This method is used in conjunction with the temperature curves of Section 3.2.

3.2 TEMPERATURE GRADIENTS

Curves of temperature versus time are presented in Figures 3.2-1 through 3.2-20 for the elemental structural T section. Temperatures are given in dimensionless form by expressing them as a ratio of the boundary layer temperature, T_{aw} and assuming that initial temperatures are zero. The curves are extended sufficiently in time to give the maximum stresses of Section 3.3. Time is also expressed in dimensionless form by the term θ which is defined in the nomenclature preceding Section 3.1.

[redacted]

[redacted]

The temperature curves were obtained from a lumped mass-heat-flow analysis in which the T was divided into 15 elements as shown in the following diagram. Also shown is the notation used for these elements, and the points at which temperatures are given are identified. The diagram also gives the geometry of the T section and summarizes the dimensionless parameters.

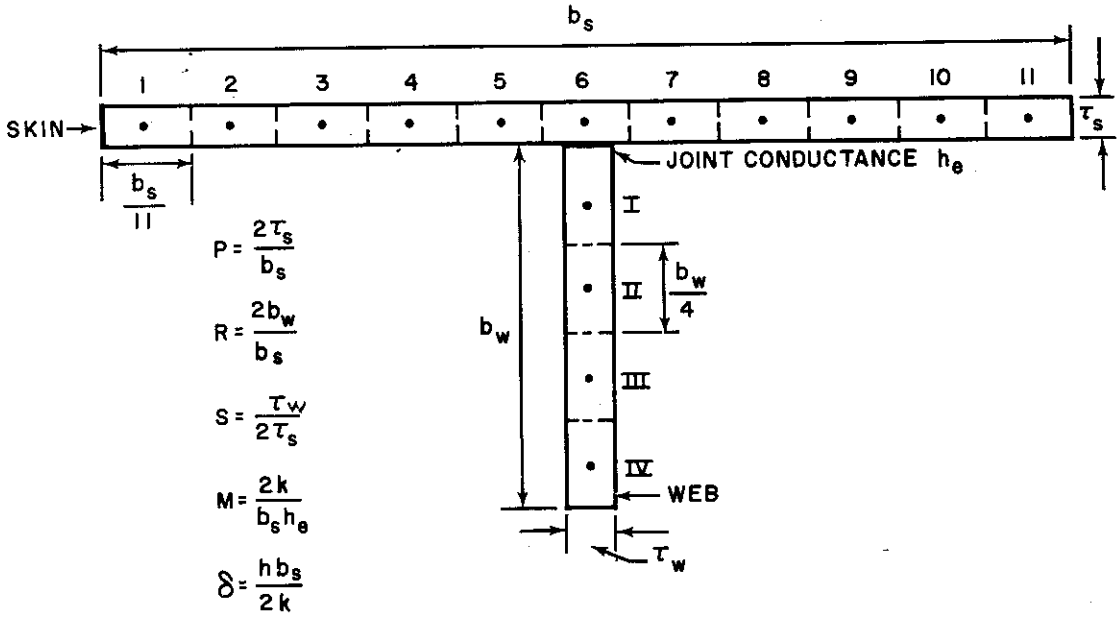

TEMPERATURES GIVEN AT
POINTS 1, 6, I, II, III, IV

Although experimental data on joint resistance are meager, Part II summarizes all that is available. The data are generally expressed as a conductance in terms of heat flow per unit of contact area. For the calculation of the parameter M, it must be modified to an effective value, h_e to account for the difference between the actual contact area of the flange and the thickness of the web. This is done by increasing the conductance of the joint by the ratio of flange width to web thickness.

Also, in a typical riveted construction, some allowance must be made for the heat capacity and conduction path added by the interface flange. It is recommended that the dimension b_w be taken around the flange to the rivet centerline. When an outstanding flange exists, its developed length should similarly be added to b_w.

EXAMPLE

The skin-stringer element shown in the following diagram is convectively heated by a boundary layer having a temperature of 900°F and a heat transfer coefficient of 30 BTU/ft^{2}hr°F. The material is 18-8 stainless steel which has a thermal conductivity of 134 BTU in./ft^{2}hr°F, a specific heat of 0.133 BTU/lb°F, and a density of 0.29 lb/in.^{3}. The thermal conductance across the joint is assumed to be 40 BTU/ft^{2}hr°F. Find the temperature at point A after 200 seconds.

[redacted]

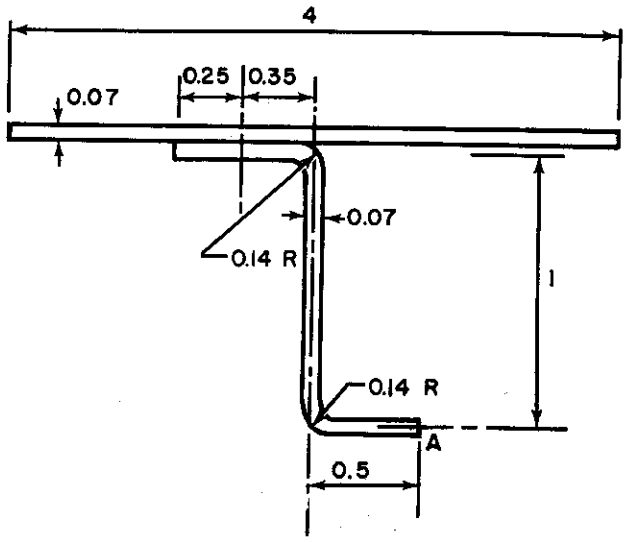

ALL DIMENSIONS IN INCHES.

Assume contact width at joint is 0.45 in. so that $h_e = 40 \times \frac{0.45}{0.07} = 257$ BTU/ft^{2}hr°F. Then, $M = \frac{2 \times 134}{4 \times 257} = 0.26$. From the diagram, $b_w = 0.46 + 0.72 + 0.21 + \pi \times 0.14 = 1.83$ in. Calculating the nondimensional parameters gives

$$\delta = \frac{h}{k}(b_s/2) = \frac{30 \times 2}{134} = 0.448,$$

$$P = \frac{2\tau_s}{b_s} = \frac{2 \times 0.07}{4} = 0.035,$$

$$\delta/P = 0.448/0.035 = 12.8,$$

$$S = \tau_w/2\tau_s = 0.50, \text{ and}$$

$$R = 2b_w/b_s = 2 \times 1.83/4 = 0.965.$$

Thermal diffusivity of material $= \frac{k}{wc} \times 1.93 \times 10^{-6} = \frac{134 \times 1.93 \times 10^{-6}}{0.29 \times 0.133} = 0.00671$ in.^{2}/sec. For a time of 200 seconds, $\theta = \frac{0.00671 \times 200}{4.0} = 0.335$.

Considering the available data, it will be assumed to a close approximation that $M = 0.25$ and $R = 1.0$. Then, from Figure 3.2-7, for $\delta/P = 8.0$, the temperature ratio at point A equals 0.130, and from Figure 3.2-11, for $\delta/P = 16.0$, the temperature ratio equals 0.185. Interpolating linearly, for $\delta/P = 12.8$, the temperature ratio becomes 0.163.

The boundary layer temperature is 900°F, so that the temperature rise at point A = 0.163 x 900 = 147°F.

Note that, at the same time, the maximum temperature reached in the skin is approximately 0.83 x T_{aw} = 747°F, so that a gradient of 600°F exists across the stringer.

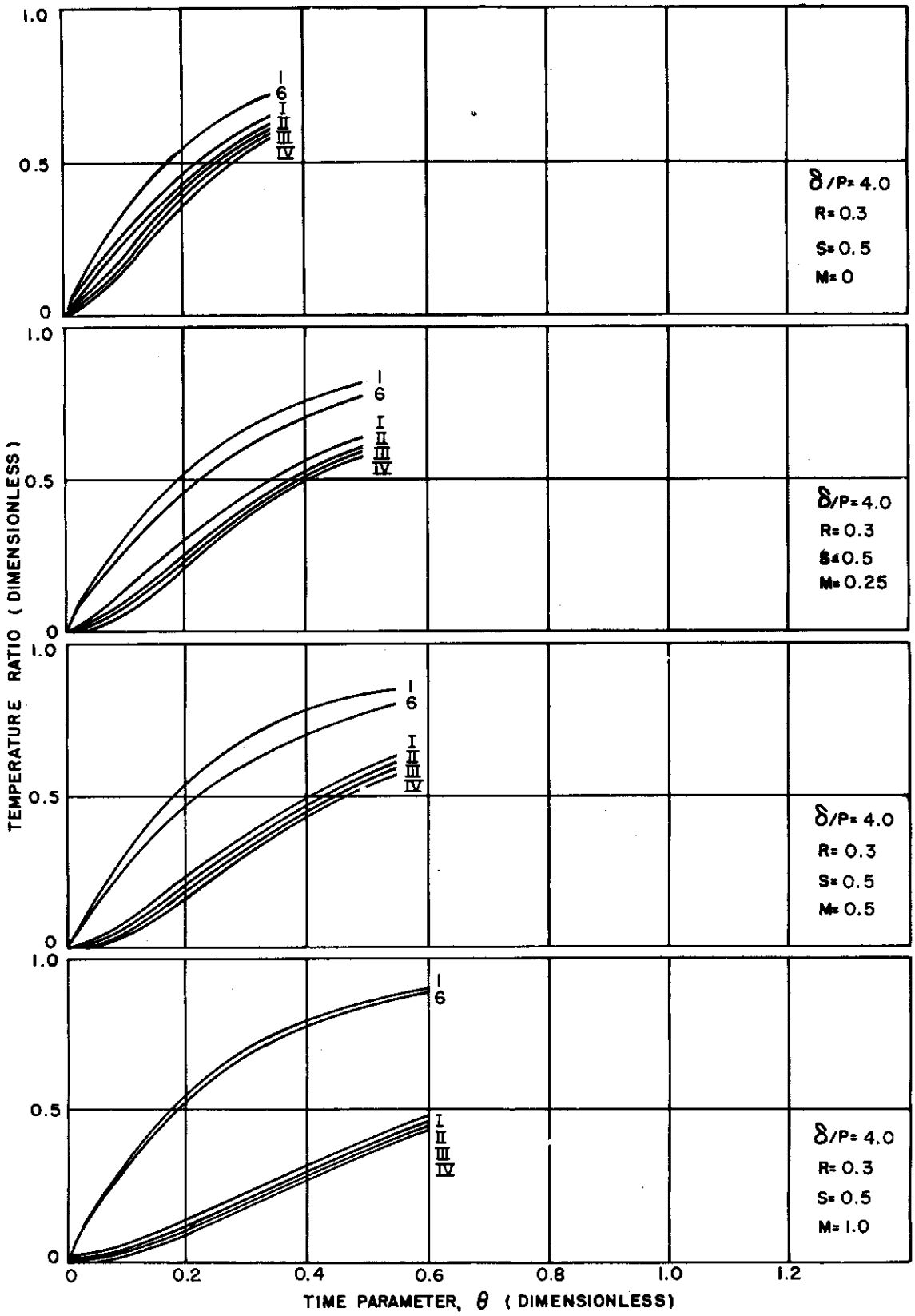

Figure 3.2-1. Temperature Gradients in a Structural T Section

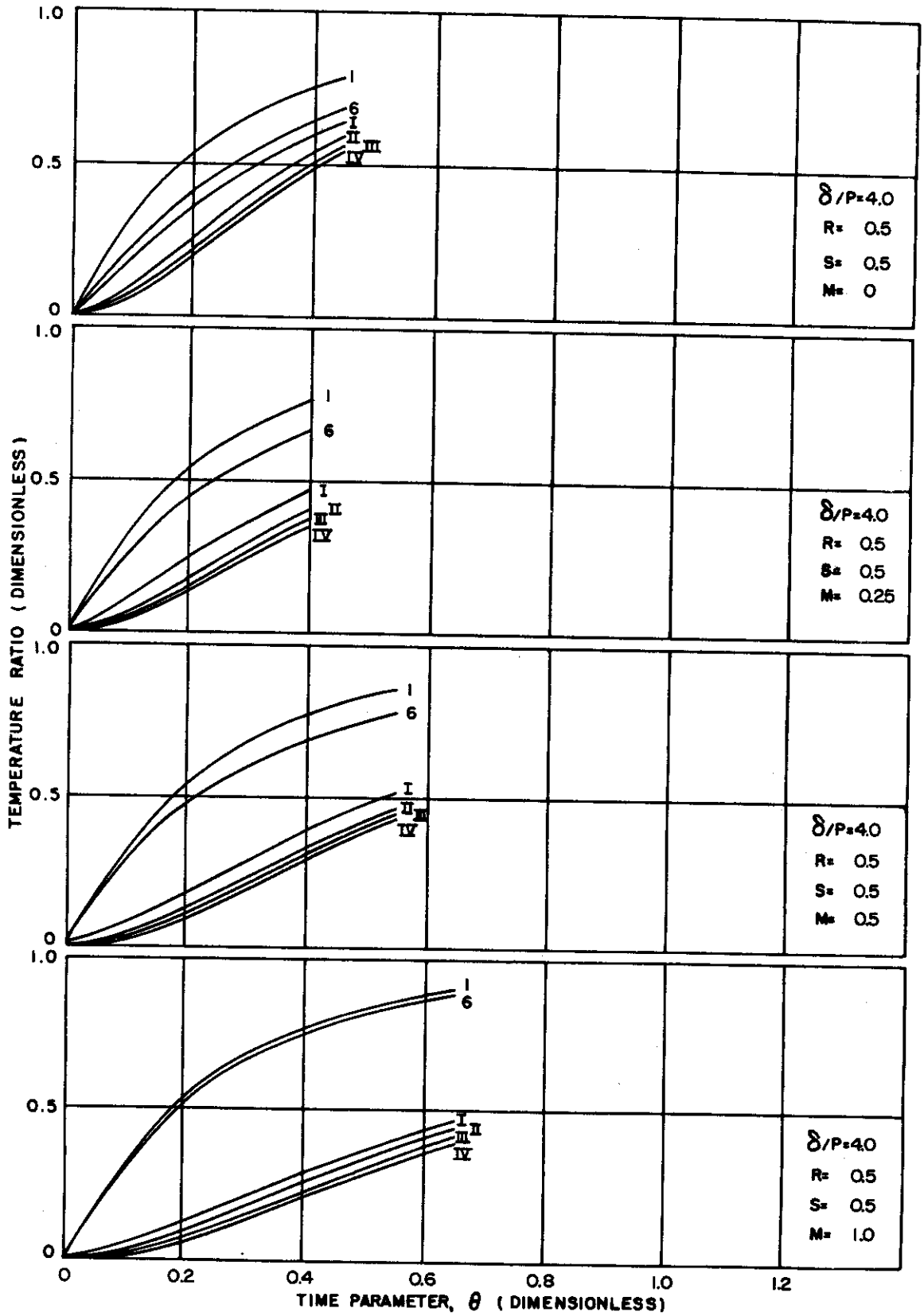

Figure 3.2-2. Temperature Gradients in a Structural T Section

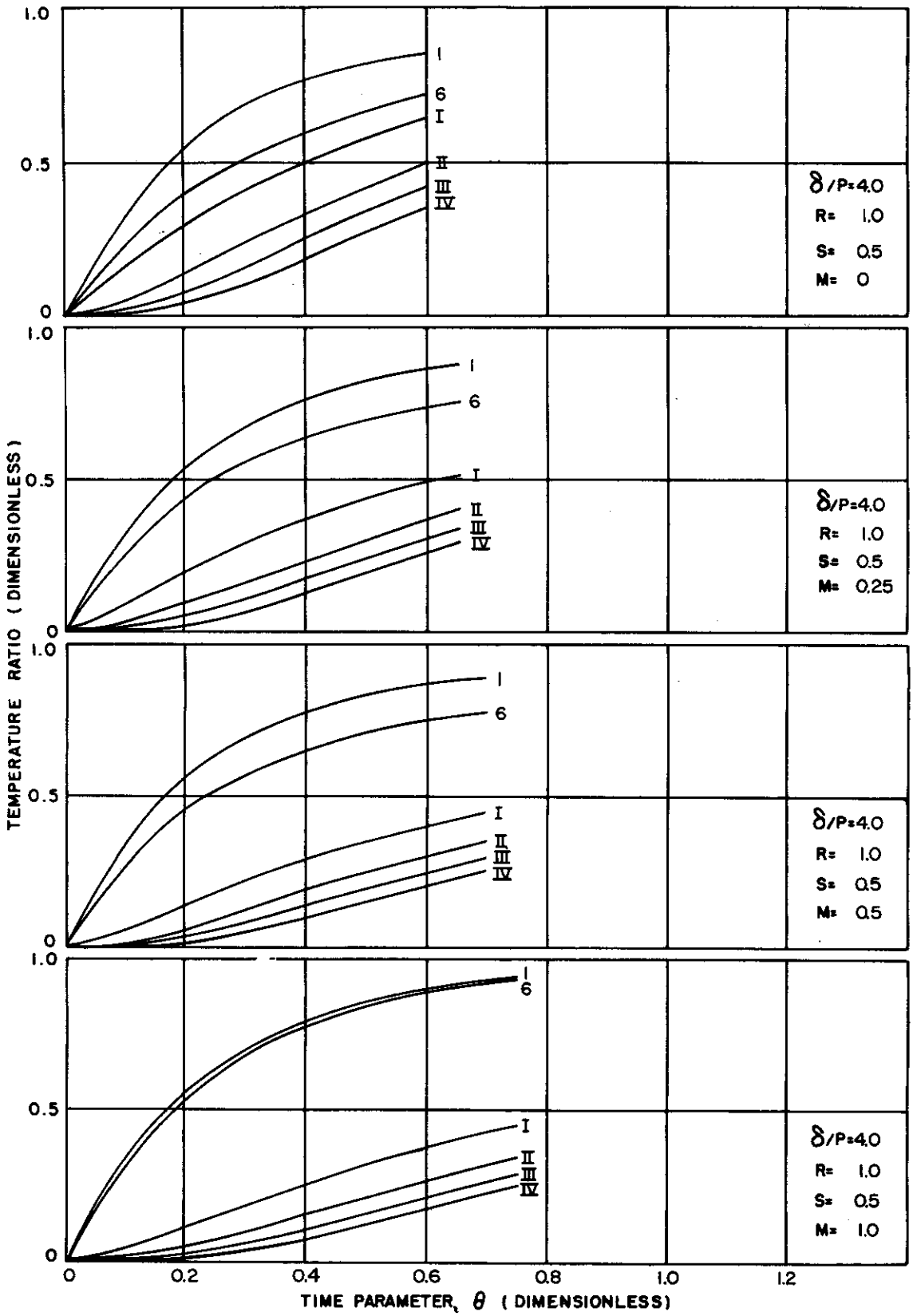

Figure 3.2-3. Temperature Gradients in a Structural T Section

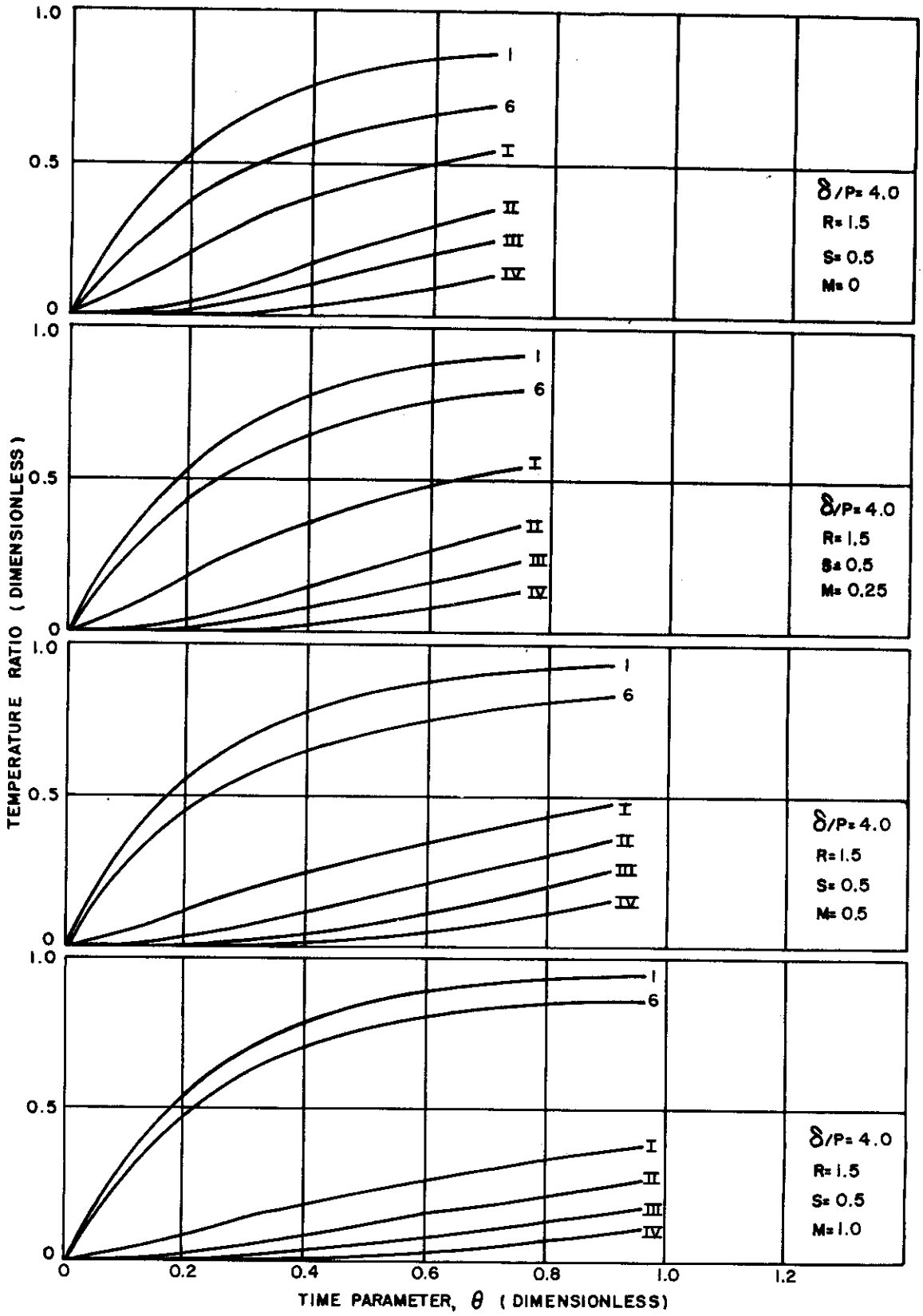

Figure 3.2-4. Temperature Gradients in a Structural T Section

[redacted]

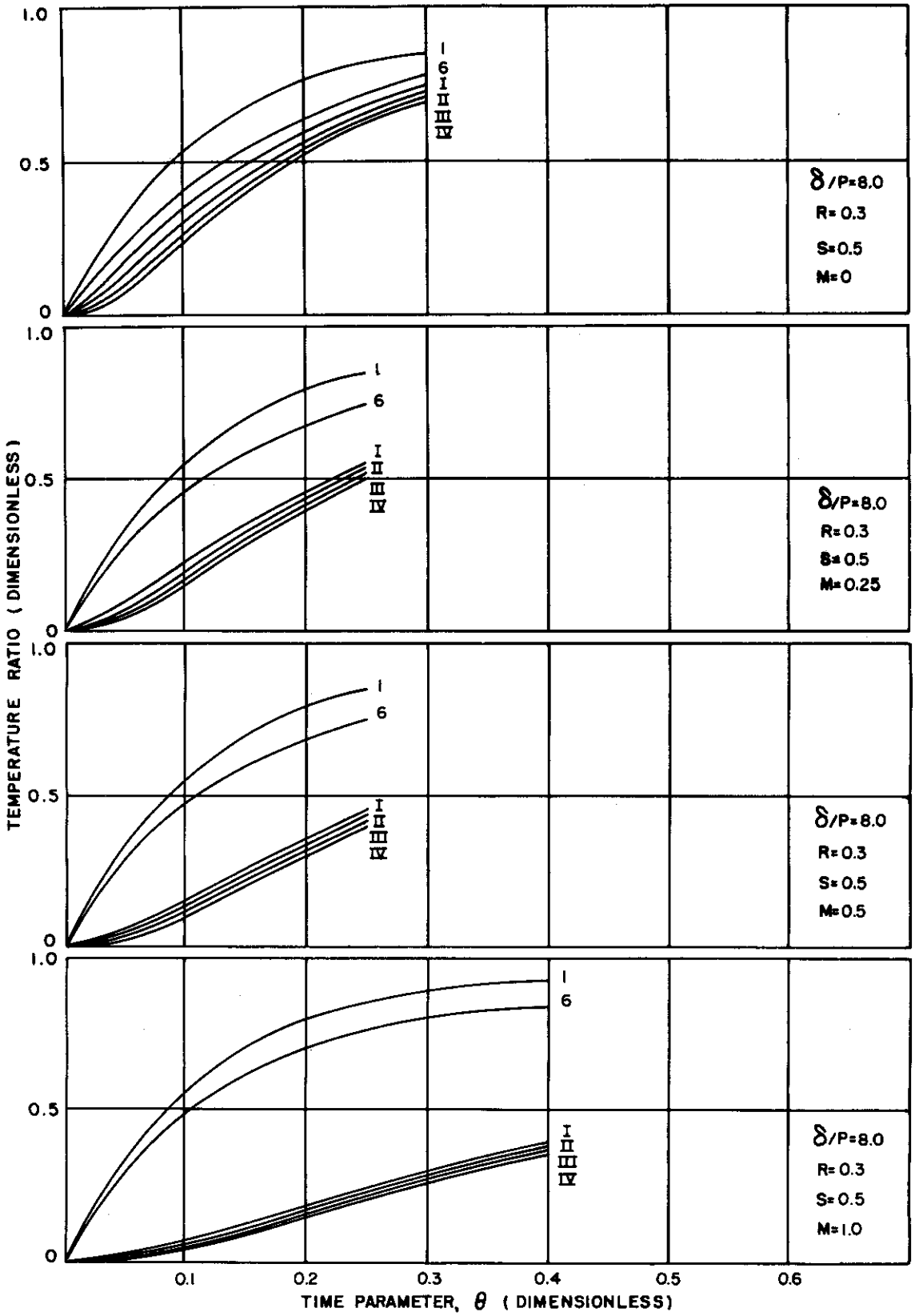

Figure 3.2-5. Temperature Gradients in a Structural T Section

[redacted]

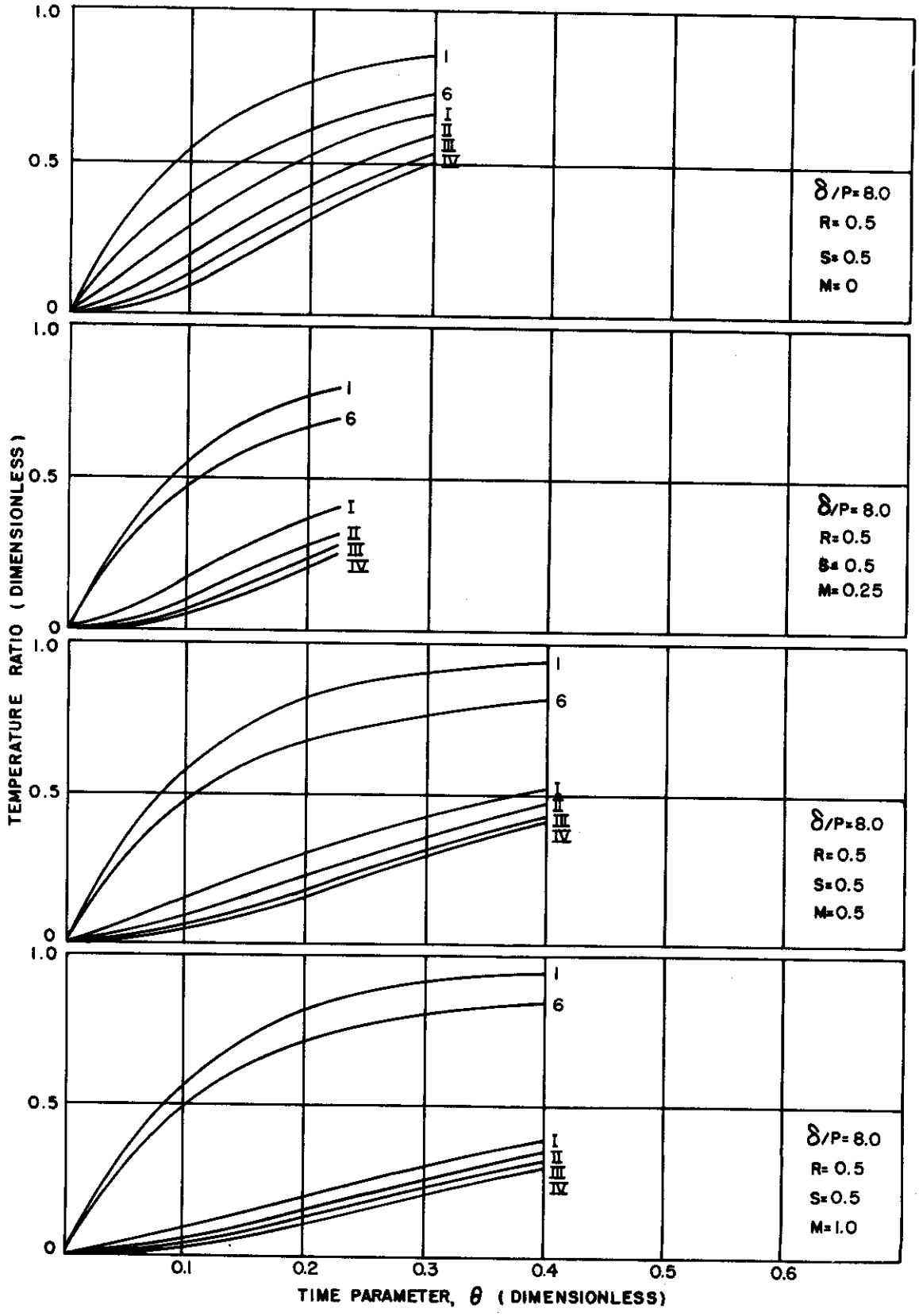

Figure 3.2-6. Temperature Gradients in a Structural T Section

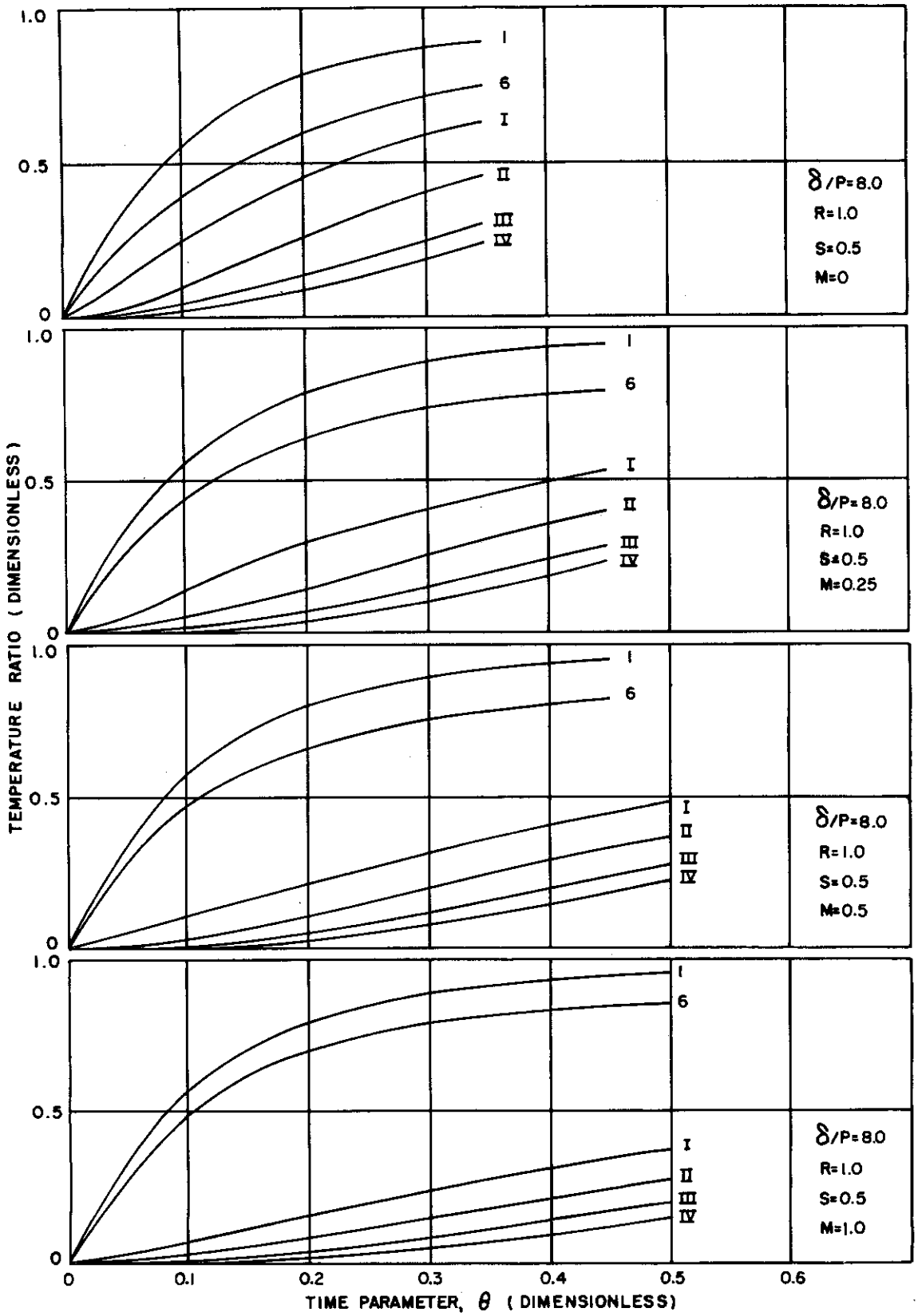

Figure 3.2-7. Temperature Gradients in a Structural T Section

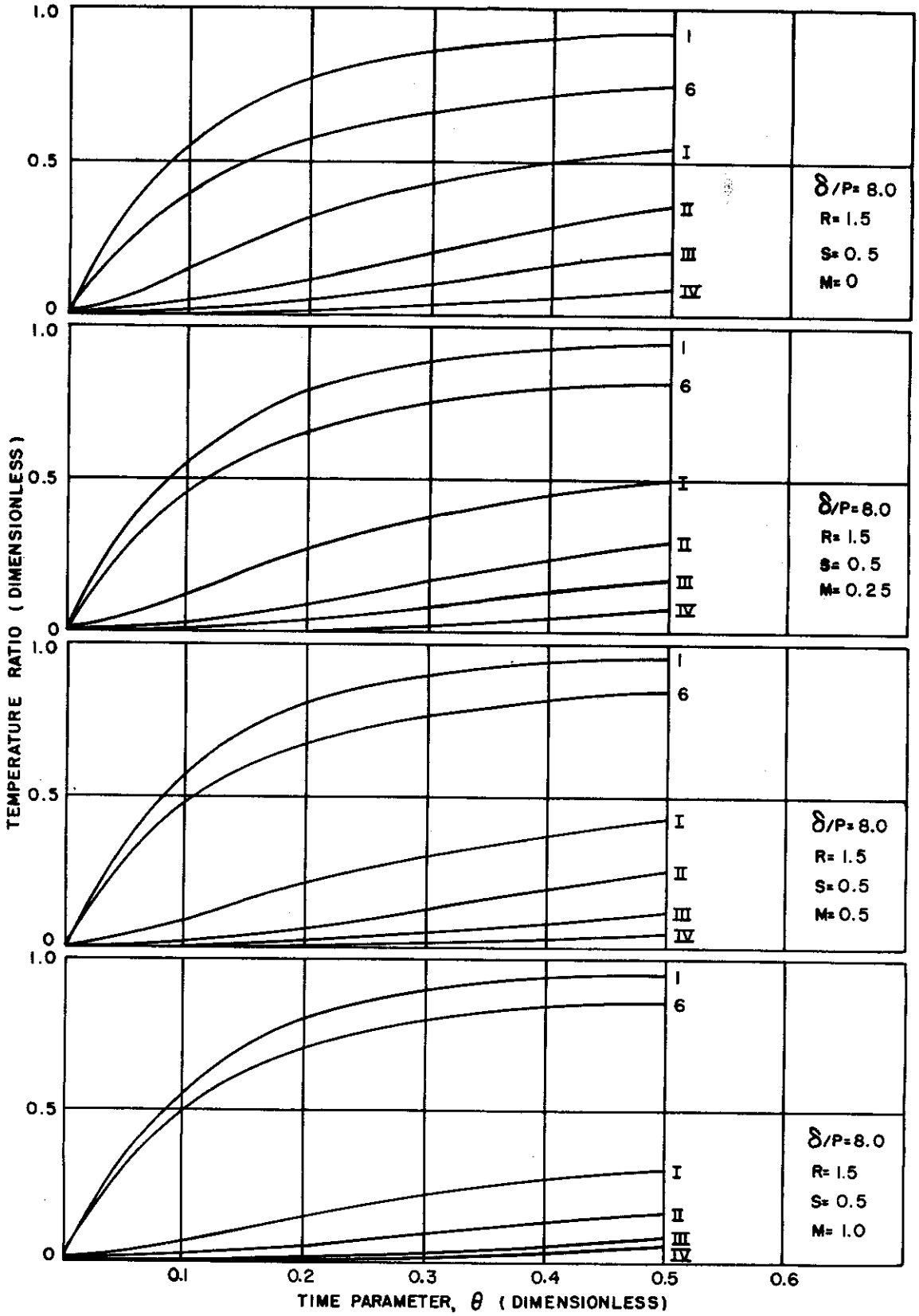

Figure 3.2-8. Temperature Gradients in a Structural T Section

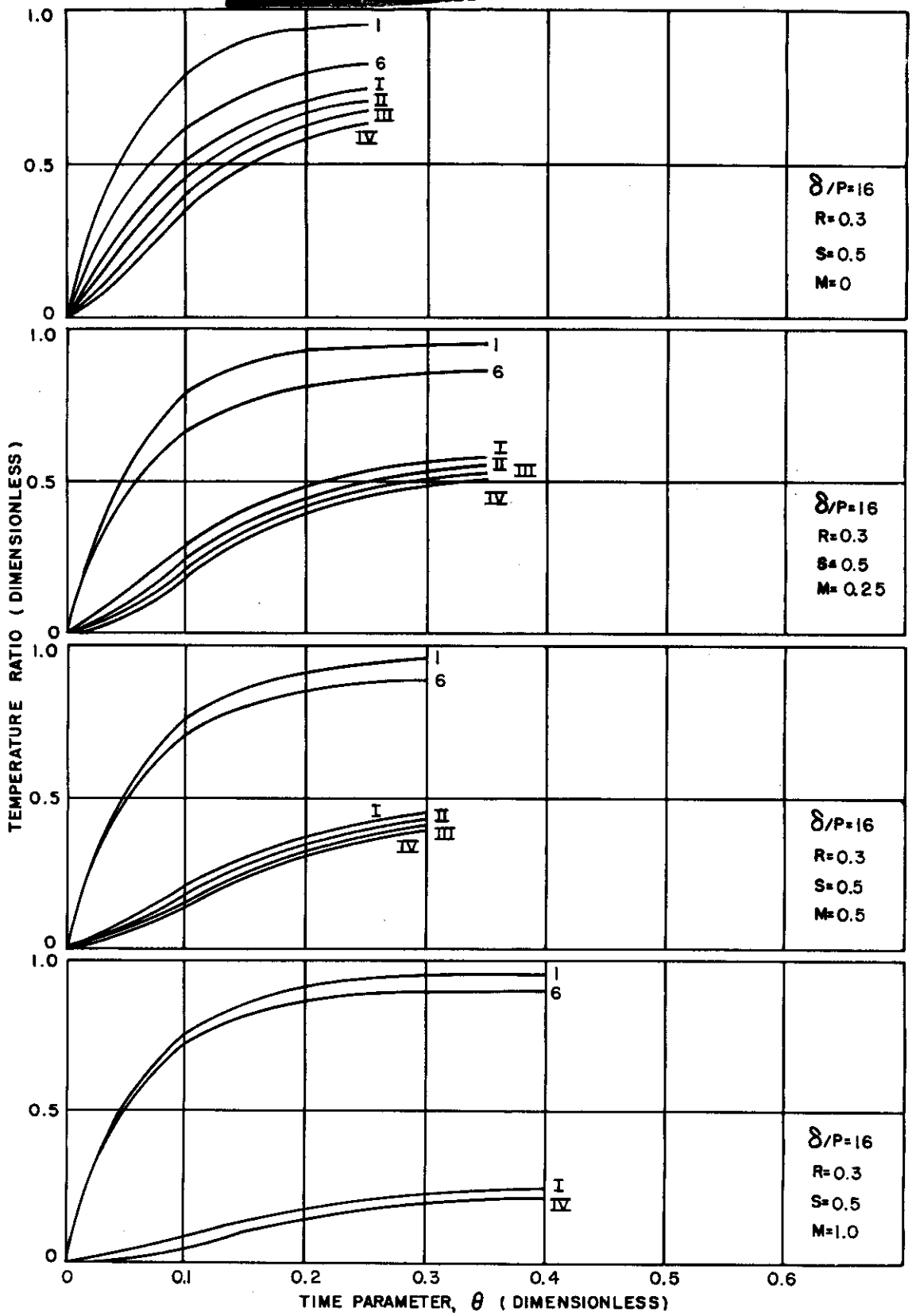

Figure 3.2-9. Temperature Gradients in a Structural T Section

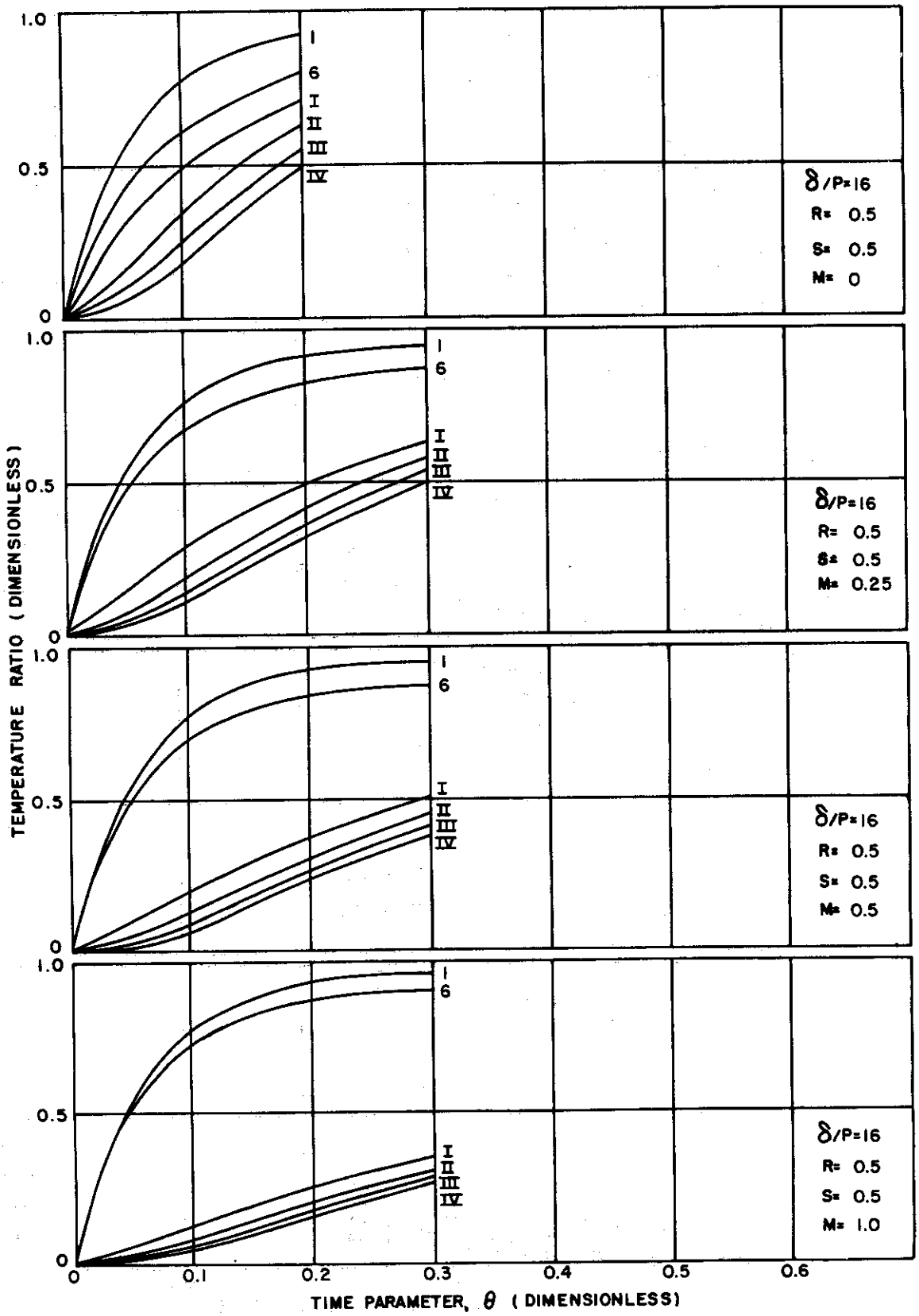

Figure 3.2-10. Temperature Gradients in a Structural T Section

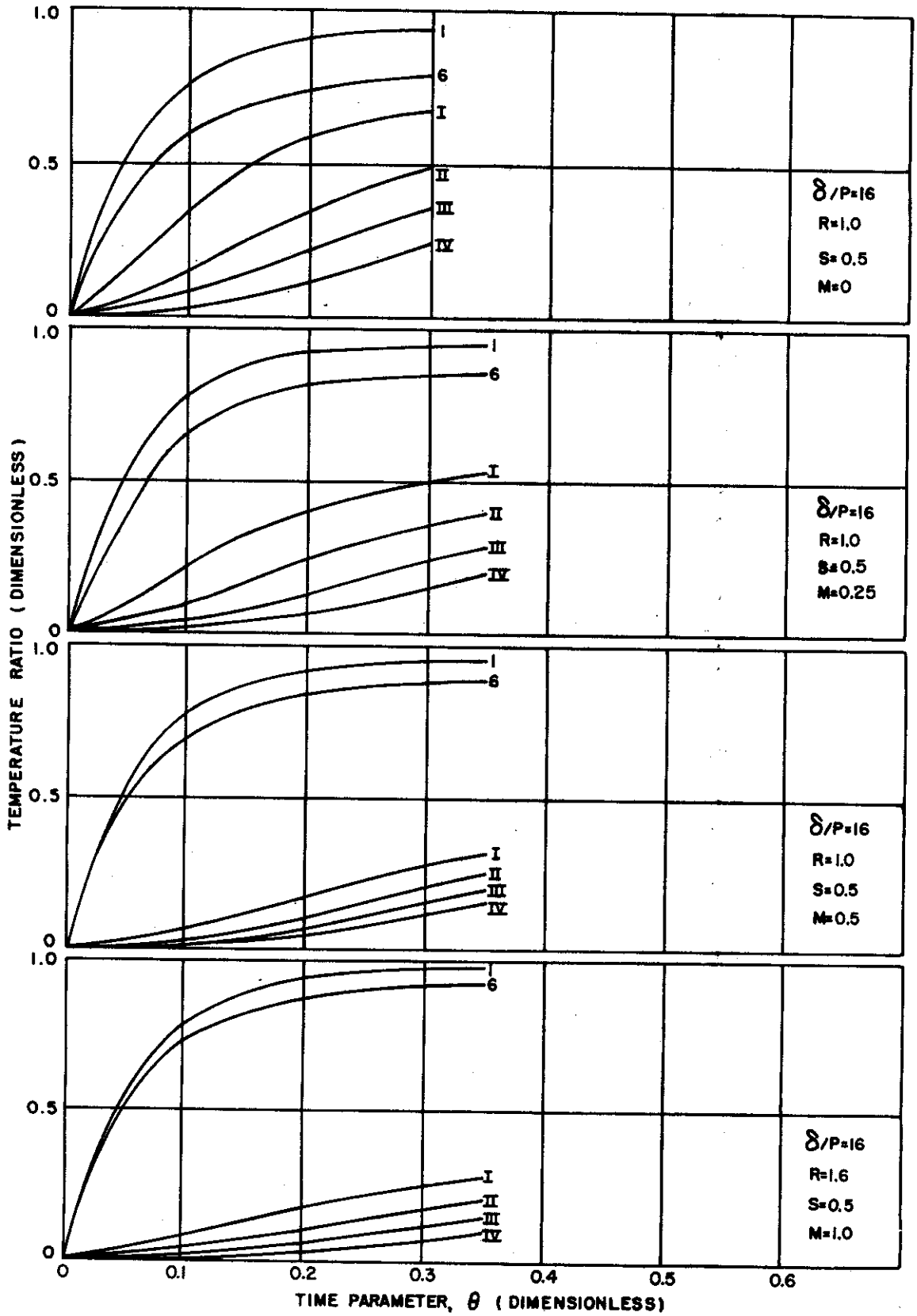

Figure 3.2-11. Temperature Gradients in a Structural T Section

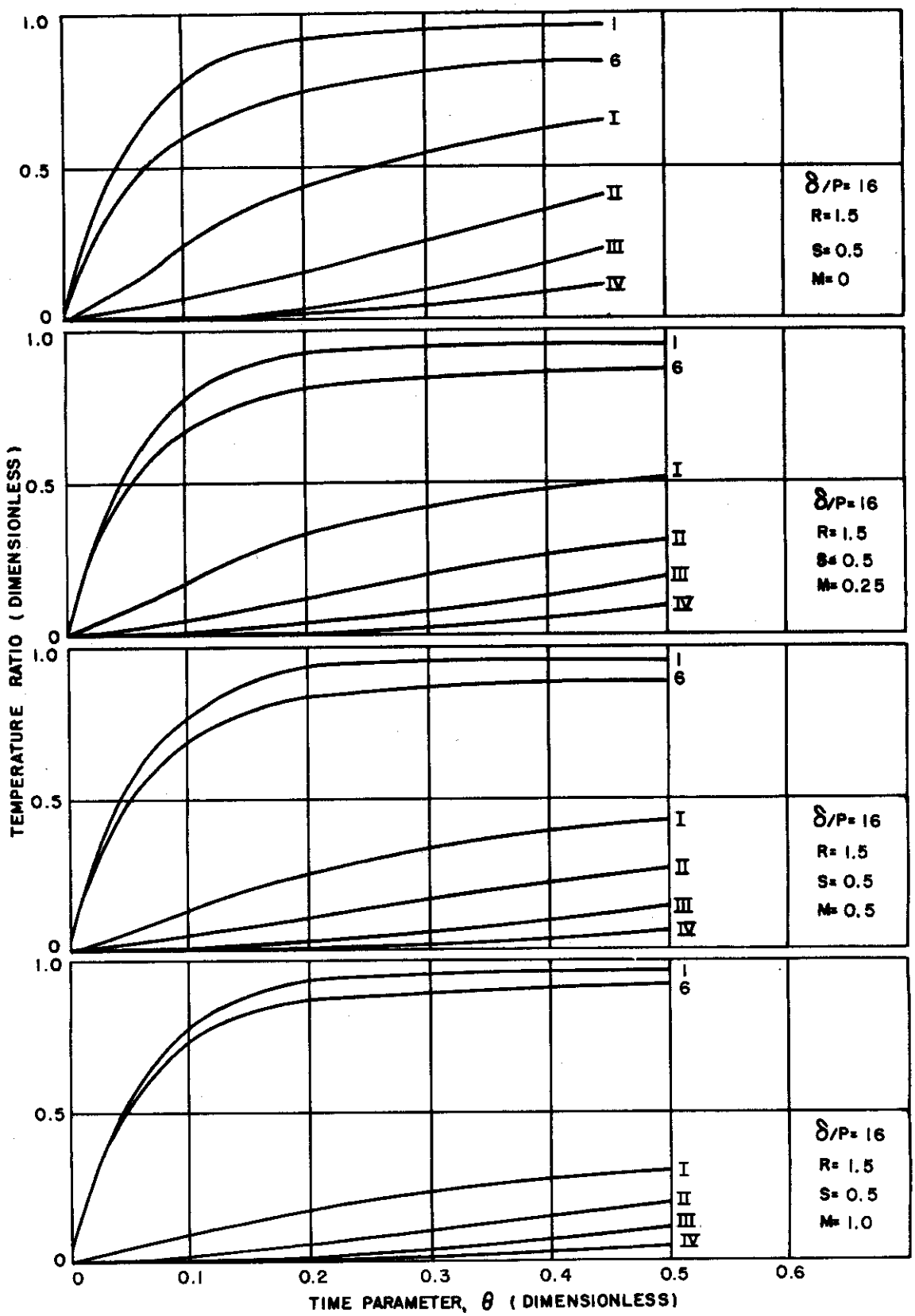

Figure 3.2-12. Temperature Gradients in a Structural T Section

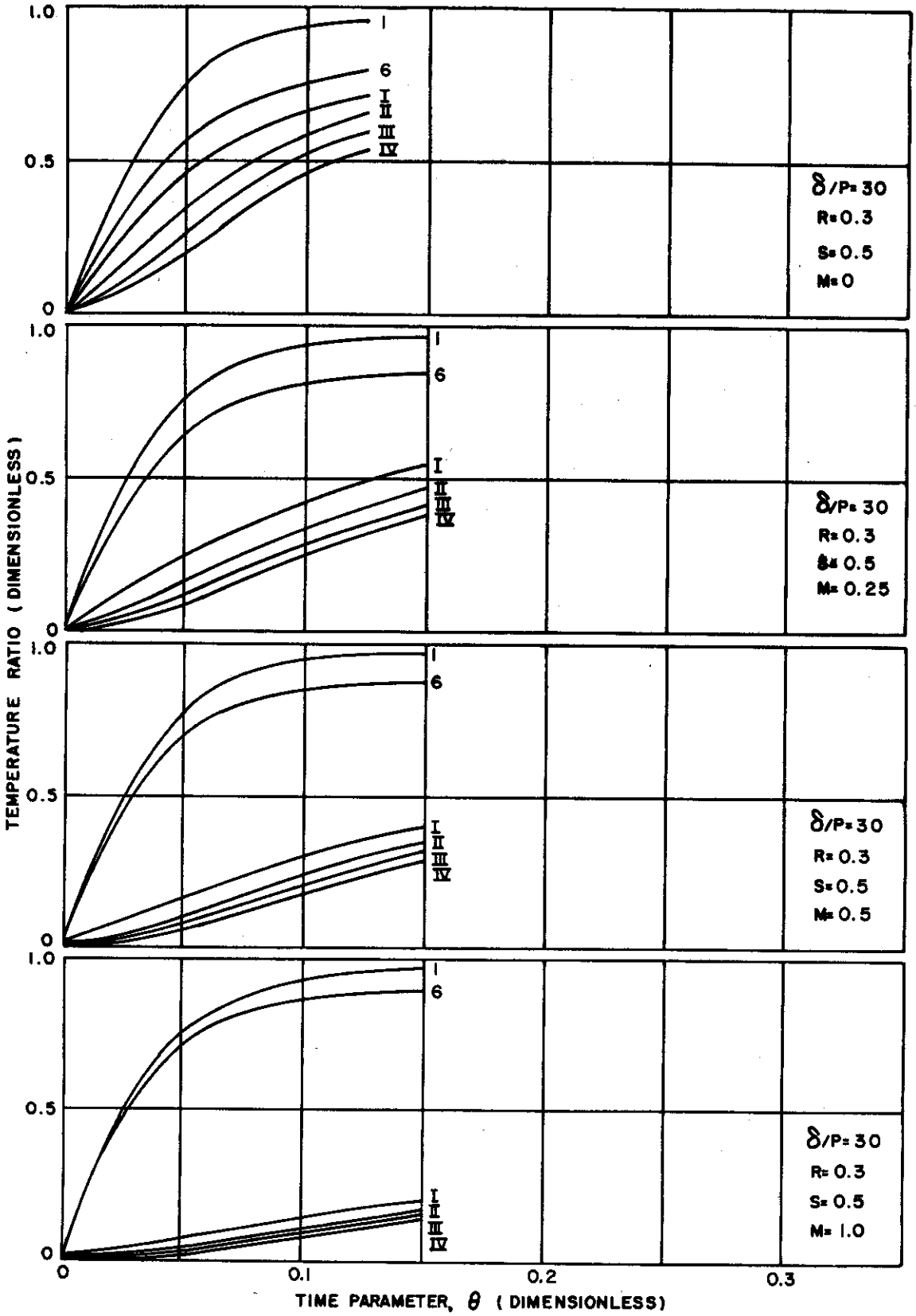

Figure 3.2-13. Temperature Gradients in a Structural T Section

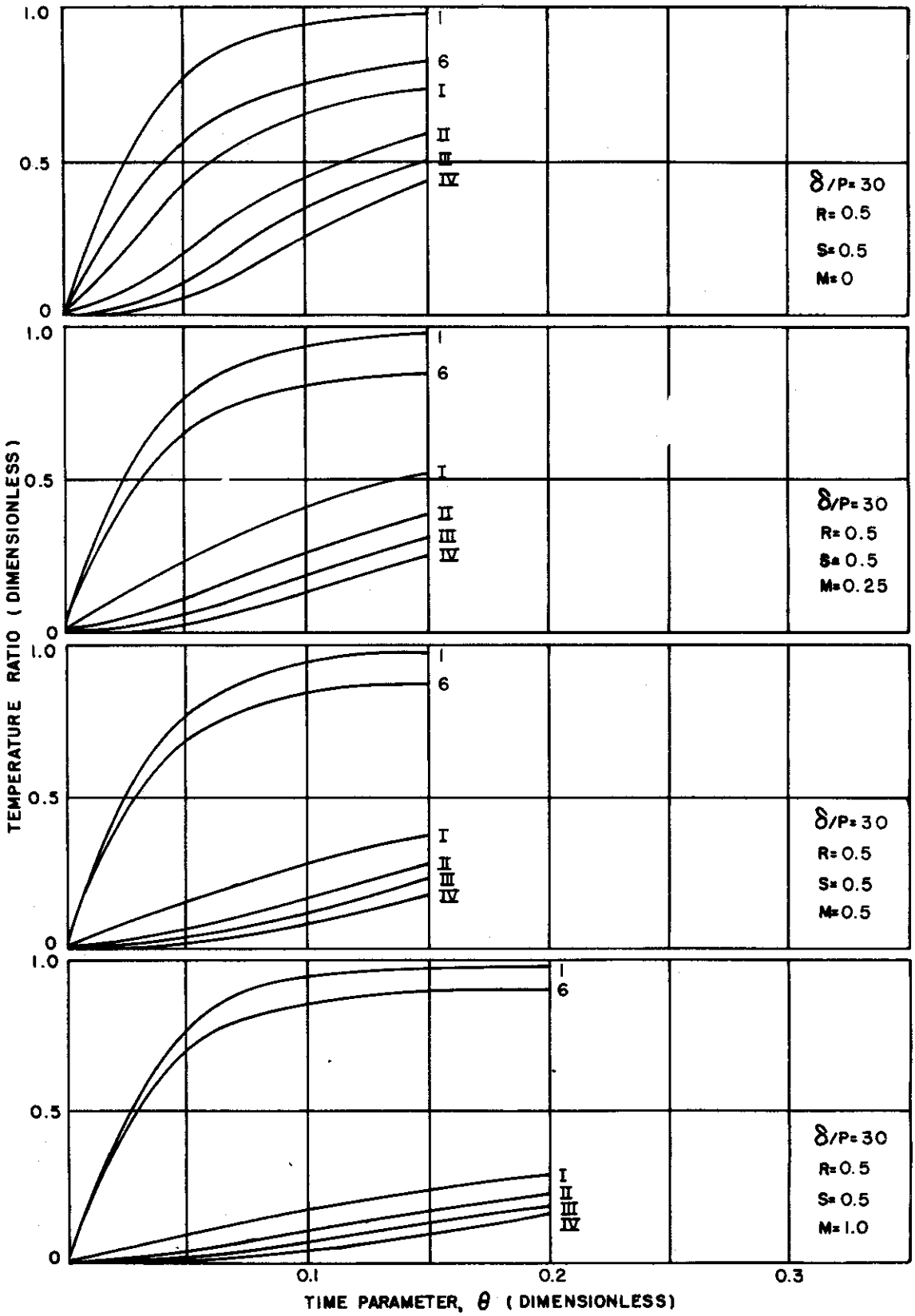

Figure 3.2-14. Temperature Gradients in a Structural T Section

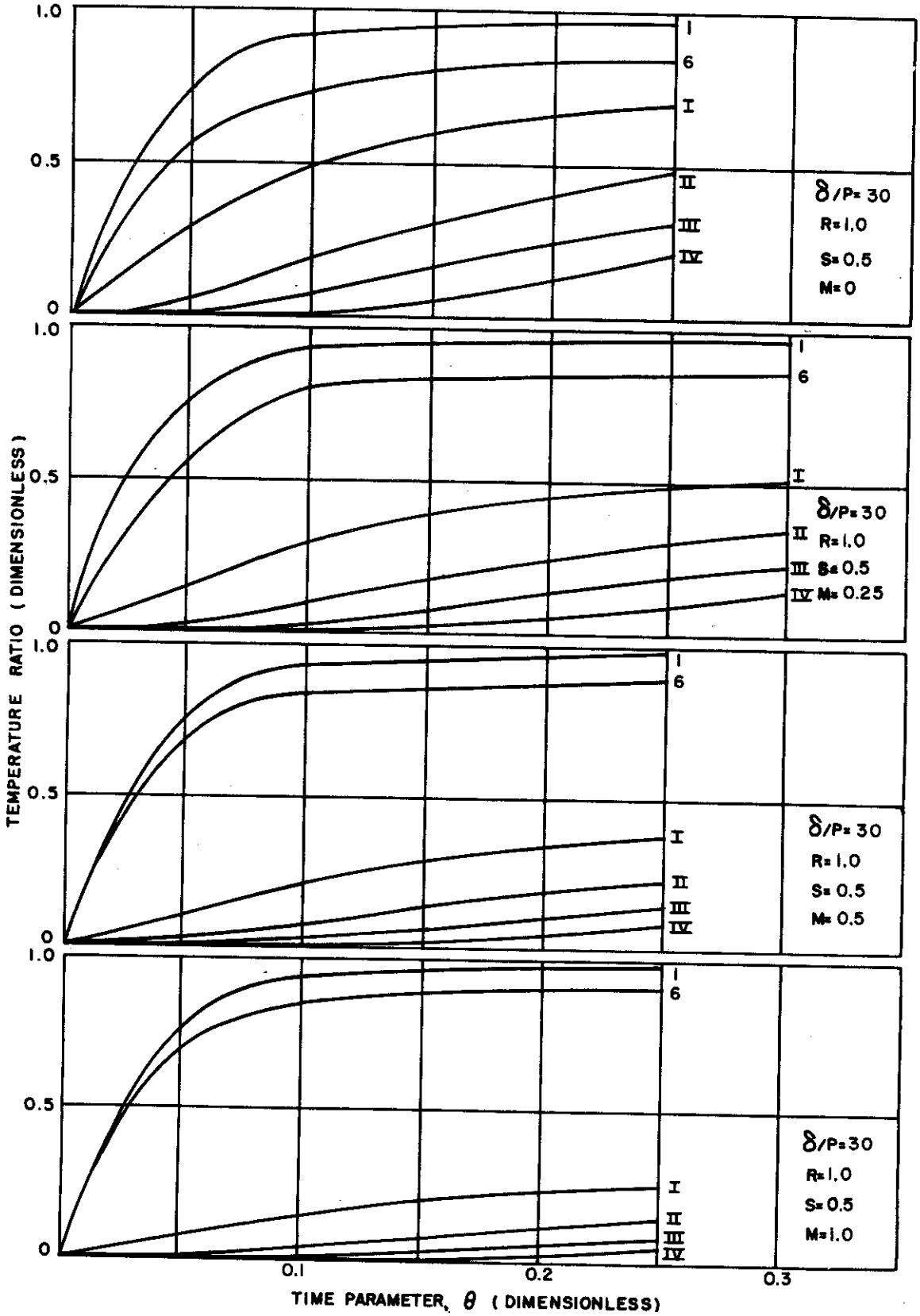

Figure 3.2-15. Temperature Gradients in a Structural T Section

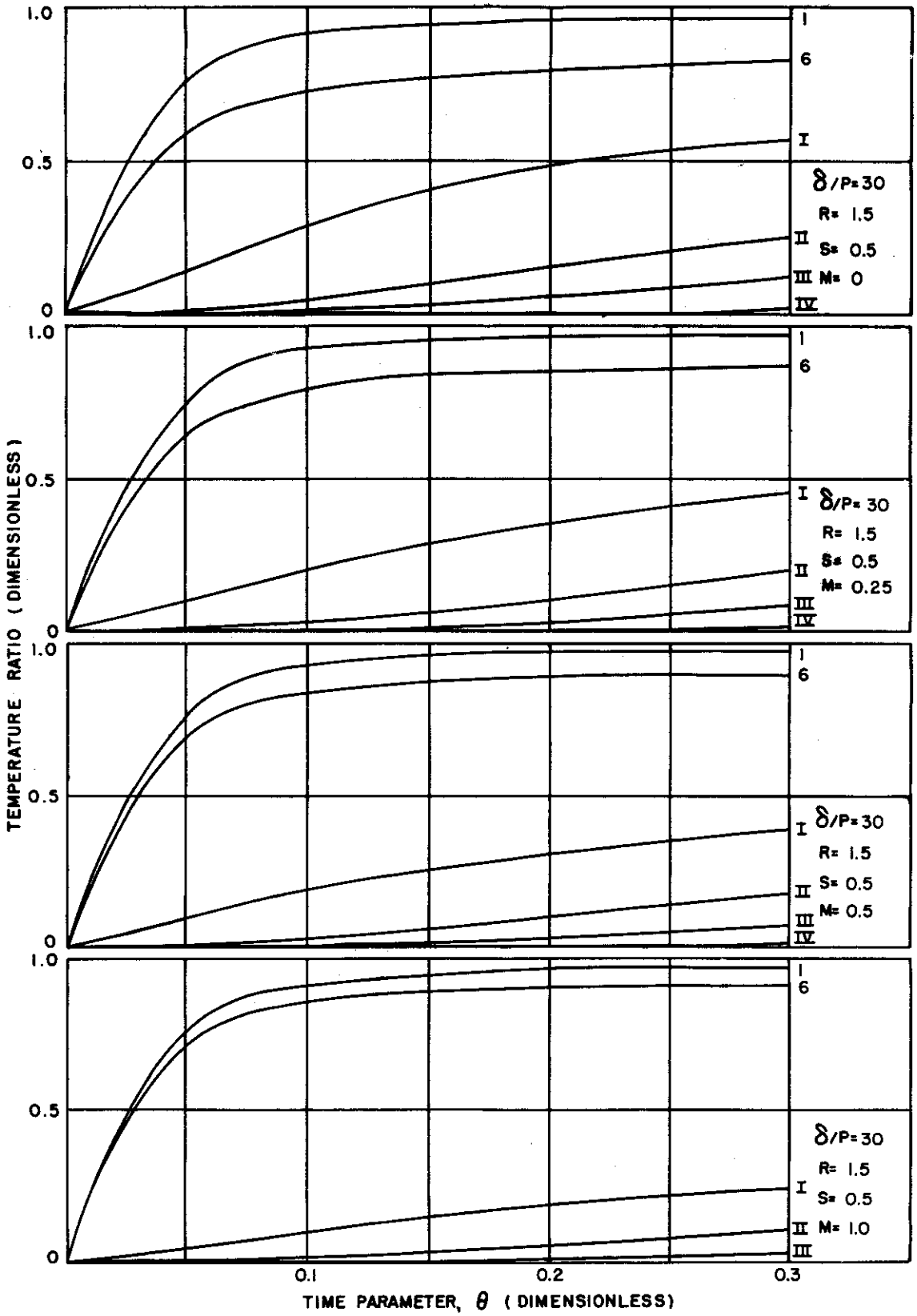

Figure 3.2-16. Temperature Gradients in a Structural T Section

[redacted]

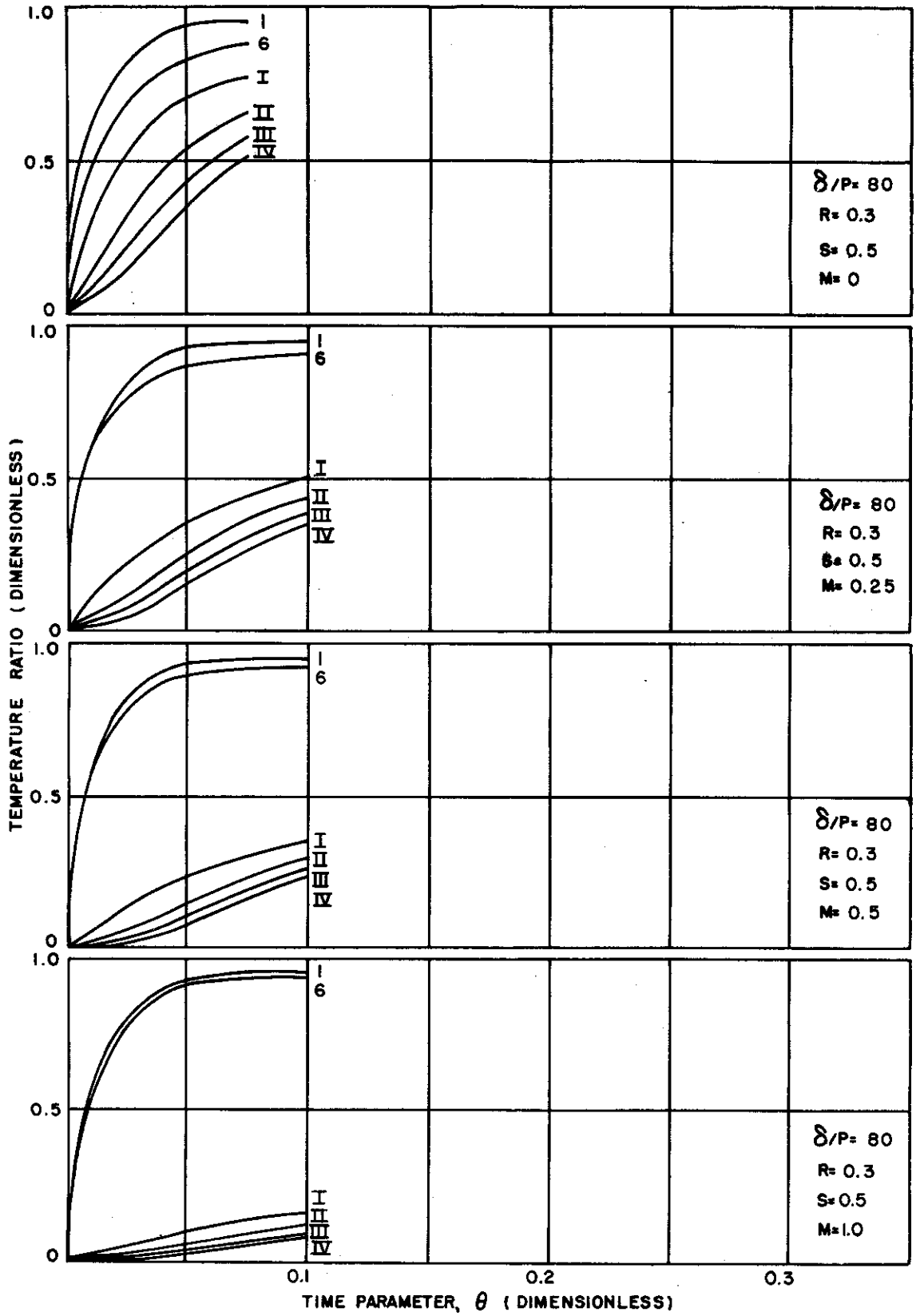

Figure 3.2-17. Temperature Gradients in a Structural T Section

[redacted]

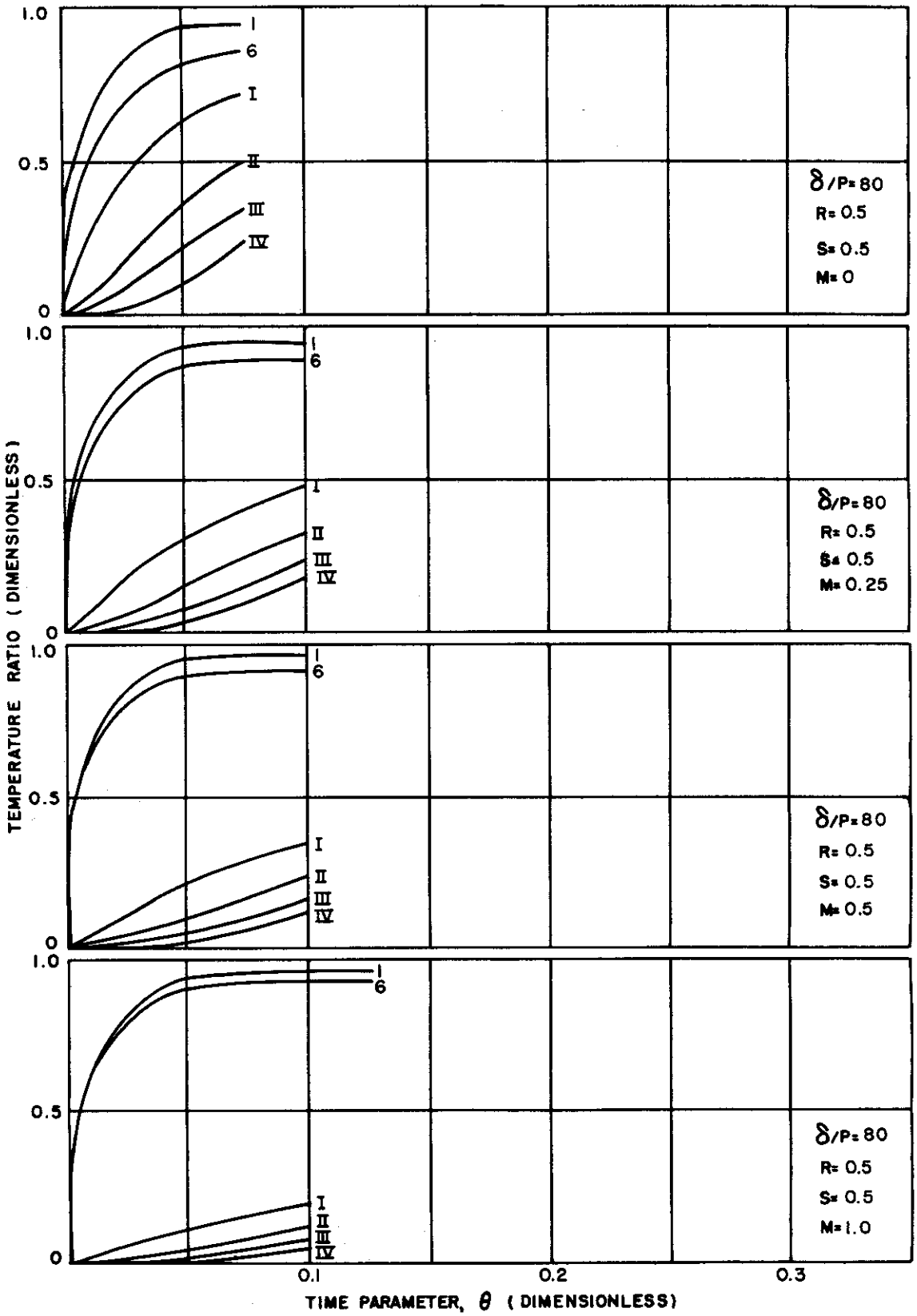

Figure 3.2-18. Temperature Gradients in a Structural T Section

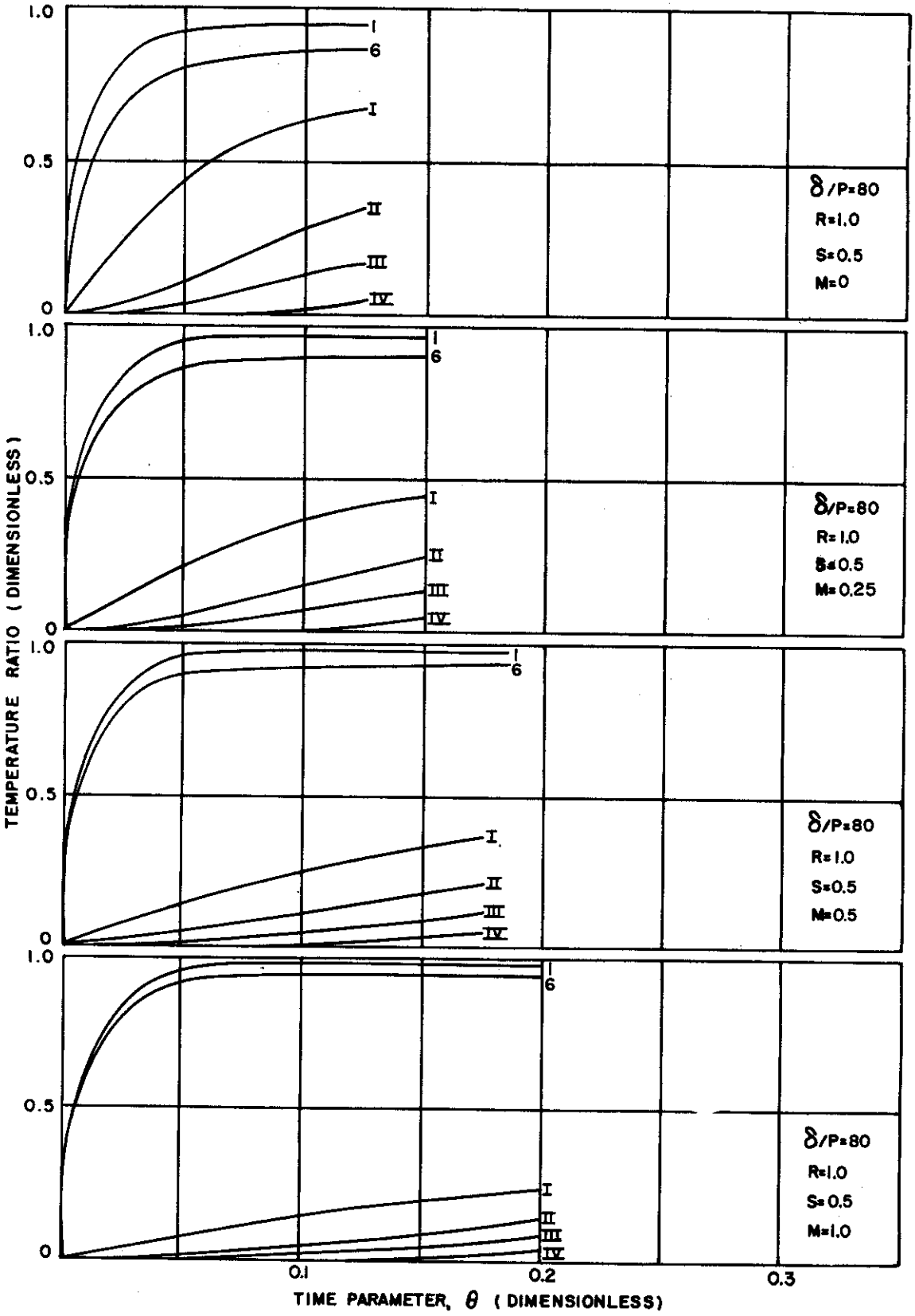

Figure 3.2-19. Temperature Gradients in a Structural T Section

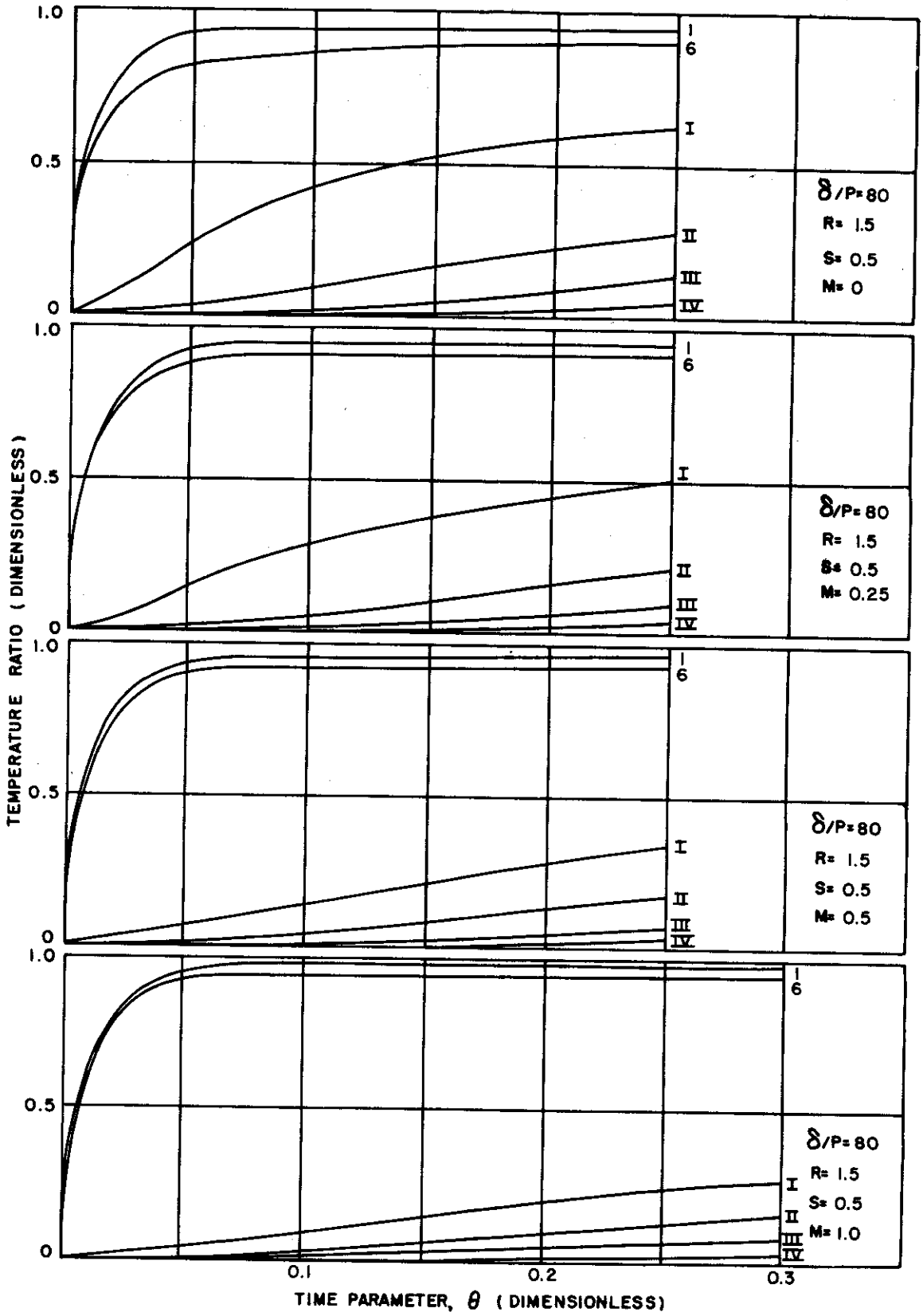

Figure 3.2-20. Temperature Gradients in a Structural T Section

[redacted]

3.3 THERMAL STRESSES

The curves of temperature ratio in Section 3.2 are completely general and may be applied to any structural T section that can be isolated by the condition of no heat flow across the boundaries where the cuts are made. The resulting material expansions, however, may be absorbed by either stress or deflection (axial and bending), or combinations of both, the actual proportions of each depending upon the restraints provided by the surrounding structure. General expressions for calculating normal stresses, given any temperature distribution and structural arrangement, are presented in Part II.

If two simplifying assumptions are made in conjunction with the general equations for thermal stress, the concept of an isolated T section can be continued and stresses readily calculated for the range of geometric and aerodynamic parameters for which temperature gradients are presented in Section 3.2. These two assumptions are:

(1) Plane cross-sections remain plane.

(2) The temperature distribution and geometry must be symmetrical about two perpendicular axes so that thermal stresses produce no bending, and the average temperature of the T section must be equal to the average temperature of the entire structural cross-section.

The first assumption limits the results to applications away from free or elastically restrained ends of structural members. The second assumption restricts the results to a single beam comprising two similar T sections joined at the extremities of the webs, and with heating conditions symmetrical about the joint. This latter case may be extended to a multiweb wing if the geometry and heating conditions are constant across the chord. For most practical cases of multiweb wings, this will be a close approximation. It is also shown in Part II that these stress values apply to a continuous stringer supported by ribs, or to a fuselage ring.

With these assumptions, maximum values of the dimensionless thermal stress ratio, σ, are plotted in Figures 3.3-1 through 3.3-8 for the skin station 1 and the web station IV, against the heat input parameter $\sqrt{\delta/P}$. A range of values of the geometric parameter R and a single value of the parameter S are included. The curves are repeated for different values of the joint resistance M.

EXAMPLE

Find the maximum thermal stresses for the example given in Section 3.2. For this example, $M = 0.26$, $\delta/P = 12.8$, $R = 0.965$, and $S = 0.50$. From Figure 3.3-6 for $M = 0.25$, $R = 1.0$, and $\delta/P = 12.8$, maximum nondimensional stress in skin equals 0.241. From Figure 3.3-2 for the same parameters, maximum nondimensional stress in lower flange of stringer equals 0.55. For 18-8 stainless steel, $\alpha = 9 \times 10^{-6}$ in./in.°F, and $E = 26 \times 10^{6}$ psi, so that for a boundary layer temperature of 900°F,

$$\alpha E T_{aw} = 9 \times 26 \times 900 = 210{,}500 \text{ psi.}$$

Therefore, maximum stress in skin = 210,500 x 0.241 = 50,700 psi, and maximum stress in lower flange = 210,500 x 0.55 = 115,900 psi.

[redacted]

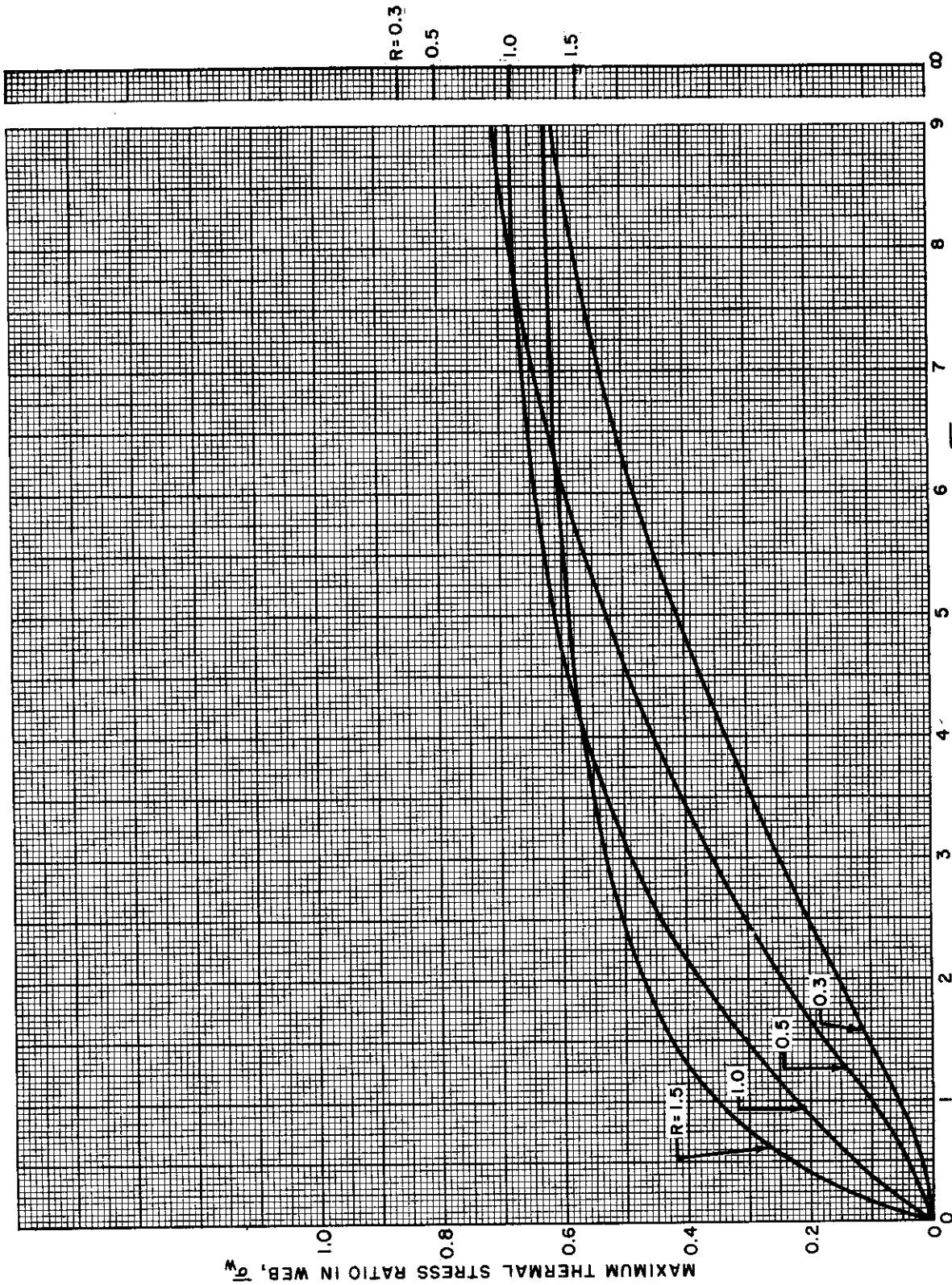

Figure 3.3-1. Maximum Thermal Stress in a Structural T Section (Web), M = 0

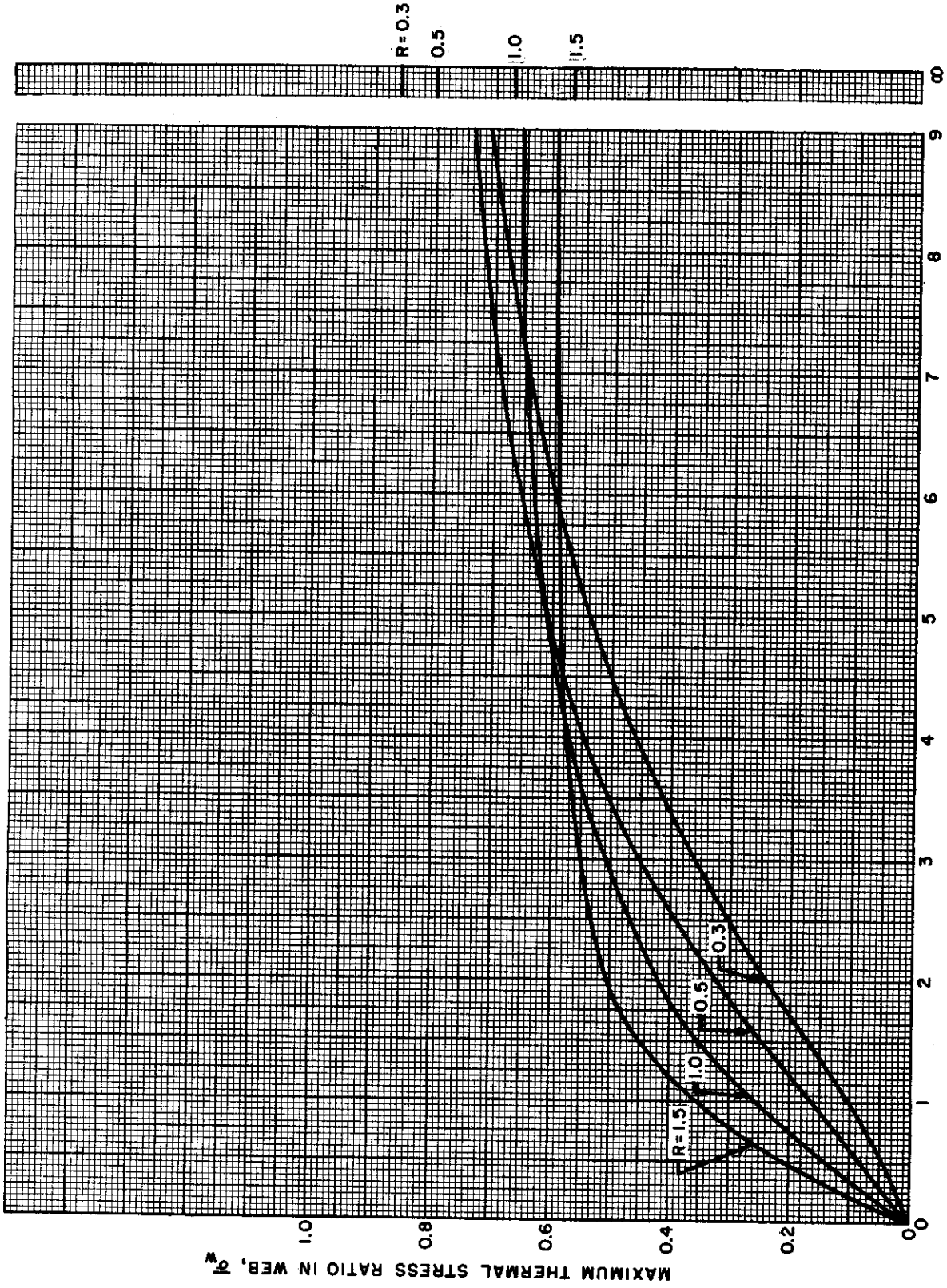

Figure 3.3-2. Maximum Thermal Stress in a Structural T Section (Web), M = 0.25

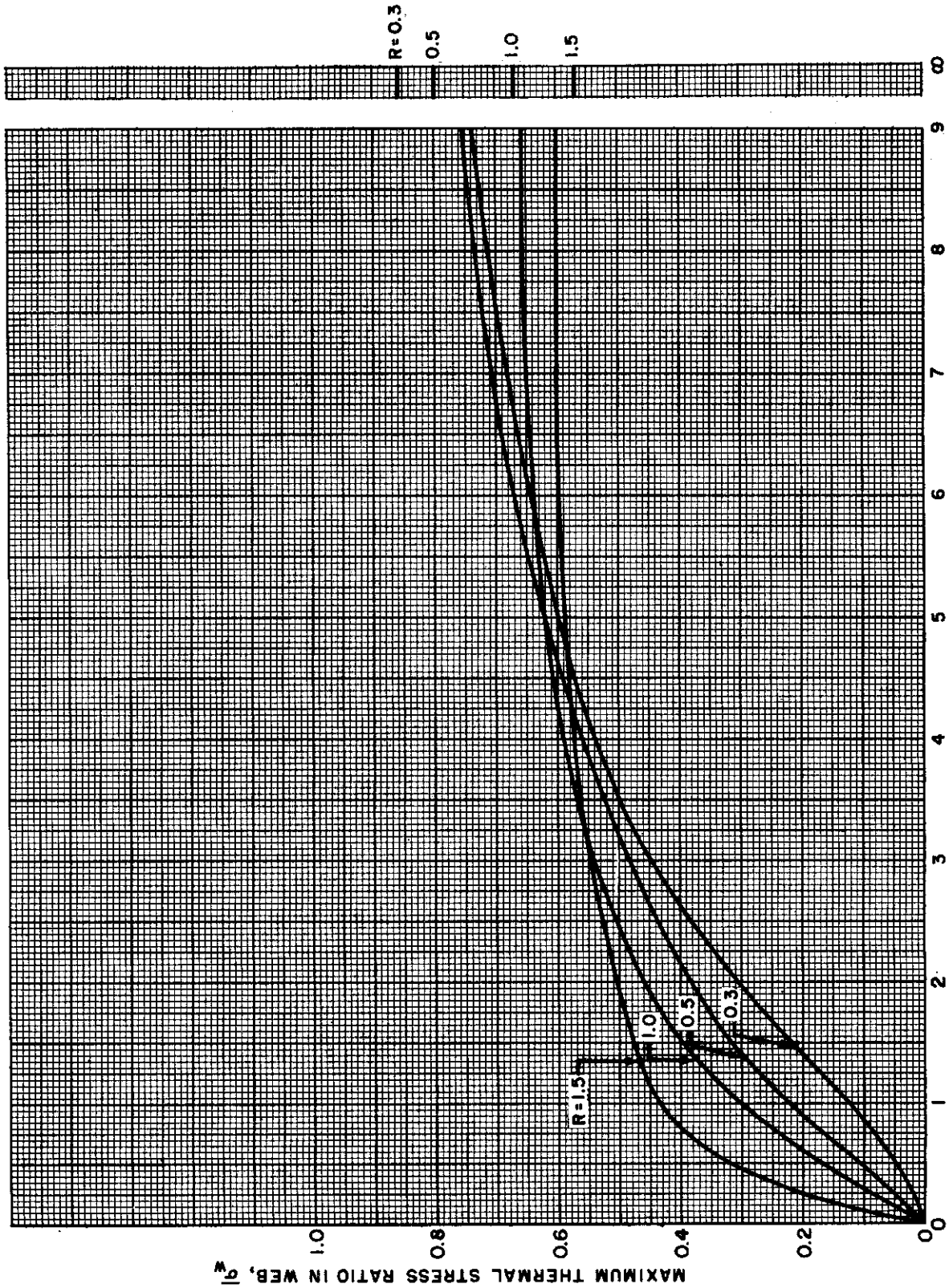

Figure 3.3-3. Maximum Thermal Stress in a Structural T Section (Web), M = 0.5

[redacted]

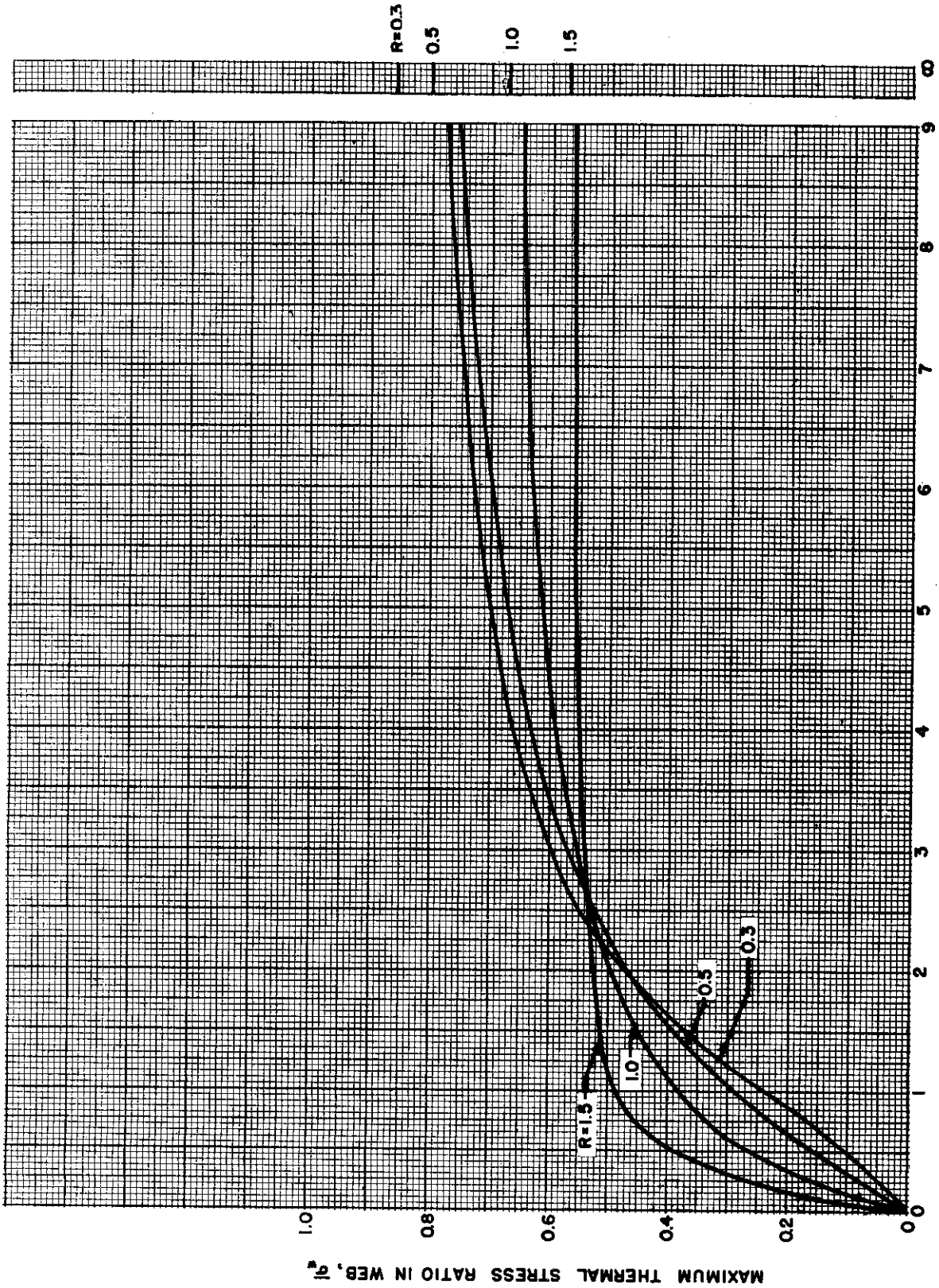

Figure 3.3-4. Maximum Thermal Stress in a Structural T Section (Web), M = 1.0

[redacted]

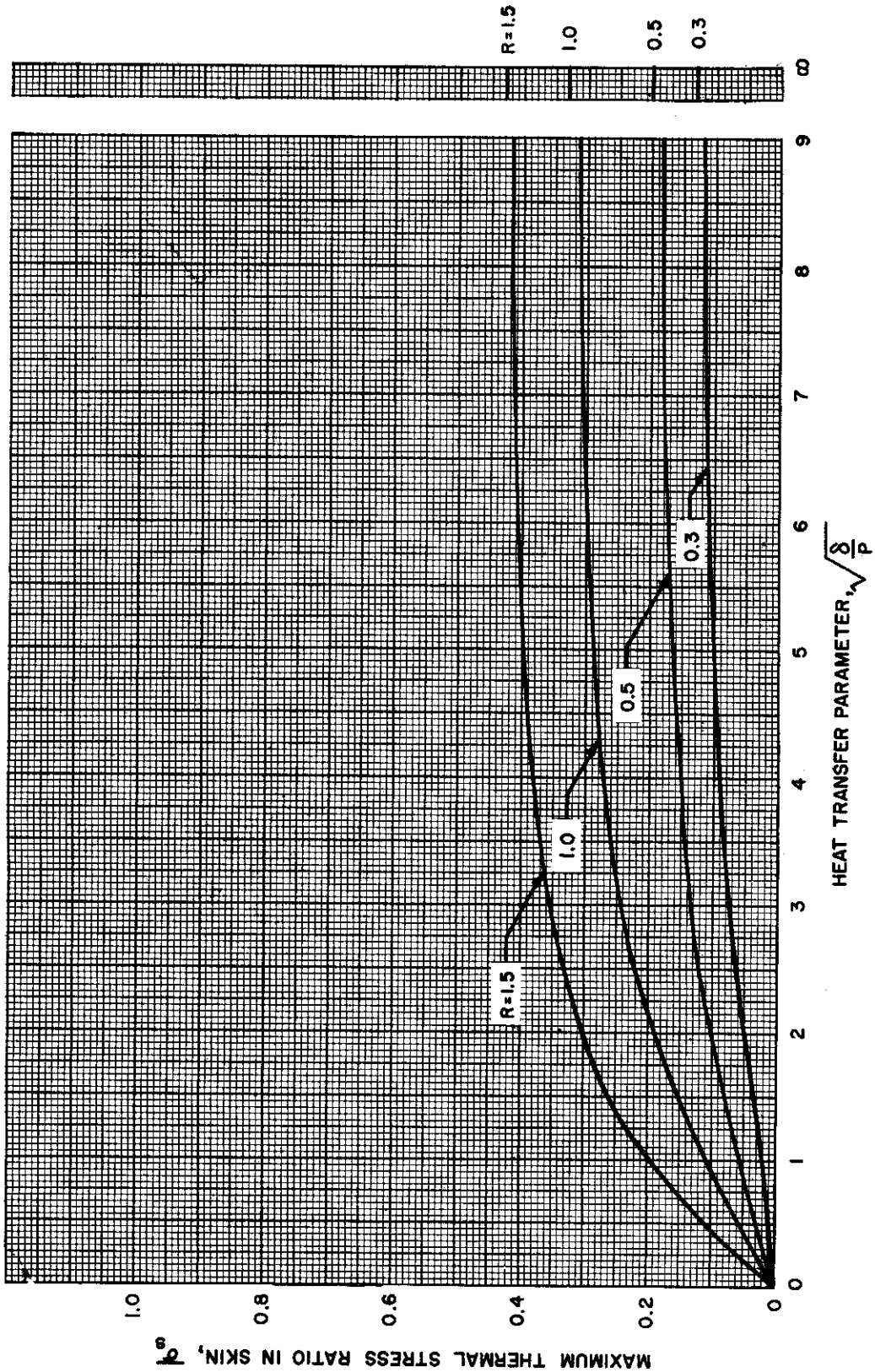

Figure 3.3-5. Maximum Thermal Stress in a Structural T Section (Skin), M = 0

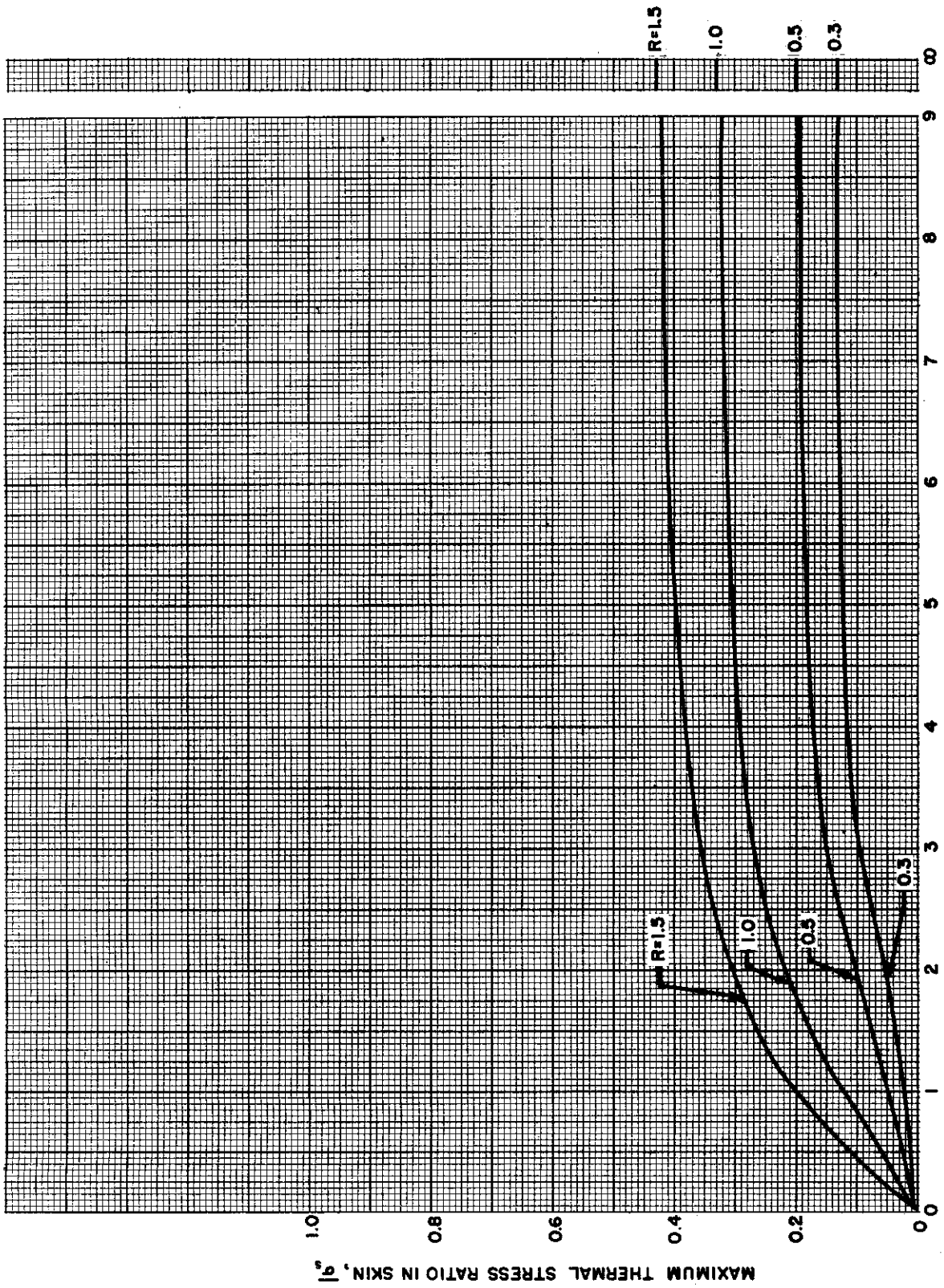

Figure 3.3-6. Maximum Thermal Stress in a Structural T Section (Skin), M = 0.25

[redacted]

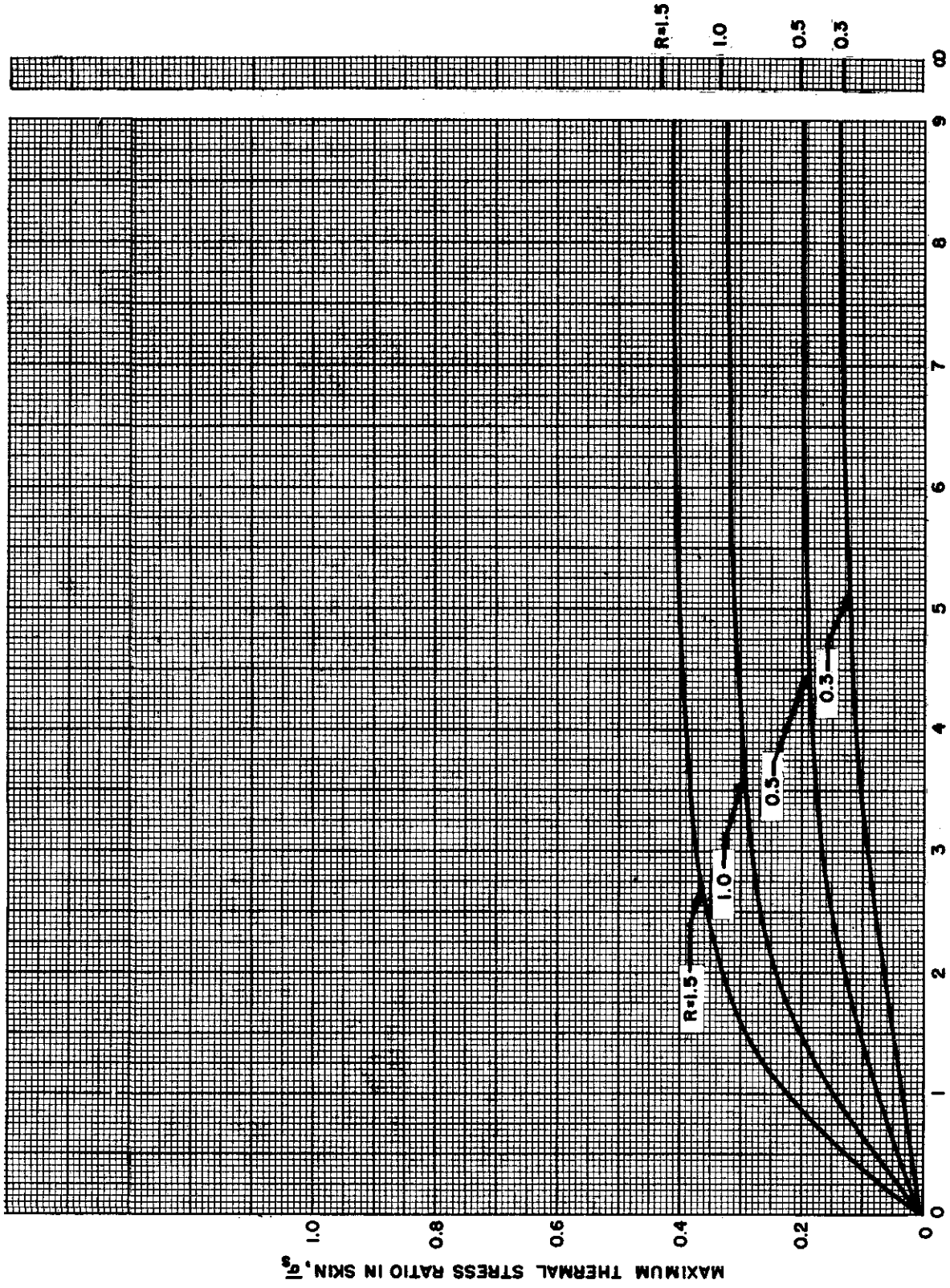

Figure 3.3-7. Maximum Thermal Stress in a Structural T Section (Skin), M = 0.5

[redacted]

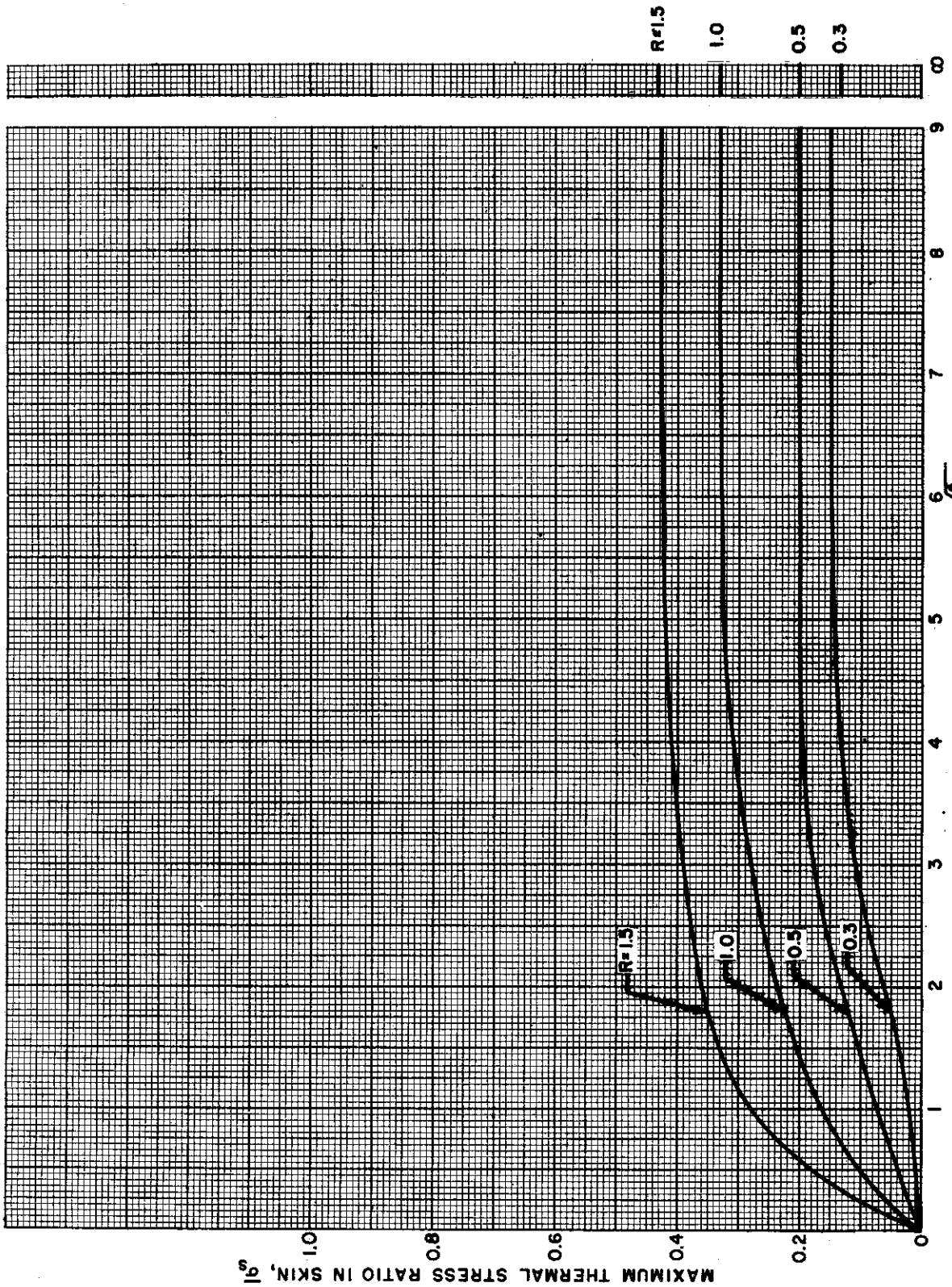

Figure 3.3-8. Maximum Thermal Stress in a Structural T Section (Skin), M = 1.0

3.4 TRANSIENT CONDITIONS

As explained in Section 3.1, it is impractical to produce generalized charts giving temperature gradients and thermal stresses in structures when the external aerodynamic conditions vary arbitrarily with time. A simple numerical method is presented in this section, therefore, for the particular case when the boundary layer temperature varies arbitrarily with time, and the heat transfer coefficient is constant. This method uses the curves of Section 3.2 to calculate temperatures, and a simple formula is given by which the corresponding thermal stresses may be calculated.

In using this method, the geometric and aerodynamic parameters are calculated as before, and the appropriate graph of dimensionless temperature ratios is selected from Figures 3.2-1 through 3.2-20. If attention is focused on the temperature at only one point, say station IV, the method will apply equally to the temperatures at all other stations.

Dividing the flight time into equal time increments, $\Delta\bar{\theta}$, the corresponding incremental value of dimensionless time, $\Delta\theta$, is calculated. Denoting the values of θ at the end of each time increment as $\theta_1, \theta_2, \theta_3$, etc., these values are marked on the curve of v_{IV} against θ, and corresponding values of v_{IV} are noted. Denote the values of v_{IV} at the end of each increment as $(v_{IV})_1, (v_{IV})_2, (v_{IV})_3$, etc.

It is now necessary to calculate, from the flight conditions, an average value of boundary layer temperature, T_{aw}, for each time increment. Denote these values as $(T_{aw})_1, (T_{aw})_2, (T_{aw})_3$, etc.

Then the temperature at station IV at the end of the nth time interval is given by

$$(T_{IV})_n = \left[(T_{aw})_n - (T_{aw})_{(n-1)}\right](V_{IV})_1 + \left[(T_{aw})_{(n-1)} - (T_{aw})_{(n-2)}\right](V_{IV})_2$$
$$+ \left[(T_{aw})_{(n-2)} - (T_{aw})_{(n-3)}\right](V_{IV})_3 + \text{- - - - - - - - -}$$
$$+ \left[(T_{aw})_2 - (T_{aw})_1\right](V_{IV})_{(n-1)} + \left[(T_{aw})_1 - T_a\right](V_{IV})_n + T_a .$$

While this procedure appears complex when expressed algebraically, it is numerically simple, as will be shown in the following example.

EXAMPLE

In the example of Section 3.2, find the lower flange temperature after 200 seconds if the boundary layer temperature increases steadily from 100° to 900°F as given by the following:

Time (sec)	0	40	80	120	160	200
T_{aw} (°F)	100	300	500	700	900	900

From the previous example, the material diffusivity = 0.00671 in.^{2}/sec, and b_s = 4 in., so that for an elemental time of 40 sec

$$\Delta\theta = \frac{\Delta\theta \times a}{(b_s/2)^2} = \frac{40 \times 0.00671}{4.0} = 0.0671.$$

From the previous example, geometric and aerodynamic parameters are $\delta/P = 12.8$, $S = 0.5$, $R = 0.965$, and $M = 0.26$.

From Figures 3.2-7 and 3.2-11 for $R = 1.00$ and $M = 0.25$, interpolating for $\delta/P = 12.8$ gives the following curve of v_{IV} against θ.

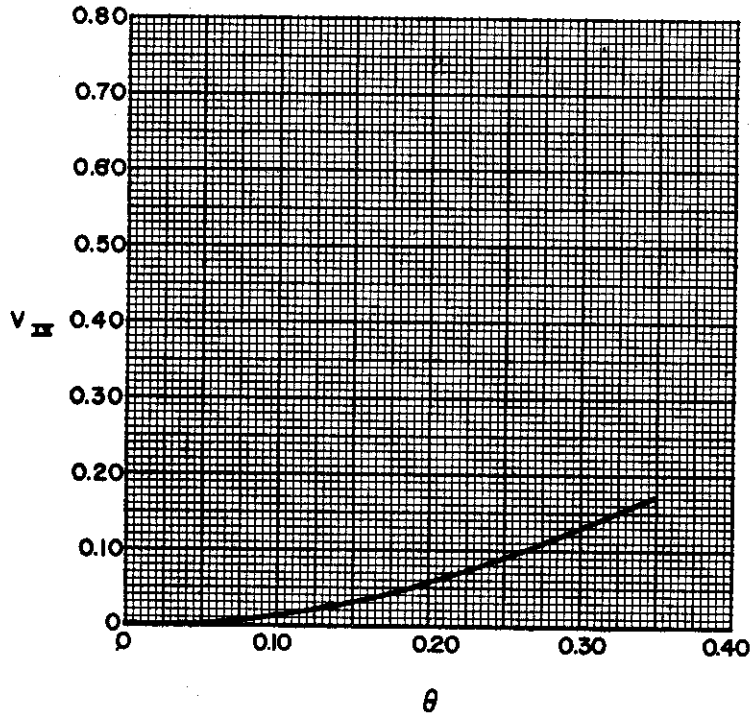

From this curve, the values of $(v_{IV})_n$ in the following table can be obtained:

Time (sec)	0	40	80	120	160	200
$\Delta\theta$		0.0671	0.0671	0.0671	0.0671	0.0671
θ	0	0.0671	0.1342	0.2013	0.2684	0.3355
$(v_{IV})_n$	0	0.008	0.024	0.057	0.104	0.162
T_{aw} (°F)	100	300	500	700	900	900
mean T_{aw} (°F)		200	400	600	800	900

From this table, the following calculation is made for T_{IV} at 200 seconds:

$$(T_{IV})_{200} = (900-800)\ (0.008) + (800-600)\ (0.024) + (600-400)\ (0.057) + (400-200) \times (0.104) + (200-100)\ (0.162) + 100 = 154^\circ F.$$

To obtain stresses for the transient condition, this temperature calculation procedure is repeated for each station in the section and the dimensionless thermal stress ratio is calculated from

$\bar{\sigma} = u_{av} - u_i$ for skin stresses, or

$\bar{\sigma} = u_{av} - v_j$ for web stresses.

where u_{av} is given by

$$u_{av} = \frac{1}{1+RS}\left\{\frac{2}{11}(u_1+u_2+u_3+u_4+u_5) + \frac{u_6}{11} + \frac{RS}{4}(v_I+v_{II}+v_{III}+v_{IV})\right\}.$$

[redacted]

SECTION 4.0

COLUMNS AND PLATES

By P. P. Bijlaard, J. Padlog, and M. A. Goldberg

[redacted]

[redacted]

[redacted]

TABLE OF CONTENTS

[redacted]

NOMENCLATURE

b = plate width (in.)

c = fixity coefficient

E = Young's modulus (psi)

K = buckling coefficient for a plate element

ℓ = column length (in.)

T_s = skin temperature (°F)

t = plate thickness (in.)

ΔT = temperature difference between two points (°F)

η = plasticity coefficient

ρ = radius of gyration (in.)

σ_{cr} = critical buckling stress (psi)

σ_{cy} = material yield stress (psi)

σ_{ULT} = ultimate buckling stress (psi)

[redacted]

SECTION 4.0

COLUMNS AND PLATES

4.1 GENERAL

Curves are presented in this section for the design of column and plate elements occurring in structures that operate at elevated temperature. There are several effects to be considered in designing compression elements in elevated temperature structures. Among those covered by the illustrations of this section are:

(a) Effects of reduced material properties: With the increase of temperature, the yield strength and elastic moduli of structural materials decrease, and the shape of the stress-strain curve changes, resulting in a decrease in the stress level at which elements become unstable. Column curves for various materials, each covering a range of temperatures, are given in Section 4.2. Similar plate buckling curves are given in Section 4.5.

(b) Effects of time: Most materials, when subjected to stress at elevated temperature for an extended period of time, continue to strain as long as load is applied. This phenomenon is called creep, and its rate increases with an increase of either stress or temperature.

Considering now a compression element operating under constantly applied load at elevated temperature, it is evident that, if a small initial eccentricity exists, the resulting stress gradient will cause varying amounts of creep across the section. Higher creep rates at the more highly stressed fibers cause an increase of eccentricity with time, until a value of deflection is reached at which the element fails.

To account for this effect, creep buckling curves for columns having stable cross-sections are given in Section 4.3, and for plates in Section 4.6.

(c) Effects of temperature gradients: During acceleration or deceleration of a supersonic aircraft, transient heating conditions exist during which temperature gradients are produced through the cross-section in many or all elements of the structure. Evidently, if a column is subjected to a temperature gradient across its section, the problem mentioned in item (a) arises in a more complicated form since now each fiber of the column has different stress-strain characteristics. In addition, the differential expansions produced within the various elements of the column may produce destabilizing deflections or thermal stresses, depending upon the restraints provided by the surrounding structure.

The effect of thermal stresses on the critical stress of columns having stable cross-sections may be evaluated readily by means of the curves in Section 4.4. Various temperature gradients are considered for a variety of cross-sectional shapes which are not subject to local crippling.

This phenomenon could be further complicated by the effects of creep, but this is considered to be a special case since transient temperature gradients are not generally sustained long enough for creep to become significant.

Further reduction of allowable stress occurs if the average temperature of a column is greater than that of the surrounding structure, so that its general expansion is restricted. No particular treatment of this problem is given since the effect is dependent upon the geometry of the surrounding structure. If the cross-sectional area of the column is small compared with the area of the cooler surrounding material, then it can be assumed that the expansion due to temperature difference is prevented. The resulting stress of $\alpha E \Delta T$ can be treated as an additional applied stress.

The effects of temperature gradients and thermal stresses in plates cannot be readily presented in simple graphical form, as is the case for columns. Therefore, design curves are not presented in this part of the report, but methods of analysis are included in Part II.

Column and plate curves are given for the following materials in the order shown:

SHORT-TIME LOADING

2024-T3 Aluminum Alloy, Clad

7075-T6 Aluminum Alloy

FSI-H24 Magnesium Alloy

RC C-110M Titanium Alloy

Alloy Steel, Heat-treated to 200,000 psi

18-8 Stainless Steel

17-7 PH Stainless Steel

Inconel X

LONG-TIME LOADING

2024-T3 Aluminum Alloy, Clad

RC C-110M Titanium Alloy

Inconel X

TEMPERATURE GRADIENTS - COLUMNS ONLY

2024-T3 Aluminum Alloy, Clad

C-110M Titanium Alloy

Inconel X

4.2 COLUMNS — UNIFORM TEMPERATURE — SHORT-TIME LOADING

Figures 4.2-1 through 4.2-9 give stable section column buckling curves for various materials, ranges of temperature, and short-time loading. The values for these curves are calculated from the Euler column formula incorporating the tangent modulus. Values of tangent moduli are taken from the data of Section 2.0.

The coefficient c is the standard end fixity factor which takes the value 1.0 for pinned ends and 4.0 for fixed ends.

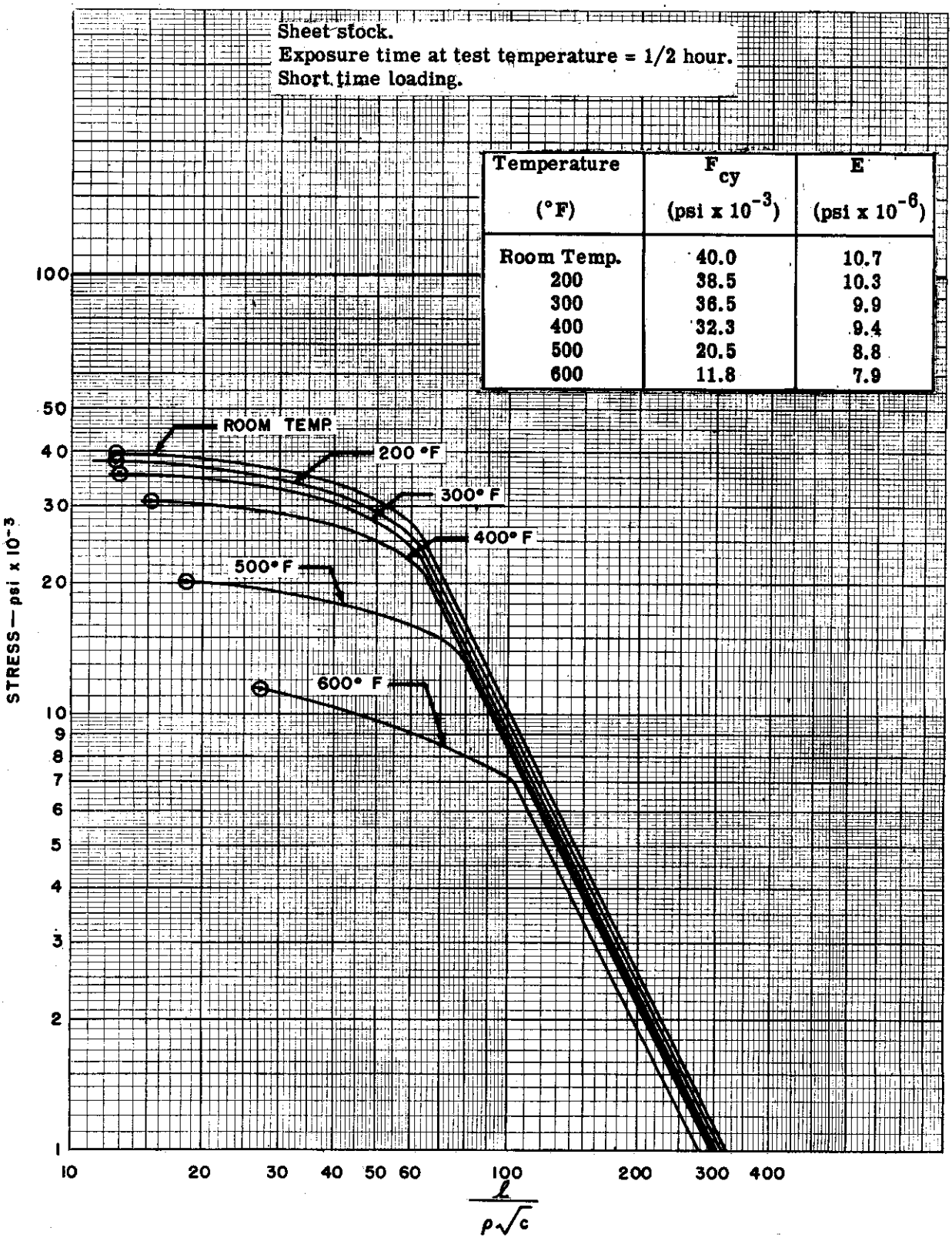

Temperature (°F)	F_{cy} (psi x 10^{-3})	E (psi x 10^{-6})
Room Temp.	40.0	10.7
200	38.5	10.3
300	36.5	9.9
400	32.3	9.4
500	20.5	8.8
600	11.8	7.9

Figure 4.2-1. 2024-T3 Clad Aluminum Alloy — Buckling Stress for Stable Section Columns

[redacted]

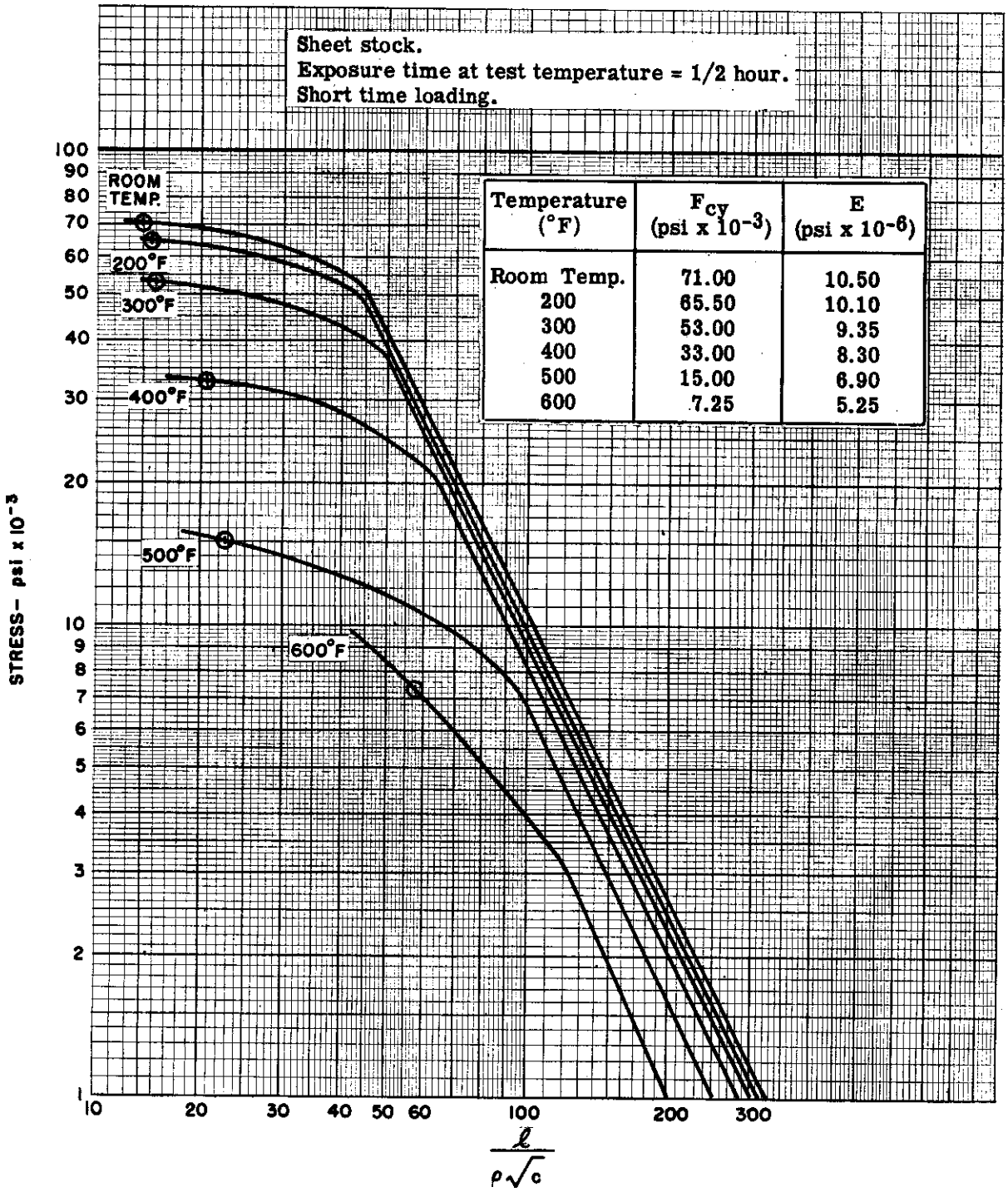

Temperature (°F)	F_{cy} (psi x 10^{-3})	E (psi x 10^{-6})
Room Temp.	71.00	10.50
200	65.50	10.10
300	53.00	9.35
400	33.00	8.30
500	15.00	6.90
600	7.25	5.25

Figure 4.2-2. 7075-T6 Aluminum Alloy – Buckling Stress for Stable Section Columns

[redacted]

[redacted]

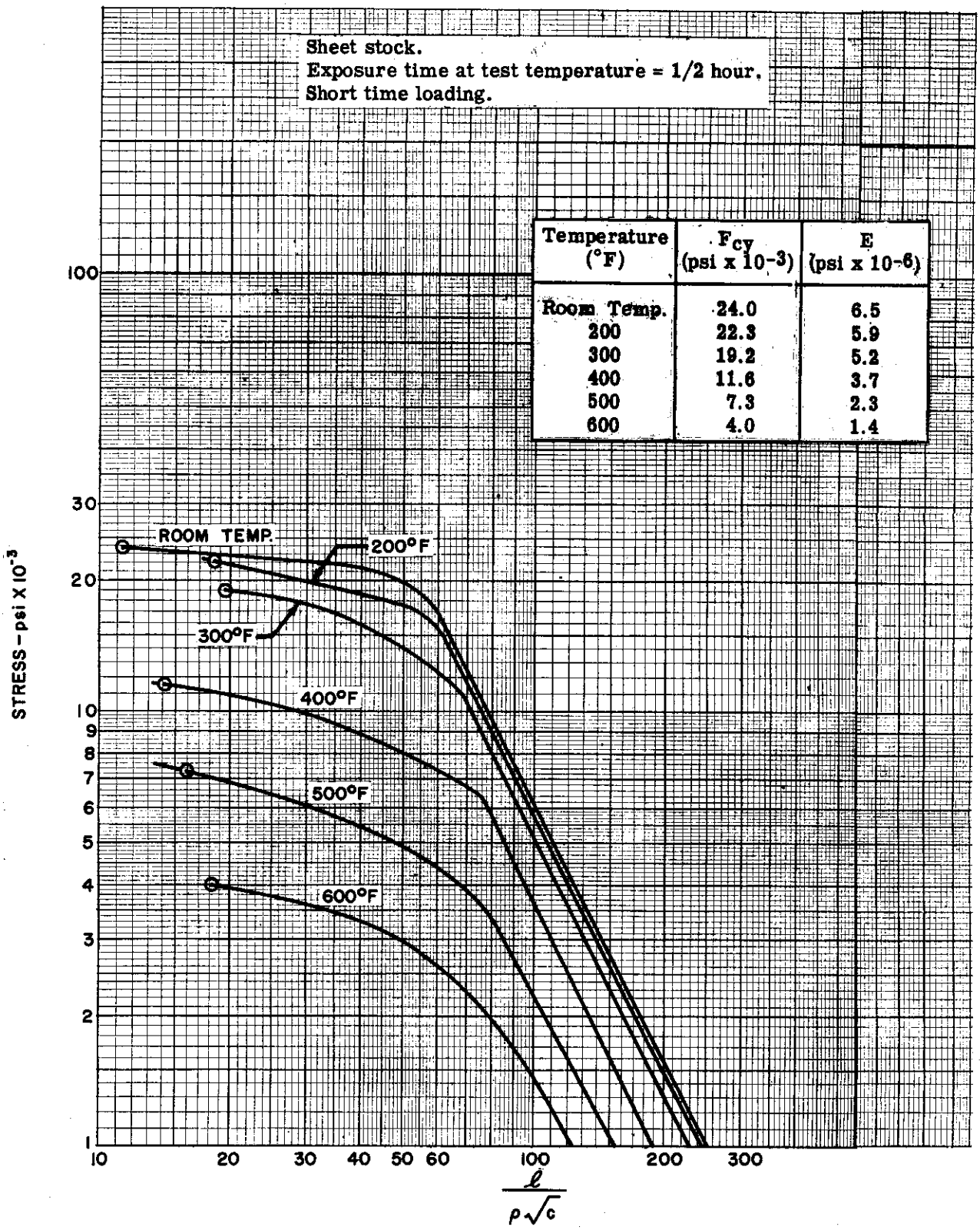

Figure 4.2-3. FSI-H24 Magnesium Alloy — Buckling Stress for Stable Section Columns

[redacted]

[redacted]

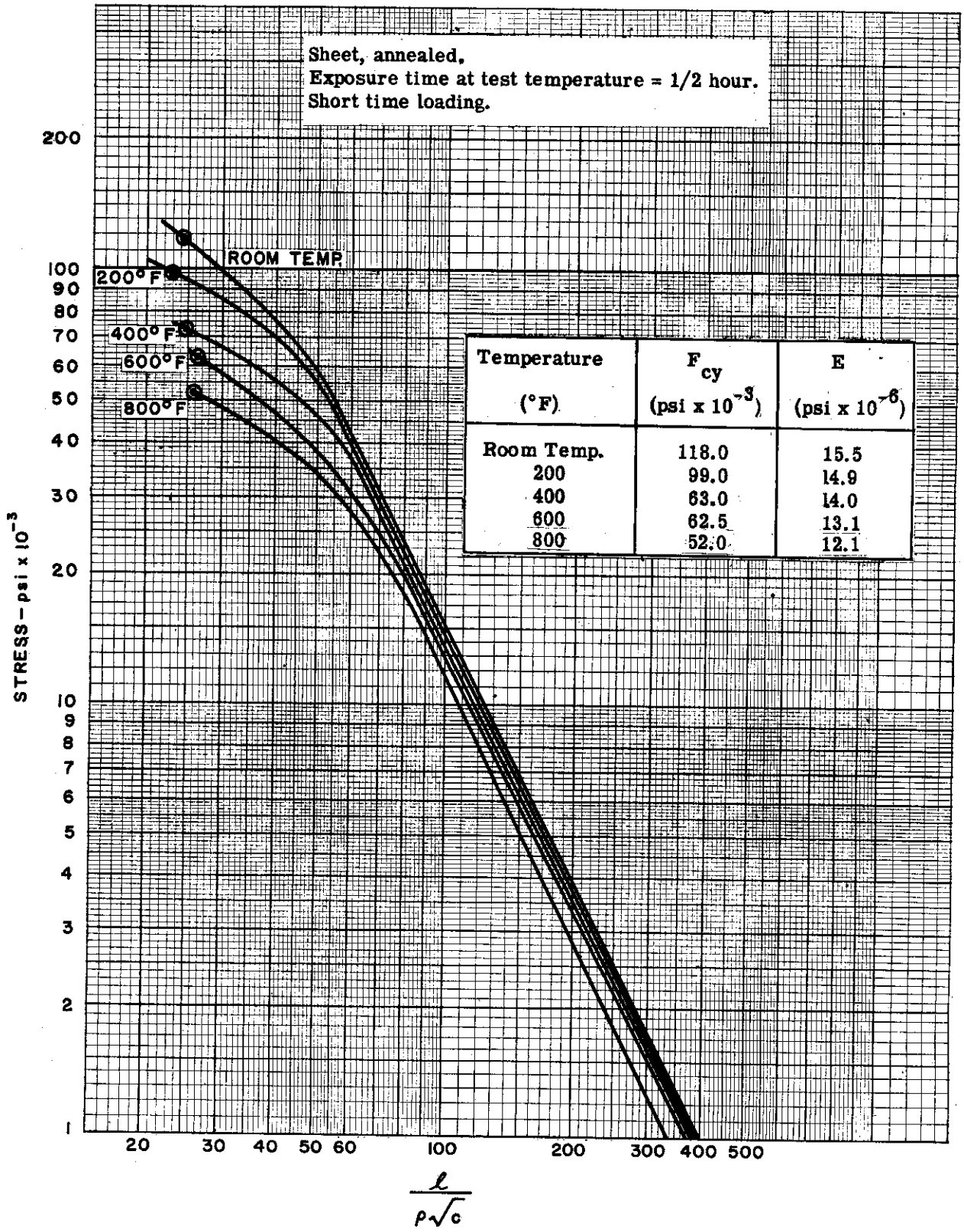

Temperature (°F)	F_{cy} (psi x 10^{-3})	E (psi x 10^{-6})
Room Temp.	118.0	15.5
200	99.0	14.9
400	63.0	14.0
600	62.5	13.1
800	52.0	12.1

Figure 4.2-4. RC C-110M Titanium Alloy — Buckling Stress for Stable Section Columns

[redacted]

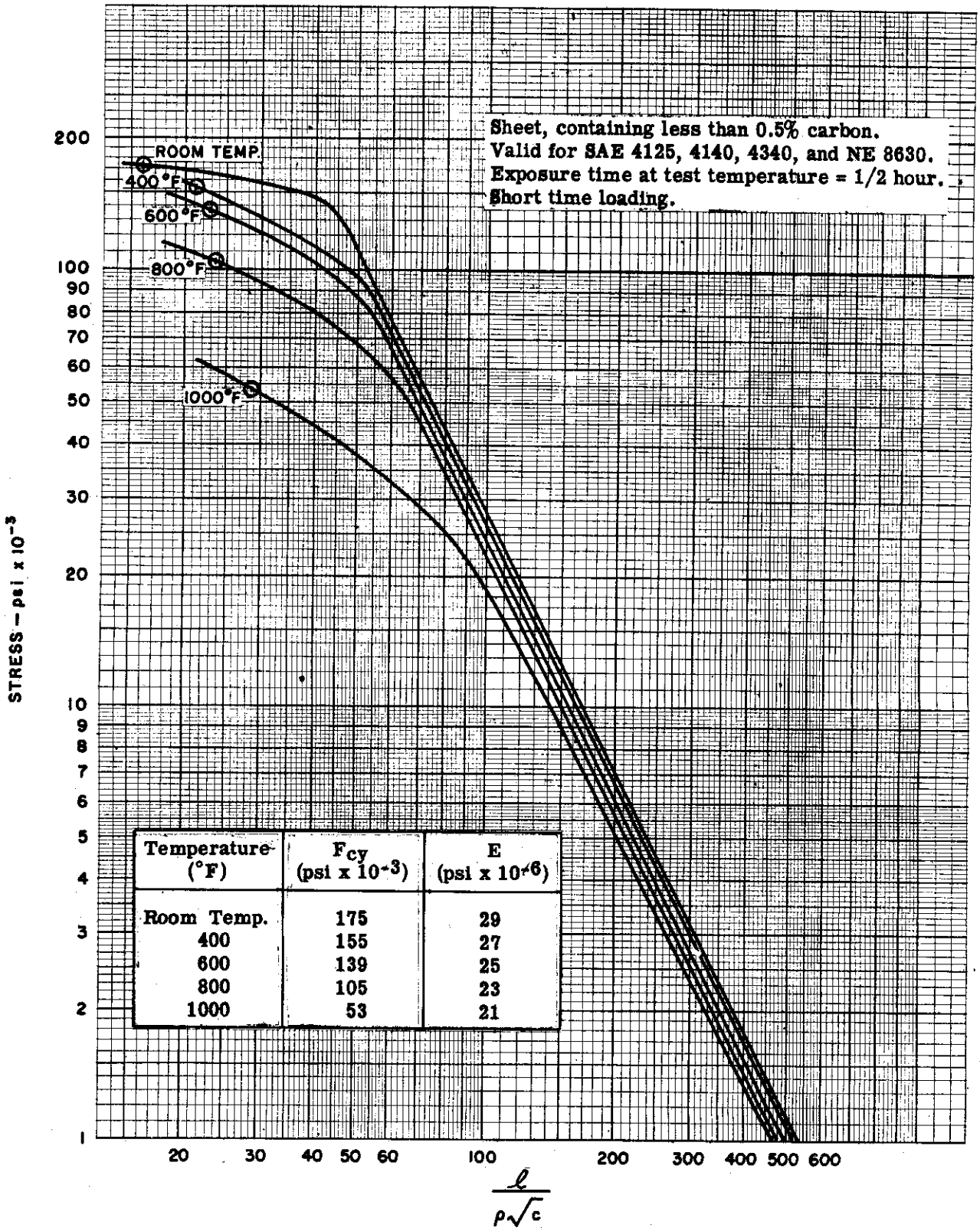

Temperature (°F)	F_{cy} (psi x 10^{-3})	E (psi x 10^{-6})
Room Temp.	175	29
400	155	27
600	139	25
800	105	23
1000	53	21

Figure 4.2-5. Alloy Steel — Heat-Treated to 200,000 psi — Buckling Stress for Stable Section Columns

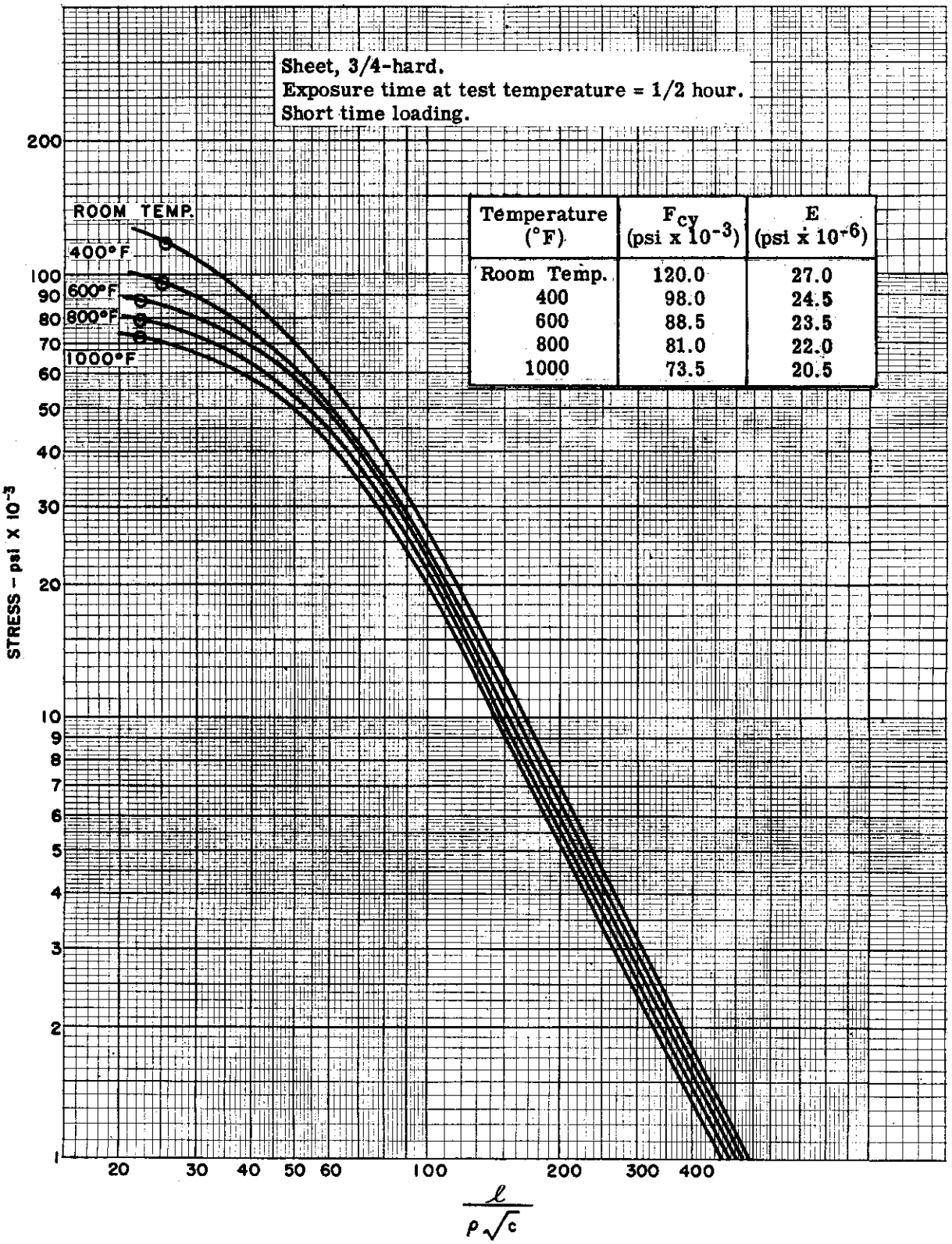

Temperature (°F)	F_{cy} (psi x 10^{-3})	E (psi x 10^{-6})
Room Temp.	120.0	27.0
400	98.0	24.5
600	88.5	23.5
800	81.0	22.0
1000	73.5	20.5

Figure 4.2-6. 18-8 Stainless Steel — Buckling Stress for Stable Section Columns

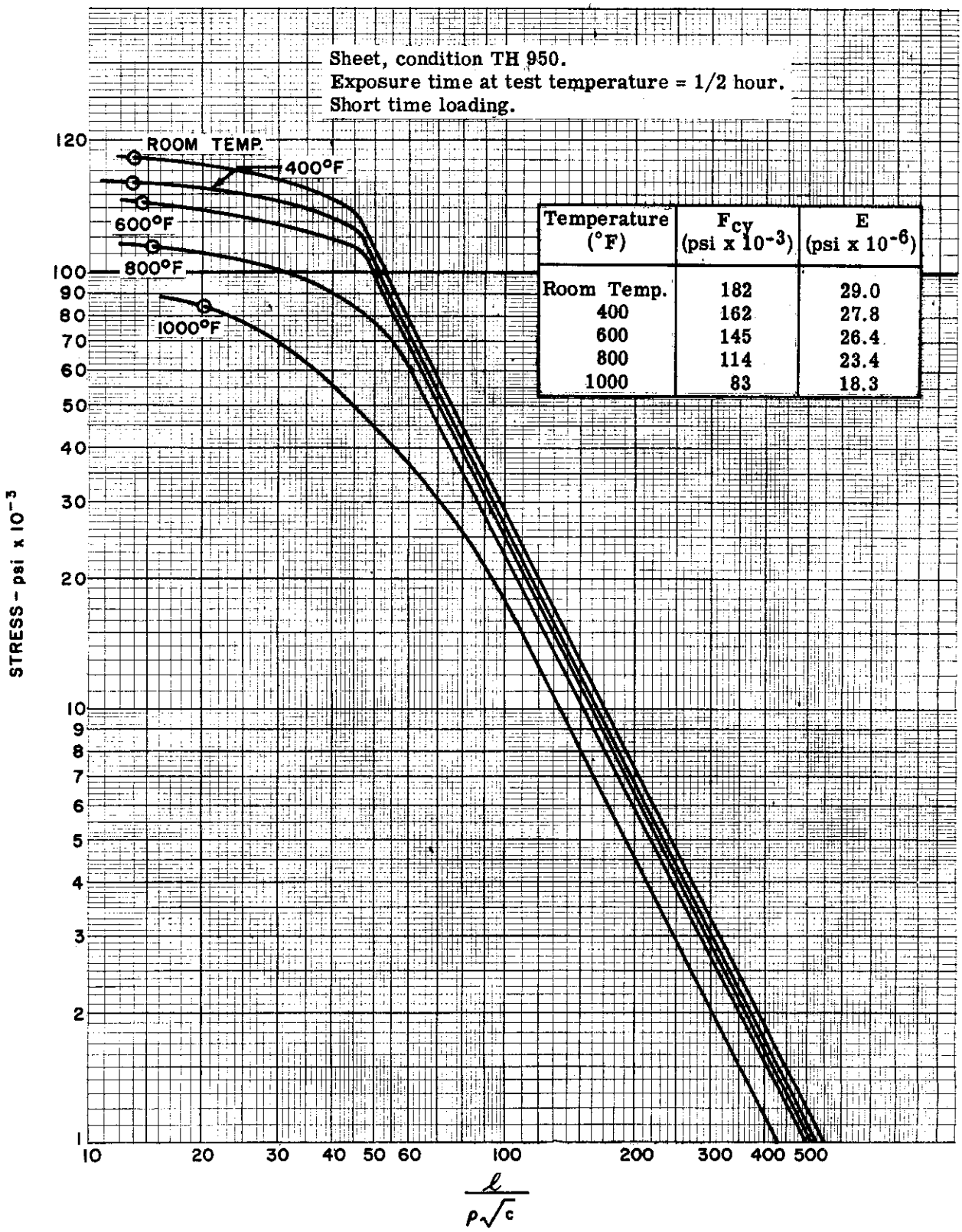

Figure 4.2-7. 17-7 PH Stainless Steel — Buckling Stress for Stable Section Columns

[redacted]

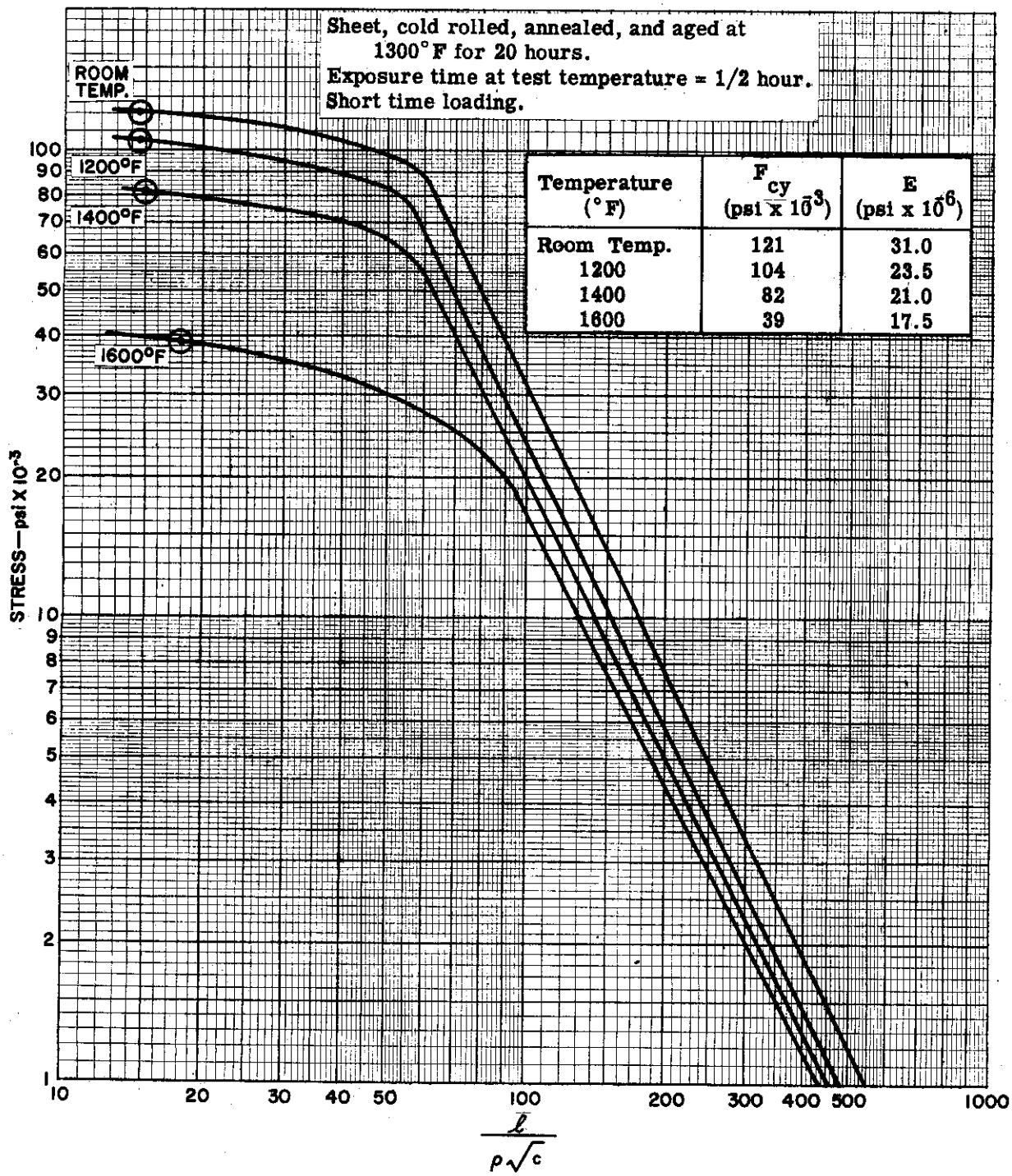

Figure 4.2-8. Inconel X — Buckling Stress for Stable Section Columns

[redacted]

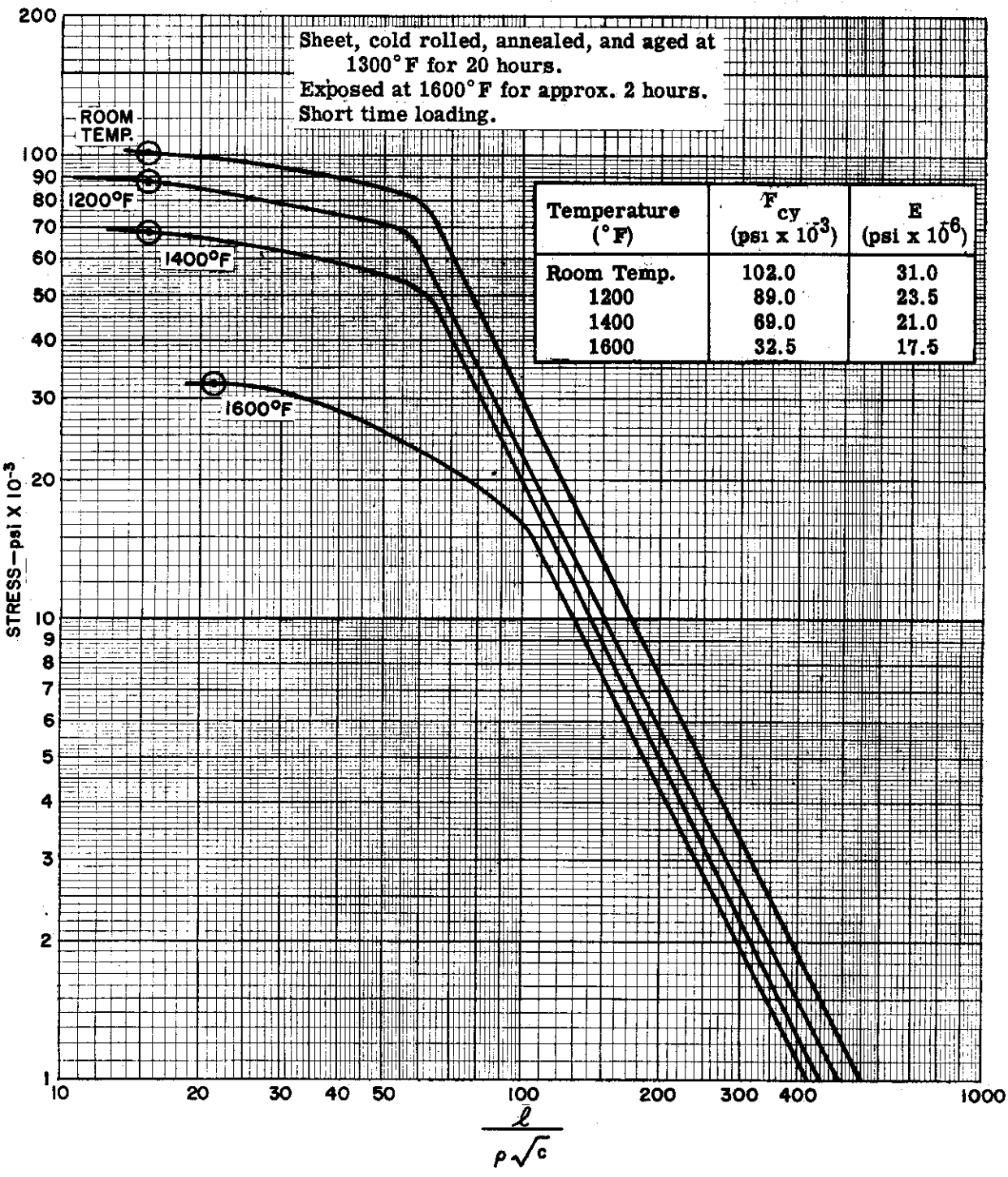

Figure 4.2-9. Inconel X — Buckling Stress for Stable Section Columns Exposed at 1600°F for 2 Hours

4.3 COLUMNS — UNIFORM TEMPERATURE — LONG-TIME LOADING

Figures 4.3-1 through 4.3-6 give creep buckling curves for stable section columns under constant load and temperature. A number of materials and times of loading are covered, and two temperatures at the level where creep is significant are included for each material.

The values for these curves have been calculated using a method detailed in Part II in which the Euler column formula is combined with a tangent modulus based upon the isochronous stress-strain curve. This method has the merits of simplicity and conservatism, but it can only be considered as an approximation to the solution of the creep buckling problem. Accordingly, comparisons between the results of this method and test data are given in Part II.

The method explained previously for the preparation of column creep buckling curves does not include consideration of initial eccentricity. This matter is discussed in Part II where it is shown that initial eccentricity can be neglected in most practical columns where the ratio of initial eccentricity to column cross-sectional width is 0.01 or less.

Creep data upon which Figures 4.3-1 through 4.3-6 are based are taken from the material properties of Section 2.0. It is explained in Section 2.0 that, because of limited data, some interpolation has been necessary. Consequently, creep buckling data should be considered provisional and suitable only for preliminary design until more comprehensive information is available.

[redacted]

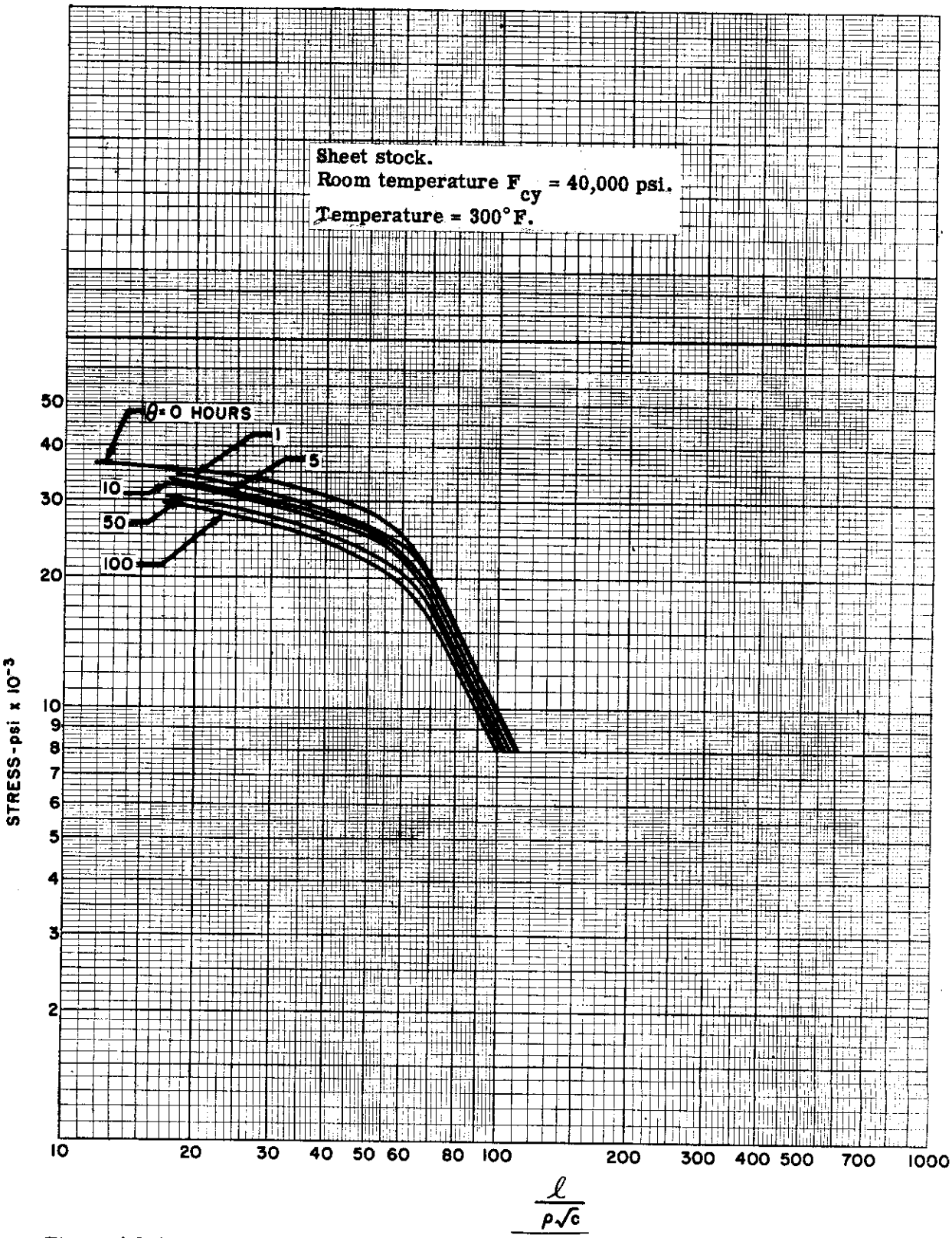

Figure 4.3-1. 2024-T3 Clad Aluminum Alloy — Creep Buckling Stress for Stable Section Columns at 300°F

[redacted]

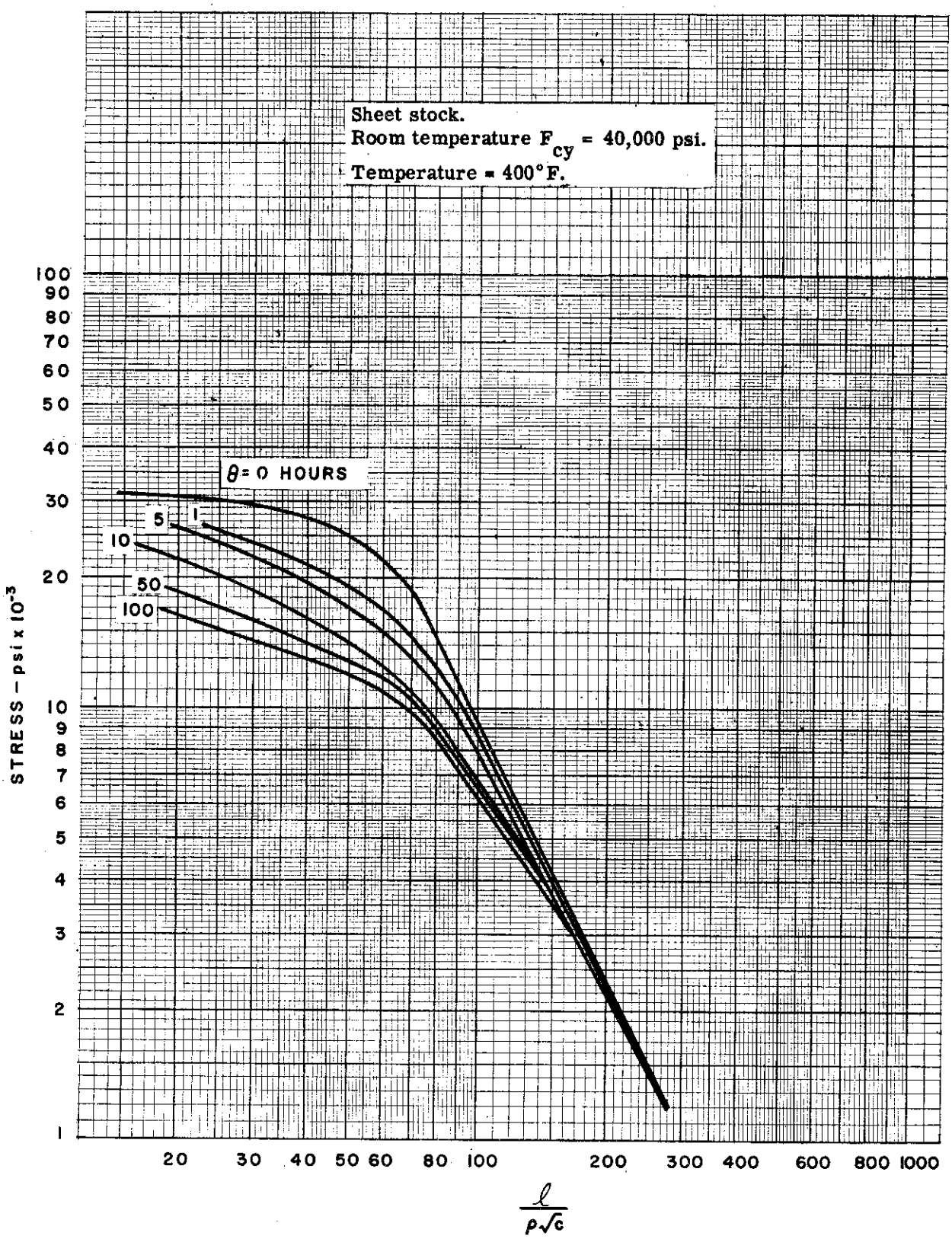

Figure 4.3-2. 2024-T3 Clad Aluminum Alloy – Creep Buckling Stress for Stable Section Columns at 400°F

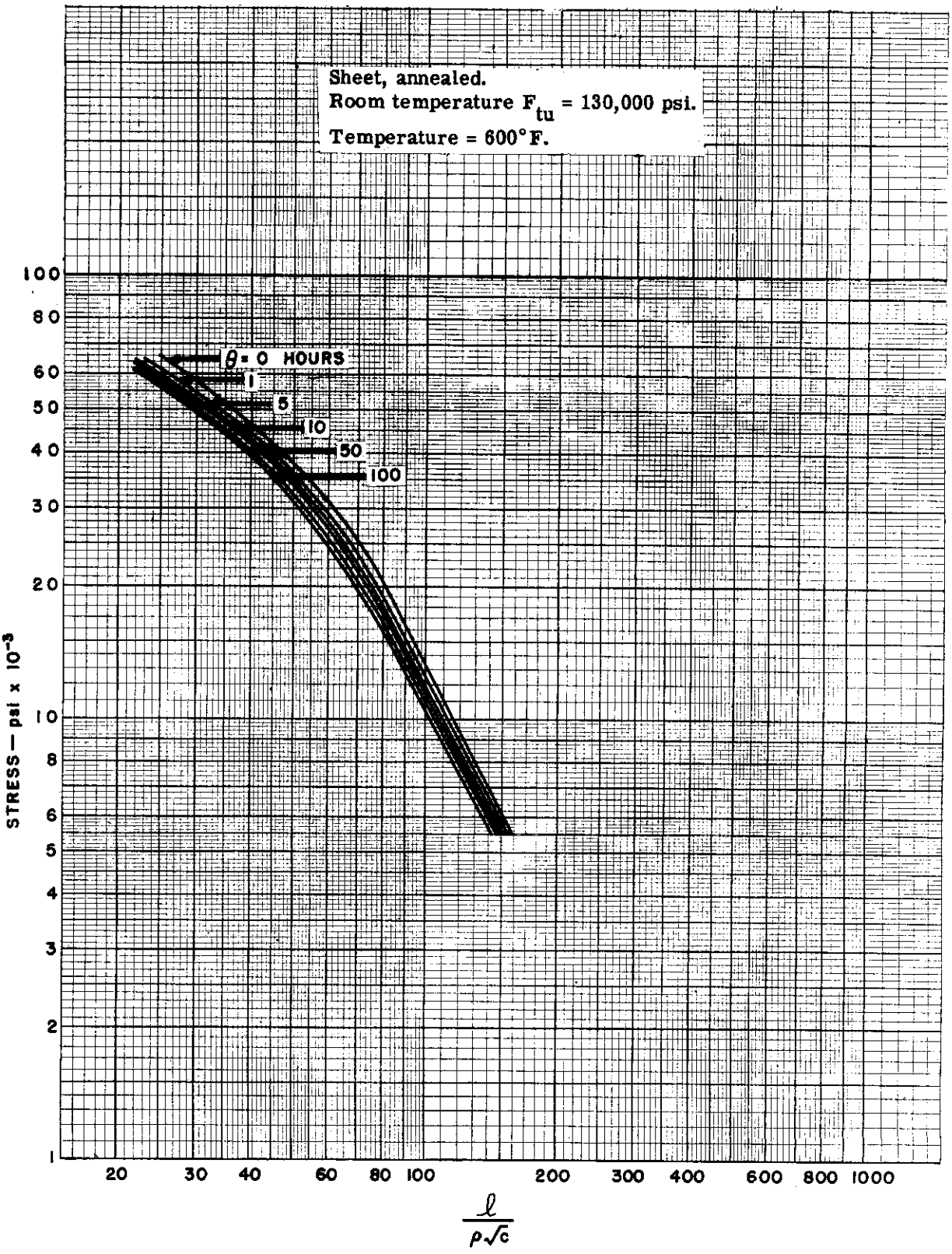

Figure 4.3-3. RC C-110M Titanium Alloy – Creep Buckling Stress for Stable Section Columns at 600°F

[redacted]

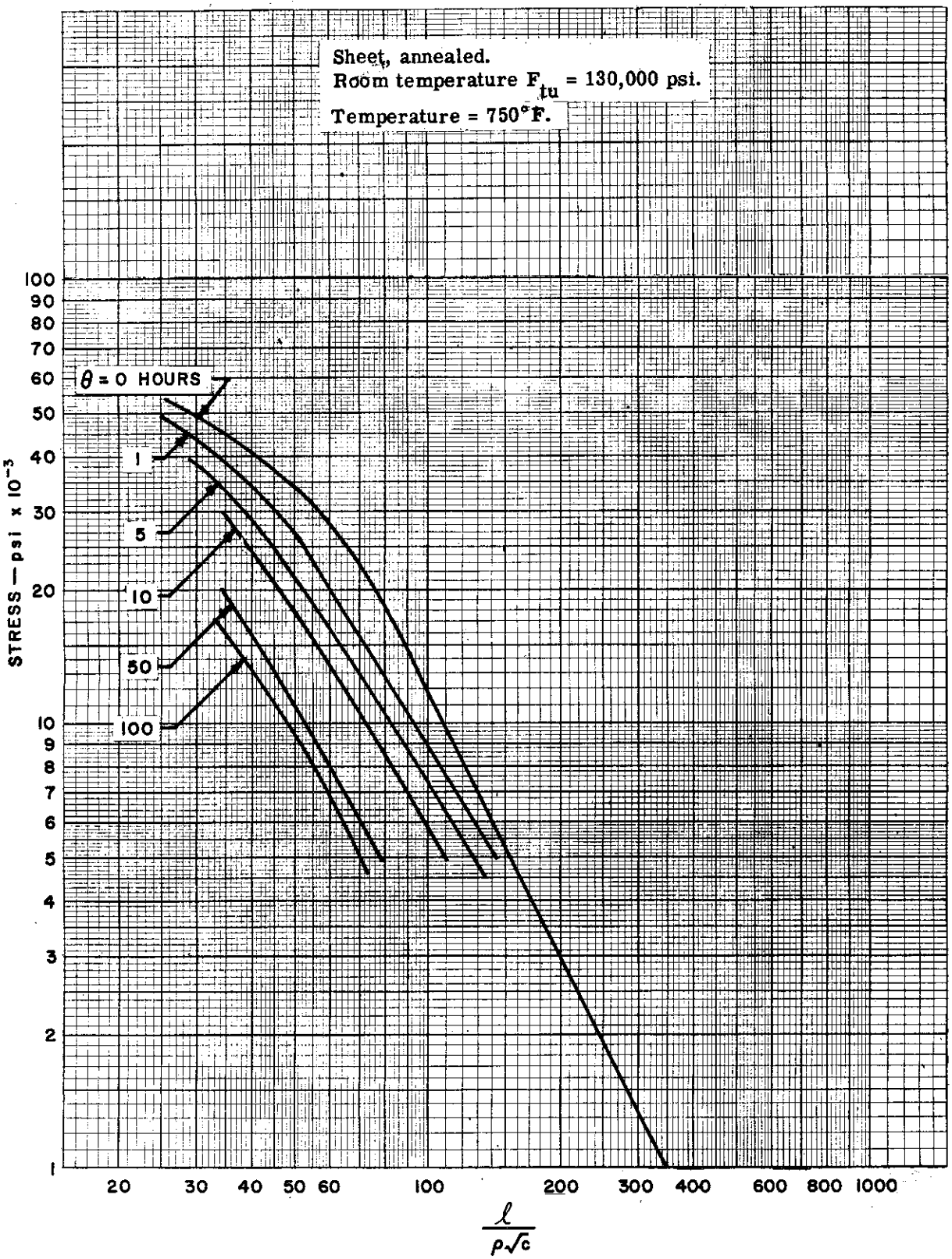

Figure 4.3-4. RC C-110M Titanium Alloy — Creep Buckling Stress for Stable Section Columns at 750°F

[redacted]

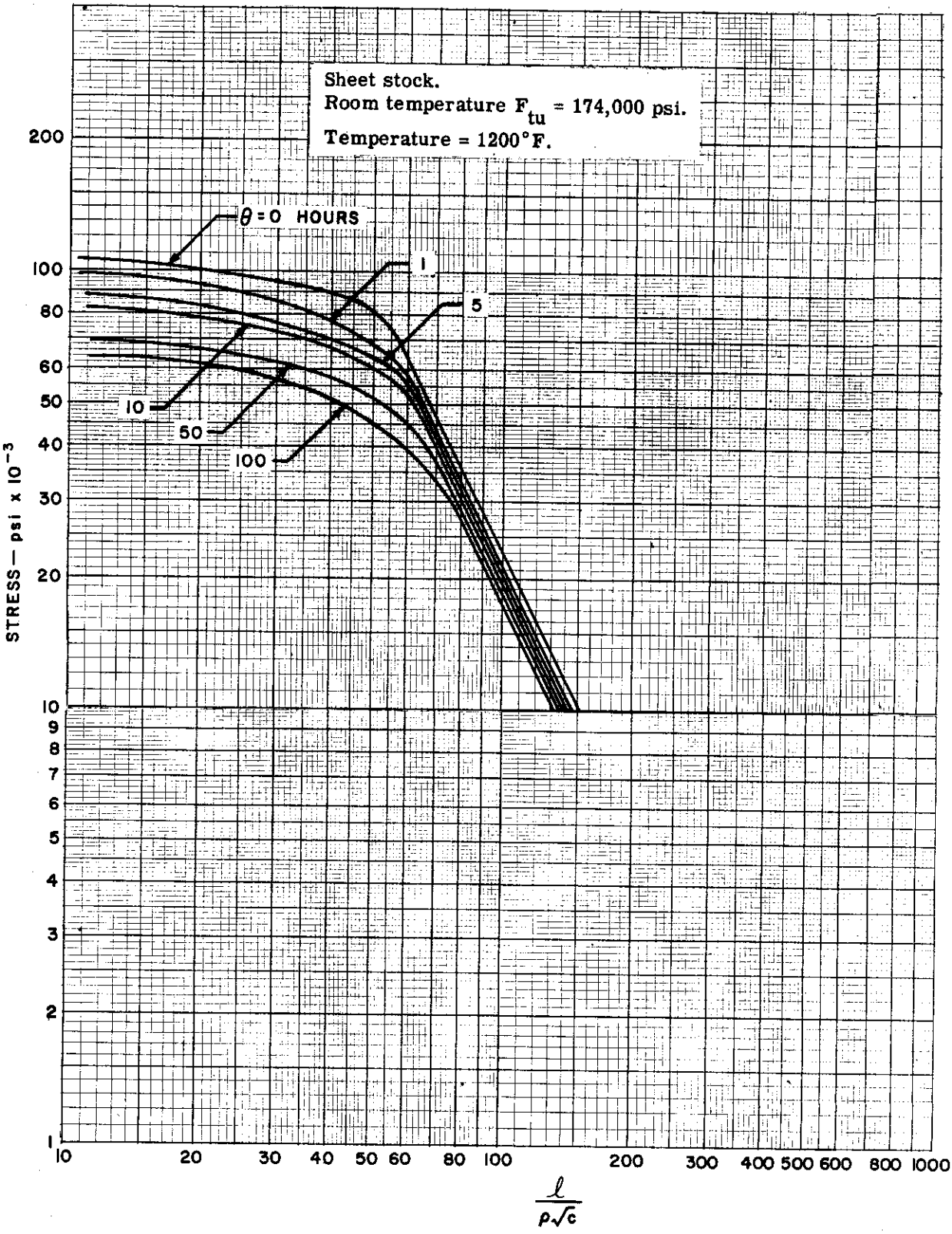

Figure 4.3-5. Inconel X — Creep Buckling Stress for Stable Section Columns at 1200°F

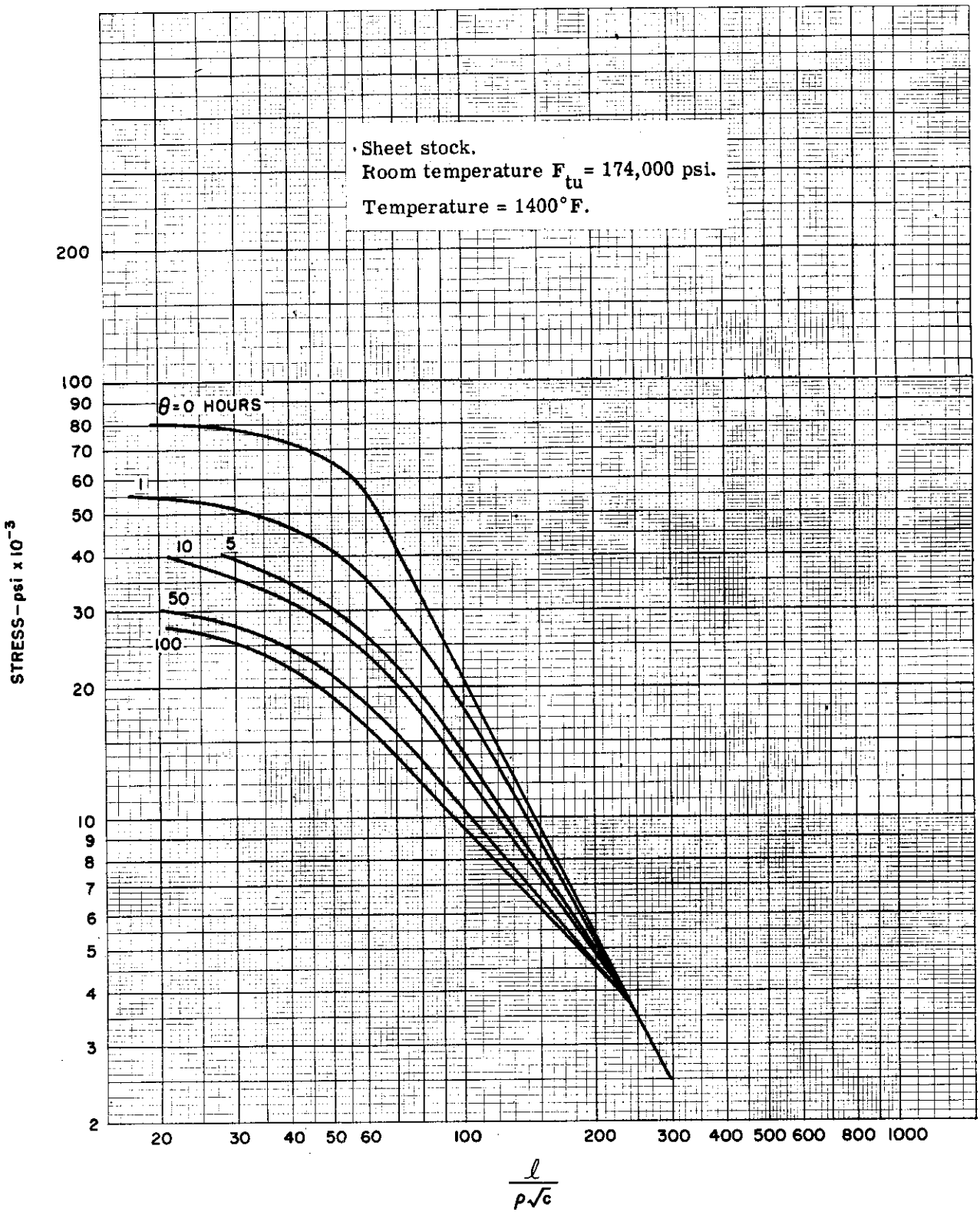

Figure 4.3-6. Inconel X — Creep Buckling Stress for Stable Section Columns at 1400°F

4.4 COLUMNS — LINEAR TEMPERATURE GRADIENTS

The temperature gradients through the cross-section of a column heated convectively from one side may be computed from the information and data presented in Section 3.0. If the nonlinearity of these gradients is neglected for engineering simplicity, and if the cross-sections are assumed stable, Figures 4.4-1 through 4.4-7 present buckling curves for such columns. A number of representative section shapes are included covering a range of dimensions. The curves apply to columns continuous over many supports ($c = 1$) and built in ($c = 4.0$), but they cannot be used in any manner for pin-ended columns since the effect of a temperature gradient is, in this case, quite different.

Figures 4.4-1 through 4.4-7, based upon tangent moduli given in Section 2.0, cover a range of temperatures in which the respective materials will be most frequently used. Each group of curves is associated with the temperature, T_s, in the skin and the gradient across the section is denoted by the increment ΔT. A value of ΔT equal to zero represents a uniform stress and these curves are identical with those of Section 4.2.

It will be noted that the effect of section shape is generally small so that interpolation for other similar shapes is readily accomplished. In interpolating for intermediate values of temperature gradient, the effect of a steadily increasing value of gradient is first to increase rapidly the column buckling stress, and then to decrease it slowly. The curves may be used directly for sections larger or smaller than those shown, provided that the proportions are retained. Similarly, they apply to elements of any thickness, provided that local instability does not occur.

The method by which the curves of Figures 4.4-1 through 4.4-7 have been calculated is given in Part II. Briefly, this method consists of assuming a strain at one extreme fiber, and from the specified temperature gradient the strains at all other points across the section are known.

Using the stress-strain and tangent moduli diagrams appropriate for the temperature at each fiber, an average stress and an effective stiffness are obtained for the column; these are used in the conventional column formulas to find an appropriate l/ρ. This process is repeated to obtain a series of values of l/ρ vs. σ_{cr}.

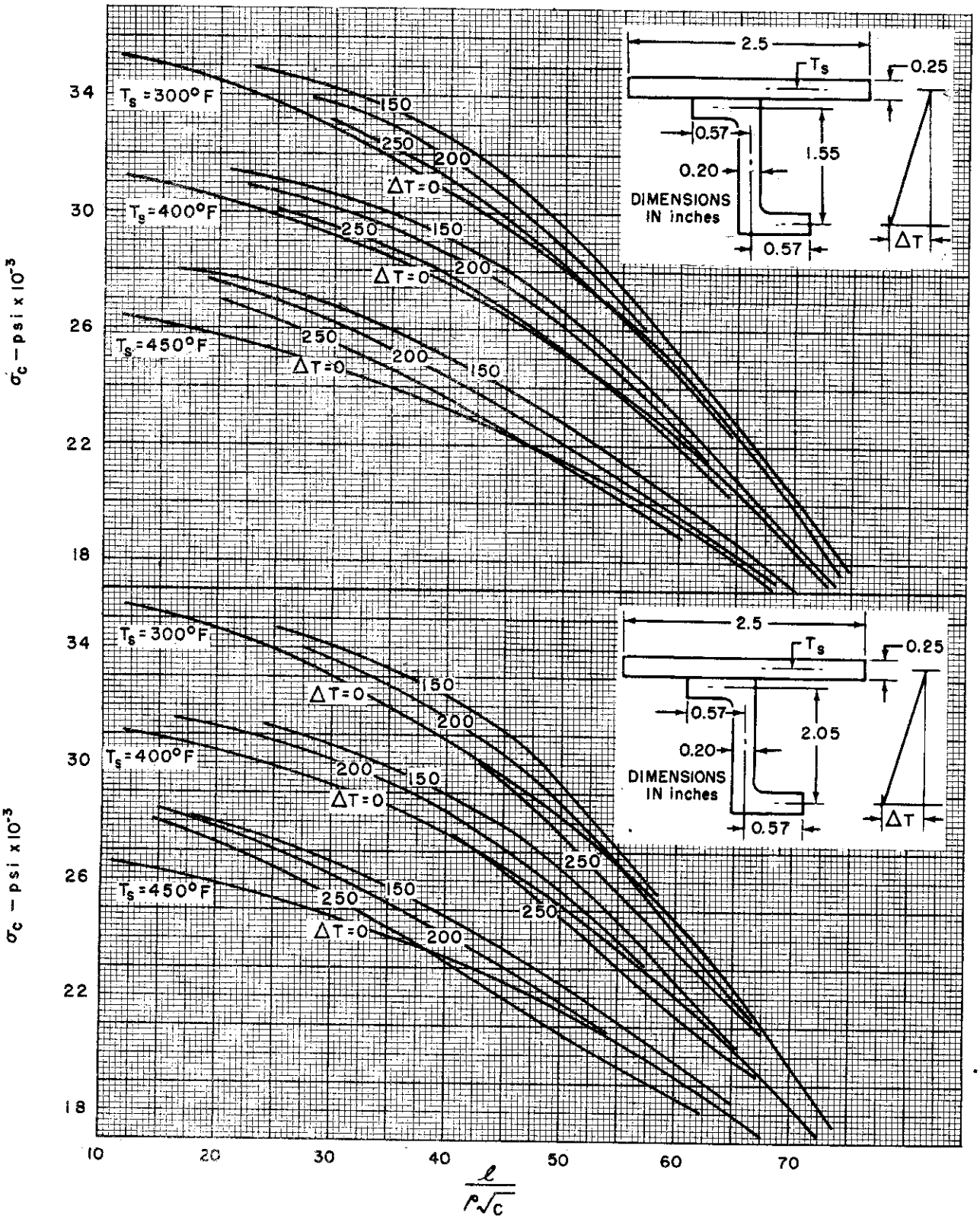

Figure 4.4-1. 2024-T3 Clad Aluminum Alloy – Buckling Stress for Columns with Temperature Gradient

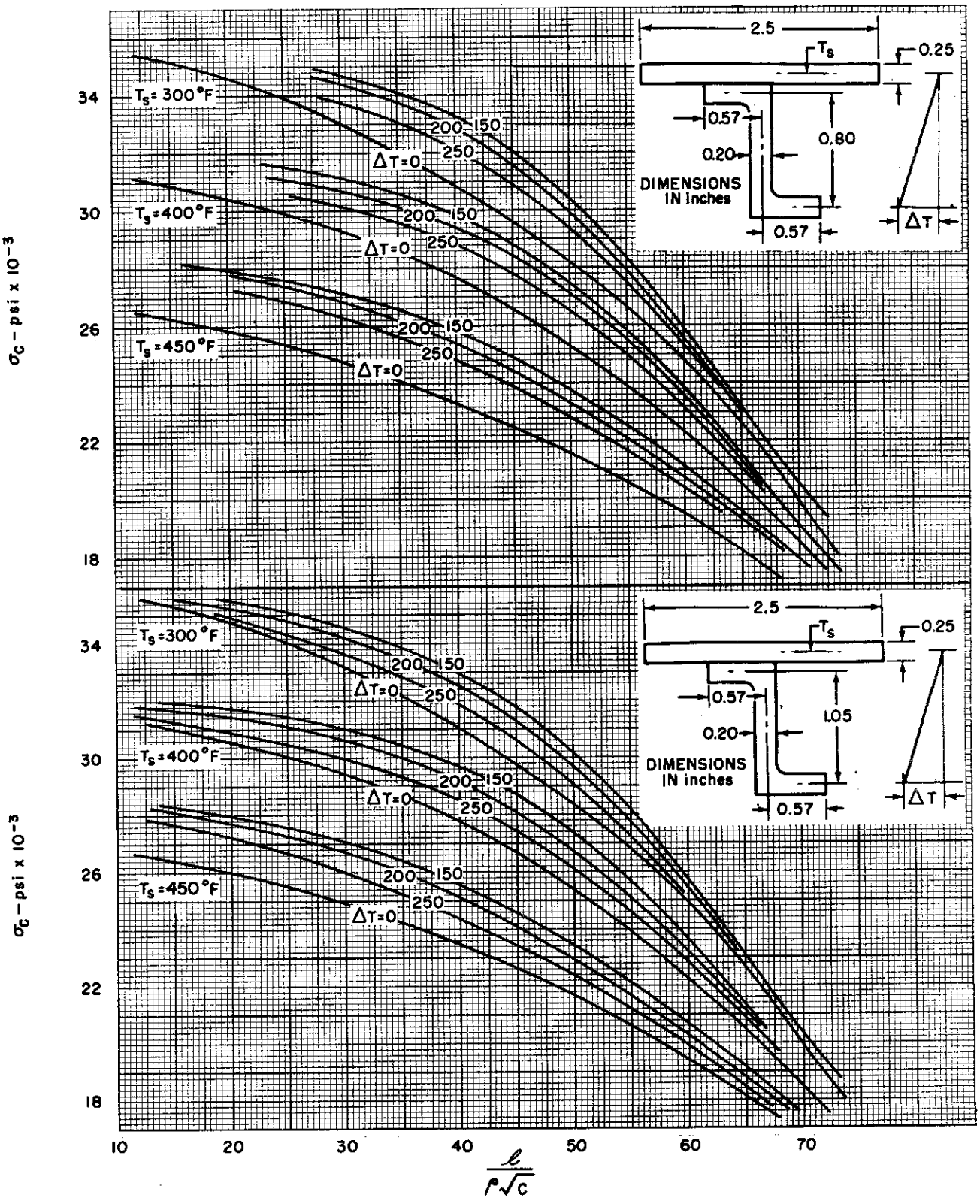

Figure 4.4-2. 2024-T3 Clad Aluminum Alloy — Buckling Stress for Columns with Temperature Gradient

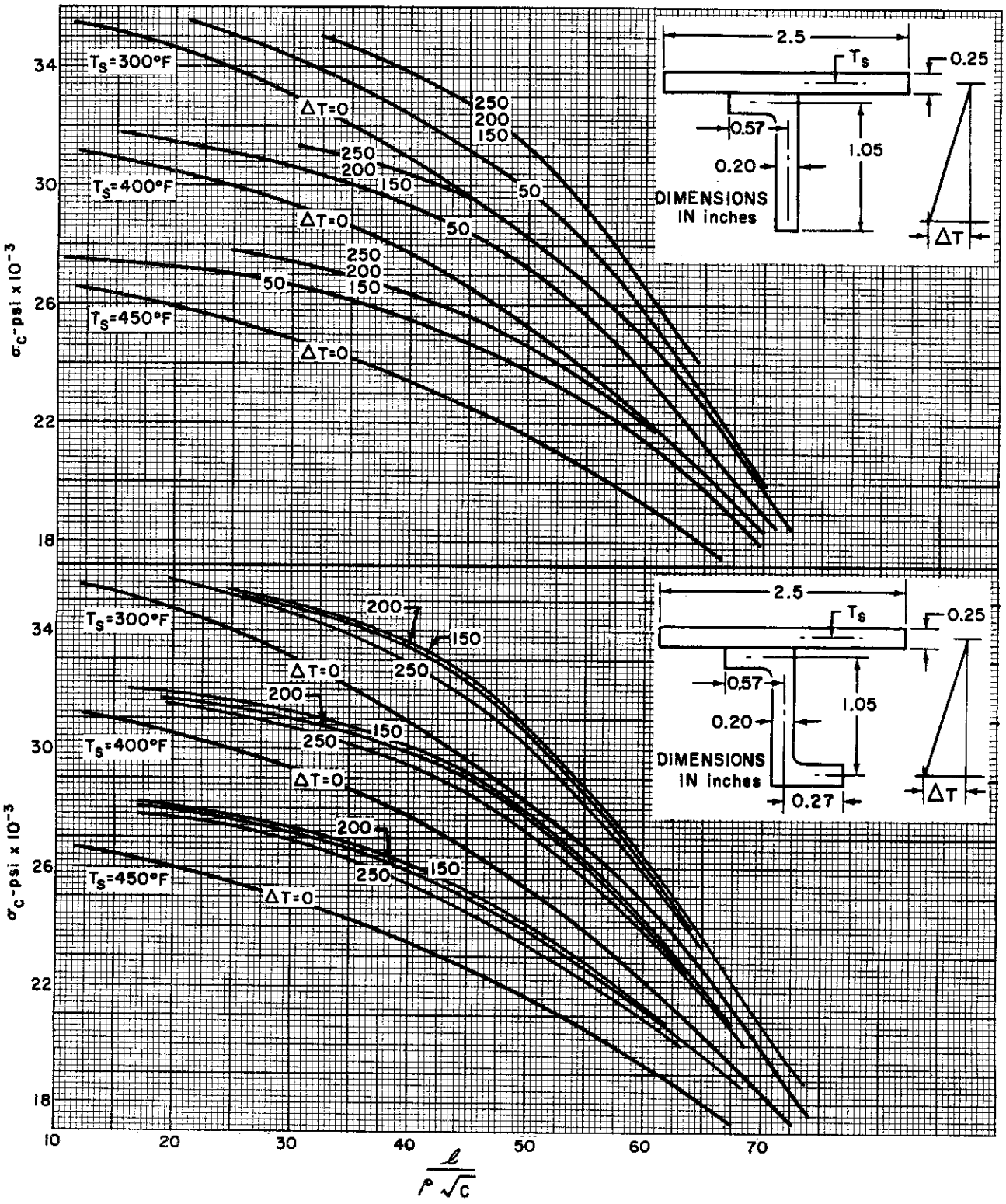

Figure 4.4-3. 2024-T3 Clad Aluminum Alloy — Buckling Stress for Columns with Temperature Gradient

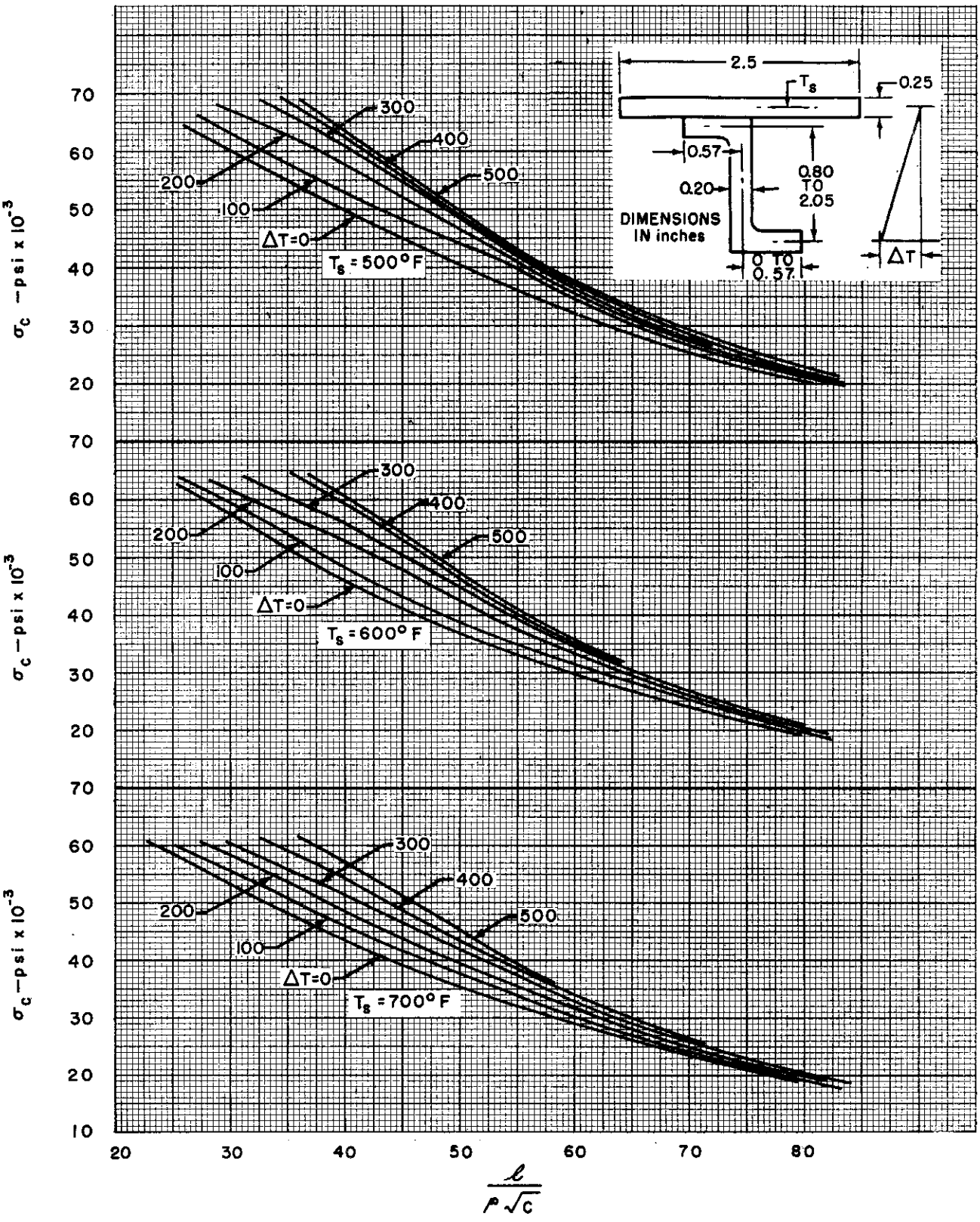

Figure 4.4-4. RC C-110M Titanium Alloy -- Buckling Stress for Columns with Temperature Gradient

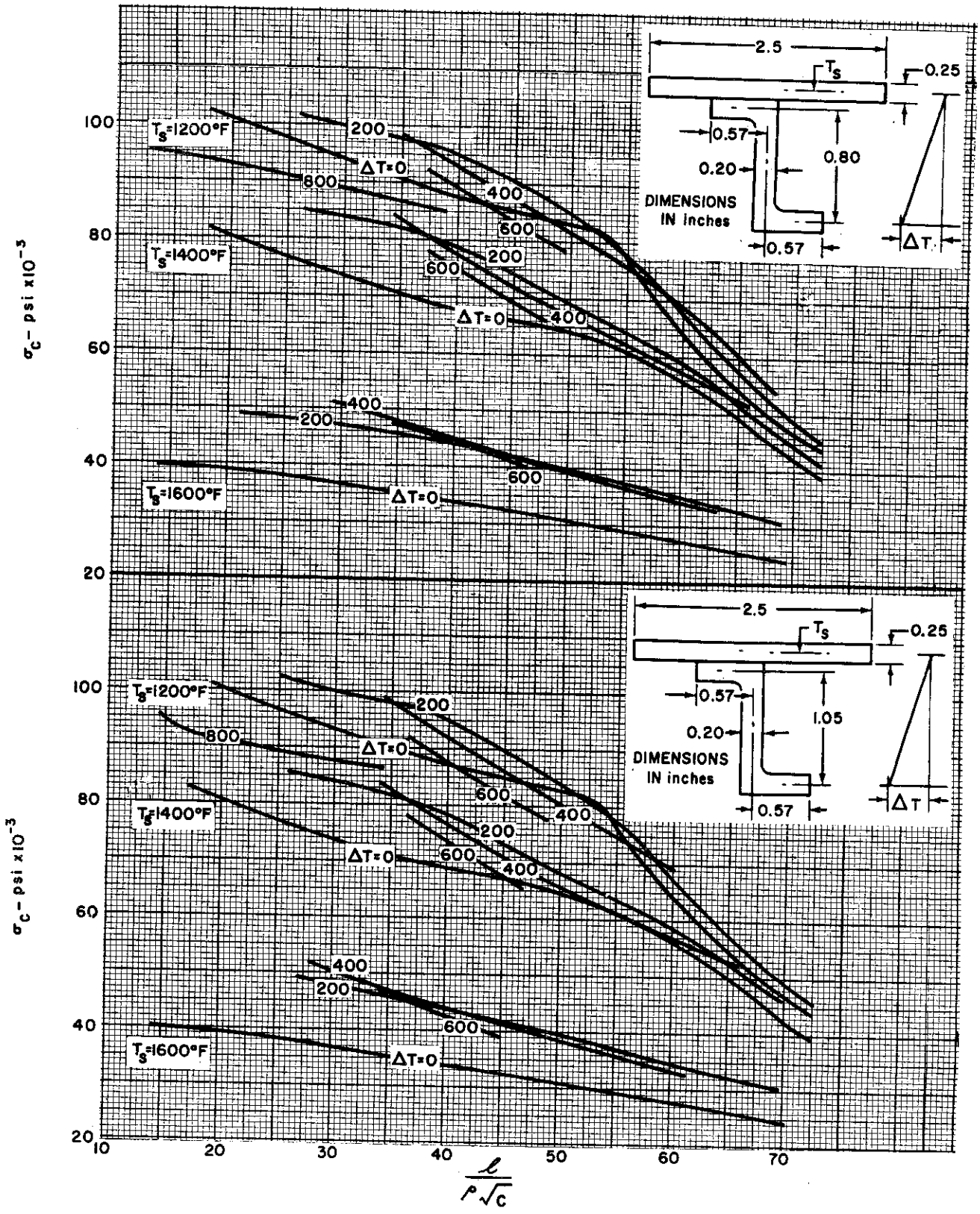

Figure 4.4-5. Inconel X — Buckling Stress for Columns with Temperature Gradient

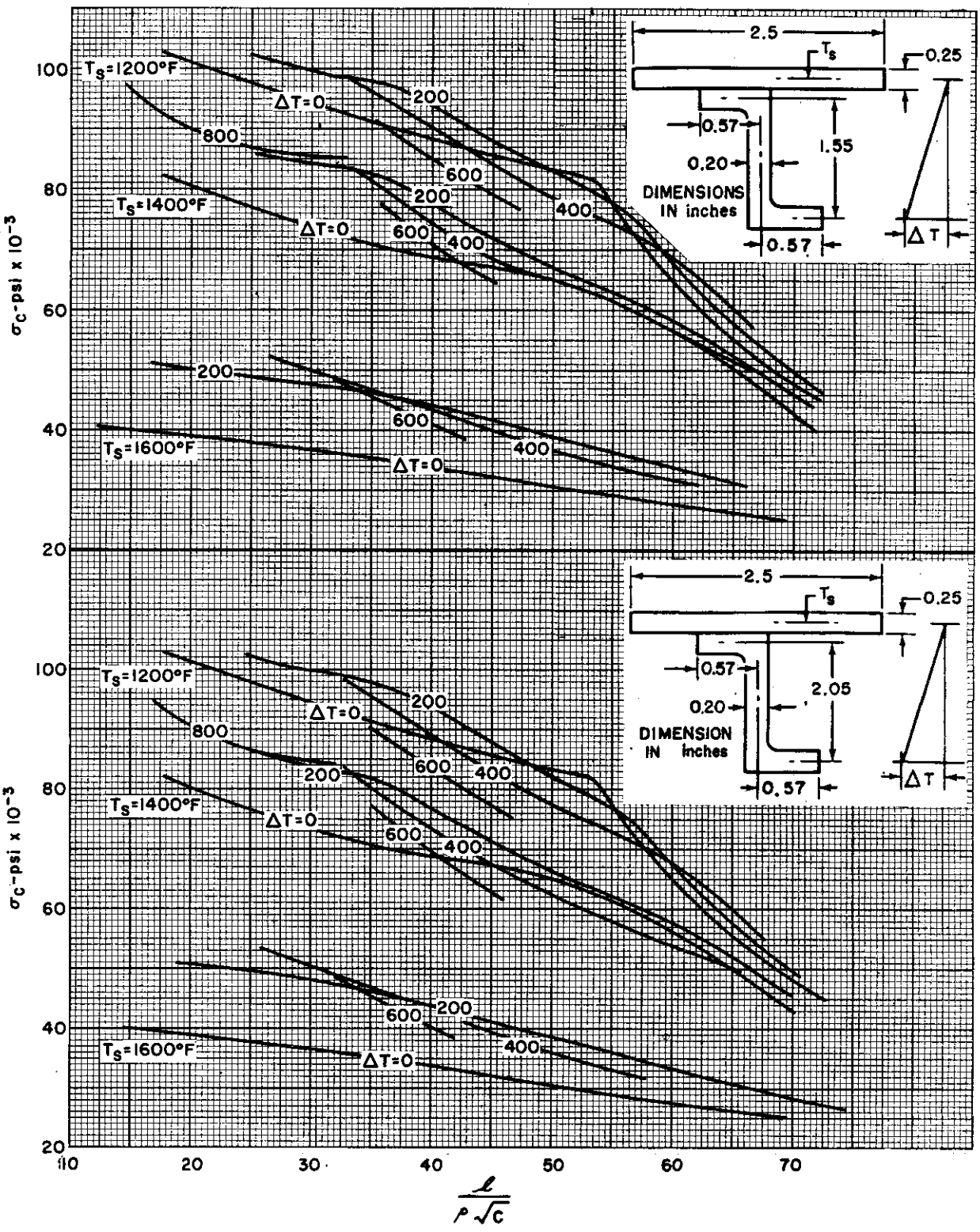

Figure 4.4-6. Inconel X — Buckling Stress for Columns with Temperature Gradient

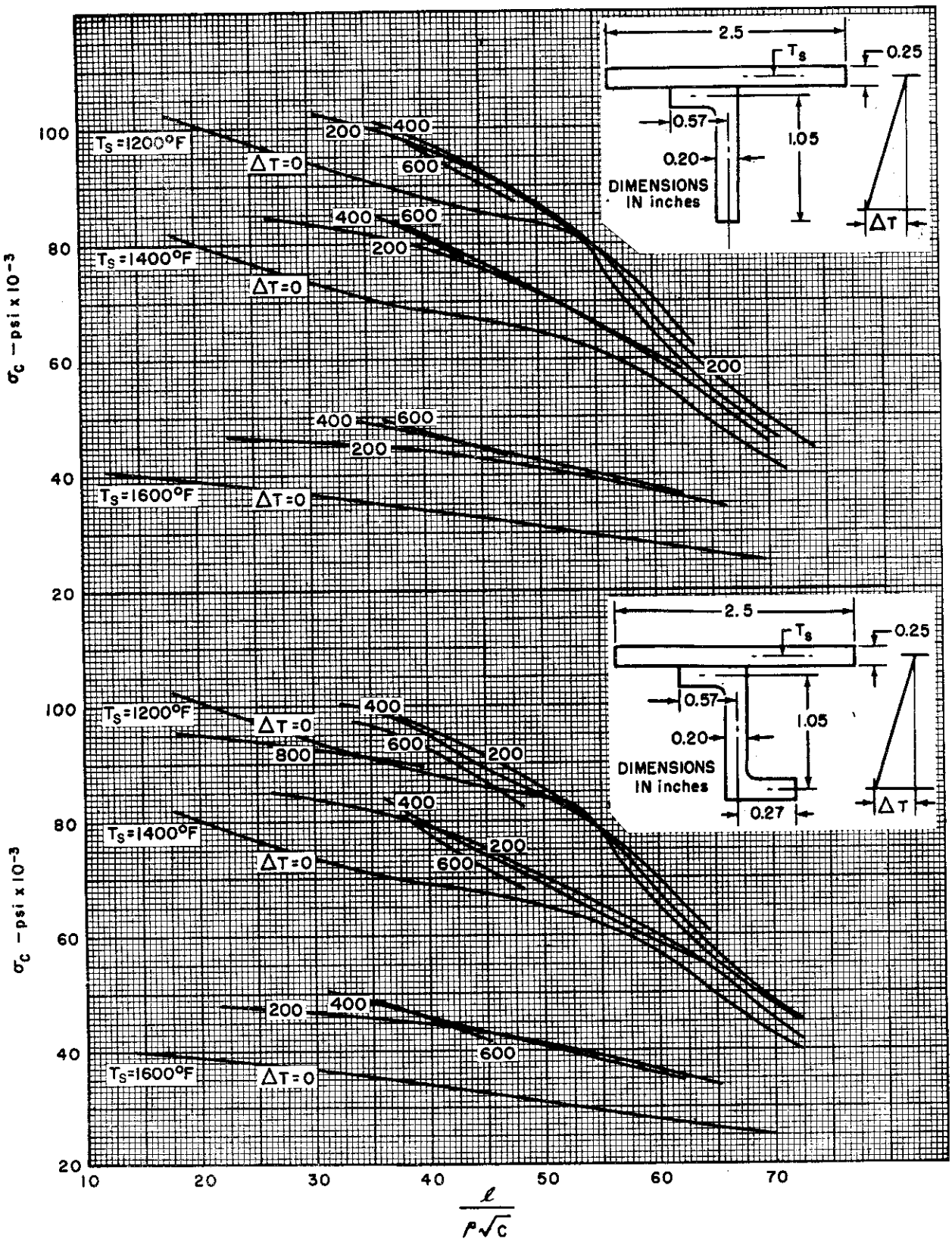

Figure 4.4-7. Inconel X — Buckling Stress for Columns with Temperature Gradient

4.5 PLATES — UNIFORM TEMPERATURE — SHORT-TIME LOADING

Figures 4.5-1 through 4.5-9 give plate buckling curves for various materials and ranges of temperatures, and for short-time loading. The values for these curves are calculated from the usual plate buckling equation

$$\sigma_{cr} = \frac{K\pi^2\eta E}{12(1-\mu^2)}\left(\frac{t}{b}\right)^2.$$

Here the plasticity coefficient η is dependent upon the type of loading, the geometry of the plate configuration, and the stress-strain curve in compression. The method of calculating η is explained in Part II.

[redacted]

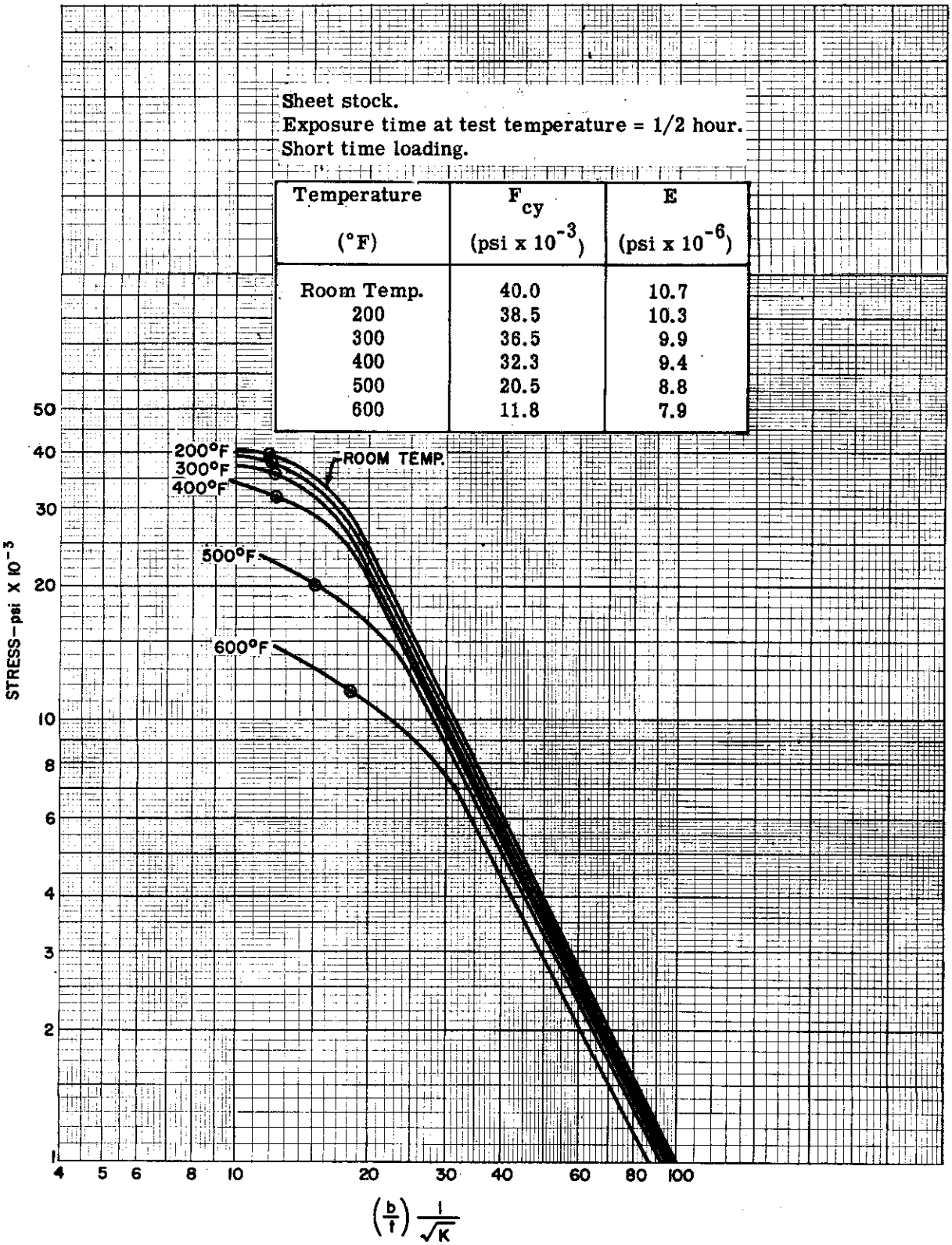

Figure 4.5-1. 2024-T3 Clad Aluminum Alloy — Buckling Stress for a Long Simply Supported Plate in Compression

[redacted]

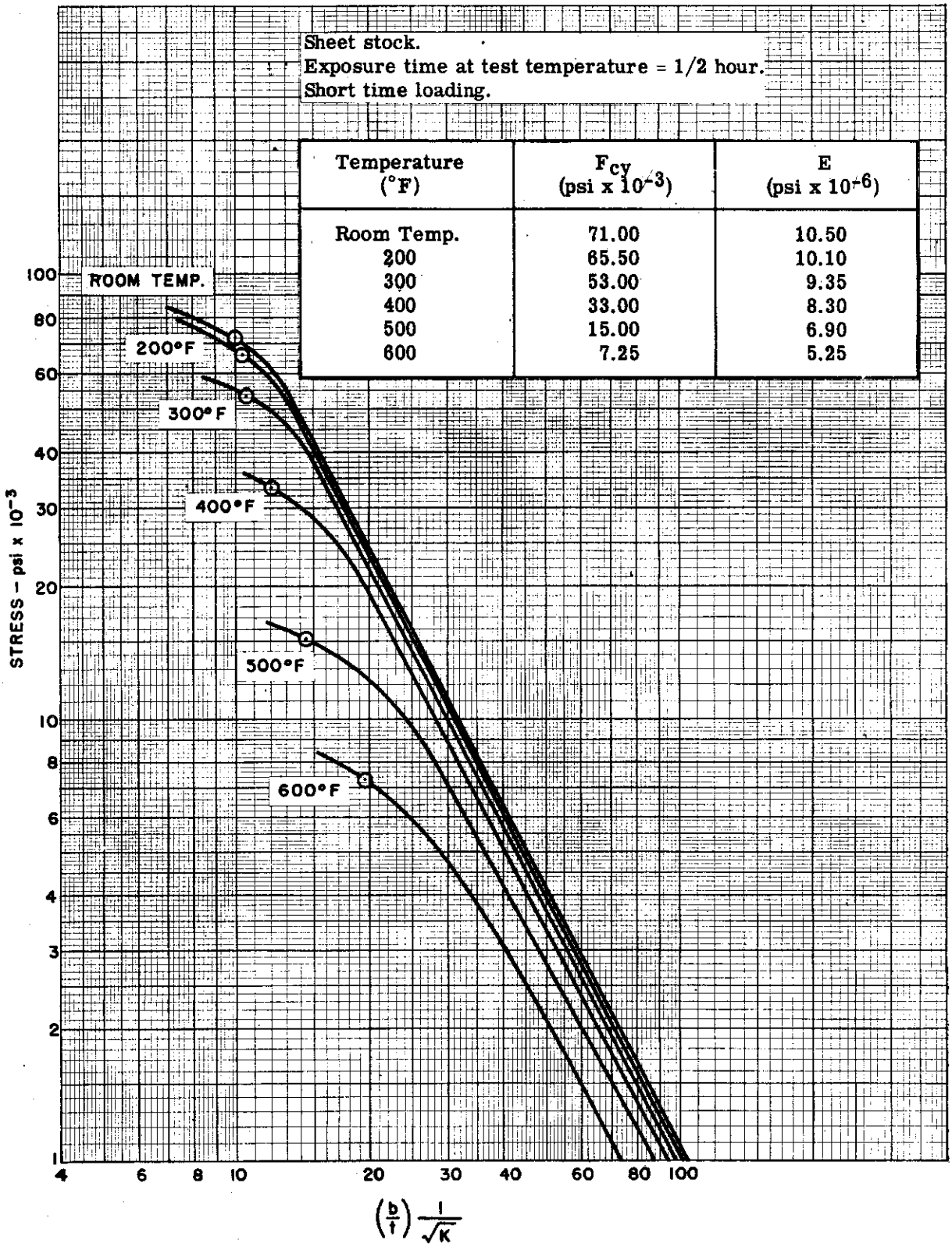

Figure 4.5-2. 7075-T6 Aluminum Alloy — Buckling Stress for a Long Simply Supported Plate in Compression

Sheet stock.
Exposure time at test temperature = 1/2 hour.
Short time loading.

Temperature (°F)	F_{cy} (psi x 10^{-3})	E (psi x 10^{-6})
Room Temp.	24.0	6.5
200	22.3	5.9
300	19.2	5.2
400	11.6	3.7
500	7.3	2.3
600	4.0	1.4

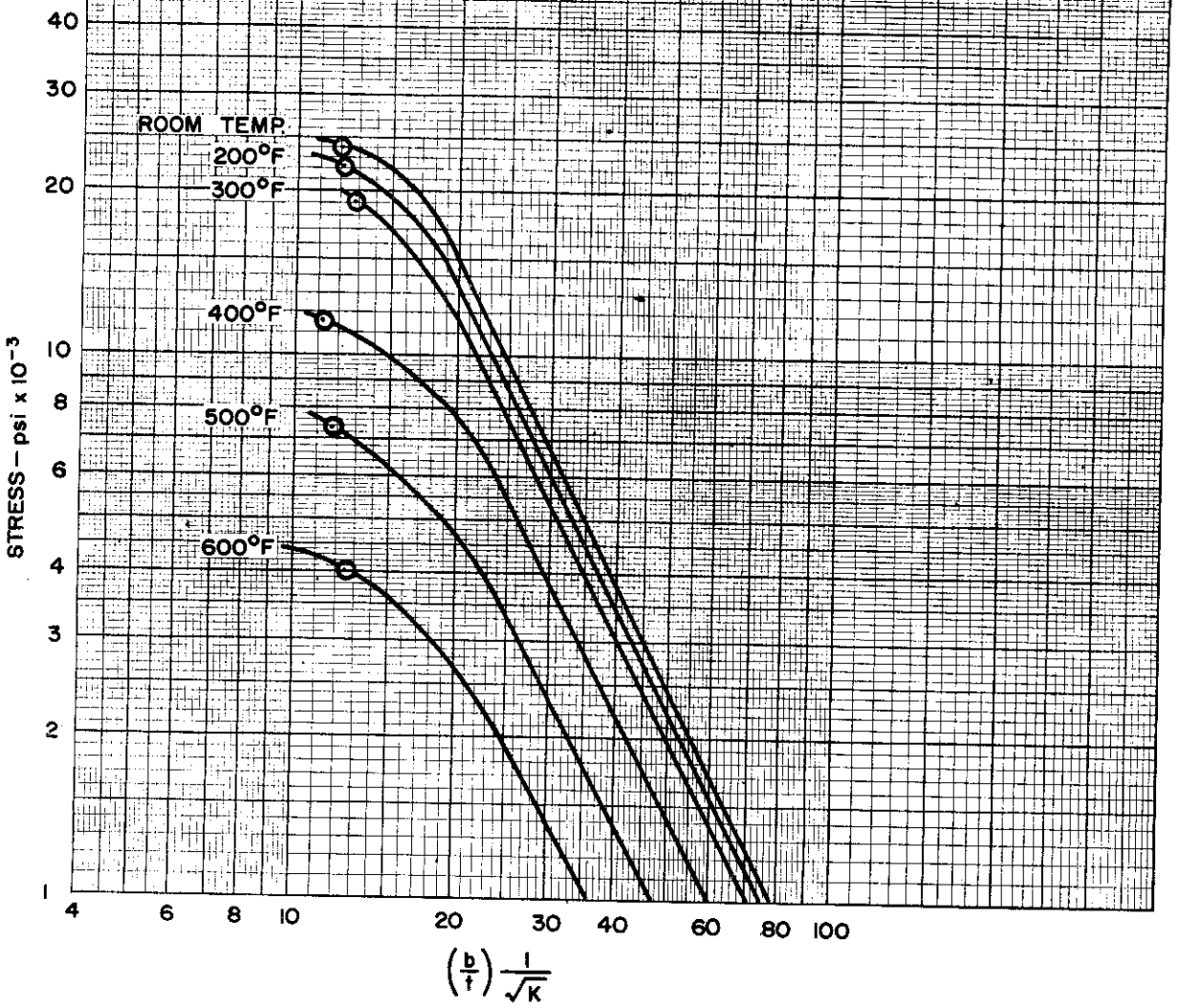

Figure 4.5-3. FSI-H24 Magnesium Alloy — Buckling Stress for a Long Simply Supported Plate in Compression

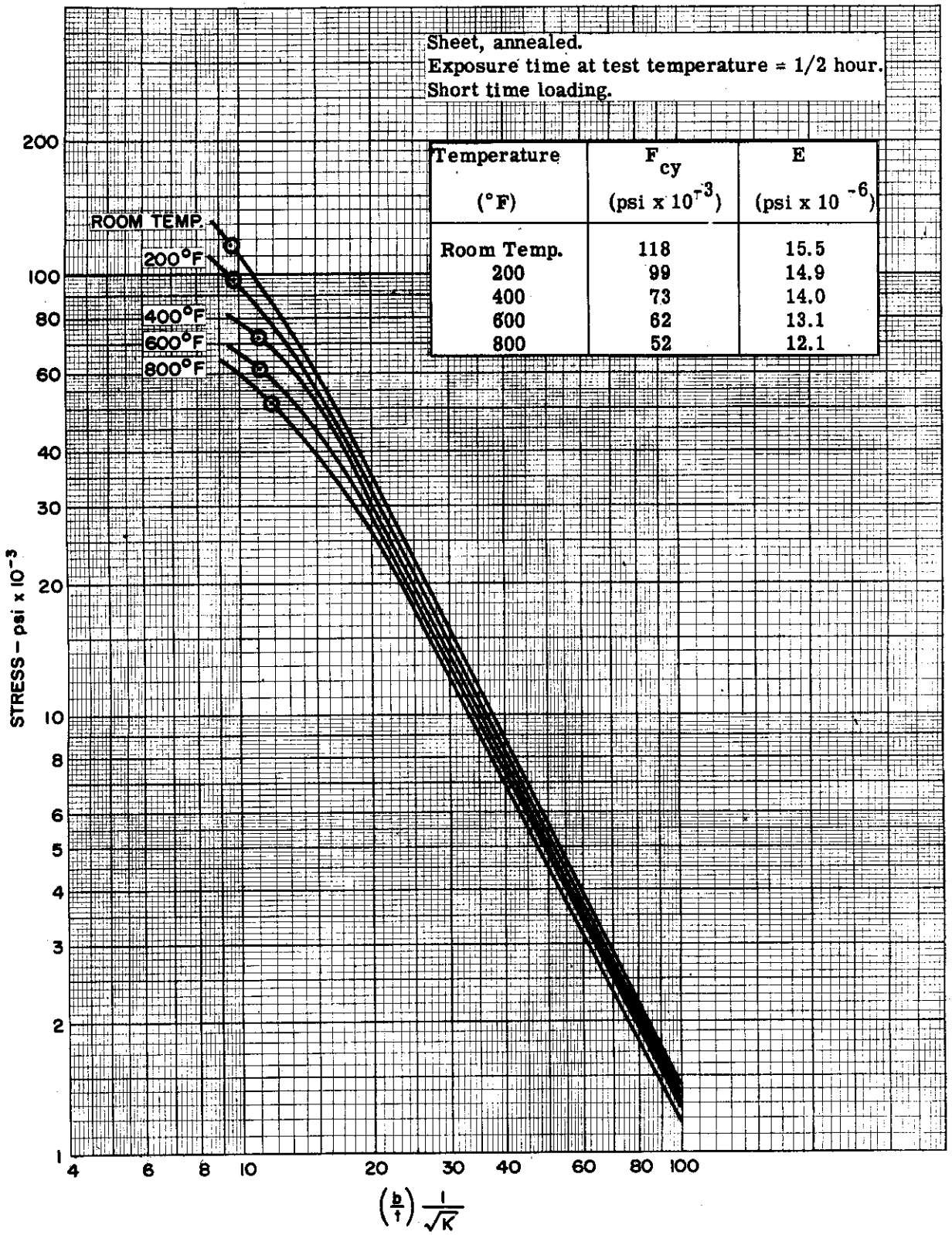

Figure 4.5-4. RC C-110M Titanium Alloy — Buckling Stress for a Long Simply Supported Plate in Compression

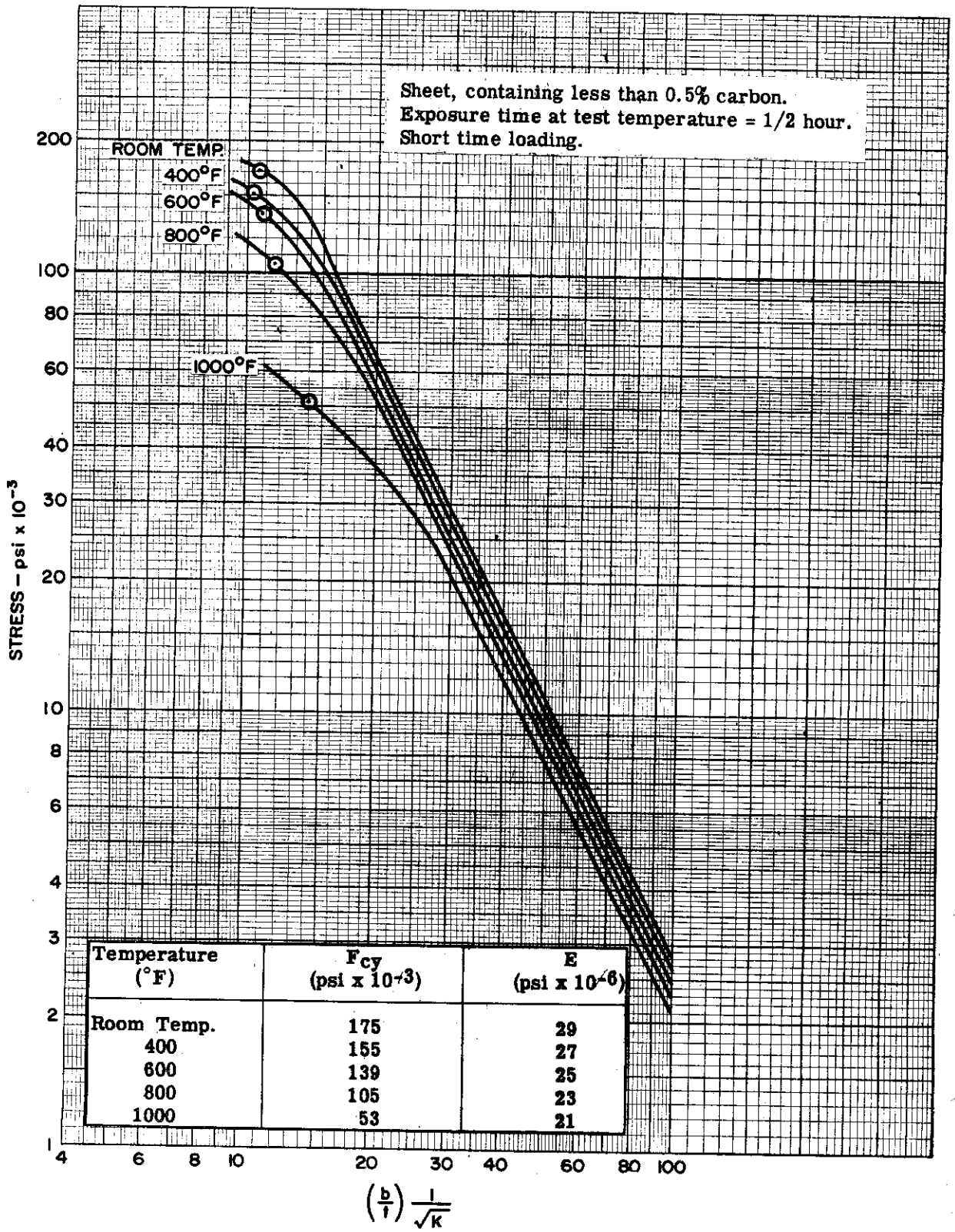

Temperature (°F)	F_{cy} (psi x 10^{-3})	E (psi x 10^{-6})
Room Temp.	175	29
400	155	27
600	139	25
800	105	23
1000	53	21

Figure 4.5-5. Alloy Steel – Heat-Treated to 200,000 psi — Buckling Stress for a Long Simply Supported Plate in Compression

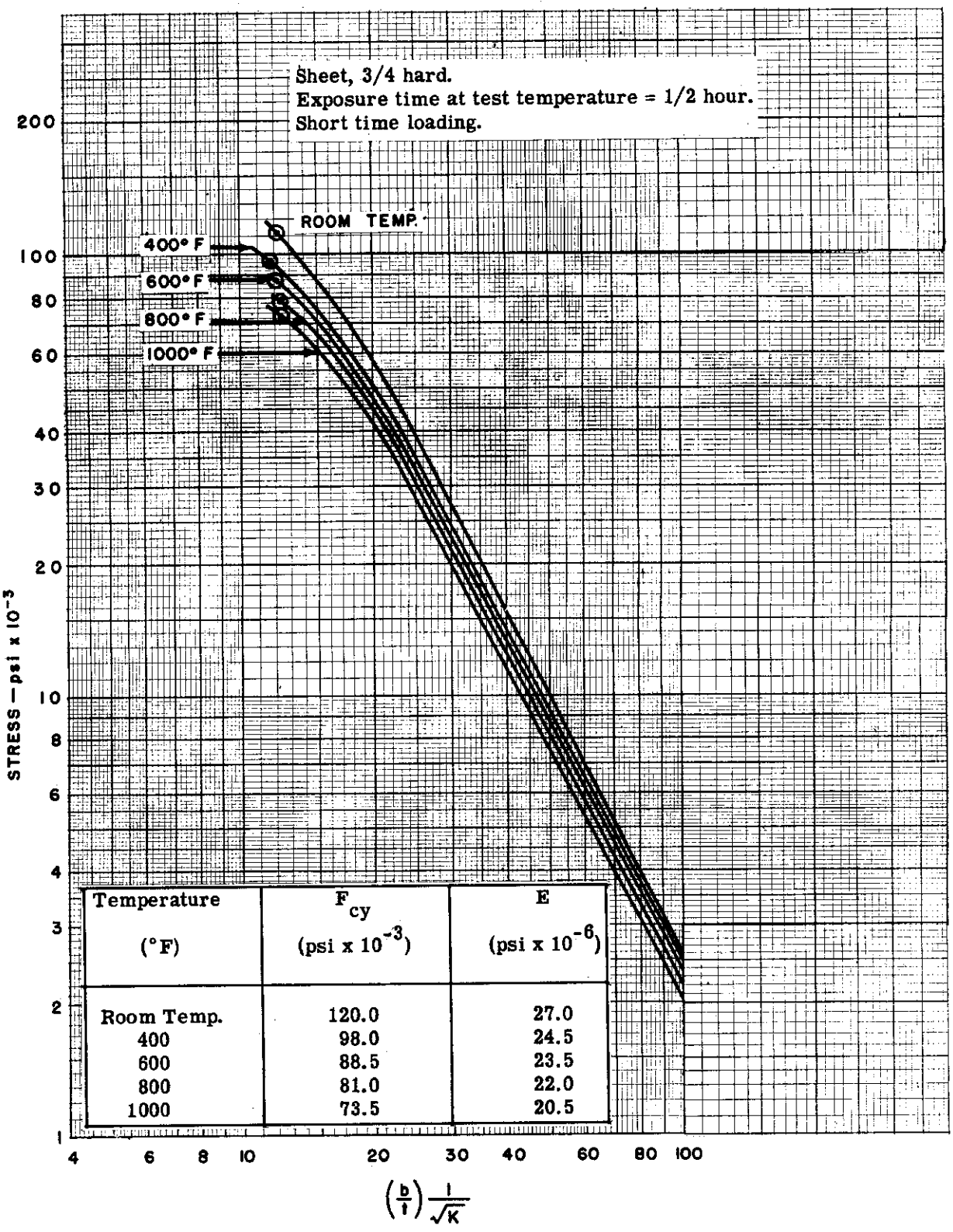

Temperature (°F)	F_{cy} (psi x 10^{-3})	E (psi x 10^{-6})
Room Temp.	120.0	27.0
400	98.0	24.5
600	88.5	23.5
800	81.0	22.0
1000	73.5	20.5

Figure 4.5-6. 18-8 Stainless Steel — Buckling Stress for a Long Simply Supported Plate in Compression

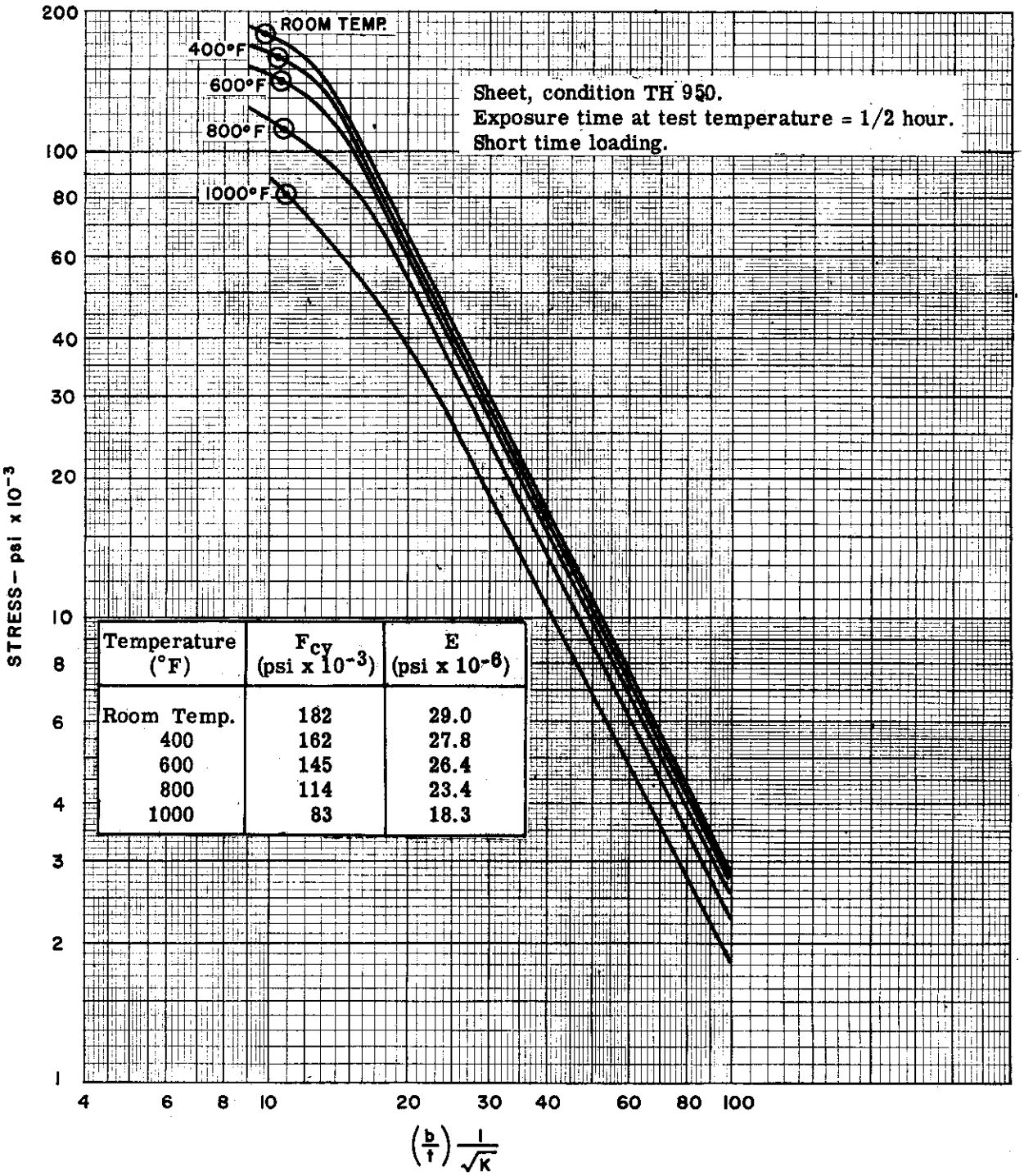

Temperature (°F)	F_{cy} (psi x 10^{-3})	E (psi x 10^{-6})
Room Temp.	182	29.0
400	162	27.8
600	145	26.4
800	114	23.4
1000	83	18.3

Figure 4.5-7. 17-7 PH Stainless Steel — Buckling Stress for a Long Simply Supported Plate in Compression

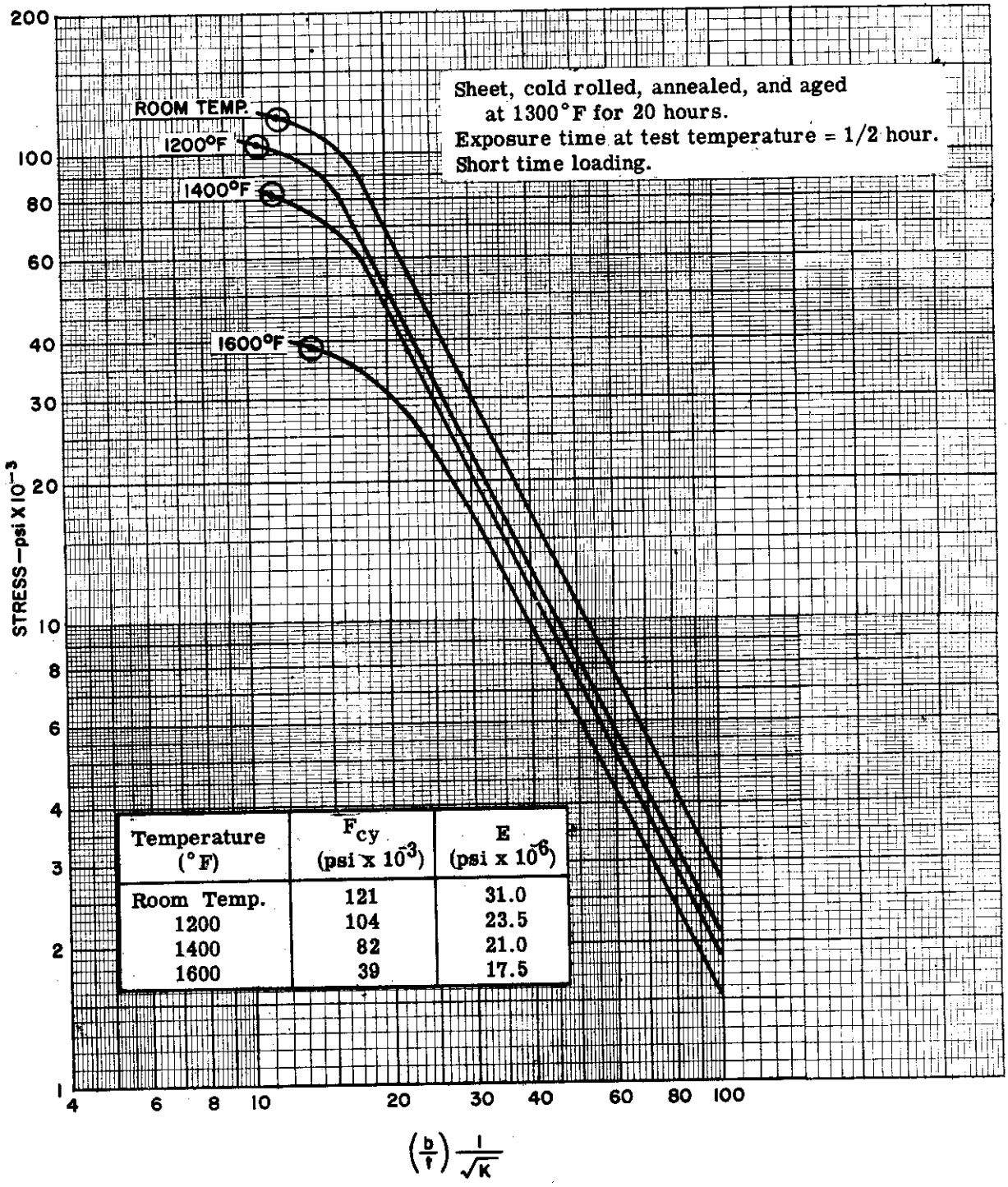

Temperature (°F)	F_{cy} (psi x 10^{-3})	E (psi x 10^{-6})
Room Temp.	121	31.0
1200	104	23.5
1400	82	21.0
1600	39	17.5

Figure 4.5-8. Inconel X — Buckling Stress for a Long Simply Supported Plate in Compression

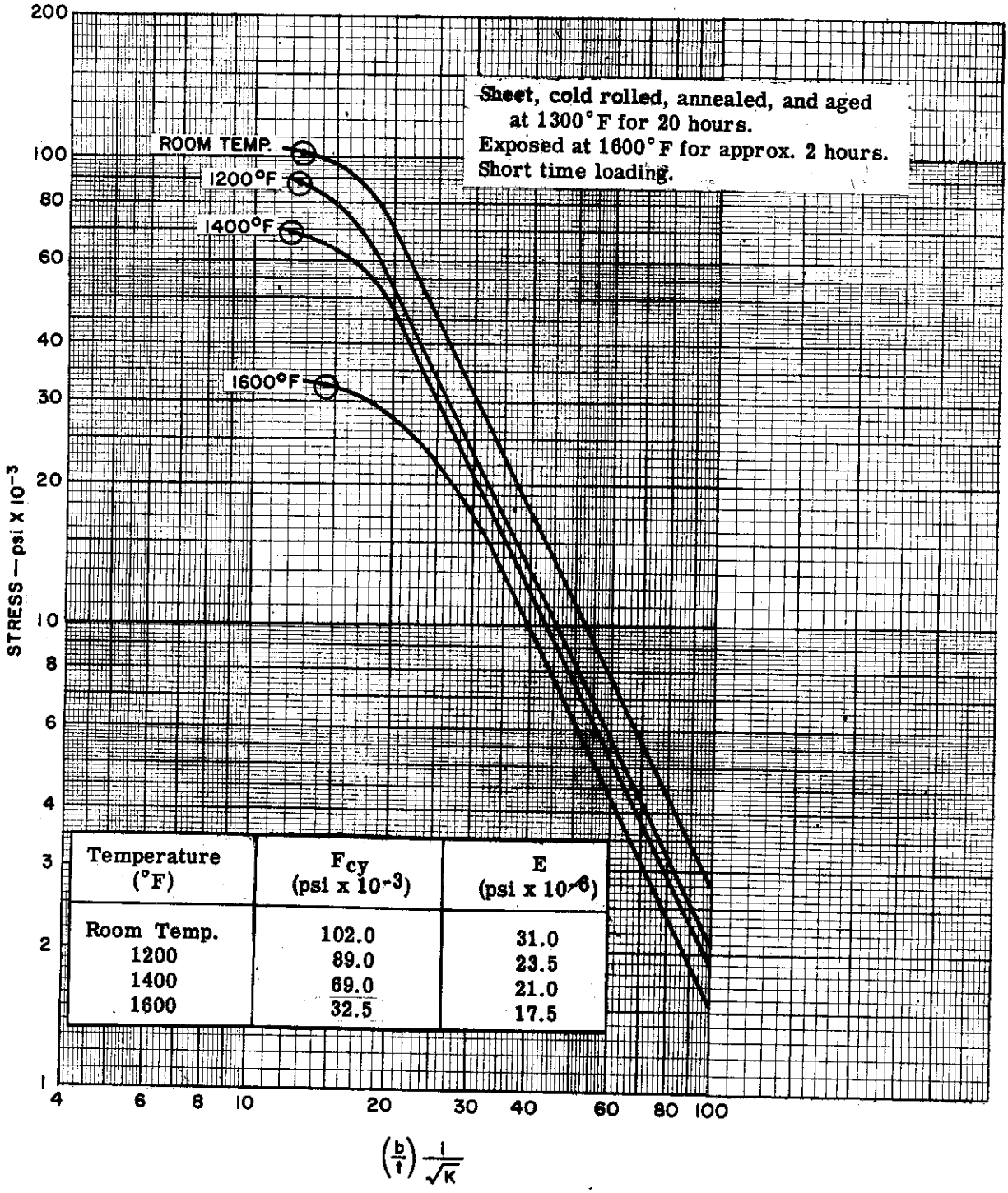

Temperature (°F)	F_{cy} (psi x 10^{-3})	E (psi x 10^{-6})
Room Temp.	102.0	31.0
1200	89.0	23.5
1400	69.0	21.0
1600	32.5	17.5

Figure 4.5-9. Inconel X — Buckling Stress for a Long Simply Supported Plate in Compression, Exposed at 1600°F for 2 Hours

4.6 PLATES — UNIFORM TEMPERATURE — LONG-TIME LOADING

Plates under long-time loading buckle and collapse owing to the creep action of materials. The method of analysis employed in predicting the creep failure of plates is slightly more complex than for columns. The method is in agreement with recent test results of long, simply supported plates.

In determining the collapse or ultimate stress of plates under long-time loading, the buckling stress, σ_{cr}, is determined at first using Figures 4.6-1 through 4.6-6. These figures are for various materials and for two temperatures at which creep is significant. The curves have been computed using the usual plate buckling equation

$$\sigma_{cr} = \frac{K\pi^2 \eta E}{12(1-\mu^2)} \left(\frac{t}{b}\right)^2,$$

where the plasticity coefficient η, dependent upon the plate configuration, corresponded to long, simply supported plates for the case presented. To include time-dependent strain, the isochronous stress-strain curves of the material for the specified time and temperature were used. When the value of $\sigma_{cr} > 0.64\,\sigma_{cy}$, σ_{cr} represents the collapse or ultimate stress. Otherwise, the ultimate stress is computed as follows

$$\sigma_{ULT} = \sqrt{\sigma_{cr}\,\sigma_{cy}} - 0.25\,\sigma_{cr}.$$

When the edges of the simply supported plate are held straight in the plane of the plate, a condition represented by a plate continuously attached to adjoining plates along the unloaded edges,

$$\sigma_{ULT} = \sigma_{cy} - 1/2\,\sigma_{cr}\left[-0.545 + \sqrt{1.54\,\frac{\sigma_{cy}}{\sigma_{cr}} - 0.0865}\right]^2$$

In all these equations, σ_{cy} is the yield stress of the material as determined from the isochronous stress-strain curve. Further discussion of the method of analysis, together with an explanation of the isochronous curves, is presented in Part II.

In the preparation of Figures 4.6-1 through 4.6-6, the isochronous curves presented in Section 2.0 were used. As explained in Section 2.0, these curves are based upon limited creep data and some interpolation was necessary in their formulation. Moreover, the method of analysis for predicting the creep buckling of plates has been checked against limited test data. For these reasons, the information presented in this section should be considered provisional until more test results become available.

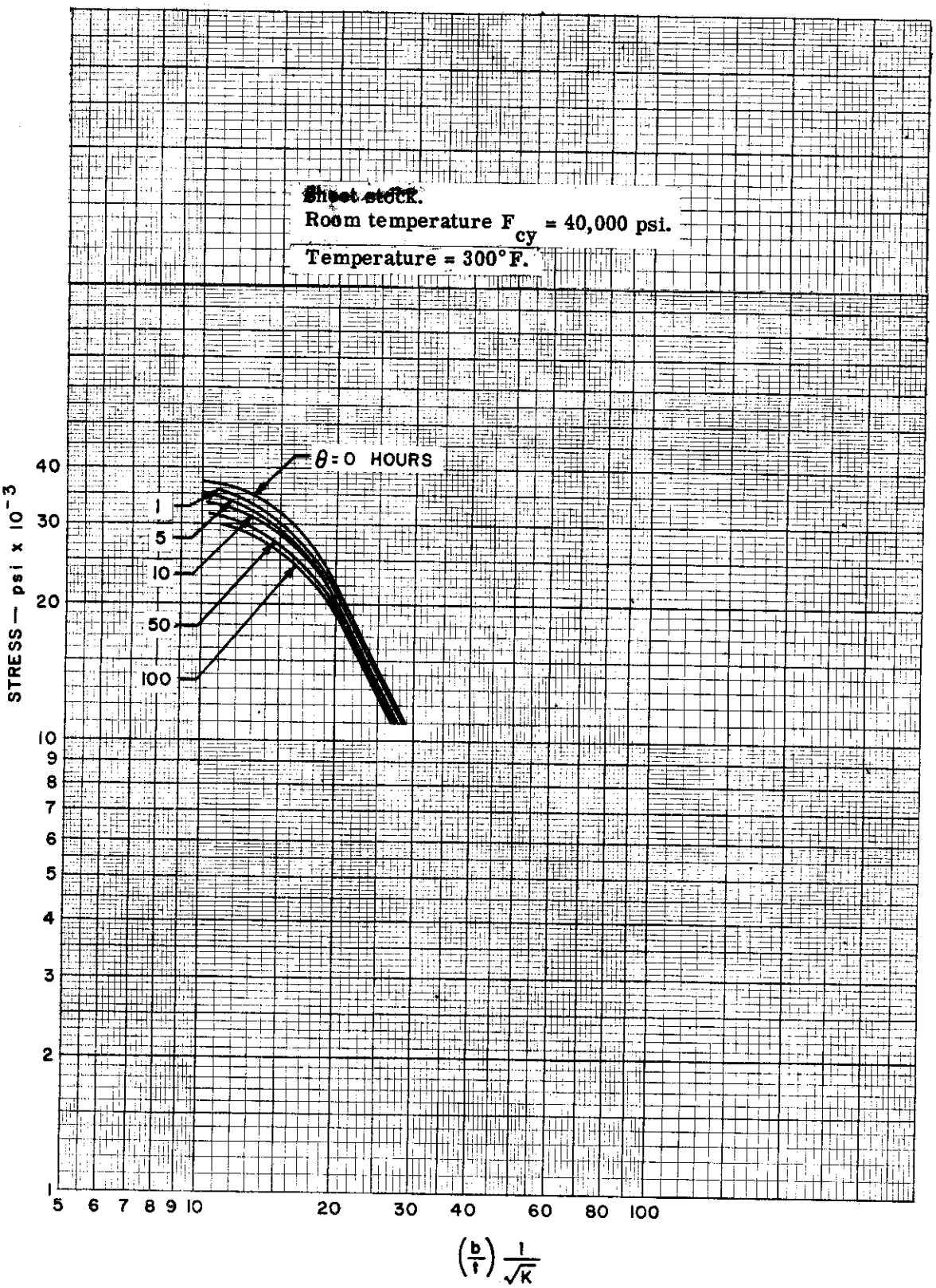

Figure 4.6-1. 2024-T3 Clad Aluminum Alloy — Creep Buckling Stress for a Long Simply Supported Plate in Compression, Temperature 300°F

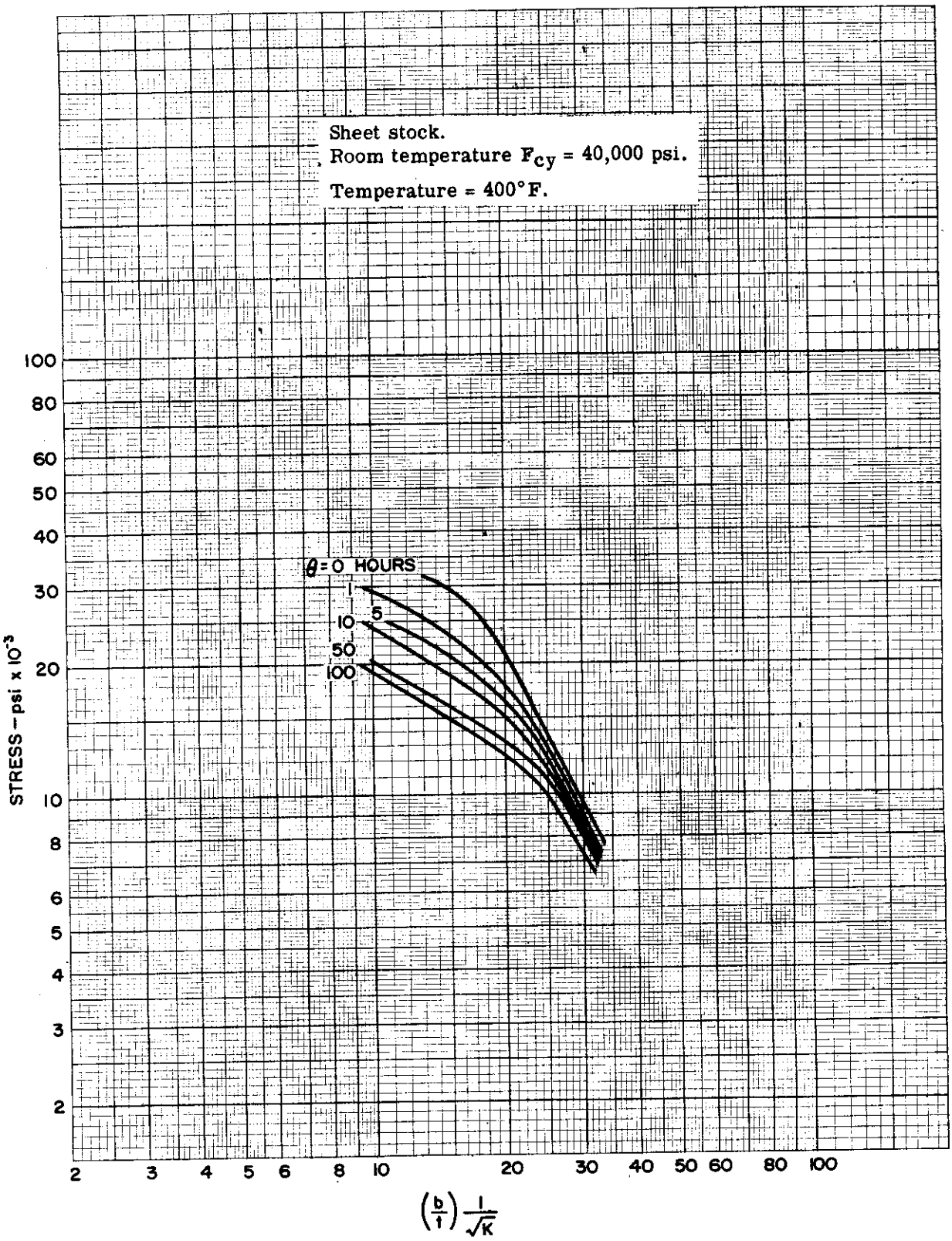

Figure 4.6-2. 2024-T3 Clad Aluminum Alloy — Creep Buckling Stress for a Long Simply Supported Plate in Compression, Temperature 400°F

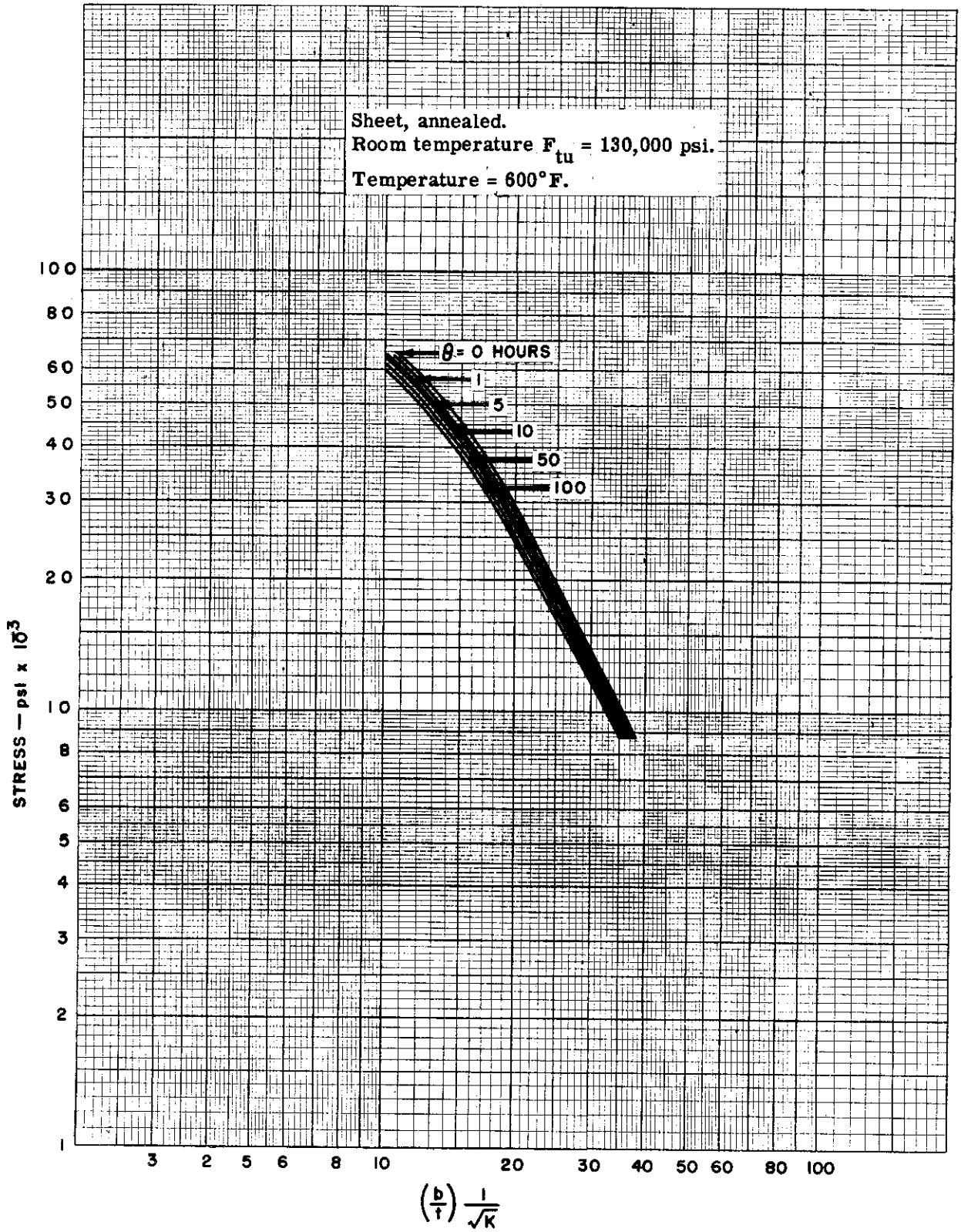

Figure 4.6-3. RC C-110M Titanium Alloy — Creep Buckling Stress for a Long Simply Supported Plate in Compression, Temperature 600°F

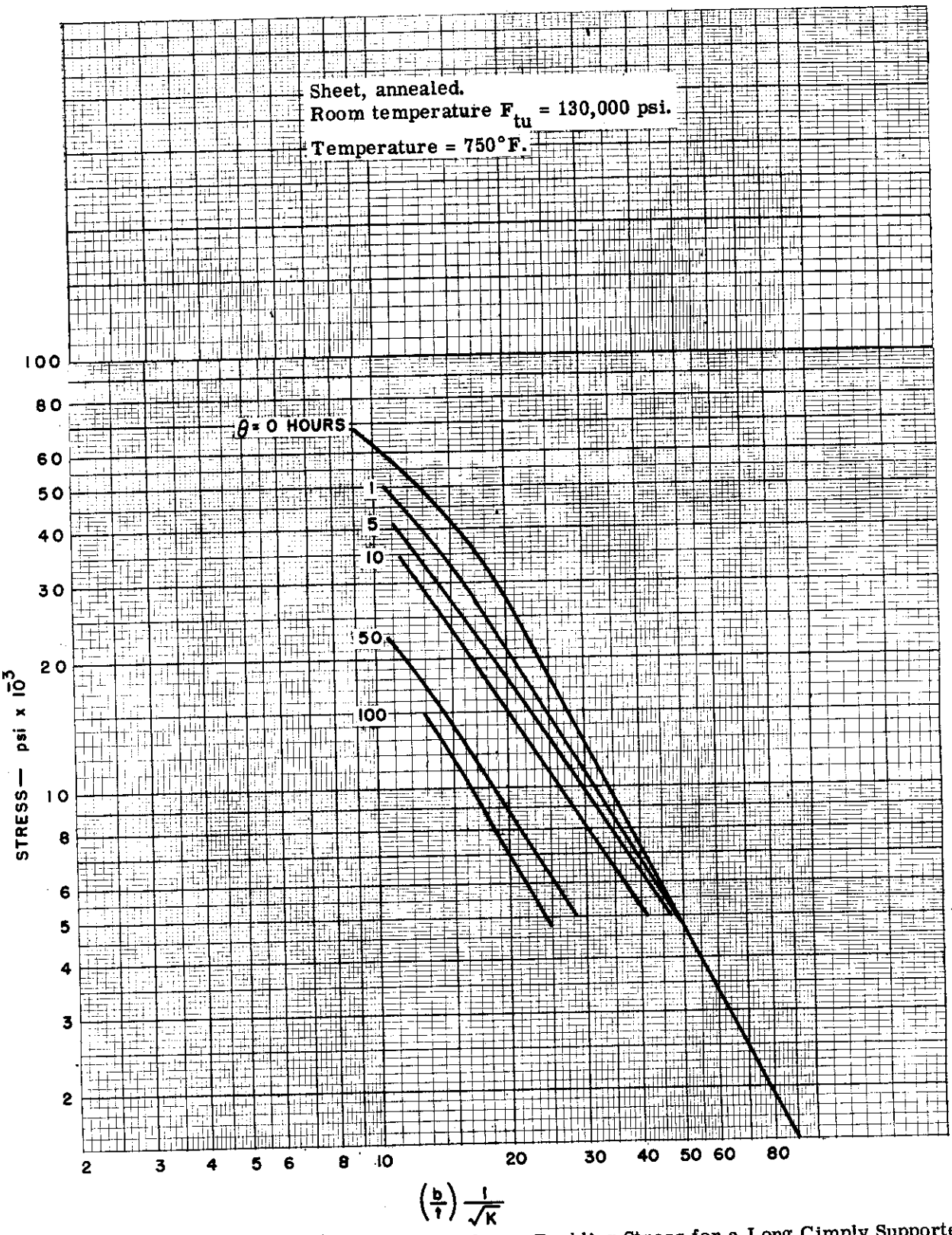

Figure 4.6-4. RC C-110M Titanium Alloy — Creep Buckling Stress for a Long Cimply Supported Plate in Compression, Temperature 750°F

[redacted]

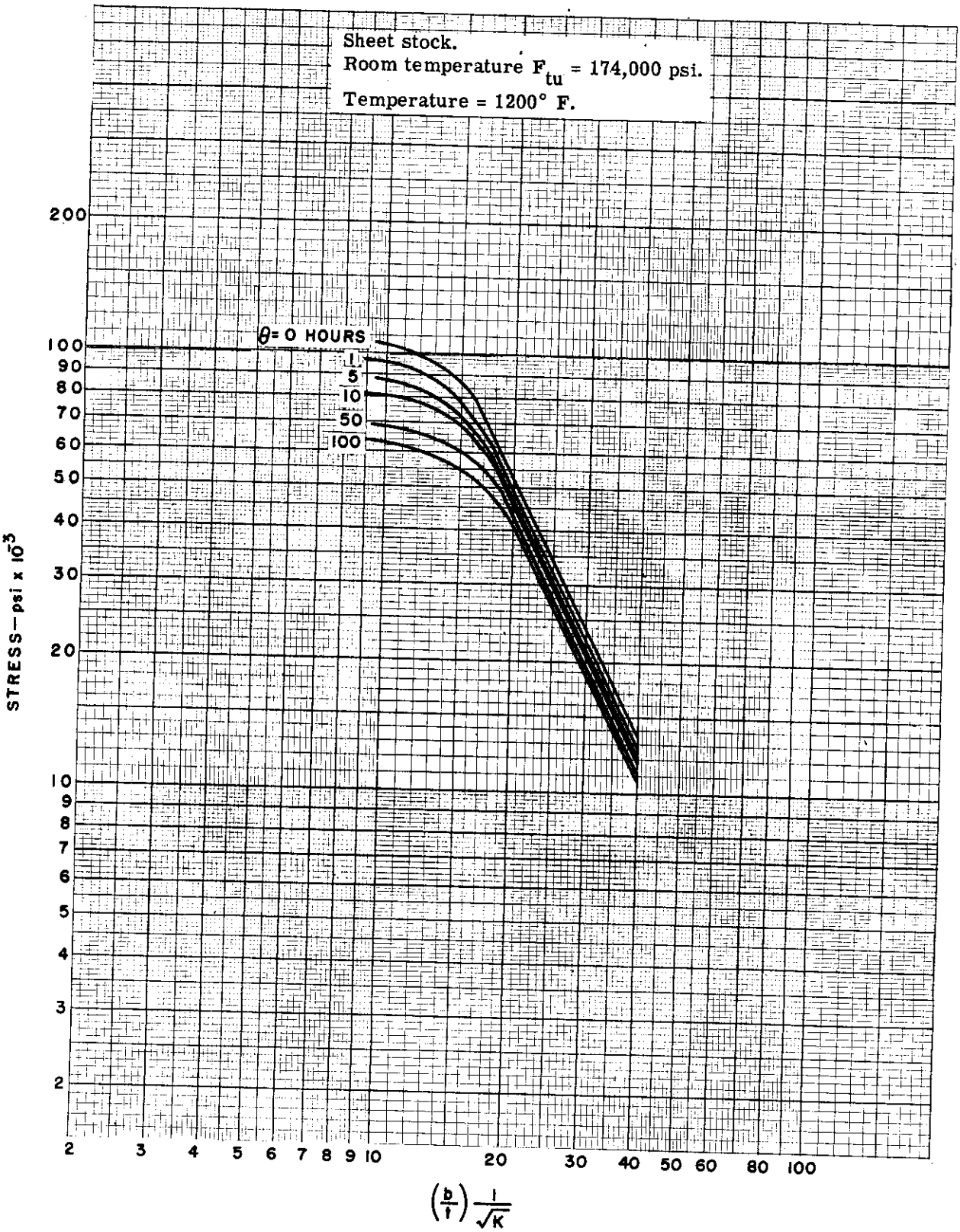

Figure 4.6-5. Inconel X — Creep Buckling Stress for a Long Simply Supported Plate in Compression, Temperature 1200° F

[redacted]

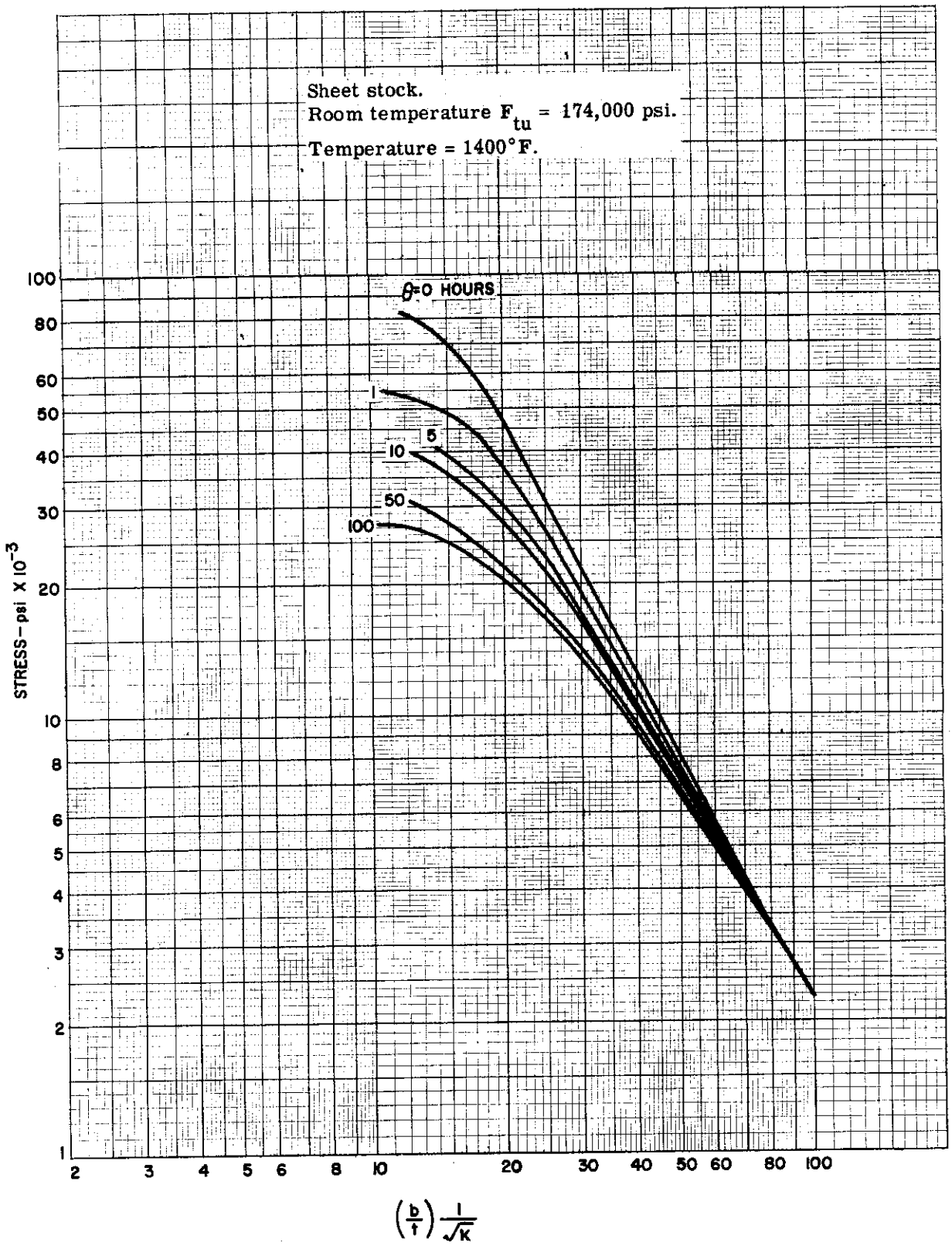

Figure 4.6-6. Inconel X — Creep Buckling Stress for a Long Simply Supported Plate in Compression, Temperature 1400° F

[redacted]L

NOTES

[redacted]

[redacted]

SECTION 5.0

PRESSURE VESSELS

By R. E. Wong, and A. Schnitt

[redacted]

[redacted]

[redacted]

TABLE OF CONTENTS

NOMENCLATURE

a = mean radius, length of semi-major axis (in.)

C = buckling coefficient

ΔC = incremental buckling coefficient

D_i = inside diameter (in.)

E = Young's modulus (psi)

k = ratio of major to minor axis of ellipse

K_k = stress concentration factor in knuckle

l = length (in.)

p = pressure (psi)

t = thickness (in.)

t_d = dome thickness (in.)

t_k = knuckle thickness (in.)

V = enclosed volume ($in.^3$)

W = weight (lb)

η = plasticity coefficient

ρ = density ($lb/in.^2$)

σ = stress (psi)

σ_{cr} = critical stress (psi)

SECTION 5.0

PRESSURE VESSELS

5.1 GENERAL

Presented in this section is design information relative to integral and nonintegral pressure vessels. A nonintegral vessel is one which contains a fluid under pressure while an integral vessel carries both external loads and fluids under pressure. Derivations and references associated with the following work are contained in Part II.

The information presented in Section 5.2 permits the rapid estimation of thicknesses and weights of nonintegral pressure vessels of shapes and materials considered common for advanced aircraft. These data can also be applied to integral pressure vessels when the external bending moment can be carried successfully by the excess strength of the cylindrical portion of the vessel and no additional material is required.

Many integral pressure vessels are unstiffened, or are ring (frame) stiffened circular cylinders. Internal pressure increases the critical stress of these structures besides decreasing the applied compression by placing the cylinder in "pretension." To facilitate the design of such structures, both with and without pressure, curves of buckling coefficients are given in Section 5.3.

5.2 WEIGHT AND THICKNESS ESTIMATION

Pressure vessels composed of right circular cylinders, oblate spheroids, and spheres are considered herein for the materials listed in Table 5.2-1. The weights of these portions of pressure vessels at room temperature and as a function of the proof pressure and volumetric capacity are shown in Figures 5.2-1 through 5.2-5. The proof pressure is selected as the "key" pressure to permit the application of an individually chosen factor between proof pressure and working or malfunction pressure. Table 5.2-1 lists the allowable stresses at proof pressure, and these are based upon the criterion that no more than 0.1% volumetric set occurs at proof pressure. As a result of this criterion, the allowable stresses for cylinders are slightly higher than for spherical shells.

The weights presented are for shells alone and do not include weights for bosses around openings and doors, and internal baffling and plumbing. Also excluded are weights of locally added structure to support nonintegral vessels, or a possible increase in cylindrical shell thickness to support external loads in integral vessels. Note that the length of the knuckle region of cylindrical tank ends is approximately one-fourth the radius of the cylindrical shell.

The parameter W/V in Figures 5.2-1 through 5.2-5 indicates that, for a given pressure and volume of vessel contents, the weight is independent of the number of vessels in which the contents is contained, provided the vessels are geometrically similar. Minimum weight for cyclindrical pressure vessels of given volume and design pressure occurs when the diameter approaches zero because, for this geometric shape, the weight of the ends also approaches zero while the weight of the cylindrical portion remains constant. This statement is valid provided that the material tolerances for all gages considered are a constant percentage of the nominal gage.

It should be noted also that minimum weights are obtained using spherical pressure vessels and that the ends of cylindrical vessels increase in weight as the ratio of major to minor axes increases from the value of one, associated with a spherical shape.

The weight of vessels composed of one or more geometric shapes can be computed with the aid of the following formulas:

Oblate Spheroid
$$\begin{cases} k = 2, & W/V = 4.32\, p\ \rho/\sigma \\ k = 3, & W/V = 11.80\, p\ \rho/\sigma \\ k = 4, & W/V = 31.35\, p\ \rho/\sigma \end{cases}$$

Sphere
$$\frac{W}{V} = \frac{96 \rho p \sigma^2}{(4\sigma - p)^3}$$

Cylinder
$$\frac{W}{V} = \frac{8 \rho \sigma p}{(2\sigma - p)^2}$$

The shell thickness can then be obtained by the use of the following formulas:

Cylinder
$$t = \frac{p D_i}{2\sigma - p}$$

Sphere
$$t = \frac{p D_i}{4\sigma - p}$$

Oblate Spheroid Dome
$$t_d = \frac{p k a}{2\sigma}$$

Knuckle
$$t = \frac{K_k\, p\, a}{\sigma}$$

where K_k varies with k as:

k	K_k
1	0.65
2	1.086
3	2.85
4	4.90

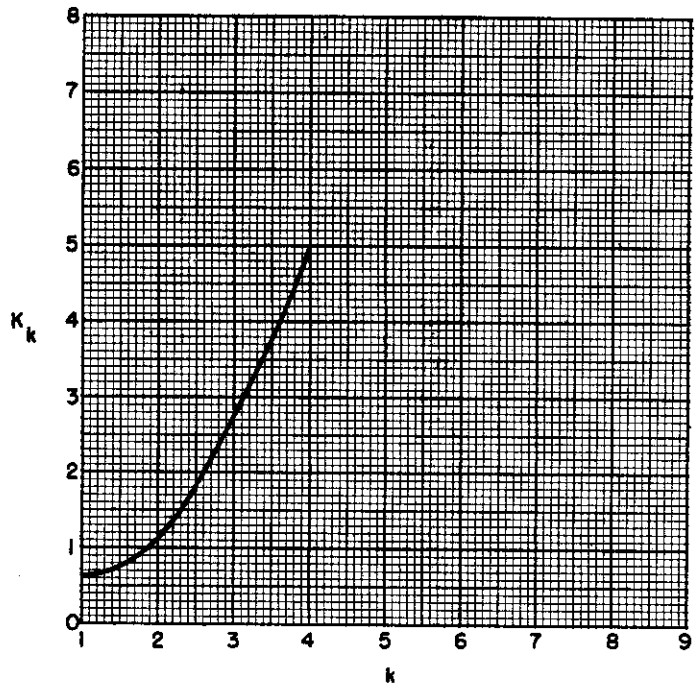

TABLE 5.2-1

RECOMMENDED ROOM TEMPERATURE PROOF PRESSURE STRESSES

Material	Condition	Density ($lb/in.^3$)	Ultimate Tensile Strength (psi)	Recommended Proof Pressure Stress Cylinders (psi)	Recommended Proof Pressure Stress Spheres (psi)
18-8 SS	Annealed	0.286	75,000	28,000	26,000
18-8 SS	1/4-hard	0.286	125,000	60,000	56,000
17-7 PH	FA (formed and aged)	0.276	170,000	112,000	100,000
4130, 4140 4340	Normalized	0.283	90,000	67,000	65,000
4130, 4140, 4340	Heat-treated	0.283	140,000	118,000	115,000
Cor-Ten	Cold-rolled	0.284	70,000	48,000	45,000
403, 410 SS	Heat-treated	0.280	180,000	126,000	120,000
K-Monel	Age-hardened after welding	0.306	134,500	80,000	77,000
6061 Aluminum	Welded in T4 Aged to T6	0.098	38,000	28,800 (for cylinder) 32,600 (for head)	28,800
Titanium	Pure-Annealed	0.163	100,000	70,000	66,000

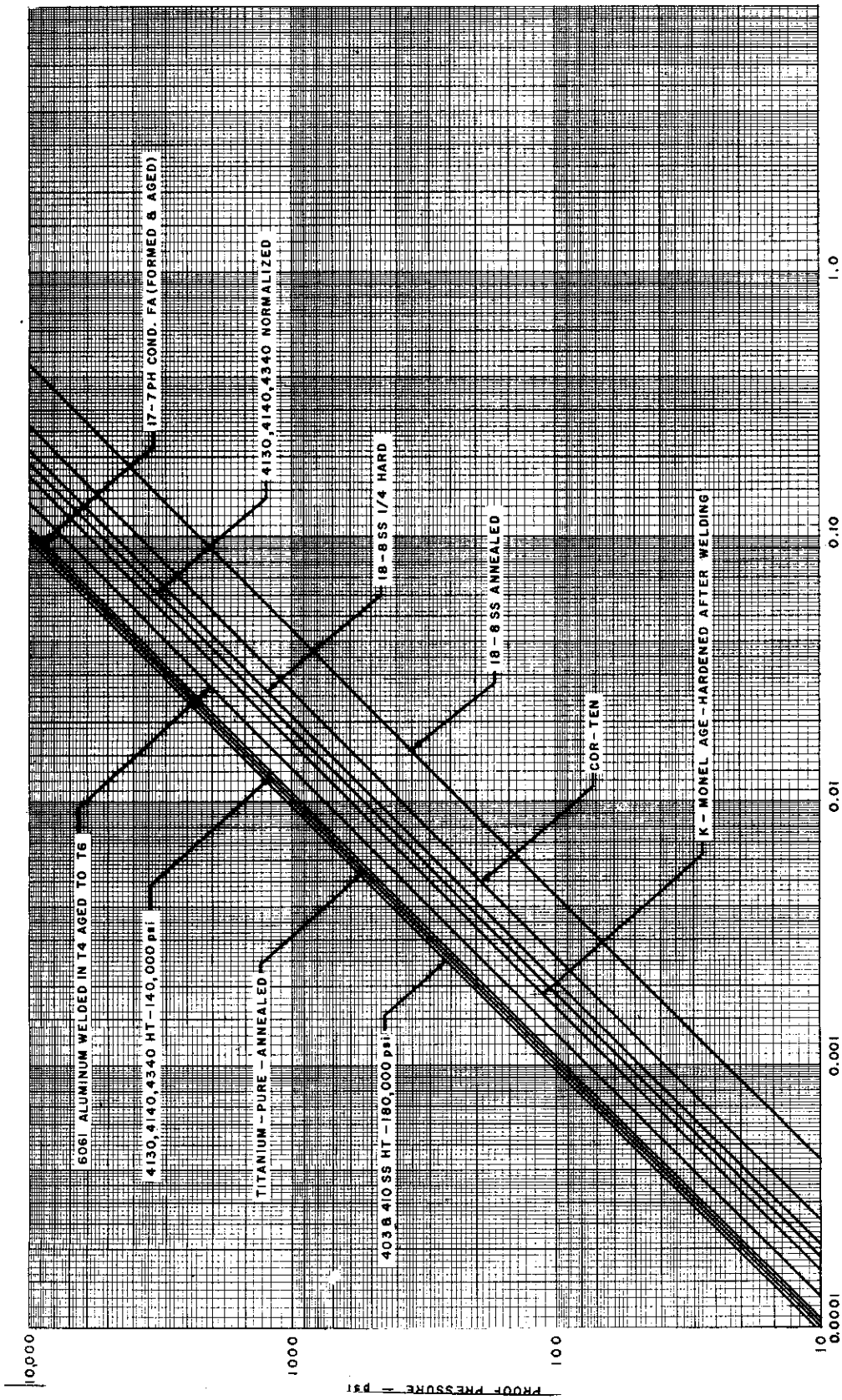

Figure 5.2-1. Weight of Cylindrical Sheels Under Internal Pressure

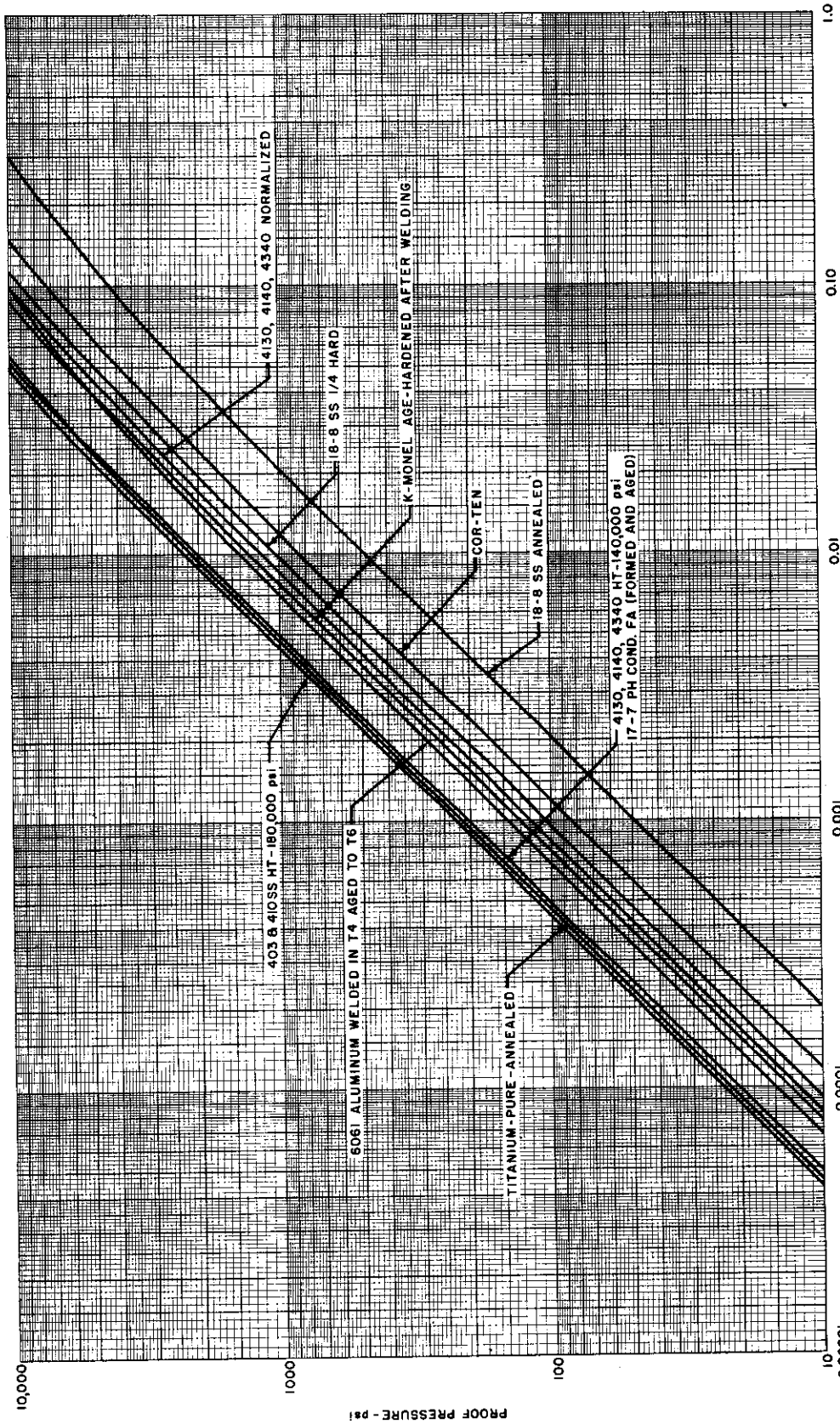

Figure 5.2-2. Weight of Elliptical (Oblate Spheroidal) Shells Under Internal Pressure, k = 2.0

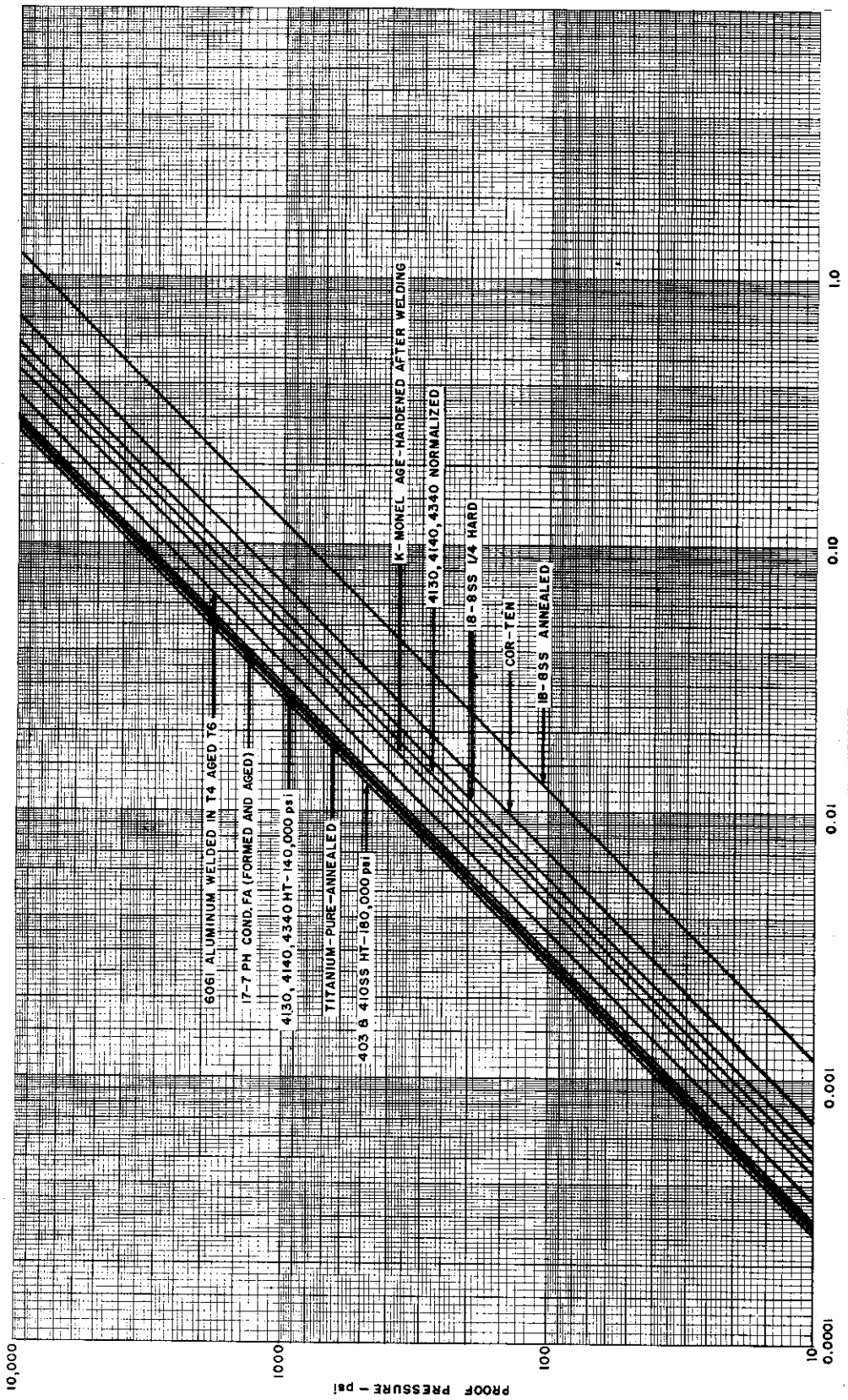

Figure 5.2-3. Weight of Elliptical (Oblate Spheroidal) Shells Under Internal Pressure, $k = 3.0$

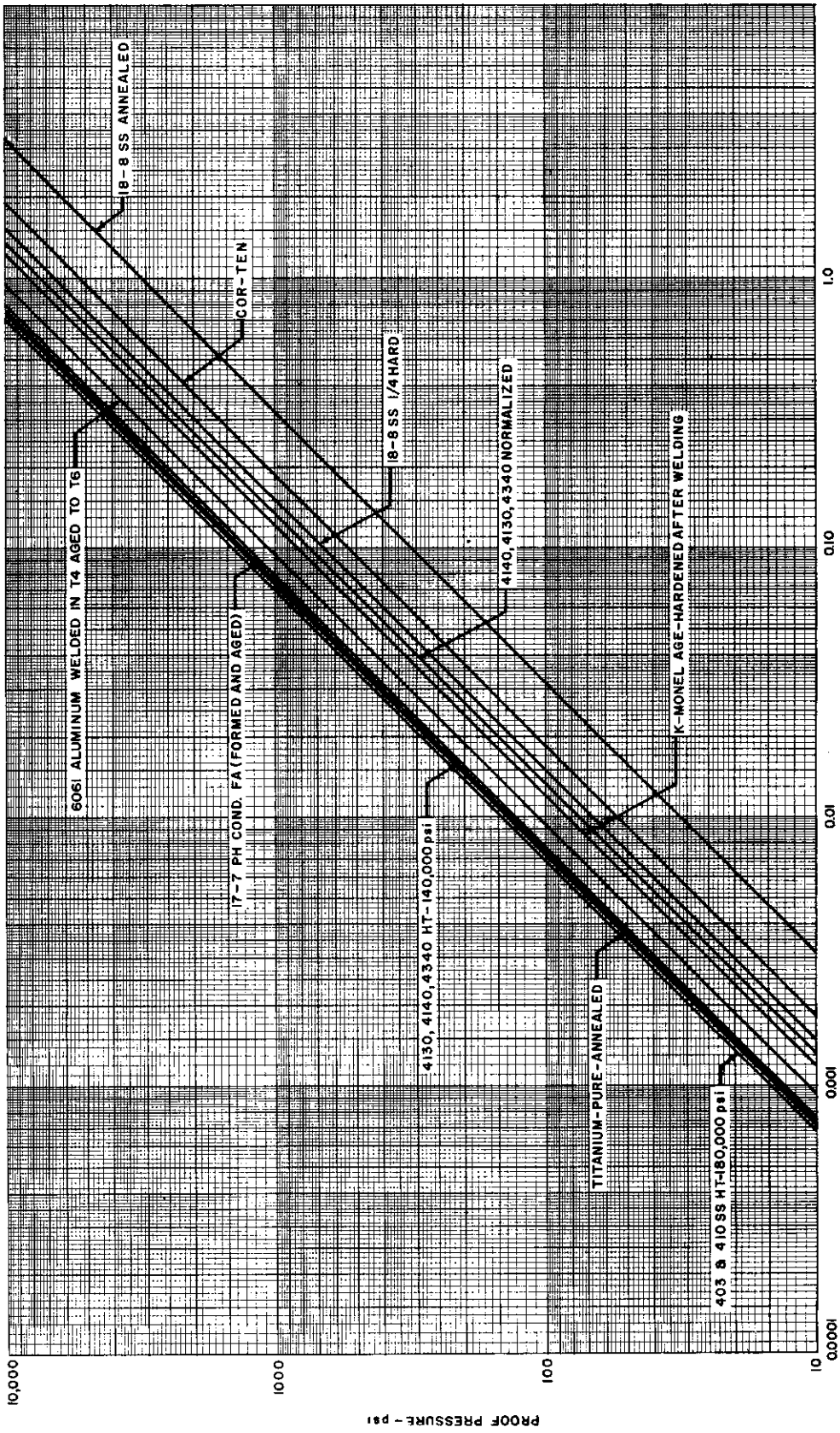

Figure 5.2-4. Weight of Elliptical (Oblate Spheroidal) Shells Under Internal Pressure, k = 4.0

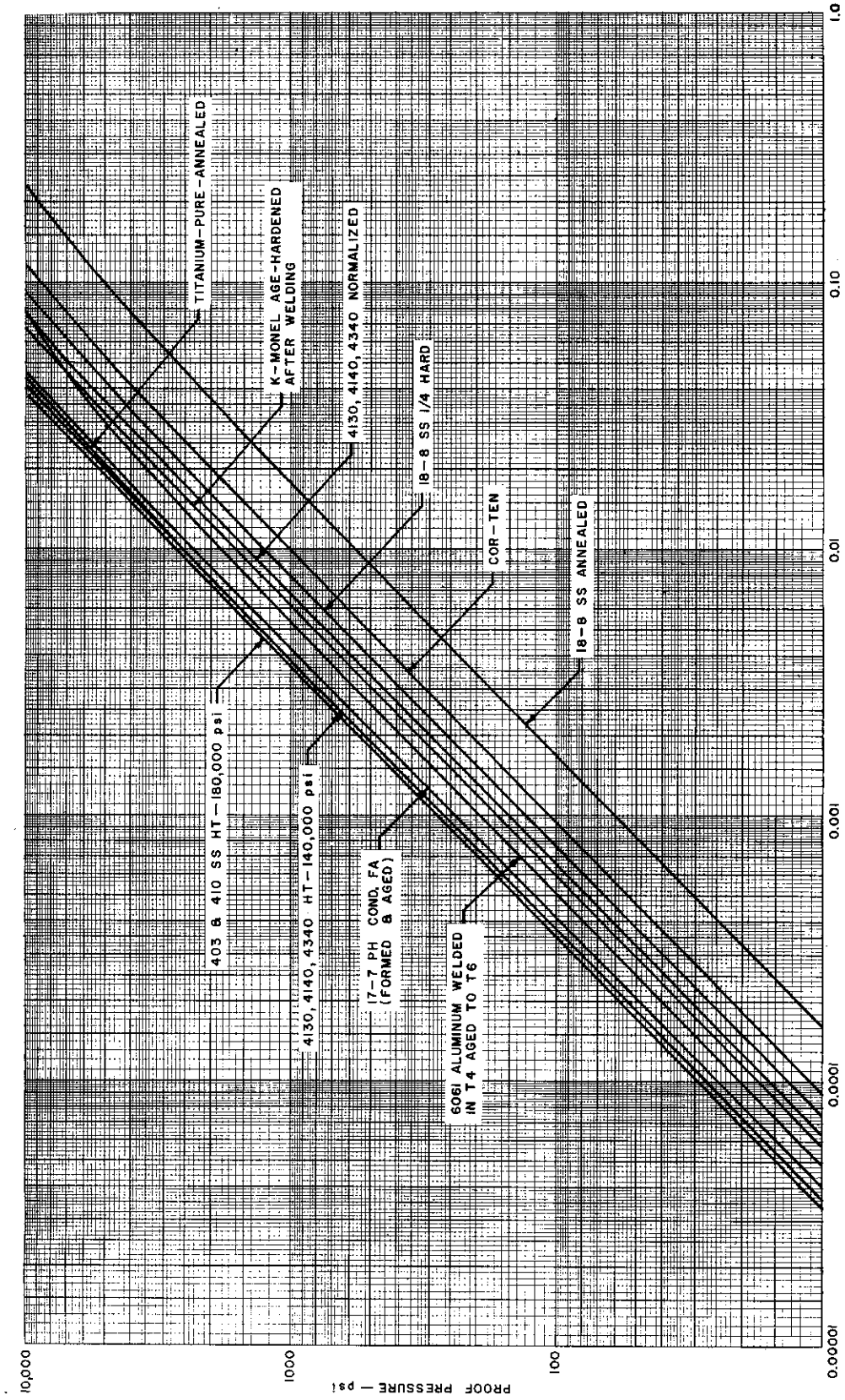

Figure 5.2-5. Weight of Spherical Shells Under Internal Pressure

5.3 BUCKLING COEFFICIENTS

Integral pressure vessels carry propellants under pressure and external body or fuselage loads in combination. As a consequence of internal pressure, buckling coefficients are increased. Buckling coefficients for pressurized unstiffened and ring (or frame) stiffened cylinders in compression are presented. The critical stress for such structure is given by

$$\sigma_{cr} = (C + \Delta C)\, \eta\, E \frac{t}{a} ,$$

where C is the buckling coefficient of cylinders without internal pressure and ΔC is the incremental buckling coefficient due to the presence of internal pressure. For cylinders in bending, the critical stress is increased by a factor of 1.3. It is noted that the applied stress should be reduced by the longitudinal pretension produced by internal pressure and it is equal to $p a/2t$; or, it can be included as an added coefficient in the critical stress formula, and it is equal to $\bar{p}/2$ where

$$\bar{p} = \frac{p}{E} \left(\frac{a}{t}\right)^2 .$$

The incremental buckling coefficient, ΔC, for long, unstiffened cylinders is given in Figure 5.3-1. In this case where

$$\frac{\ell}{a} \sqrt{\frac{t}{a}} > 20,$$

$C = 0.2$. The total buckling coefficient is limited to a value of 0.605 for values of $\bar{p} > 0.8$. The coefficients are based upon theory and experiment.

For short, simply supported or ring-stiffened pressurized cylinders, the buckling coefficients are given in Figure 5.3-2. In this plot, the coefficients are combined $(C + \Delta C)$ and are based upon theory only.

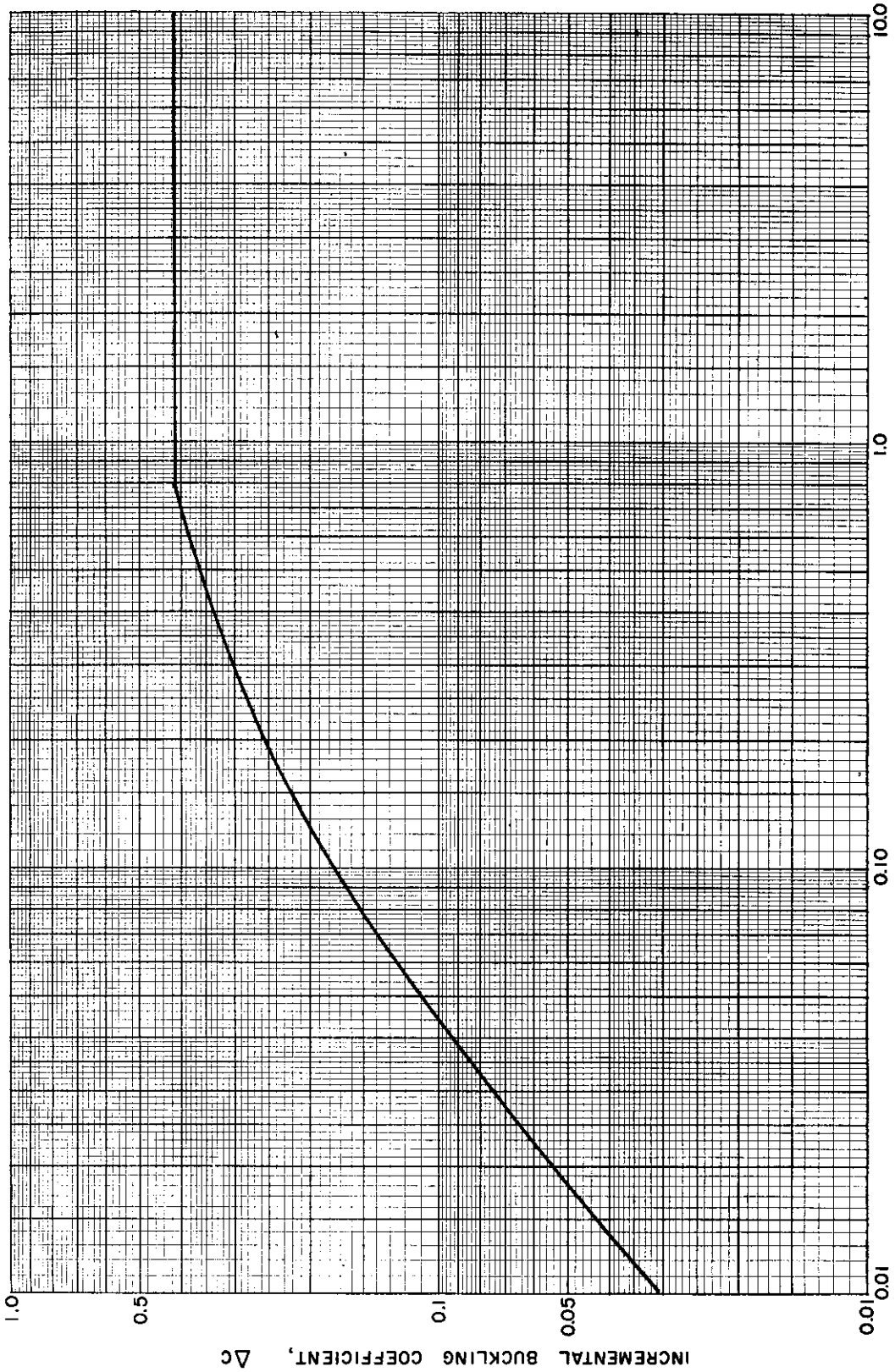

Figure 5.3-1. Incremental Buckling Coefficient for Unstiffened Cylinder Under Axial Compression and Internal Pressure

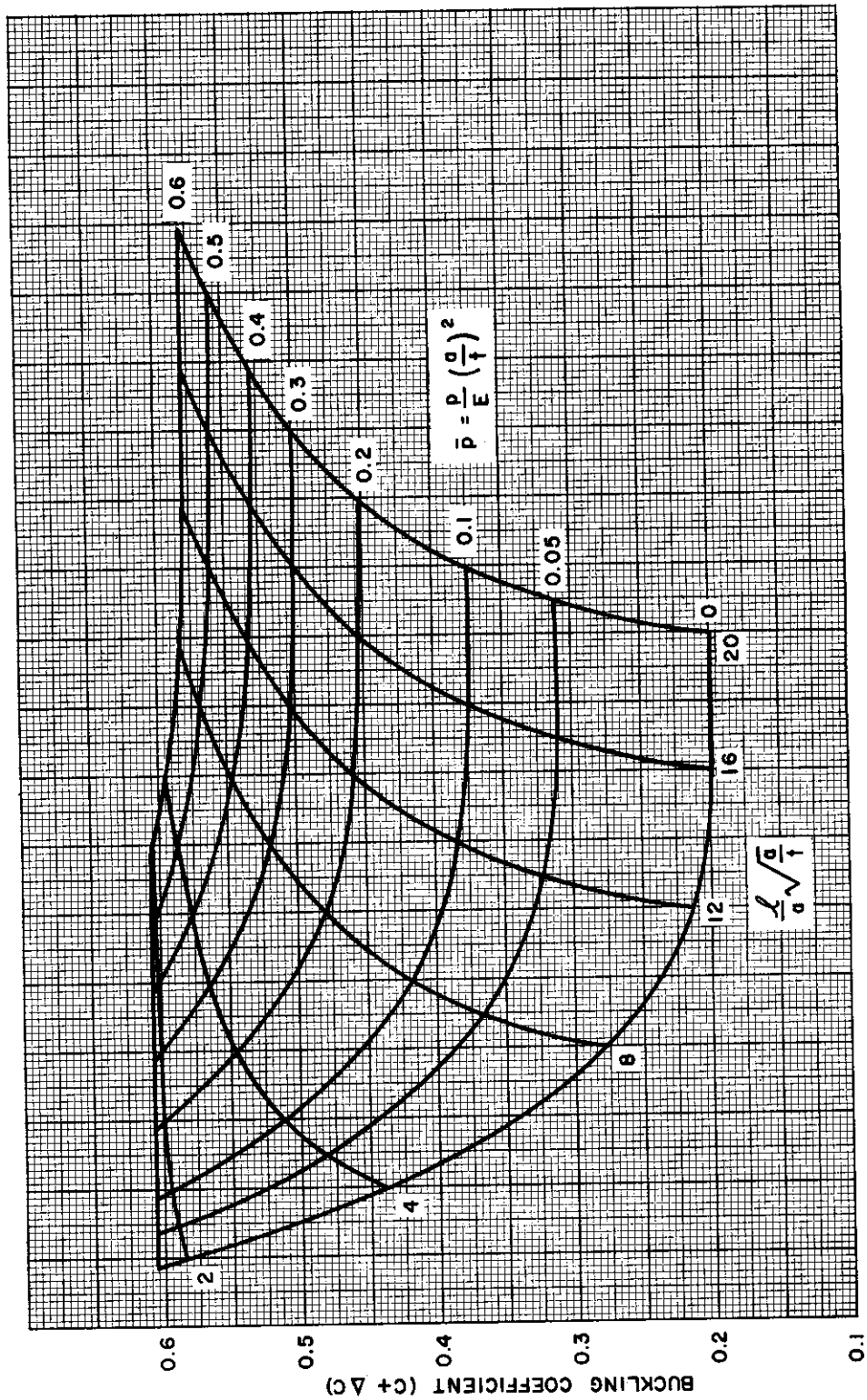

Figure 5.3-2. Buckling Coefficient for Ring-Stiffened Cylinder Under Axial Compression and Internal Pressure

[redacted]

NOTES

[redacted]

SECTION 6.0

INSULATION DESIGN

By W. H. Dukes, M. A. Goldberg, and M. A. Brull

[redacted]

[redacted]

TABLE OF CONTENTS

NOMENCLATURE

c_m = specific heat of structural material (BTU/lb°F)

g = gravity constant (ft/sec^2)

I = a function defined in Section 6.5

K_A = conductivity of outer wall attachment (BTU-in./ft^{2}hr°F)

K_a = conductivity of air (BTU-in./ft^{2}hr°F)

K_i = conducitivity of insulation (BTU-in./ft^{2}hr°F)

K_m = conductivity of structural skin (BTU-in./ft^{2}hr°F)

$2L$ = distance between outer wall attachments (in.)

m = number of intermediate radiation foils

n = number of time increments

Q_o = heat flux transferred through point-type thermal leakage (BTU/hr)

q = heat flux per unit area and unit time (BTU/ft^{2}hr)

R = parameter defining conductivity of outer wall attachment (dimensionless)

r = radial distance from the center of a point-type thermal leakage

$2s$ = thickness or diameter of outer wall attachments (in.)

t = structural skin thickness (in.)

T = structural temperature (°R)

T_1 = temperature of hot wall (°R)

T_2 = temperature of cold wall (°R)

T_i = initial structural temperature (°R)

T_j = structural temperature at time θ_j (°R)

T_m = mean temperature of air space (°R)

T_o = temperature at outer surface of insulation (°R)

T_{oj} = value of T_o during the jth time increment (°R)

ΔT = temperature difference between the two walls bounding an air space (°F)

NOMENCLATURE (cont)

x = insulation thickness (in.)

Y = temperature multiplication factor for line-type thermal leakage through insulation

Z = factor for temperature increase due to point-type thermal leakage through insulation

α_i = diffusivity of insulation (in.^{2}/hr)

α_m = diffusivity of structural skin (in.^{2}/hr)

β = coefficient of cubic expansion of air (1/°F)

ϵ = normal emissivity of each surface of a radiation barrier

ϵ_1 = normal emissivity of hot wall

ϵ_2 = normal emissivity of cold wall

η = a parameter defined in Section 6.4

θ = time (hr)

$\Delta\theta$ = length of time increment

μ = a parameter defined in Section 6.4

ν = kinematic viscosity of air (ft^2/sec)

ρ_m = density of structural skin material (lb/ft^3)

σ = Stephan-Boltzman constant = 0.173×10^{-8} BTU/hr ft^2°R^4

SECTION 6.0

INSULATION DESIGN

6.1 GENERAL

In this section, graphs are presented by which structural temperatures or insulation requirements can be readily determined for the design of insulated structures. To facilitate the use of these charts, a brief discussion of the mechanics of insulation is given in the following.

Transfer of heat through a medium occurs by one or more of the following mechanisms:

(a) Conduction - energy transfer by molecular agitation.

(b) Radiation - an electromagnetic form of energy transmission.

(c) Convection - energy transfer by mass displacement of the medium.

Conduction is predominant in solids, while liquids and particularly gases transmit relatively small quantities of heat by conduction. Since radiation can exist only through a nonabsorbing medium, it is an important form of heat transfer through gases, and is the only method of transferring heat across a vacuum. Convection, since it requires circulation and mixing of the medium to effect heat transfer, can exist only in liquids and gases.

Because of the low conductivity of gases, the most efficient methods of insulating are concerned with using a blanket of air as the heat-resisting means, with arrangements being made to minimize convection and radiation. In the fibrous, powdered, and other loose "fill" types of insulation, the material breaks up the air space into small cells so that convection is prevented, and the fill also blocks most of the radiation. Some additional conduction is provided by fibers or powder granules, but again this is minimized by the small contact areas between any two fibers. Since the heat transfer through such a material is complex, an over-all conductivity is usually determined experimentally and the material is treated theoretically as if it has only conduction characteristics. Generally, such a conducitivity will vary widely with temperature.

A second method of utilizing the low conductivity of air is to omit the "fill" material with a consequent saving in weight, but to provide the two parallel walls bounding the air space with highly reflective surfaces to minimize radiant heat transfer. Convection effects must then be included, so that this system is effective when the air pressure is low and convection small.

At high temperatures, the heat transmission by radiation may still be significant in the insulating arrangement described previously, despite the reflective surfaces of the bounding walls. Additional highly reflective metal foils can then be introduced into the air space parallel with the bounding walls, and separated from each other. By this means, radiation is reduced further, although at some cost in weight. Such an arrangement of metal foils has been termed a radiation barrier.

In this section, data are provided for the design of structural insulation of each of the forms described previously. That is, low conductivity materials (Section 6.2), air spaces (Section 6.3), and radiation barriers (Section 6.4).

Attention is concentrated generally on the transient case that occurs when insulation is used as the only means of preventing excessive structural temperatures. In such circumstances, the structure forms the only heat sink to absorb heat passing through the insulation, and its temperature rises

continuously during flight even if constant aerodynamic conditions exist. The problem of structural temperature in an insulated structure, therefore, leads to a complex differential equation, the solution of which is facilitated by the curves of this section.

When an air space is used as insulation, all three modes of heat transfer are involved and the number of variables becomes large. It is, therefore, impractical to present directly the structural temperature for this case, but instead charts are given by which heat transferred by each medium separately may be computed and summed. It is shown how the resulting total heat flux is used to calculate the transient structural temperature.

The use of an air space, or a fibrous or powdered type of insulation, implies an outer protecting wall to carry aerodymamic forces. This wall, in turn, will require attachment to the primary structure beneath. These attachments will form a thermal leakage through the insulation, permitting additional heat to be transferred into the primary structure. Section 6.5 shows a method by which the local structural temperatures due to such leakage may be estimated.

6.2 LOW-CONDUCTIVITY MATERIALS

This section presents graphs, charts, and methods applicable to the design of structures insulated by a material in which the mode of heat transfer is predominately by conduction.

In Part II, it is shown that the thickness of a low-conductivity insulating material required to maintain a specified maximum structural temperature is given

$$x/\sqrt{a_i} = A \tan^{-1} AB$$

where

$$A = \sqrt{\theta/\ln C} \qquad (\text{hr})^{1/2}$$

$$B = 12\, K_i/\left(\sqrt{a_i}\ \rho_m\ c_m\ t\right) \qquad (\text{ft/hr})$$

$$C = \left(T_o - T_i\right)/\left(T_o - T\right) \qquad (\text{dimensionless})$$

This expression includes the heat capacity of the insulating material, but considers only constant aerodynamic conditions as defined by T_o. For all practical purposes, the heat transferred through the insulation will be small enough that the outer surface will rise rapidly to equilibrium temperature (see Section 1.7). It is this equilibrium temperature which is used as T_o.

Since the afore-mentioned expression is developed for constant values of insulation conductivity and diffusivity, mean values with respect to both time and temperature gradient through the insulation must be used. For rapid evaluation of this expression, Figures 6.2-1 and 6.2-2 are provided; their use is shown in the following examples.

EXAMPLE

Find the thickness and weight of Thermoflex insulation required to protect an aluminum alloy structure from an equilibrium temperature of 1440°F sustained for 15 minutes. The structure has a skin thickness of 0.06 in., and the temperature should not exceed 350°F when the initial temperature is 100°F. Conductivity of Thermoflex is 0.50 BTU-in./hr ft^2°F at a density of 3 lb/ft^3. Assume a_i = 8.0 in.^{2}/hr.

Therefore, $C = \left(T_o - T_i\right)/\left(T_o - T\right)$ = (1440 - 100) / (1440 - 350) = 1.23.

From Figure 6.2-1 for a time of 15 minutes, A = 1.12 and $B = 12\, K_i/\left(\sqrt{a_i}\ \rho_m\ c_m\ t\right)$ = 12 x 0.50/2.825(173 x 0.21 x 0.06) = 0.971.

From Figure 6.2, $x/\sqrt{\alpha_i} = 0.91$.

Therefore, $x = 0.91 \times 2.825 = 2.57$ in. and the weight is 0.642 lb/ft^2.

EXAMPLE

Repeat the previous example using a ceramic coating as insulation. Density of the ceramic is 125 lb/ft^3 and its conductivity is 10 BTU-in./ft^{2}hr°F. $\alpha_i = 4.57$ in.^{2}/hr.

From Figure 6.2-1, A = 1.12, and

$B = 12\, K_i/(\sqrt{\alpha_i}\ \rho_m\ c_m\ t) = 12 \times 10/(173 \times 0.21 \times 0.06 \times 2.140) = 25.70.$

From Figure 6.2-2, $x/\sqrt{\alpha_i} = 1.7$.

Therefore, $x = 1.7 \times \sqrt{4.57} = 3.64$ in. and the weight is 37.9 lb/ft^2.

Figures 6.2-1 and 6.2-2 can also be used to evaluate the structural temperature if the insulation thickness and the equilibrium temperature at the outer surface of the insulation are given. To use the curves for this purpose, A is first evaluated using Figure 6.2-2 for the known values of $x/\sqrt{\alpha_i}$ and B. Figure 6.2-1 then gives C and hence T.

If arbitrary aerodynamic flight conditions are considered so that T_o varies with time, the flight must be divided into small time increments and the afore-mentioned procedure applied over each increment. The final temperature of the first time increment then becomes the initial temperature of the second, etc. If the insulation conducitivity and specific heat vary with temperature, this effect can be included by using appropriate average values for each time increment.

If the variation of insulation characteristics with temperature is neglected, and the flight is divided into equal time increments, then, as is shown in Part II, the structural temperature is given by

$$T_j = \left(1 - \frac{1}{C}\right)\left[T_{oj} + \frac{1}{C}\, T_{o(j-1)} + \frac{1}{C^2}\, T_{o(j-2)} + \frac{1}{C^3}\, T_{o(j-3)} + \text{---------} + \frac{1}{C^{(j-1)}}\, T_{o1} \right] + \frac{1}{C^j}\, T_i ,$$

in which the subscript j denotes a particular time increment and n is the total number of time increments. Therefore,

$$n = \theta_j/\Delta\theta .$$

Then, c is evaluated, using Figures 6.2-1 and 6.2-2 from the equation

$$x/\sqrt{\alpha_i} = A \tan^{-1} AB ,$$

in which the value of A is based upon the incremental time $\Delta\theta$.

EXAMPLE

A boost glide vehicle having a range of approximately 1500 nautical miles has a flight plan, from the end of boost, as follows:

Time from boost (min)	0	5	10	15	20	25	30
Velocity (ft/sec)	10,000	8,300	6,600	4,700	2,900	1,400	300
Altitude (ft)	138,000	133,000	126,000	114,000	92,000	61,000	20,000

Assuming a constant angle of attack of 5°, and a turbulent boundary layer, Figure 1.7-1 gives for the equilibrium temperatures at the one-foot station:

Time from boost (min)	0	5	10	15	20	25	30
Equilibrium temperature (°F)	1440	1240	1050	780	440	100	60

Dividing the problem into six equal time intervals of 5 minutes each, and taking the mean equilibrium temperature in each interval, gives:

$$T_{o_1} = 1800°R \quad T_{o_2} = 1605°R \quad T_{o_3} = 1375°R$$

$$T_{o_4} = 1070°R \quad T_{o_5} = 730°R \quad T_{o_6} = 540°R$$

It is assumed that the structure is 0.070-inch thick aluminum alloy skin protected by a one-inch thickness of Thermoflex insulation of 3 lb/ft^3 density. Average conductivity of the insulation is 0.5 BTU-in./hr ft^2°F, so that the diffusivity $\alpha_i = 8.0$ in.^{2}/hr.

Therefore, $x/\sqrt{\alpha_i} = 0.354$, and $B = 12\,K_i/(\sqrt{\alpha_i}\,\rho_m\,c_m\,t) = 12 \times 0.5/(2.825 \times 173 \times 0.21 \times 0.07) = 0.832$.

From Figure 6.2-2, A = 0.69.

For a time increment of 5 minutes, from Figure 6.2-1, C = 1.2. Assume that the initial temperature of the structure is 100°F, then the structural temperature at 30 minutes is given by:

$$T_{30} = (1 - \frac{1}{1.2})(540 + \frac{1}{1.2} \times 730 + \frac{1}{1.2}2 \times 1070 + \frac{1}{1.2}3 \times 1375 + \frac{1}{1.2}4 \times 1605 +$$

$$+ \frac{1}{1.2}5 \times 1800) + \frac{1}{1.2}6 \times 560$$

$$= (1 - 0.833)(540 + 608 + 741 + 795 + 775 + 724) + 188$$

$$= 0.167 \times 4183 + 188 = 698 + 188 = 886°R \text{ or } 426°F.$$

With this type of flight plan, maximum temperatures may be reached before the end of the flight. Checking at 15 minutes gives

$$T_{15} = (1 - 0.833)(1375 + \frac{1}{1.2} \times 1605\,\frac{1}{1.2}2 \times 1800) + \frac{1}{1.2}3 \times 560$$

$$= 0.167\,(1375 + 1338 + 1250) + 324$$

$$= 0.167 \times 3963 + 324 = 662 + 324 = 986°R \text{ or } 526°F$$

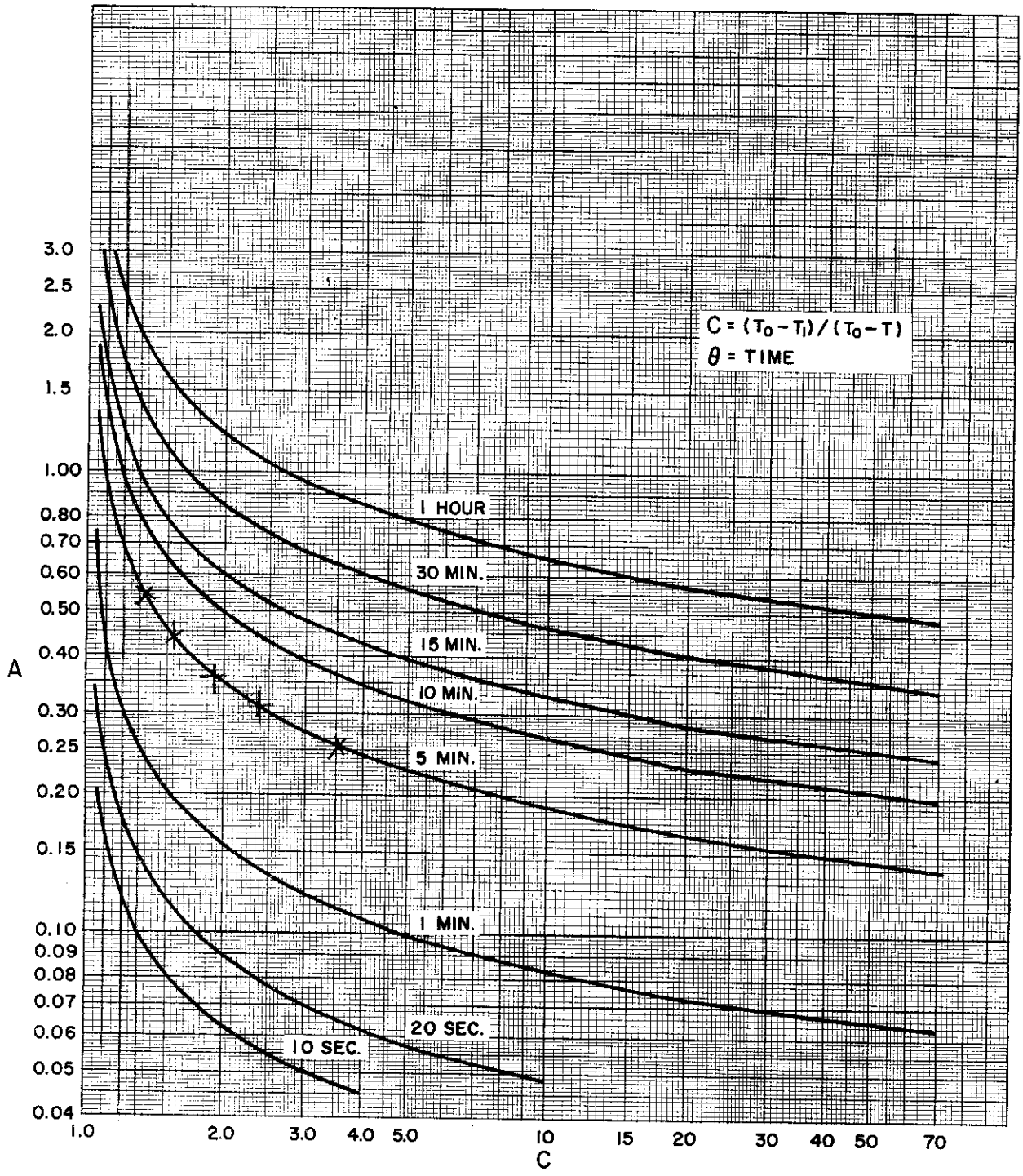

Figure 6.2-1. Graph of the Function $A = \sqrt{\theta / \ln C}$

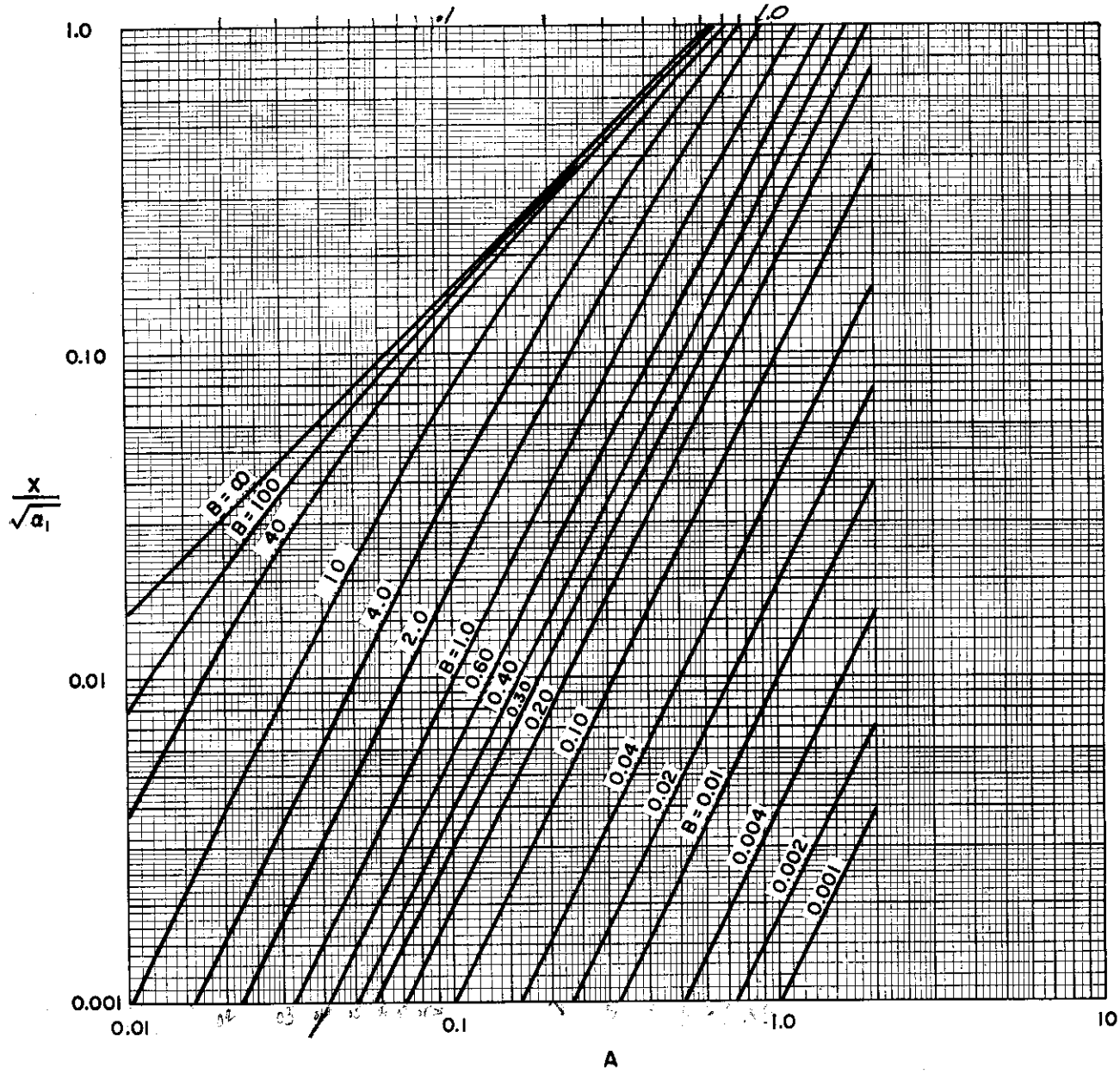

Figure 6.2-2. Graph of the Function $\frac{X}{\sqrt{a_1}} = A \tan^{-1} AB$

6.3 USE OF AN AIR SPACE

The efficiency of an air space as a means of insulating a structure has been mentioned in Section 6.1, and this section gives a method by which the heat flux across such an insulation may be calculated. Also included is a means of using the heat flux in conjunction with the curves of Section 6.2 to obtain transient structural temperatures.

Heat is transferred across an air space by the three methods explained in Section 6.1; conduction, convection, and radiation. In this section, the heat flux due to each of these modes of transfer is considered separately, and the total is obtained by summing.

(a) Heat Transfer Across an Air Space by Conduction

The heat transfer by conduction across an air space bounded by two parallel walls is given by

$$q = \frac{K_a}{x} \Delta T .$$

The conductivity K_a depends upon the mean temperature of the air, and values are given in Section 2.0. This expression is presented graphically in Figure 6.3-1 for a practical range of values of air space depth and mean temperature. Values obtained from this figure should be multiplied by the temperature difference across the air space to obtain heat flux per unit area and time.

(b) Heat Transfer Across an Air Space by Convection

In Part II, it is shown that for horizontal air spaces with the hot wall below, the heat transferred when natural convection exists is given by

$$q = 0.080\, K_a\, (\Delta T)^{1.333} \left(\sqrt[3]{\beta g / \nu^2} \right) .$$

A horizontal air space with the hot wall below is typical of conditions that occur when such insulation is used on the lower surface of a wing or fuselage. If the hot wall is on top, such as occurs on the top surface of a wing, convection will not exist. This equation includes the heat transfer by both conduction and convection, and is plotted for a practical range of values of mean temperature and pressure in Figure 6.3-3. Dependence of the equation upon air pressure arises from the density effect on kinematic viscosity.

Natural convection can exist, in a horizontal air space, only if the Grashof number exceeds 2000. This limitation is reduced to a readily useable form by Figure 6.3-2 which shows whether convection exists for any combination of air pressure, mean temperature, air space depth, and temperature difference. If, for a particular example, the air space thickness and the temperature difference give a point which lies below the appropriate pressure-temperature line, then convection does not exist, and Figure 6.3-1 should be used for heat transfer by conduction. If the point lies above the appropriate line, then convection will exist, and Figure 6.3-3 should be used for heat transfer by combined conduction and convection.

EXAMPLE

An air space one-inch thick is formed by a double-shell type of construction in which the inner shell is a conventional aluminum alloy skin. The aluminum is maintained at 200°F by a water cooling system, and on the bottom surface of the wing the outer shell is at an equilibrium temperature of 1000°F. What is the rate of heat transfer across the insulation? The altitude is 35,000 feet.

$\Delta T = 1000° - 200° = 800°F.$

Mean temperature of insulating air is $(1000° + 200°)/2 = 600°F.$

Air space thickness = 1.0 in.

Assuming ambient air pressure between the shells, atmospheric pressure at 35,000 ft = 500 lb/ft^2.

From Figure 6.3-2, the intersection of x = 1.0 in. and ΔT = 800°F gives a point which lies to the right of the line for a pressure of 500 lb/sq ft and a mean temperature of 600°F. Therefore, both convection and conduction are present.

From Figure 6.3-3, heat transferred = 295 BTU/ft^{2}hr.

(c) Heat Transfer Across an Air Space by Radiation

The heat transfer by radiation, between two parallel flat plates is given by

$$q = \epsilon_o \sigma \left(T_1^4 - T_2^4\right)$$

where, ϵ_o equals the effective surface emissivity for two parallel flat plates:

$$\epsilon_o = \frac{1}{\frac{1}{\epsilon_1} + \frac{1}{\epsilon_2} - 1} .$$

The surface emissivity depends primarily upon the plate material and the condition of the surface. Some variation of emissivity also occurs as a result of plate temperature, and typical values are given in Section 2.0. Using these values of emissivity, the equation for heat flux is presented in graphical form in Figure 6.3-4 for a number of typical plate surfaces. In selecting typical plate surfaces, the precious metals have been included since they are a means of maintaining a low emissivity surface under high-temperature oxidizing conditions. Because of cost, such materials will generally be used in the form of thin foil, or as a cladding.

EXAMPLE

In the example of the previous section, how much additional heat flux is transmitted across the insulating air space by radiation if the outer shell is a nickel base material?

With T_1 = 1000°F and T_2 = 200°F, from Figure 6.3-4, heat transferred by radiation = 350 BTU/ft^{2}hr.

(d) Total Heat Transferred Across an Air Space

The total flux transferred across an air space is the sum of the flux transferred by conduction, convection, and radiation as calculated by the use of Figures 6.3-1 through 6.3-4.

It will be noted that heat transfer by conduction and convection is based upon the average air temperature and the temperature difference across the air space, while heat transfer by radiation is referred to the temperatures of the bounding walls. This apparent inconsistancy is necessary since conduction and convection depend upon the air properties, while radiation depends upon the characteristics of the bounding walls. The relationship between the two temperature systems is as follows:

$$T_m = (T_1 + T_2)/2$$

$$\Delta T = (T_1 - T_2)$$

$$T_1 = T_m + \frac{1}{2}\Delta T$$

$$T_2 = T_m - \frac{1}{2}\Delta T$$

For steady-state insulation systems where temperatures are constant, as is the case if the structure is also cooled, the total flux transmitted across the insulation is a complete solution to the problem. For transient conditions, when the structural temperature is changing as heat passes through the insulation, an average value of total flux should be obtained by using average temperatures. An effective conductivity is then obtained by dividing the average flux by the average temperature difference, ΔT, and multiplying by the depth of the air space, x. This average conductivity should then be used with the method of Section 6.2 to calculate structural temperatures.

Since radiant heat transfer depends upon the fourth power of the surface temperature, the technique of using an average conductivity, based upon average temperatures, can be in error if radiation is significant. In this case, the step-wise procedure described in Section 6.2 should be used, and the flight divided into small time increments. An average value of effective conductivity is then calculated as explained previously for each time increment. It will be evident from Section 6.2 that this procedure can be used either for constant or transient flight conditions.

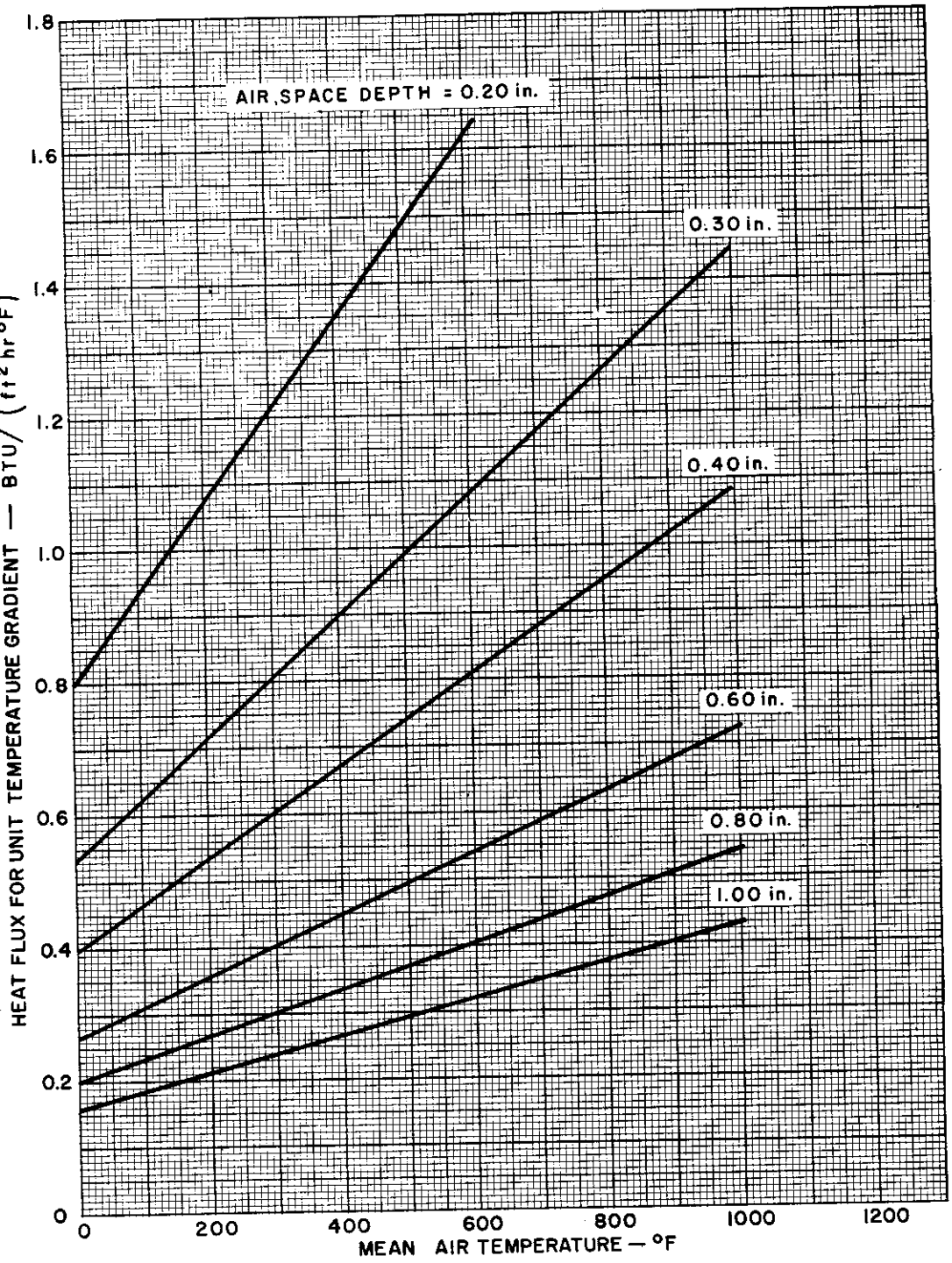

Figure 6.3-1. Heat Transferred by Conduction Across an Air Space

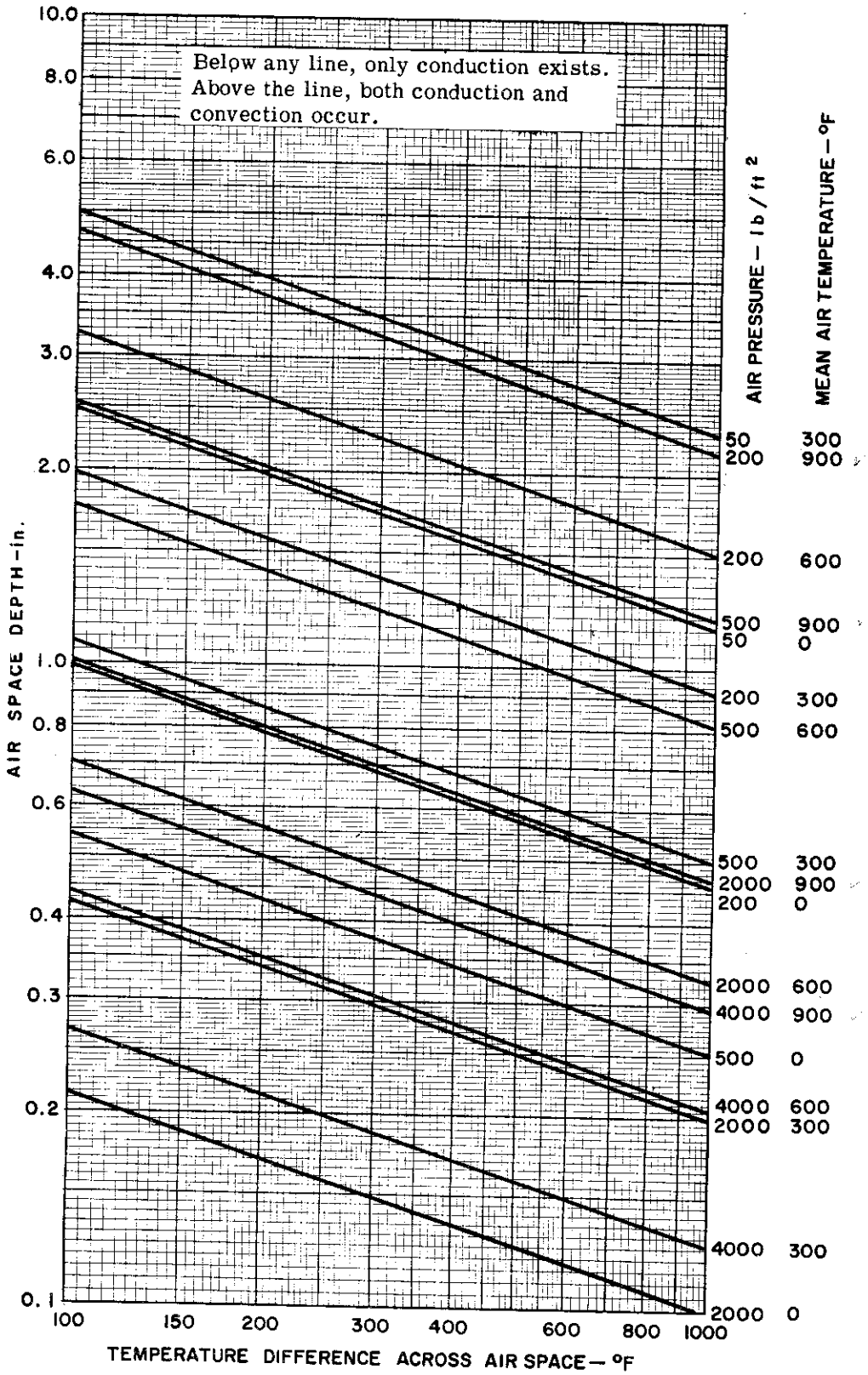

Figure 6.3-2. CHECK FOR CONVECTION IN HORIZONTAL AIR SPACE

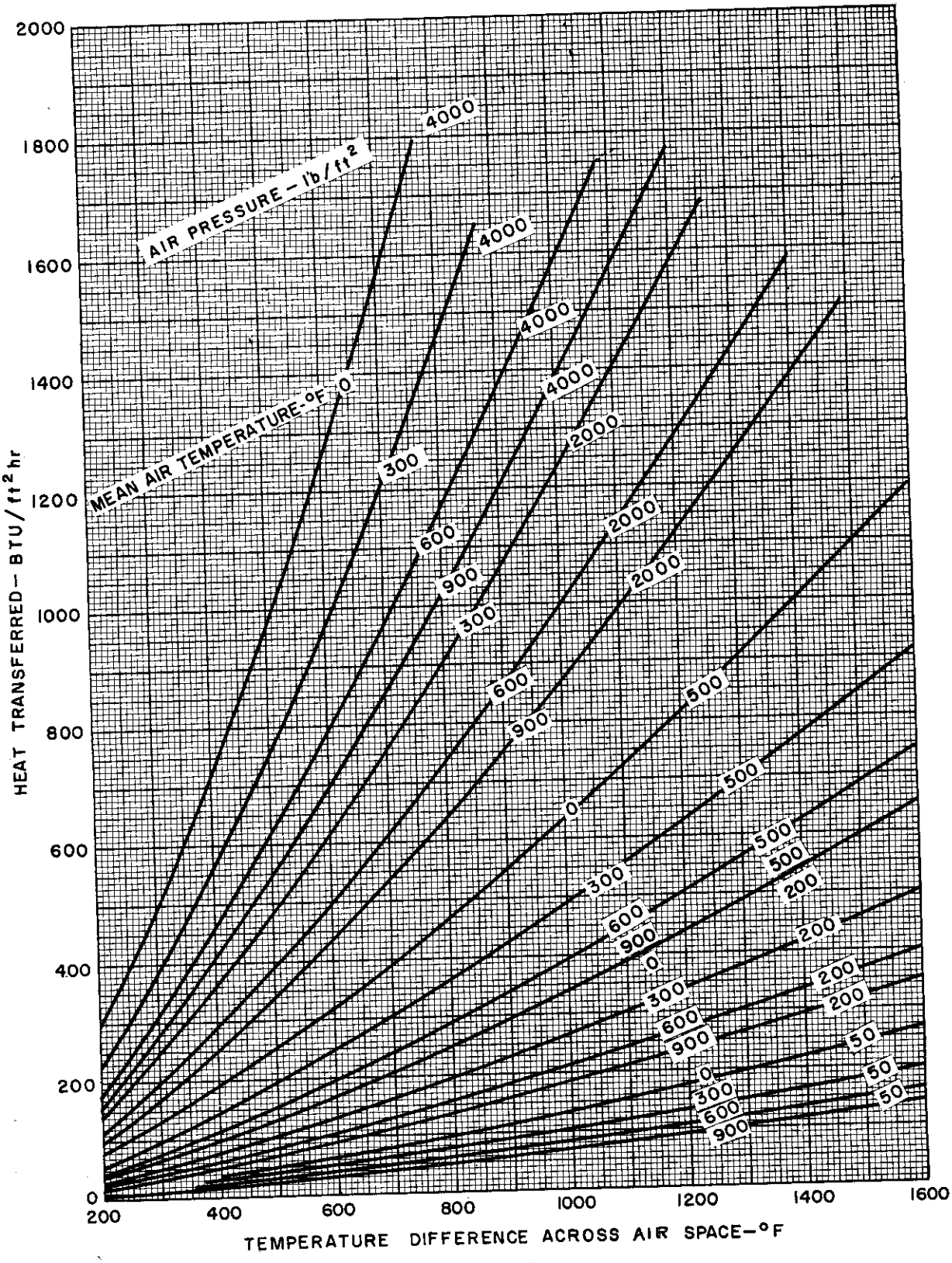

Figure 6.3-3. Heat Transferred by Convection Across a Horizontal Air Space

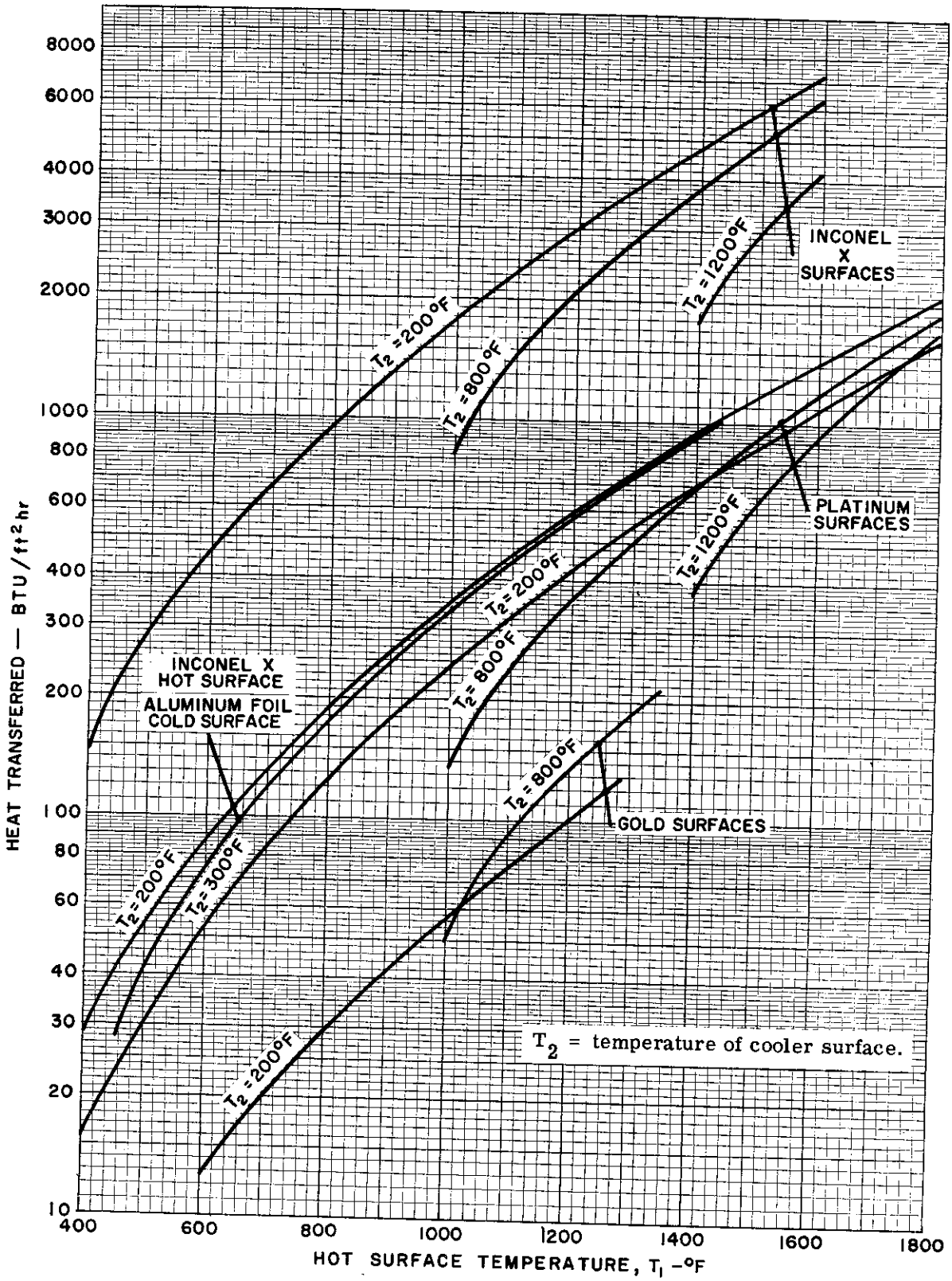

Figure 6.3-4. Heat Transferred by Radiation Across an Air Space

6.4 RADIATION BARRIERS

At high temperatures, the heat transmission across an air space by radiation may still be significant despite the use of highly reflective surfaces on the bounding walls. It may then be advantageous to use additional highly reflective metal foils within the air space, each parallel to the bounding walls and each appropriately separated. Such an assembly of metal foils is termed a radiation barrier.

The case in which radiation barriers are used as heat protection in conjunction with the structure as a heat sink has been solved analytically in Part II on the basis of the following assumptions:

(a) No heat capacity in the insulation.

(b) Infinite conductivity through the thickness of the structural skin; applicable to thin shell structures.

(c) Constant external temperature at the outer layers of the insulation, equal to the surface equilibrium temperature.

(d) Constant emissivity, with temperature, of all surfaces of the radiation foils.

(e) No heat transfer by convection between the radiation foils, since generally the foils can be spaced sufficiently close to satisfy this condition.

(f) Constant conducitivty of the air between the foils.

The required number of radiation foils to limit the structural temperature to a specified maximum value is given by the following expression taken from Section IV of Part II:

$$\mu\theta = \log_e \left(\frac{T_o - T_i + \eta/\mu \, T_o^4}{T_o - T + \eta/\mu \, T_o^4} \right),$$

where $$\mu = \frac{K_i}{x_i} \cdot \frac{12}{\rho_m c_m \tau} \quad \text{and}$$

$$\eta = \frac{\sigma \epsilon}{(m+1)(2-\epsilon)} \cdot \frac{12}{\rho_m c_m \tau} .$$

The term μ, therefore, describes the conduction characteristics of the air as a ratio of the heat capacity of the structural skin, and η does similarly for the radiation characteristics of the foils.

For convenient graphical presentation, this expression can be written in the form

$$\frac{T_i - T e^{\mu\theta}}{\left(1 - e^{\mu\theta}\right)} = T_o \left(1 + \eta/\mu \, T_o^3\right) .$$

Symbols are defined in the nomenclature of Section 6.1, but it should be noted particularly that the dimension x is the total thickness of the air space from the outer wall of the insulation to the structural surface.

Because of the approximations that have been made, the afore-mentioned equation cannot be used when the air conductivity is very small, as may be the case at extreme altitudes or if a vacuum can

be artifically produced between the foils. Again, from Section IV of Part II, the equation for this condition is

$$\eta\theta = \frac{1}{4T_o^3}\left[2\left(\tan^{-1}\frac{T}{T_o} - \tan^{-1}\frac{T_i}{T_o}\right) + \log_e\left(\frac{T_o+T}{T_o-T}\cdot\frac{T_o-T_i}{T_o+T_i}\right)\right].$$

The solution of these equations for transient heating of a structure insulated by a radiation barrier is facilitated by the use of Figures 6.4-1 and 6.4-2 which are based upon an initial temperature T_i of 100°F. In using these curves to find the number of radiation foils required to maintain a specified maximum structural temperature, the required value of η is obtained, given the structural temperature and the surface equilibrium temperature T_o for the flight time θ. η is then solved for by using the expression given previously. The reverse procedure is followed if the insulation is specified and the structural temperature is required.

EXAMPLE

Repeat the first example given in Section 6.2 using gold radiation foils in 2.6 inches of air space, as a means of insulation. Assume the gold has an emissivity of 0.020 and that over the range of temperatures involved, the air has an average conductivity of 0.24 BTU-in./ft^{2}hr°F. How many foils are required if the air can be evacuated?

In the example mentioned, the structure is aluminum, 0.06-inch thick, having an initial temperature of 100°F and a final temperature after 15 minutes that must not exceed 350°F. The equilibrium temperature at the outer surface of the insulation is 1440°F.

$$\mu\theta = \frac{0.24}{2.8} \times \frac{12}{173 \times 0.21 \times 0.06} \times \frac{15}{60} = 0.1175 .$$

Entering with this value and a structural temperature of 350°F on the left-hand side of Figure 6.4-1, and continuing across to the right-hand side of the figure gives, for T_o = 1440°F, $\eta/\mu = 0.007 \times 10^{-8}$.

The required value of η is therefore

$$10^{-8} \times 0.007 \times \frac{0.1175}{0.25} = 0.00329 \times 10^{-8}.$$

But
$$\eta = \frac{\sigma\epsilon}{(m+1)(2-\epsilon)} \cdot \frac{1}{\rho_m c_m t} = \frac{0.173 \times 10^{-8} \times 0.02}{(m+1) \times 1.98} \cdot \frac{12}{173 \times 0.21 \times 0.06}$$

$$= \frac{0.00962 \times 10^{-8}}{(m+1)} .$$

Therefore,
$$(m+1) = \frac{0.00962}{0.00329} = 2.92 ,$$

so that two radiation foils are required.

If the air conduction is neglected from Figure 6.4-2, the required value of $\frac{\eta\theta}{\sigma} = 0.011$, so that η must equal 0.00762×10^{-8}.

Therefore, $(m+1) = \frac{0.00962}{0.00762} = 1.26$,

so that one radiation foil is required.

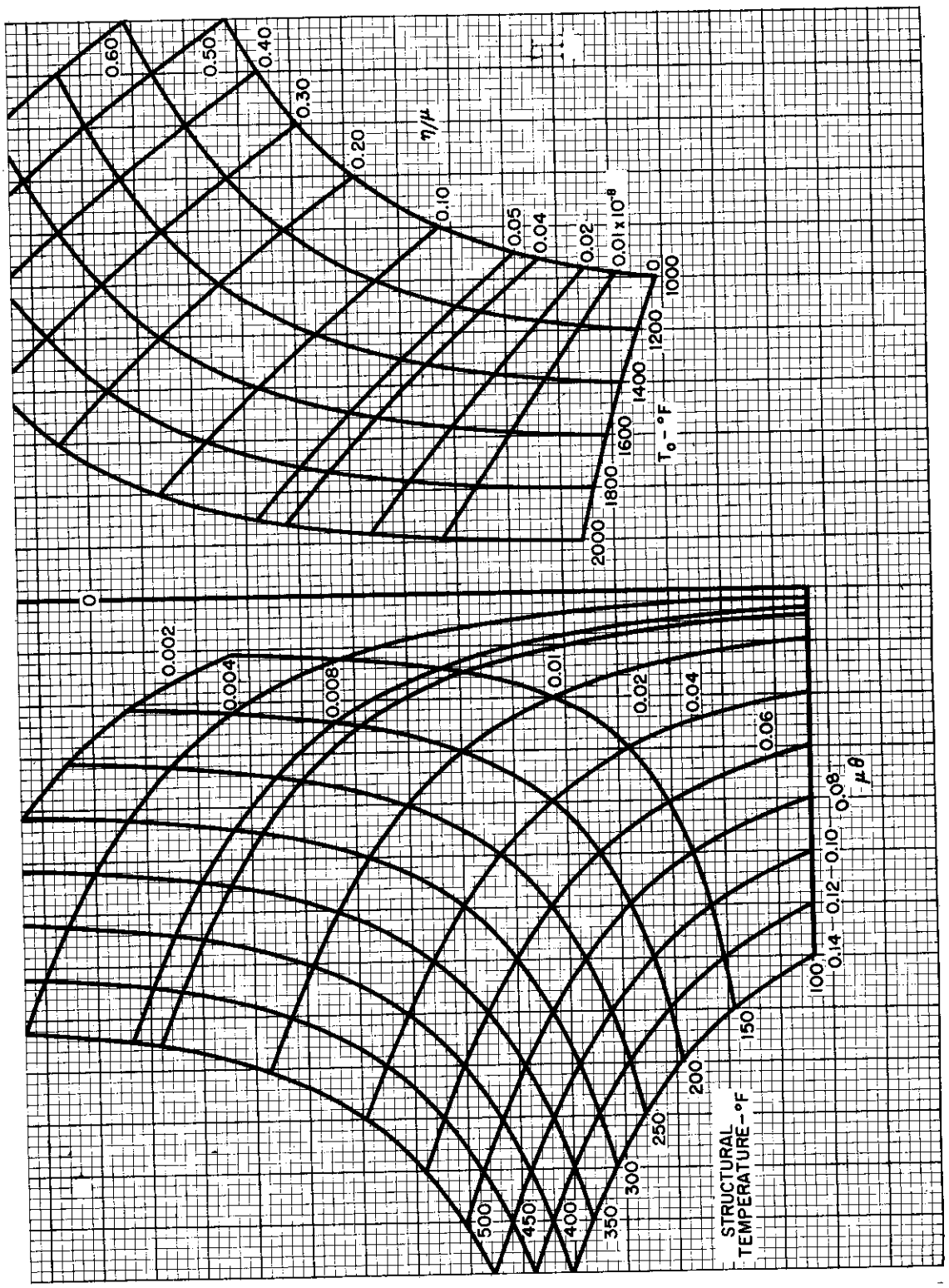

Figure 6.4-1. Radiation Barrier Design — Including Air Conduction

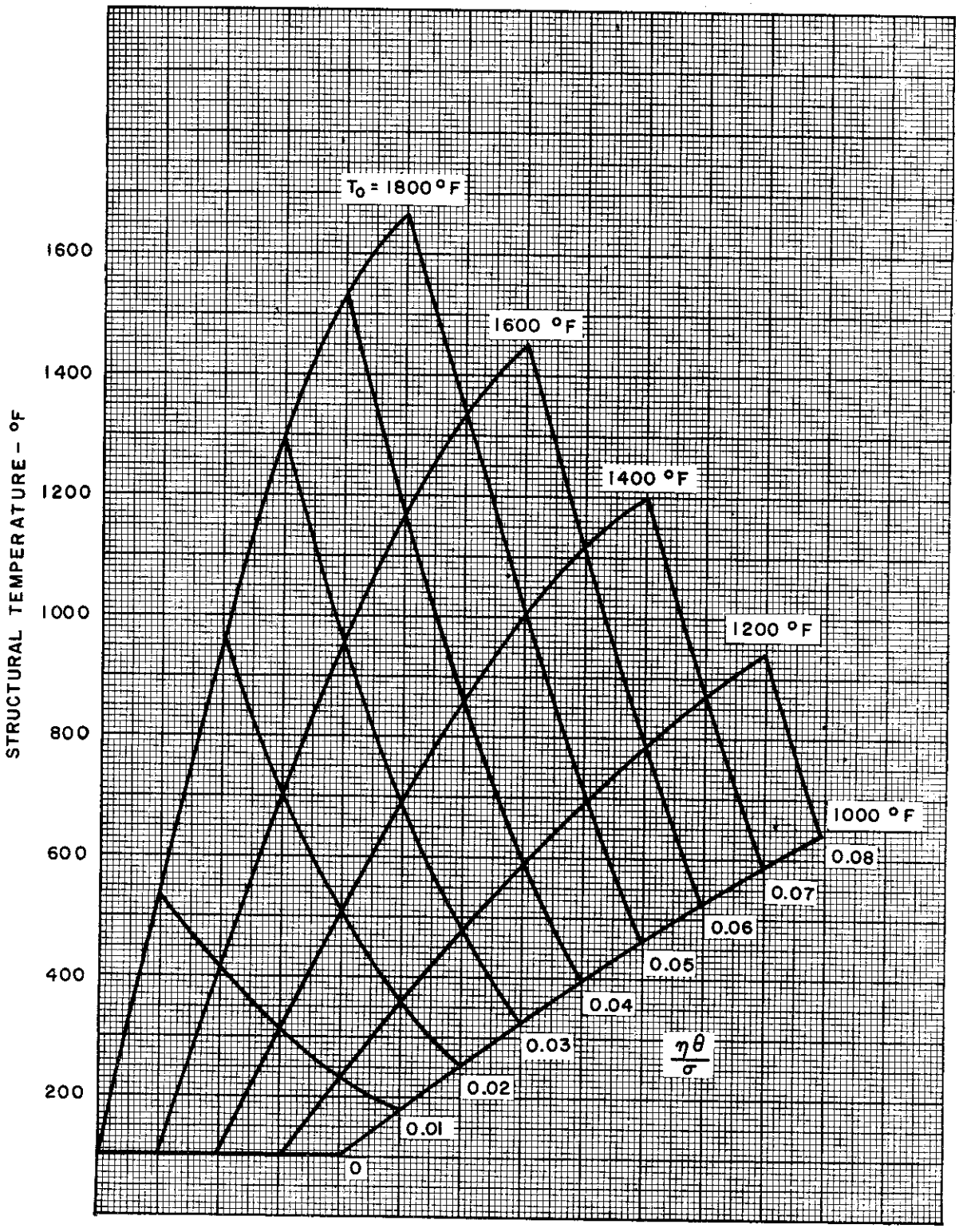

Figure 6.4-2. Radiation Barrier Design — No Air Conduction

[redacted]

6.5 THERMAL LEAKAGE THROUGH INSULATION

Materials which offer sufficient insulating efficiency for use as airframe insulation include air, and fibrous, granular, or other loose type of "fill." None of these materials has mechanical strength, so that their use around the primary structure of an airframe implies a protective outer wall of high temperature material, capable of resisting the aerodynamic forces. Such an outer wall will require load-carrying attachments into the primary structure beneath, and these will form a source of thermal leakage through the insulation.

Curves are presented in this section by which the effect of such a leakage on the temperatures in the primary structural skin can be readily calculated. Two general types of outer wall attachment are considered:

(a) Continuous, line type of attachment.

(b) Equally spaced, point type of attachment.

In both cases, a temperature increase factor is given by which the structural temperatures calculated by the methods of Sections 6.2 must be increased to include the effects of thermal leakage. This factor can be applied successively for each thermal leakage that may be present, such as when a line type of attachment exists in two perpendicular directions. Temperature increase factors are given only for constant external aerodynamic conditions; that is, a constant value of T_o. Theoretical basis for the methods of this section can be found in Part II.

(a) Continuous Line Type of Attachment

A section through this type of attachment, having the idealized form used in the solution of the problem, is shown in the following diagram, which also explains the notation:

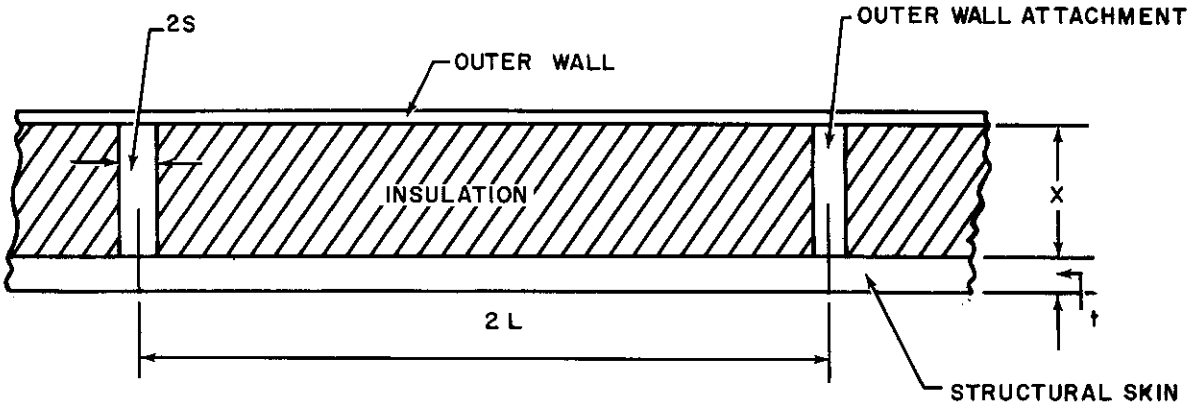

The temperature multiplication factor Y is given in Figure 6.5-1 for various values of time from the start of heating, and conductivity ratio between the skin and attachment, and for the point in the skin immediately BENEATH the attachment. Time is expressed by the ratio $\alpha_m \theta / L^2$, and the attachment conductivity ratio by the parameter R, where

$$R = \frac{K_m t}{L} \cdot \frac{x}{K_A s} .$$

Values of Y below 0.6 have not been included in Figure 6.5-1 since such values will generally represent impractical reductions of the insulation efficiency by leakage through the attachments. Similarly, for the range of values of Y and R included in Figure 6.5-I, and for $\alpha_m \theta / L^2$ greater than 0.5, the temperature gradient along the structural skin is small, and has been neglected.

To obtain the final structural temperature, the temperature of the structural skin for the condition without outer wall attachments, is calculated for the time θ, by the method of Section 6.2. Denote this temperature by T'. Then, the structural temperature including the effect of outer wall attachments is given by

$$(T_o - T) = (T_o - T')Y .$$

EXAMPLE

Referring to the first example of Section 6.2, what will be the maximum structural temperature if the Thermoflex insulation is covered by an outer wall which is attached to the primary structure by continuous channels of Inconcel X material, 0.02-inch thick, spaced 10 inches apart?

For an aluminum alloy skin:

Diffusivity $\alpha_m = 277$ in.^{2}/hr

$\theta = 15$ min $= 0.25$ hr

$L = 5$ in. so that $L^2 = 25$ in.^{2}

Therefore, $\alpha_m \theta / L^2 = 277 \times 0.25/25 = 2.77$.

Conductivity of aluminum structural skin = $K_m = 840$ BTU in./ft^{2}hr°F

Thickness of structural skin = $t = 0.06$ in.

Conductivity of Inconel X attachment = $K_A = 150$ BTU in./ft^{2}hr°F

Thickness of outer wall attachment = $2s = 0.050$ in.

Thickness of insulation = $x = 2.57$ in.

Therefore, $R = \frac{840 \times 0.06}{5} \times \frac{2.57}{150 \times 0.010} = 17.3$.

From Figure 6.5-1, $Y = 0.83$. From Section 6.2, $T_o = 1440$°F and the structural temperature, neglecting attachment effects, $T' = 350$°F. Therefore,

$(1440 - T) = (1440 - 350) \times 0.83$, and

$T = 1440 - 905 = 535$°F.

(b) Point Type of Attachment

The diagram and notation shown for the line type of attachment again applies except that dimension s now becomes the radius of the point-type attachment. Then, again using the notation T' for the structural temperature neglecting thermal leakage through the insulation, the final structural temperature is given by

$$T = T' + \frac{ZQ_o}{K_m t} .$$

Values of the factor Z are given by Figure 6.5-2 plotted against the dimension less time parameter $\frac{r^2}{4\alpha_m \theta}$ Note that in this expression, Q_o, the heat flux transmitted through the leakage path

is assumed constant. This is an approximation since, even with a constant temperature, maintained at the outer surface of the insulation, the temperature of the inner structural skin will increase with time, thus decreasing the value of Q_o. Since, however, the leakage effect is necessarily secondary and should make only a small change in structural skin temperature, it is sufficient to use an average value of Q_o.

It should also be noted that the term r, which equals the radial distance from the center of the leakage path through the insulation to the point at which the structural temperature increase is required, cannot be put equal to zero when using Figure 6.5-2. The minimum value of r, giving the maximum temperature increase is S.

EXAMPLE

Repeat the previous example for the case when the attachments of the outer wall are formed by equally spaced 0.50-inch diameter bolts of Inconel X material having a conductivity of 150 BTU/ft^{2}hr°F.

Maximum structural temperature will occur at the attachment so that r takes its minimum value which is 0.25 inch. Then, the value of the parameter $\frac{r^2}{4\alpha_m\theta}$ is

$$\frac{0.25^2}{4 \times 277 \times 0.25} = 0.000225.$$

From Figure 6.5-2, $Z = 0.64$.

For the calculation of an average value of Q_o, assume an average skin temperature of 300°F so that, with a temperature at the outer surface of the insulation of 1440°F, the heat flux through the attachment is

$$\frac{150}{2.57} \cdot \left(\frac{\pi \times 0.5^2}{4 \times 144}\right) \cdot (1440 - 300) = 58.4 \times 0.001364 \times 1140 = 91 \text{ BTU/hr.}$$

Then, the maximum structural temperature is

$$T = 350 + \frac{0.64 \times 91 \times 144}{840 \times 0.06} = 350 + 166 = 516°F.$$

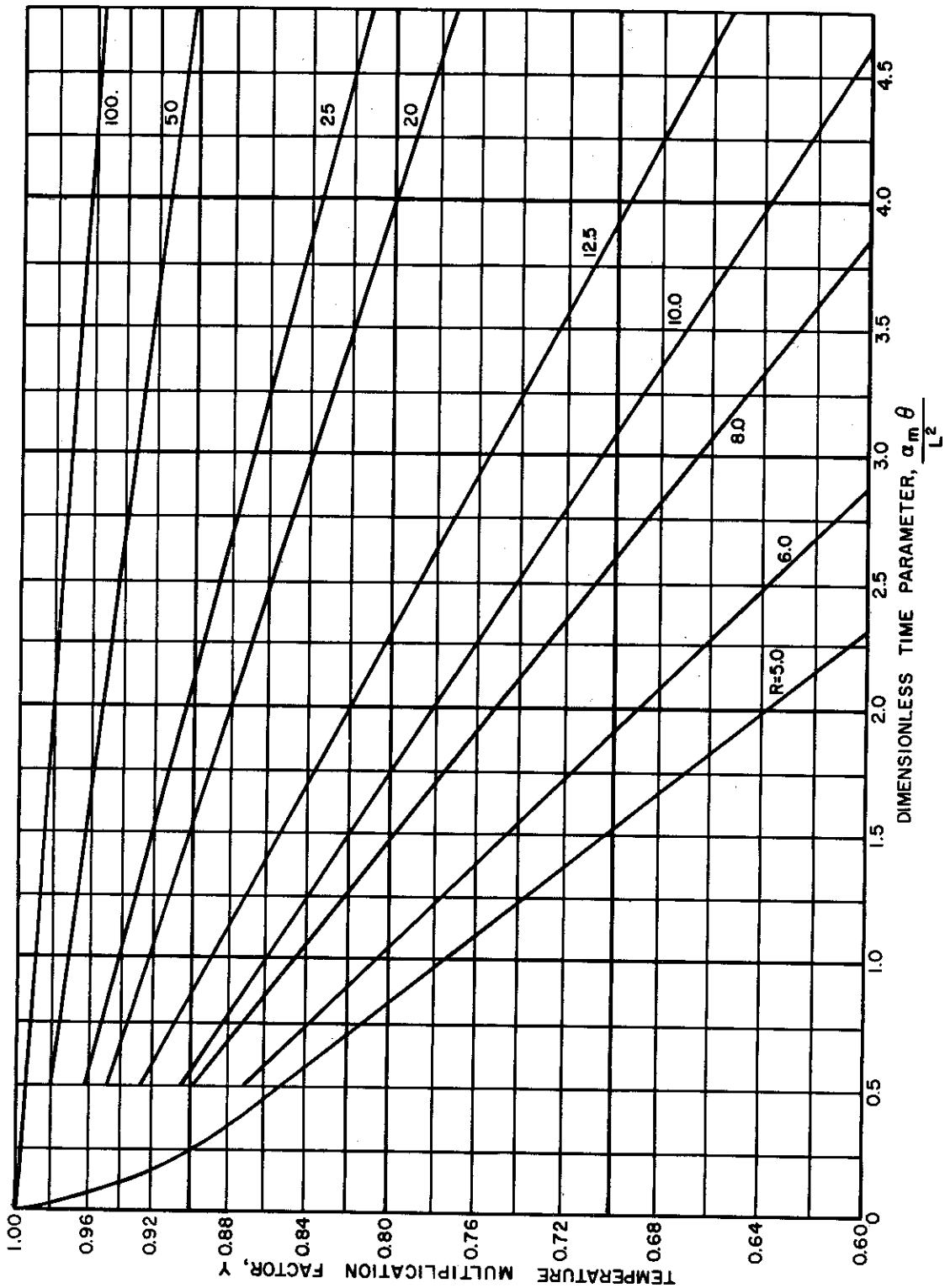

Figure 6.5-1. Temperature Multiplication Factor for Line-Type Thermal Leakage

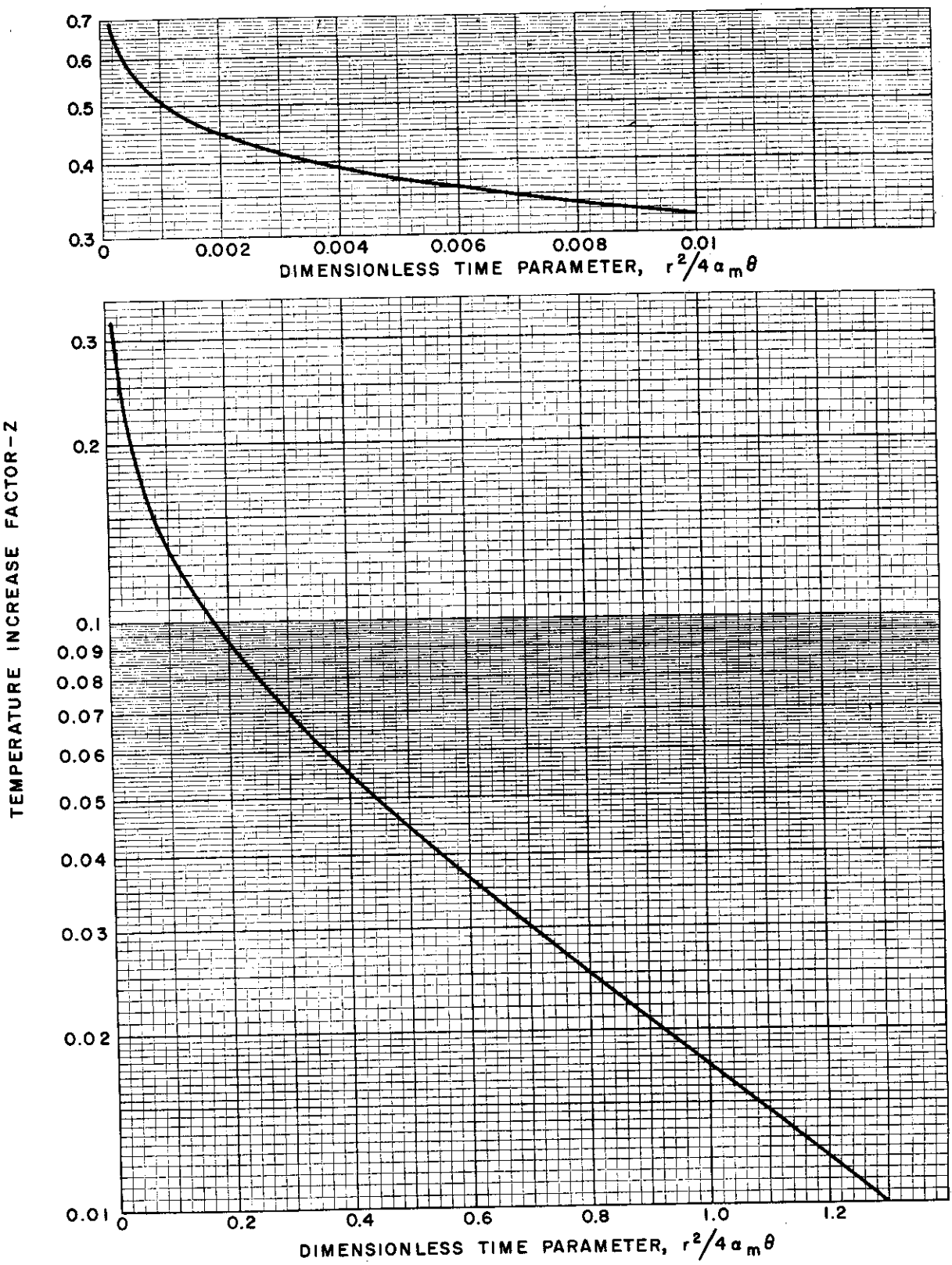

Figure 6.5-2. Temperature Increase Factor for Point-Type Thermal Leakage

[redacted]

NOTES

[redacted]

APPENDIX

EXPLANATION OF GRAPHICAL PRESENTATION BY CARPET PLOTTING

By A. Krivetsky

[redacted]

APPENDIX

EXPLANATION OF GRAPHICAL PRESENTATION BY CARPET PLOTTING

Many of the problems covered in this Manual, for which graphical presentations have been given, involve the interdependence of three variables. To present this information as concisely as possible, and also to permit accurate interpolation, a presentation known as carpet plotting is employed. Since this technique is not in general use, this appendix is included to explain how to read carpet plots to obtain the maximum amount of information.

The more conventional form of graphical presentation for functions having three variables is to associate two of the variables with a pair of perpendicular axes, and to plot curves for specific values of the third variable. Since there is no scale for this third variable, there is no precise means of interpolating for values intermediate between those plotted. This is particularly so if the function is not linear in this third variable.

In the carpet plot, however, the axis for the second variable has a new origin for each value of the third variable; and since these origins are spaced in proportion to the magnitude of the third variable, it is apparent that this latter then has its own scale. In Figure 6.4-1, for instance, the origin of the scale of $\frac{\eta\theta}{q\theta}$ is moved one large unit to the right for each value of T_o. The large unit produced by the vertical lines thus represents, simultaneously, 200°F on the T_o scale and 0.010 on the $\frac{\eta\theta}{q\theta}$ scale. Such a procedure permits precise interpolations to be made, as will be shown.

For the purposes of an example, a portion of Figure 6.4-2 is reproduced in the following.

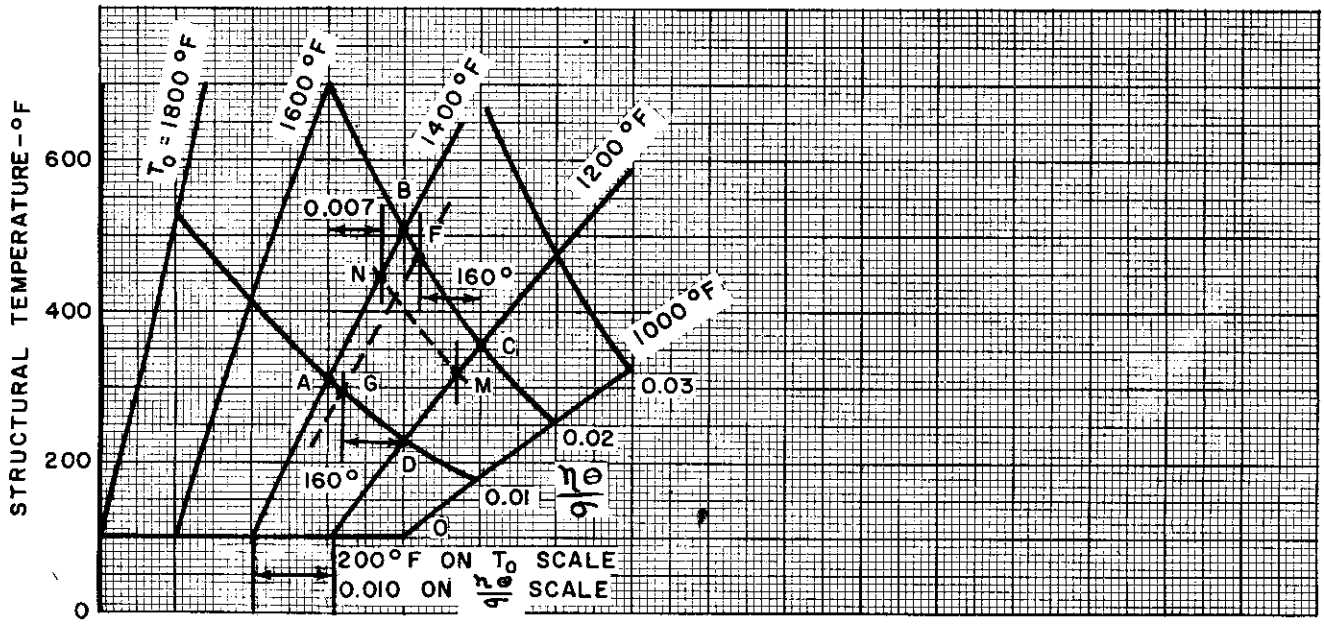

In the example, it is necessary to find the structural temperature when T_o = 1360°F and $\frac{n\theta}{\sigma}$ = 0.017. The required point obviously lies in the area ABCD. First draw a portion of the curve T_o = 1360°F, as follows.

Treating the horizontal distance AD as 200° of T_o draw a vertical line at 160°F to the left of point D and mark the point G where this line intersects the line AD. Similarly, find the point F on line BC where T_o = 1360°F. Draw in the line T_o = 1360°F.

A portion of the curve $\frac{n\theta}{\sigma}$ = 0.017 is now drawn by repeating this procedure with respect to points CD and AB, giving the points M and N. The intersection of the curves T_o = 1360°F and $\frac{n\theta}{\sigma}$ = 0.017 gives the value of structural temperature as 420°F.